Spatiotemporal mapping of spontaneous smooth muscle motility in capacious organs: the *ex vivo* urinary bladder and *in vivo* gravid uterus of the rabbit.

A thesis presented in partial fulfilment of the requirements for the degree of

Doctor of Philosophy

in

Anatomy & Physiology

at Massey University, Manawatū, New Zealand

Corrin Murray Hulls

2023

Dedicated to my father.

Abstract

The temporal and spatial dynamics of propagating myogenic contractions in the wall of the resting *ex vivo* urinary bladder and *in vivo* gravid uterus of the rabbit were characterised by spatiotemporal maps of area strain rate, of linear strain rate and contractile patch analysis, and related to cyclic variation in intravesical pressure (p_{ves}) in the bladder, and electrophysiological recordings in the gravid uterus.

In the urinary bladder, patches of propagating contractions (PPCs) enlarged and involuted with a frequency in near synchrony with peaks in intravesical pressure. Maximum area percentage of the anterior surface of the bladder undergoing contraction and the sizes of individual PPCs also coincided with the peak in p_{ves}. Moreover, p_{ves} varied cyclically with total area of contraction and with the indices of the size and aggregation of PPCs, indicating that PPCs grew and involuted by a combination of peripheral enlargement or shrinkage and by coalescence or fission with other PPCs, their areas being maximal at or around the peak in p_{ves}.

Bladder PPCs originated and propagated within temporary patch domains (TPDs) and comprised groups of near synchronous cyclic individual contractions (PICs). The TPDs were located principally along the vertical axis of the anterior surface of the bladder, either to the left or the right of midline and changed in location from one side to side and from side to tip or base. The sites of origin of PICs within PPCs were inconsistent, consecutive contractions often propagating in opposite directions along linear maps of strain rate. Similar patterns of movement of PPCs within TPDs of the same form occurred in areas of the anterior bladder wall that had been stripped of mucosa.

The synchronisation and extended propagation of PICs within PPCs and the concurrent variation in p_{ves} of the bladder were sometimes lost or diminished, uncoordinated PICs then occurred, propagated shorter distances, and had little effect on p_{ves}. There was no evidence that any influence of bladder shape on stress influenced the principal direction of propagation of either PCCs or PICs or the disposition of TPDs.

The disposition and dynamics of PPCs and their component individual myogenic contractions in the wall of the resting *ex vivo* tetrodotoxinized urinary bladder of the rabbit were characterised by spatiotemporal maps and

related to cyclic variation in p_{ves} before and after the administration of carbachol, isoprenaline, carbenoxolone, and the RhoA-inhibitor Y-27632. The results confirm that the bladder wall can exhibit two contractile states that are of similar frequencies to those of the two types of electrophysiological discharge described by previous workers. In the first of these, large low frequency cyclic PPCs predominate. In the second, small irregular, higher frequency PICs predominate. Comparison of the effects of the drugs on the timing and disposition of contraction suggested indicated that the local spatial spread of contractions in PPCs was governed largely by myocytes, whilst the propagation, frequency, and duration of PPCs was likely governed via gap junctions between interstitial cells of cajal- intermuscular (ICC-IM) and myocytes.

Spontaneous and oxytocin-induced contractile activity was quantified in the bicornuate uteri of pregnant rabbits maintained *in situ*, using data from electrophysiological recordings and spatiotemporal maps, and compared statistically.

Spontaneous contractions occurred over a range of frequencies in gravid animals at 18-21 and at 28 days of gestation and propagated both radially and longitudinally over the uterine wall overlying each foetus. Patches of contractions were randomly distributed over the entire surface of the cornua and were pleomorphic in shape. No spatial coordination was evident between longitudinal and circular muscle layers nor temporal coordination that could indicate the activity of a localised pacemaker. The density and duration of contractions decreased, and their frequency increased with the length of gestation in the non-labouring uterus.

Increasing intravenous doses of oxytocin had no effect on the mean frequencies, or the mean durations of contractions in rabbits of 18-21 days gestation but caused frequencies to decrease and durations to increase in rabbits of 28 days gestation, from greater spatial and temporal clustering of individual contractions. This was accompanied by an increase in the distance of propagation, the mean size of the patches of contraction, the area of the largest patch of contraction and the overall density of patches.

Together these results suggest that progressive smooth muscle hypertrophy and displacement with increasing gestation is accompanied by a decrease in smooth muscle connectivity causing an increase in wall compliance

and that oxytocin restores connectivity and decreases compliance, promoting volumetric expulsion rather than direct propulsion of the foetus by peristalsis. The latter effects were reversed by the β2 adrenergic receptor agonist salbutamol thus reducing area of contraction, duration, and distance of propagation.

The characteristics of smooth muscle contraction that are associated with the maintenance of tone during accommodation appear to be to be similar in the capacious organs discussed. Hence, it appears there is patchy rather than uniform local revision of the state of tonal contraction over the surfaces of the various capacious organs during accommodation that can undergo neural modulation.

There appears to be less similarity in regard to the mechanisms that secure the voiding contractions in these capacious structures. Whilst the actuation of the necessary shorter term increase in tone may be ultimately dependent upon a mechanosensitive myogenic reflex, the relative contributions of autonomic, hormonal, mechanical and voluntary reflexes that reset the threshold of this reflex and aid in the relatively rapid expulsion of the contents, appear to vary between organs.

Acknowledgements

Though only my name appears on the cover of this thesis, a great many people have contributed to its production. I owe my gratitude to all those people who have made this thesis possible- to say it has been 'quite the journey' is an understatement.

My deepest gratitude is to my Chief Supervisor, Prof. Roger Lentle. I have been amazingly fortunate to have a supervisor who granted me this opportunity, the freedom to explore on my own and at the same time the guidance to recover when my steps faltered. Roger taught me how to question and express ideas. His direction, patience and support has been unfaltering and his enthusiasm toward the sciences an inspiration.

My co-supervisor and conference wingman, Dr Quintin King. Thank you for your proficiency and expertise in everything urological. Your help, experience, guidance, professionalism, and competence were, and are, invaluable. I am indebted to him for his continuous support and encouragement, his advice and friendship.

My other co-supervisor, Dr Wei-Hang Chua. For in whom I found a colleague and a friend. Thank you for all the laughter, encouragement, and advice in all things.

Dr Patrick Janssen for designing the amazing piece of software which made this body of work possible. Dr Gordon Reynolds for his early supervision. I am grateful to both for their immense technological knowledge, advice, competence, and skills.

Thank you to Professor David Mellor for my academic introduction to Massey University, for his early career advice and support.

I would like to acknowledge Assoc. Prof. Paul Chambers and Dr Joanna Chagas for all their professional and veterinary help. Lauren Stewart, Erin Wilson, Dr Fran Wolber and Aimee Hamlin for their animal husbandry, care, and technical competence. Thank you all for your flexibility, help and co-operation.

Thank you to my friends, too numerous to name, but you know who you are. Their support and care helped me stay sane. I greatly value their friendship and I deeply appreciate their belief in me.

Most importantly, none of this would have been possible without the love and patience of my family. To my immediate family and wife thank you for your constant source of love, concern, support, and strength all these years.

I know it seems cliché to say I have the best parents in the world- but it is fact. Mum and Dad, thank you. In my life's brightest and darkest times, you have been there- unflinching, unwavering. The opportunities you have given me in life, the experiences, your generosity and love, I am indebted and will never forget.

In Glenn, I could not find a better brother. Thank you for being there and know I will always be there for you in return. In what you yourself have achieved in life I am extremely proud.

Finally, to my wife Ana- to express what you have done for me and how you have helped me is difficult to put into words and will always be insufficient. What you have accomplished and achieved, the goals you set for yourself are an inspiration. You have always encouraged me, supported me, and motivated me in every endeavour. Simply put- I am a better person having met you and a greater person by being with you. I love you, Ana.

Copyright and Permissions

Permissions to reproduce the figures from authors/publishers and material from my published journal articles have either been obtained or are in the process of being approved by the relevant authorities at the time of submission of this thesis.

Table of Contents

List of Figures

List of Tables

List of Abbreviations

$\%/s^{-1}$	Strain Rate (percentage change in area per unit time)
%PLAND	Patch Density (The total areas of all patch contractions occurring in a given A-type ST elliptical map as a percentage of the total area of the ellipse)
+ve	Positive
ΔL	Change in Length
µm	Micrometer
µM	Micromolar
µV	Microvolts
2D	two-dimensional
3D	three-dimensional
Ach	Acetylcholine
ADP	Adenosine Diphosphate
AI	Aggregation Index (an expression describing the number of patches that are adjacent to the largest patch in the field of view)
ANOVA	Analysis of Variance
AP's	Action Potentials
ASR	Area Strain Rate
ATP	Adenosine 5'-triphosphate
A-type ST Maps	Area Strain Type Spatiotemporal Maps

Ca	Calcium
cm	Centimetre
cpm	Cycles per minute
Cx	Connexin
Cx#	Connexion # Subtype
DSM	Detrusor Smooth Muscle
D-type ST Maps	Diameter Type Spatiotemporal Maps
ECG	Electrocardiogram
ECM	Extra Cellular Matrix
EHG	Electrohysterogram
EMG	Electromyography
EtHal	End Tidal Halothane
FFT	Fast Fourier Transform
G	Gauge (needle size)
H = PR/t	La Place's equation (H= Hoop stress, P= Pressure, R= Radius, t= thickness of wall
HBS	Earle's HEPES Buffer Solution
Hz	Hertz
IC	Interstitial Cells
ICC	Interstitial Cells of Cajal

ICC-IM	Interstitial Cells of Cajal- Intermuscular
ICCLC's	Interstitial Cells of Cajal Like Cells
ICCLC-LP	Interstitial Cells of Cajal Like Cells- Lamina Propria
I-Maps	Luminous Intensity Maps
IU	International Units
IUPC	Intrauterine Pressure Catheter
IV	Intravenous
K	Potassium
K_{ATP}	Adenosine 5'-triphosphate Sensitive Potassium Channels
K_{ca}	Calcium Gated Potassium Channels
kg	kilogram
K_v	Voltage Gated Potassium Channels
L#	Lumbar (Vertebrae #)
LHS	Left Hand Side
LOI	Line of Interest
LPI	Largest Patch Index (The area of the largest Propagating patch contraction as a percentage of the total area of the view)
L-type ST Maps	Longitudinal Type Spatiotemporal Maps
m/M#	Muscarinic (# subtype)
mg	Milligram

m-ICLC	Myometrial Cajal-like Interstitial Cells
min	Minute
ml	Milliliter
MLK	Myosin Light chain Kinase
MLP	Myosin Light chain Phosphatase
mm	Millimetre
mm/s	Millimetres per second
mmHg	Millimetres of Mercury (pressure)
MPS	Mean Patch Size (mm^2)
MRI	Magnetic Resonance Imaging
mU	Milliunits
mV	Millivolts
MVUs	Montevideo Units
NA	Noradrenaline
NANC	Non-adrenaline non-cholinergic
nm	Nanometer
nM	Nanomolar
nmol/L	Nanomoles per Litre
NO	Nitric Oxide

NP	Number of Patches (mean number of patches of contraction occupying the anterior surfaces of the bladder)
NVA	Non Voiding Activity
OD	Outer Diameter
P	Phosphate
P	Pressure
PBS	Physiologically Buffered Saline
PIC's	Propagating Individual Contractions
pm	Picometer
PMTA	Percentage Mean Total Area (mean percentages of the anterior surfaces of the bladders undergoing contraction)
PPC's	Propagating Patch Contractions
p_{ves}	Intravesical Pressure
R_G	Greater Curvature
RhoA	Rho-associated kinase
RHS	Right Hand Side
R_L	Lesser Curvature
ROI	Region of Interest
rtMRI	Real Time Magnetic Resonance Imaging
R-Type ST Maps	Radial Type Spatiotemporal Maps

s	Second
S#	Sacral (Vertebrae #)
sec	Seconds
SNS	Somatic Nervous System
SR	Sarcoplasmic Reticulum
ST maps	Spatiotemporal Maps
ST	Spatiotemporal
T#	Thoracic (Vertebrae #)
T/r	T= Wall Tension, r= Radius
TPD's	Temporal Patch Domains
TTX	Tetrodotoxin
UDS	Urodynamic Study
v	Volume
-ve	Negative
VSTM	Video Spatiotemporal Mapping
λ	Stretch
$б_t$	Hoop Stress

1 Introduction

Distinct layers of smooth muscle cells are found within the walls of various anatomical structures, including blood vessels, stomach, small and large bowel, urinary bladder, and uterus. When these cells contract, they shorten longitudinally and expand transversely. This directional shortening may generate short lived propulsive (phasic) contractions, or long-lived (tonic) contractions. The latter are important in hollow capacious organs that have evolved for storage, i.e., to accommodate inflow and vary capacity and luminal pressure by the adjusting wall compliance and distensibility (Gregersen & Christensen, 2000).

Smooth muscle cells can receive stimuli from the somatic and autonomic nervous systems via afferent nerves and can also respond, both directly and indirectly, to changes in wall stress. Hence, both myogenic cellular and neural circuits (Lentle, Reynolds, & Janssen, 2013) can generate either the localized short-lived 'phasic' contractions that are important in mixing and propulsion, or the 'tonic' contractions that adjust local wall compliance and influence the capacity of the structure. Tonic contraction can be maintained for long periods in primitive animals such as shellfish (Rüegg, 1971) however, there is debate as to the duration of tonic contractions in higher animals, because an increase in tone will compromise local blood supply (K. E. Andersson, Boedtkjer, & Forman, 2017).

All smooth muscle cells contract by establishing cross-bridges between uni-dimensionally orientated actin and myosin fibres to generate force. Such contractions are initiated by changes in transient concentration of calcium ions (Ca^{2+}) which activates myosin light chain kinase that in turn induces phosphorylation of myosin light chains of using energy derived from ATP to link actin with myosin via cross bridges. In a phasic contraction, the rate of myosin light chain phosphorylation corresponds well with the shortening velocity of smooth muscle (Hai & Murphy, 1988). However, sustained tone has been attributed to a state in which the actin myosin cross-bridges(termed latch-bridges), persist longer, allowing force to be maintained for a longer period and at a lower energy cost (Aguilar & Mitchell, 2010). This process is thought to be fundamental for the action of tonically active smooth muscle (Lentle, Reynolds, et al., 2013).

Myogenic changes in wall compliance of a capacious organ allow accommodation of incoming material (i.e., volumetric expansion) without a large change in luminal pressure. Compliance is controlled by a combination of the inherent elasticity of the tissue of the wall (passive tone) coupled with a change in the frequency of tonic contractions (active tone) (Gregersen & Christensen, 2000).

When the walls of a hollow spherical structure are distended by a volumetric increase in its luminal contents, the resultant force of this distension on each of the two halves of the structure is disposed at right angles to the circumferential plane and is referred to as hoop stress (Miftahof & Nam, 2013). Thus, the increase in hoop stress brought about by distension is acting to pull apart the two halves of the structure. Whilst it is possible that neural and cellular mechanoreceptors in the wall of the bladder initiate changes in tone and wall thus compliance so as to accommodate any volumetric increase without undue increase in luminal pressure, such responses are mechanistically more complex than might at first appear.

Firstly, it is important to note that that mechanoreception, like the force it detects, occurs in a particular direction. Thus, for example, for a myocyte to respond to a particular force the 'mechanoreceptor' and the cell that bears it must be orientated in the direction in which the force operates. Experimental work suggests that mechanoreception results from distraction of elements within the plasma membrane of myocytes or neurons (Brierley, 2010) and that, in the case of smooth muscle cells, where the bulk of the plasma membrane is orientated longitudinally it follows that mechanoreception operates in this dimension.

A simple first hypothesis would suggest that the overall compliance of each half of the wall of the cylindrical structure is adjusted by synchronous action of all smooth muscle cells within it in response to an increase in the volume of the contents and thus modulates hoop stress. This would require that all the component myocytes reduce their state of contraction by an equal amount on each side of the bladder in response to any local increase in stress. This could be achieved either directly, by the mechanosensitivity of the long axes of individual myocytes, or indirectly by mechanosensitive neural reflexes.

In regard to myogenic mechanoreception, it must be remembered that myocytes, like all cells, consist largely of incompressible fluid so that their lengthwise contraction must be accompanied by their width-wise expansion. Thus, if the long axes of all the component myocytes were aligned at right angles to a plane of hoop stress, their synchronous longitudinal relaxation and lengthening to reduce tension at right angles to that plane would be accompanied by a synchronous increase in tension in the circumferential plane at right angles to the first, this resulting from a concomitant decrease in cross sectional area of each myocyte. Thus, a relaxation of hoop stress in one circumferential plane would be accompanied by an increase in tension in the circumferential plane at right angles to it. This latter action would thus increase bladder wall compliance in one plane but decrease it in the other, a situation that would complicate prompt accommodation of incoming fluid. However, the orientation of the long axes of myocytes within the walls of such capacious structures as the bladder (K.-E. Andersson & Arner, 2004) and uterus (Escalante & Pino, 2017) is irregular. Hence the orientation of their long axes to a given plane will vary, as will the degree of stimulation of their mechanoreceptor organelles to any increase in hoop stress at right angles to that plane. In such a situation the contractile response will be correspondingly patchy, and compliance will result from oscillation in contractile response around the two planes that transect a spherical structure. A similar situation will likely arise if we consider neural mechanoreception as again mechanosensory neurones are unlikely to be all orientated with respect to hoop stress in a particular plane. This train of logic fits in with the experimental findings regarding the spontaneous contractile activity of the bladder and uterus.

The bladder wall exhibits rhythmic localised, tonic contractions or 'micromotions' (Bo Coolsaet, 1985) that may be superimposed on (Poley, Dosier, Speich, Miner, & Ratz, 2008) or "reset" (Lentle et al., 2015a) baseline tone. Autonomous bladder activity, and the associated micromotions persist in *ex vivo* preparations (M. J. Drake et al., 2017; Van Os-Bossagh et al., 2001) and thus do not depend on extrinsic innervation.

The urinary bladders of terrestrial mammals are of broadly uniform gross morphology across species i.e., a distensible spheroid structure that sits within the pelvis. However, the morphology of other tonically active organs i.e., the uterus, varies between mammalian species, from a duplex tubiform shape that accommodates

multiple foetuses, in the rabbit, to a uniloculate spheroid structure that generally accommodates a low number of foetuses, as in humans. The uterus increases in mass (Ferrell, Garrett, & Hinman, 1976) and augments its capacity during gestation (Tan, Tan, & Ng, 2008) to accommodate the growing foetus.

The mechanical means by which tonic or phasic contractions subsequently expel the fully developed foetus at delivery is not completely understood. It is entirely possible that, at the commencement of, and during labour, tonal adjustment is altered to reduce wall compliance and the capacity of the uterus, thus initiating expulsion of the foetus by 'volumetric expulsion' rather than direct myogenic propulsion.

The localised patches of contractions that are found in the wall of the non-gravid uterus (Akerlund, 1998) continue in the gravid uterus throughout gestation until near term (Caldeyro-Barcia & Poseiro, 1959; Carter, Naaktgeboren, & Van Zon-Van Wagtendonk, 1971; Cushny, 1906; Dubin, Ghodgaonkar, & King, 1979; Mackler, Ducsay, Veldhuis, & Yellon, 1999; R. Wilson, Allen, Nandi, Giles, & Thornton, 2001). Hence, there is a gradual decrease in basal tone of the uterus throughout gestation so as to avoid any increase in uterine pressure consequent on any increase in the volume of contents (Apostolakis, Rice, Longo, Seron-Ferre, & Yellon, 1993; Baguma-Nibasheka, Wentworth, Green, Jenkins, & Nathanielsz, 1998; Haluska & Novy, 1993; Honnebier, Jenkins, Wentworth, Figueroa, & Nathanielsz, 1991; Sigger, Harding, & Jenkin, 1984). Thus, the ongoing resetting of smooth muscle tone could result from the same localised tonic events that maintain "resting' capacity in the non-gravid uterus. Ultimately, a further resetting of tone via hormonal stimuli, such as oxytocin, would increase basal tone as to decrease wall compliance and promoting a relative increase in pressure of the contents and the expulsion of the foetus.

Both the uterus and urinary bladder have been hypothesized to possess a localised region of pacemaker tissue that initiates contractile activity, but such sites have not been located or their actual existence remains controversial (W. J. Lammers, Stephen, Al-Sultan, Subramanya, & Blanks, 2015; Lutton, Lammers, James, van den Berg, & Blanks, 2018a; Yu, He, Li, & Cheng, 2017). Whilst a body of work describes both 'tonic' and 'phasic'

contraction at a cellular level in both organs, the mechanism of tonic smooth muscle contraction and its disposition have received very little attention.

The aims of this thesis are to investigate *ex* and *in vivo* the patterns of spontaneous smooth muscle motility in two capacious organs, the urinary bladder, and the gravid uterus of the rabbit.

Several methods have been used to quantify the contractile activity of smooth muscles in these organs. They include the measurement of variations in isometric force in isolated muscle strip preparations (Longhurst, Kang, Wein, & Levin, 1990; Schofield & Wood, 1964), the determination and mapping of electromyographic activity (Arpad I Csapo & Takeda, 1965; Iggo, 1955; M. Kinder, Gommer, Janknegt, & Van Waalwijk van Doorn, 1997; W. J. Lammers, 2013; Ursillo, 1961), and the variation in intraluminal pressure (Arpad I Csapo & Takeda, 1965; Robert M. Levin, Goldman, & Wein, 1984; Suzuki & Tsutsumi, 1981). However, all these methods are essentially derivative in that they do not measure motility in the whole organ directly.

The technique of 'length dependent' spatiotemporal mapping has been used to map variation in length and linear strain in a number of organs including the *ex vivo bladder* (Bijos & Drake, 2015; J. Gillespie, Harvey, & Drake, 2003; W. J. Lammers et al., 2008; Lentle et al., 2015a; C. Rabotti & Mischi, 2015; R. C. Young, 2016).This technique allows the timing, locus, speed, and frequency of smooth muscle contractile activity to be measured. I have used a novel two dimensional spatiotemporal mapping algorithm that was developed in this laboratory to measure variation in area strain rate, to quantify and map spontaneous contractile activity in the urinary bladder and gravid uterus. Further, through observation, how a targeted range of pharmacological agents influence this tonic activity. Together these two methods shed light on the manner in which neurogenic and myogenic muscle activity together modulate wall tension to accommodate any increase in content.

This thesis will be presented in the following order: firstly, a literature review describing the morphology, physiology, and modulation of control in of the urinary bladder and gravid uterus, followed by a detailed description of what is currently understood of the physics and biomechanics of accommodation in these capacious structures. A review of current methodologies to measure contractile activity of these organs will be

presented. Further, the methodology of the spatiotemporal mapping of strain rate, its evolution, and its application will then be described. The subsequent chapters that detail the results of these studies will begin with an analysis of the myogenic contraction of the *ex vivo* rabbit urinary bladder, quantifying and characterising its spontaneous contractile motility. A further chapter will describe the pharmacological modulation of its spontaneous contractions with the aim to investigate the levels of myogenic and neurological control. The next chapter will describe the spontaneous contractile activity of the gravid uterus *in vivo* and *in situ* detailing and describing the spontaneous myogenic contractile activity and its hormonal modulation. Lastly, a discussion chapter will summarize key results, compare, and contrast findings and discuss their implications. Lastly, limitations and future direction of work will also be addressed.

Preface: Literature Review

In this review the relevant anatomy of the two organs investigated will be discussed, notably the urinary bladder and the gravid uterus. Next, the mechanics of tone in capacious structures will be detailed. Finally, the manner in which smooth muscle behaves i.e., the dynamics of accommodation, and these features will be described and contrasted with those of phasic contraction.

2 Literature Review

2.1 The Bladder

2.1.1 Anatomy of the Urinary Bladder

The human bladder is located under the peritoneum and behind the pubic symphysis. It is a hollow organ with walls of smooth muscle, internally lined by an epithelial layer and in its upper regions externally protected by a layer of serosa. Although it is capable of storing up to 1 litre of urine, the bladder holds an average volume of 300-400 ml (Lukacz et al., 2011) during the normal filling stage.

The shape of the bladder changes as it fills and empties. The volume of its contents and pressure from neighbouring organs affects its shape and position. During filling it changes from a tetrahedral shape and becomes oval, rising into the abdominal cavity. When empty the bladder is situated entirely in the lower region of the pelvis and flattened by the overlying bowel.

The anatomy of the bladder consists of:

- **The Dome or Body** – Main part of the bladder, the detrusor muscle is thickest in the dome and produces the strongest and most significant contractions during micturition
- **The Trigone** – located on the posterior surface. It is triangular-shaped, with the tip of the triangle pointing downwards. The slit-like openings of the ureters are approximately 2.5 cm apart, and these openings insert at the rear of the bladder. The epithelial layer here is smooth and the trigone acts as a funnel that assists in channelling urine into the urethra.
- **Bladder neck or urethral entrance** – is a cone shaped structure formed by the convergence of the fundus and the two inferolateral surfaces. It is continuous with the urethra.

The bladder wall consists of the outer serosa; detrusor (smooth) muscle layer; the lamina propria or suburothelium; and the uroepithelium (urothelium). The lamina propria and urothelium are collectively described as the mucosa (Fig 2-1).

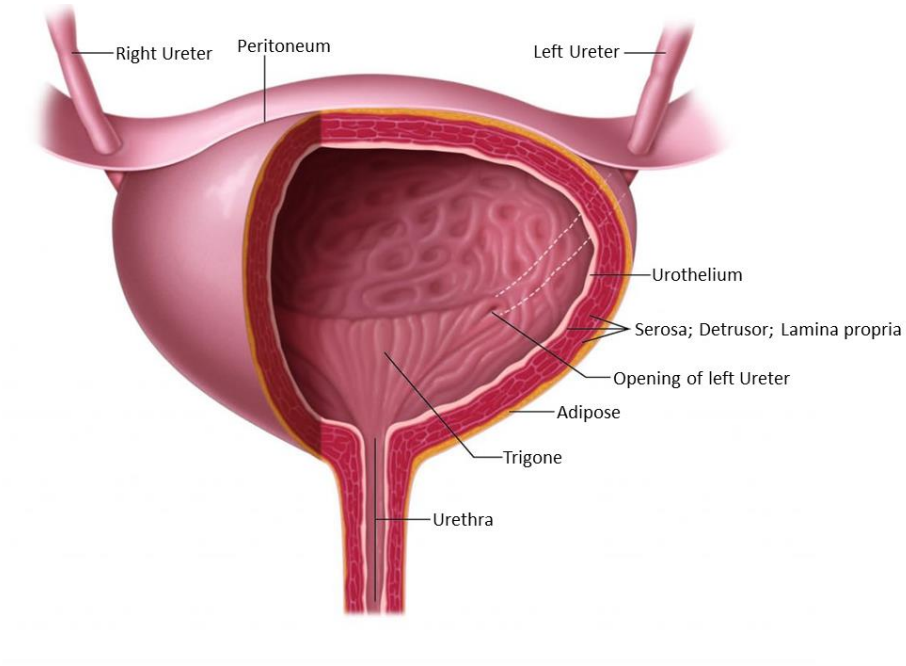

Figure 2-1 Anatomy of the Bladder (Urology, 2022)

Each layer that makes up the wall of the bladder varies in its function and complexity. The innermost urothelium consists of the polyhedrally shaped cells that form a stratified transitional epithelium, containing basal cells, intermediate cells, and umbrella cells.

The innermost umbrella cell layer prevents bacterial attachment and diffusion of urine components across the epithelium and has low permeability to urea and water. (Apodaca, 2004; Lewis, 2000). This layer maintains a barrier even as the bladder undergoes cycles of filling and voiding. Hence, the mucosal surface is able to unfold from a highly wrinkled state, and, as it enlarges, increasing the surface area (Christopher H. Fry & McCloskey, 2019).

The *lamina propria* consists of numerous interstitial cells (ICs), interspersed with afferent nerve fibres and blood vessels (Hossler & Monson, 1995; Miodonski, Litwin, Nowogrodzka-Zagorska, & Gorczyca, 2001).

The bulk of the bladder wall consists of detrusor muscle which consists of bundles of smooth muscle cells that are orientated in various circumferential and longitudinal directions. The longitudinal axes of the smooth muscle cells in of the inner and external layers orientate predominantly longitudinally- from the base of the bladder to its apex- while those of the middle layer run predominantly in a circumferential direction (Miftahof & Nam, 2013). The muscular layer also contains a loose network of three-dimensional stroma as well as a fine arrangement of collagen and elastin fibres which explains the walls great level of extensibility.

The serosa covers only the superior and lateral walls of the bladder and originates from the visceral peritoneum. The remainder of the bladder wall is covered by an adventitia that merges with pelvic floor organs.

2.1.2 Dual Function of the Urinary Bladder

The function of waste control in all living organisms is one of the vital importance. Almost universally, terrestrial animals have a urinary bladder with a storage function and it has been hypothesized that storage function allows for an evolutionary selective advantage in reducing the likelihood of successful predation (McCarthy & McCarthy, 2019). The dual function of the bladder is usually divided into two phases: bladder filling and voiding. The simplistic view of the filling phase is that the bladder muscle (detrusor) remains relaxed, so that a large volume of urine can be accommodated without much increase in pressure. During voiding, the detrusor contracts to empty the bladder to completion (Hinman & Cox, 1967). Given this view, the bladder is basically an on-off control system, but in reality, the process of bladder is control is far more complex. The preceding work will document the unique physiological properties of the diverse array of cells within the bladder wall, and the multiple levels of hierarchical control that modulate urine storage and ultimately govern its normal functions of filling and emptying.

2.1.3 The Detrusor

2.1.3.1 The Morphology of the Detrusor Smooth Muscle Cell

The structural unit of the detrusor muscle is the smooth muscle cell- the myocyte (Fig 2-2). Their contractility and temporal repertoire depend on the balanced function of plasmalemmal ion channels. The detrusor myocytes are very similar to visceral smooth muscle cells (A. Brading, 1987). Each myocyte contains a characteristic spindle-like shape measuring ≈100–300 μm in length and ≈5–6 μm in diameter (Miftahof & Nam, 2013). When relaxed, the cell has a smooth surface and a polygonal shape in cross section. When the muscle contracts in the longitudinal direction, the cells become scalloped in appearance with an irregular surface.

Detrusor myocytes contain an organized longitudinal matrix of thinner-actin and thicker myosin filaments, and an associated family of special proteins and kinases, e.g., light chain myosin, tropomyosin, myosin light chain kinase, caldesmon and myosin phosphatase. Actin filaments are single helical coils of actin associated with tropomyosin and caldesmon. Myosin filaments are made from two coil rod-like structure heavy chains with a globular head domain.

The cell membranes contain cavaeoli which generally associate with elements of the subsurface sarcoplasmic reticulum. The cytoplasm contains a centrally located nucleus, intracellular thin α- and β-actin (≈6 nm), intermediate, mainly desmin (≈10 nm) (U. Malmqvist, A. Arner, & B. Uvelius, 1991; Ulf Malmqvist, Anders Arner, & Bengt Uvelius, 1991) and thick (≈20–25 nm) filaments and mitochondria. Thin α- and β-actin filaments are arranged into a lattice that is attached to the cell membrane at the sites of dense bodies. They provide the integrity, strength, and high degree of deformability to the bladder wall as well as associating with myosin thick filaments. The regularly spaced dense bodies establish direct structural and functional contacts between the intracellular cytoskeleton and the extracellular matrix (ECM). The anchoring plaques of these dense bodies transmit the forces generated by the contraction-relaxation of the actin myosin complex to the surrounding tissue, and may act as mechanosensors in gene expression signalling pathways, cell migration, growth, and adaptation (Geiger & Ginsberg, 1991; Yamada & Geiger, 1997; Zamir & Geiger, 2001)

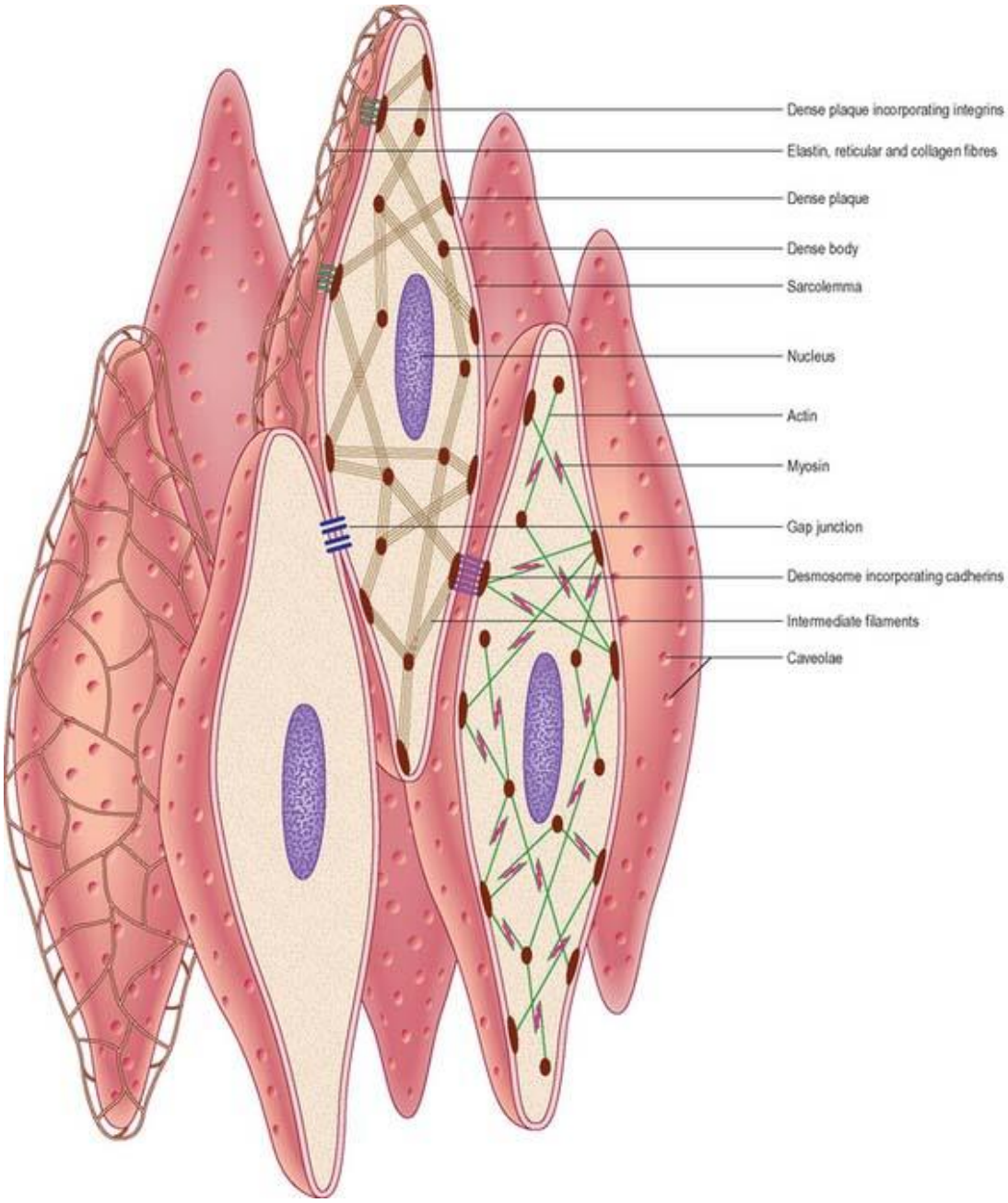

Figure 2-2 Three-dimension representation of smooth muscle cells

For clarity, some structural features have been separated for illustration in different cells. The spindle-shaped cells interdigitate with their long axes parallel; mechanical continuity between the cells is provided by a reticular layer of elastin and collagen fibres. The cytoskeletal framework consists of intermediate filament arrays (mainly longitudinal) and bundles of actin and myosin filaments (shown in separate cells) inserted into cytoplasmic dense bodies and sub membranous dense plaques to form a three-dimensional network. The sarcolemma contains anchoring desmosomes (adherens junctions), gap junctions and caveolae. Modified from (ClinicalGate, 2015, 18 March).

Individual detrusor smooth muscle cells are linked to other smooth muscle cells via gap junctions (Gabella, Bulbring, Brading, Jones, & Tomita, 1981). Gap junctions are thought to consist of symmetrically arranged protein channels in each membrane that create a continuous pathway from one cell to the other that allows the transit of ions and water-soluble molecules between cells. Gap junctions also connect the cells electrically, making groups of cells into a functional syncytium allowing electrical charge to distribute between the component cells of the syncytium.

2.1.3.2 Electromechanical Activity of the Detrusor Muscle

The resting membrane potential of human bladder myocytes range between -55 and -38 mV. There is confusion around the existence of a spontaneous slow wave activity. One author (A. F. Brading, 2006) claims that intracellular recording from isolated and intact strips of detrusor do not show low amplitude resting potential oscillations consistent with slow waves. However, other studies (A. Visser & Van Mastrigt, 1999; A. Visser & van Mastrigt, 2000; A. J. Visser & van Mastrigt, 2001) on mechanical and intracellular electrical activity in human detrusor smooth muscle obtained show spontaneous fluctuations of the resting membrane potential of varying amplitude (~8-10 mV) and at a wide range of frequencies ν = 0.33–25 (Hz).

Contractility of the smooth muscle is influenced by patterns of spontaneous and/or induced electrical charge. A depolarisation phase is mediated via an inward current of Ca^{2+} via L-type Ca^{2+} channels (Kajioka, Nakayama, McMurray, Abe, & Brading, 2002). The principal control of the muscle cell contraction is free cytosolic calcium (Ca^{2+}) that triggers the cyclic actin–myosin complex formation. An increase of the sarcoplasmic Ca^{2+} from a basal level of 50–100 nM initiates contraction, half maximal activation is achieved at about 1 µM (Changhao Wu, Kentish, & Fry, 1995). The source of Ca^{2+} can be extracellular (Montgomery & Fry, 1992) via channels in the membrane mentioned i.e., L-type Ca^{2+} channels , or from intracellular stores (C. Fry, Gallegos, & Montgomery, 1994). The increase in free Ca^{2+} is short lived and is either removed from the cell via Na+/Ca2+ exchange (C Wu & Fry, 2001) and an ATP-dependent Ca-pump (Liu, Ishida, Okunade, Shull, & Paul, 2006) or moved back into cellular stores (Nobe, Sutliff, Kranias, & Paul, 2001).

Like other smooth muscle cell types, K^+ channels play a critical role in the modulation of detrusor myocyte tone, and a number of K^+ channels have been identified in detrusor myocytes from various species (Christ & Hodges, 2006). The main function of detrusor smooth muscle K^+ channels is to regulate and control Ca^{2+} entry via voltage gated Ca^{2+} channels, and thus the intracellular Ca^{2+} concentration that controls bladder muscle contraction and relaxation (Petkov, 2011). K^+ channels are the largest and most diverse group of ion channels which includes several varieties of channels including voltage-gated K^+ (K_V) channels, Ca^{2+} activated K^+ (K_{Ca}) channels and ATP sensitive K^+ (K_{ATP}) channels. The K^+ channels have an important role in maintaining the detrusor smooth muscle cell resting potential via the negative equilibrium potential for K^+. The opening of K^+ channels cause cell membrane hyperpolarization, limits Ca^{2+} entry via L-type Ca^{2+} channels and causes detrusor smooth muscle relaxation. By contrast, inhibition of detrusor smooth muscle K^+ channels lead to membrane depolarization and activation and opening of L-type Ca^{2+} channels causing detrusor smooth muscle contraction.

Studies on isolated detrusor muscle from humans and several animal species (K. E. Anderson, 1993) have shown that drugs that open K_{ATP} channels not only reduce spontaneous contractions, but also contractions induced either by direct electrical stimulation, by the drug carbachol (acetylcholine receptor agonist), and by low, external K^+ concentrations. (Malmgren, Andersson, Andersson, Fovaeus, & Sjögren, 1990). These drugs effect on preloaded tissue, their suppression of phasic activity, and the supporting view that they relax bladder tissue by K_{ATP} channelling opening and subsequent hyperpolarization, suggest K^+ channels are intimately involved in the modulation of bladder tone (Malmgren et al., 1990).

2.1.4 Control of Contractile Behaviour of the Detrusor Muscle

The detrusor exhibits two types of contractions; a longstanding tonic contraction associated with the accommodation of incoming urine and a short-lived, quasi-phasic contraction associated with urine expulsion. Thus, during bladder filling the muscle modulates the tonic contractions that control wall compliance, and it undergoes phasic contractions during micturition.

During bladder filling, the spontaneous contractile activity of an individual myocyte may spread to a few nearby cells, which can then be regarded as a module or ‘‘active unit’’ (Marcus J Drake, Fry, & Eyden, 2006). However, if several active units are coordinated, the size of the functional unit may increase. In the isolated detrusor muscle strip, this is reflected by increased amplitudes of the spontaneous contractions (A. F. Brading, 1997). Corresponding contractions (as reflected by changes in intravesical pressure) can be observed in isolated perfused bladders (M. Drake, Harvey, & Gillespie, 2003; Marcus J Drake et al., 2003) and in intact bladders during cystometry, even in humans (Marcus J Drake, Harvey, Gillespie, & Van Duyl, 2005). The difficulty in observing such contractions during cystometry in the human bladder may be explained by their lack of coordination- some units are contracting when others are relaxing- and no consistent change in intravesical pressure is recorded. However, in isolated bladder preparations from patients with detrusor overactivity, there seems to be increased coordination leading to large amplitude contractions (A. F. Brading, 1997), possibly reflecting increased changes in inter-cellular communication.

After micturition, spontaneous contractions are minimal, and filling occurs with little increase in overall intravesicular pressure but with a background of small phasic increases in pressure. These rhythmic pressure oscillations are a result from uncoordinated myogenic contractions which arise at many different sites throughout the bladder. As filling proceeds, the rhythmic pressure waves increase in amplitude and eventually cause the urge to micturate. The bladder must at this point change from an ordered set of oscillators which provide background tone to a well-coordinated propulsive system capable of efficient emptying. How both of these functions are controlled is not yet fully understood but it is clear that there must be many pacemaking loci which generate the fundamental rhythmic activity. A brief description of the controlling features bladder activity will be discussed below.

2.1.4.1 Neural Control

The generation of a graded receptor potential in afferent sensory neurons in response to stretch requires the gating of a channel, which in the case of physiological bladder filling must be sensitive to incremental increases in bladder pressure/muscle stretch and can be rapidly activated to compensate for these changes (Brierley, 2010), and thus influence the frequency of the action potentials generated (Fig 2-3). One hypothesis for direct neural mechanotransduction relies on the direct distortion of the architecture of the ion channel by change in membrane bilayer tension, a 'tugging' of the ion channel, physically opening the pore (Hamill & Martinac, 2001). An alternative hypothesis is that the ion channel is physically tethered to the extracellular matrix or intracellular cytoskeleton and thus the stretch activated domains that initiate a reflex change respond to tension throughout the entire cell membrane, which results in an opening of the channel (Christensen & Corey, 2007; P. G. Gillespie & Walker, 2001).

2.1.4.2 Mechanosensitivity of Pores

The physical stretching of detrusor myocytes has also been shown to open non-selective cation channels, depolarise the cell and augment Ca^{2+} influx through Ca^{2+} channels (Wellner & Isenberg, 1994), thus causing tone to increase and compliance to decrease. However, this effect requires a high level of stretch (ΔL=20% (M. C. Wellner & G. Isenberg, 1993)) and thus may occur during quick stretch or overfill. It therefore seems that accommodation of urine is more likely achieved by action of mechanoreceptors in the ICCs (see section below) or by stretch of some other yet to be identified channel in the myocyte that reduces depolarisation.

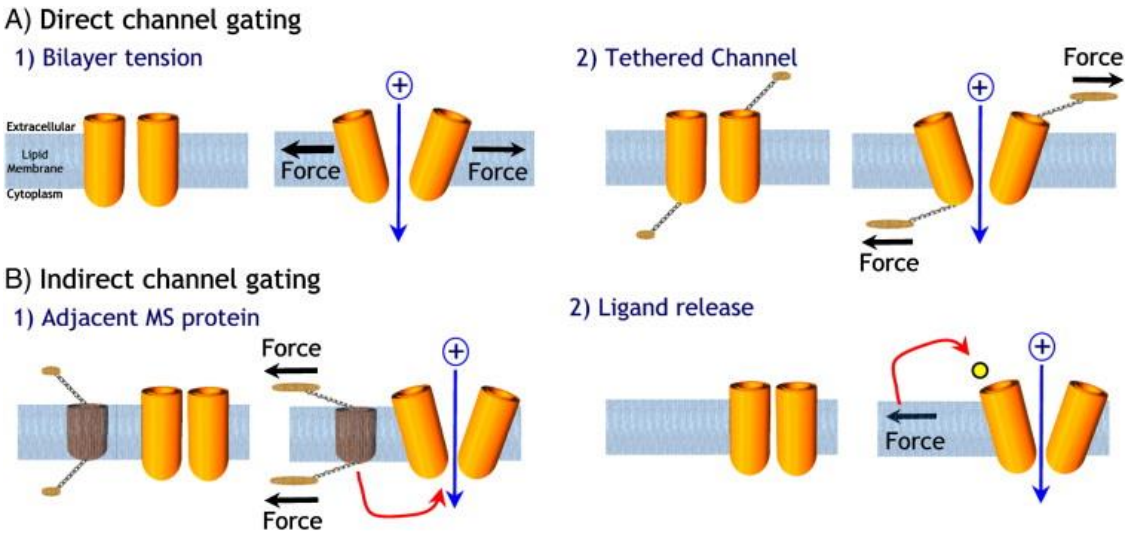

Figure 2-3 Proposed models by which a putative mechanotransduction channel is gated by mechanical stimuli in the myocyte (Brierley 2010).

2.1.4.3 Role of Gap Junctions Between Myocytes

Bladder smooth muscle is an excitable tissue, which means that it responds to electrical, chemical, or physical stimuli by a rapid depolarization of the membrane, creating an action potential that can be transmitted to other cells. Detrusor smooth muscle cells are electrically coupled to one another via low-resistance electrical pathways formed by gap junctions, thereby resulting in a three-dimensional electrical syncytium (Christopher H Fry, Sui, Severs, & Wu, 2004). This implies that the electrical activity recorded from a particular cell in the syncytium need not necessarily have been initiated in that cell but may have originated at any other cell within its electrical "reach". However, even though there is evidence of intracellular current and also support of intercellular electrical communication, the degree of coupling is significantly less than that in well coupled tissues, such as the myocardium (C. Fry, Cooklin, Birns, & Mundy, 1999; Seki, Karim, & Mostwin, 1992). The extent and velocity of the spread of electrical activity in a network of cells depends on the shape of the signal itself and the passive electrical properties of the tissue- in particular, the magnitude of gap junction resistance. A variety of conditions is illustrated in Figure 2-4, where gap junction resistance increases gradually. An increase in gap junction resistance limits the extent of electrical current flow in the network and thus reduces

conduction velocity of a regenerative signal (an action potential) and decreases the extent of spread of other electrical activity. In summary, smooth muscle cells in the detrusor tissue are able to behave as a functional syncytium, however, the mechanisms underlying the generation of this excitation and its propagation in the bladder are still to be described.

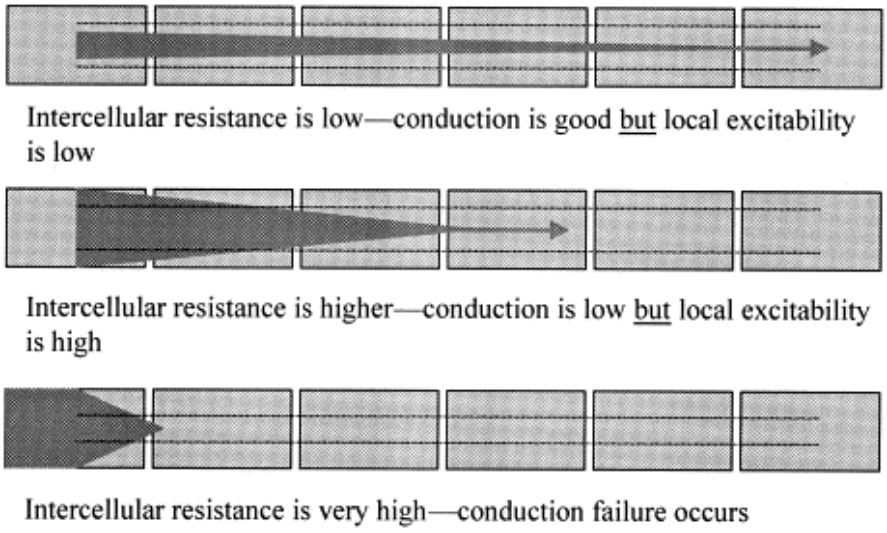

Figure 2-4 Schematic representation of current flow in an electrically couple system of cells.

The diagrams show a linear array of several cells coupled by low, intermediate, and very high resistances in the 3 arrays. The dark arrow represents the flow of current in the intracellular space from a source on the left-hand side. The thickness of the arrow represents the current density in a particular cell, and the 2 parallel lines show the current density required to elicit regenerative electrical activity (Christopher H Fry et al., 2004).

2.1.4.4 Role of Interstitial Cells of Cajal

Interstitial cells of Cajal-like cells (ICCLC's) are found in both the upper and lower urinary tract. They are mesenchymal cells located within the muscle layers of the alimentary tract that mediate communication between the autonomic nervous system and smooth muscle. In the gastrointestinal tract, interstitial cells of cajal act as primary pacemaking cells which propagate depolarising currents into neighbouring smooth muscle cells to initiate spontaneous slow waves and corresponding phasic contraction (Sanders, 1996), and play a functional role in the transmission of signals from enteric neurons to smooth muscle cells (Hirst & Ward, 2003). In the urinary tract, including the renal pelvis, ureter, bladder, and urethra, ICCLC's have been identified by

their morphological characteristics (M. Drake, Mills, & Gillespie, 2001; H. Hashitani, 2006; Lang et al., 2006), but show variability among tissues, which may account for individual characteristics of the organs (H. Hashitani, 2006).

ICCLC's in the bladder are distributed throughout the bladder wall (R. A. Davidson & McCLOSKEY, 2005) and can be divided into at least two subpopulations by their morphology and orientation. Firstly, ICCLC's in the detrusor smooth muscle layer (ICCLC-IM), and ICCLC's in the suburothelial layer or lamina propria (ICCLC-LP) (R. A. Davidson & McCLOSKEY, 2005; McCloskey & Gurney, 2002a; G. Sui, Rothery, Dupont, Fry, & Severs, 2002). These ICCLC's are closely associated with detrusor smooth muscles and make structural interactions with cholinergic nerves in each region (R. A. Davidson & McCLOSKEY, 2005; Johnston, Carson, Lyons, Davidson, & McCloskey, 2008; McCloskey & Gurney, 2002a; G. Sui et al., 2002).

In the detrusor smooth muscle layer, ICCLC's are preferentially located along the boundary of smooth muscle bundles and are also distributed between muscle bundles. They run in parallel with the smooth muscle bundles and are closely associated with intramural nerves (R. A. Davidson & McCLOSKEY, 2005). The role of ICCLCs in the urinary bladder as pacemaker cells has remained controversial due to difficulty in their identification.

Suburothelial ICCLCs have a spindle- and stellate-shaped morphology with several branches emanating from a central soma (R. A. Davidson & McCLOSKEY, 2005; Johnston et al., 2008; McCloskey, 2010a; McCloskey & Gurney, 2002a; G. Sui et al., 2002). They are extensively linked by gap junctions to form a functional syncytium (G. Sui et al., 2002). Further, these ICCs are in close apposition to one another and nerves, and form an interconnected cellular network (Smet, Jonavicius, Marshall, & De Vente, 1996), supposedly involved in signalling pathways of the bladder, and may play a role in moderating the sensory process, leading to the initiation of the micturition reflex (G. Sui et al., 2002) (Fig 2-5).

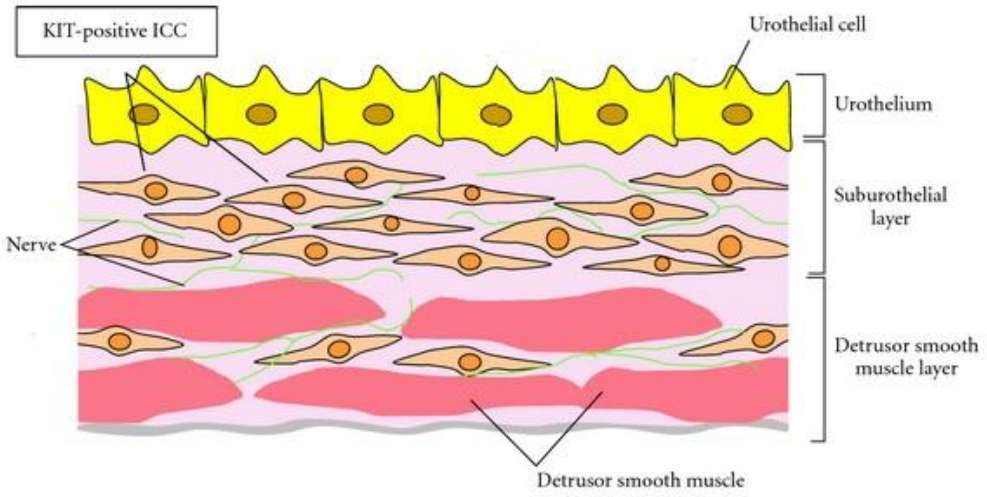

Figure 2-5 Distribution and morphology of Kit positive suburothelial and detrusor ICCs and interaction with the urothelium, nerves, and smooth muscle (adapted from (Kubota et al., 2011)).

Spontaneous electrical activity has been identified, and various transmembrane ion channels have been described particularly in bladder ICCLC's-LP and ICCLC's-IM. Already, differences in the ion channels in the various bladder ICCLC subtypes may be indicative of their distinctive functions. Oscillations in membrane potential indicate physiological activity in the absence of agonists or neurotransmitters. Isolated ICCLC's-LP and ICCLC's-IM loaded with calcium indicators display spontaneous changes in intracellular Ca^{2+} concentration (McCloskey & Gurney, 2002a; G. P. Sui, Wu, & Fry, 2003). Like signal transmission in smooth muscle, Ca^{2+} excitability in these cells show an important signalling mechanism likely to support a number of different cellular processes such as pacemaker activity or the release of signalling molecules (De Jongh et al., 2007; Johnston et al., 2008).

The relationship between ICCLC's and smooth muscle cell Ca^{2+}-signalling remains rather elusive, and it is not clear which ICCLC's act as pacemakers or indeed in that ICCLC's have any meaningful role in spontaneous activity of the bladder.

2.1.4.5 Electrophysiological Control

The detrusor muscle produces spontaneous action potentials (APs) or spikes (H. Hashitani & A. F. Brading, 2003; Hikaru Hashitani & Alison F Brading, 2003b; A. Visser & Van Mastrigt, 1999). A change in membrane potential, brought on by the firing of action potentials or by activation of stretch-dependent ion channels in the plasma membrane (see above), can also trigger contraction. Electrical activity has been observed at the cellular level (Ursillo, 1961), in bladder strips (W. Van Duyl, 1980), and in intact bladders *in vivo* (BLRA Coolsaet, 1984). They occur as single, clusters, or bursts and each spike have a relatively constant duration. The force developed depends on the width of the contracting and relaxing areas and the amplitude of the spontaneous contractions increase with increasing stretch (Bo Coolsaet, 1985). The origin of these spontaneous action potentials is still open to debate, however, the current understanding is that regular/periodic action potential firing is likely to be myogenic in origin, perhaps generated by pace making cells electrically coupled to the smooth muscle cells, whereas asynchronous/stochastic action potential firing may be driven by spatiotemporally random ATP release from autonomic nerve terminals (Appukuttan, Padmakumar, Young, Brain, & Manchanda, 2018). Spontaneous APs are resistant to tetrodotoxin (TTX) suggesting that extrinsic innervation and shifts in intracellular calcium stores do not contribute to their generation.

2.1.5 Neurophysiology of the Bladder

The bladder has two essential functions: store urine that is continually produced from the kidney without its pressure rising above kidney filtration pressure and it must empty quickly when required. However, as previously discussed, the bladder is simply not a static bag but rather a spontaneously active muscular organ. The coordination within the organ is mediated by a complex neural control system and involves the brain, the spinal cord, and the major pelvic and intramural ganglia.

Bladder function is controlled by autonomic and somatic nerve input (Fig 2-6). The autonomic nervous system can also be further divided into the sympathetic and parasympathetic. The sympathetic nervous system

prepares the body for the fight/flight response (e.g., Increasing heart rate, dilating airways) while the parasympathetic nervous system controls normal bodily processes. The somatic nervous system (SNS)

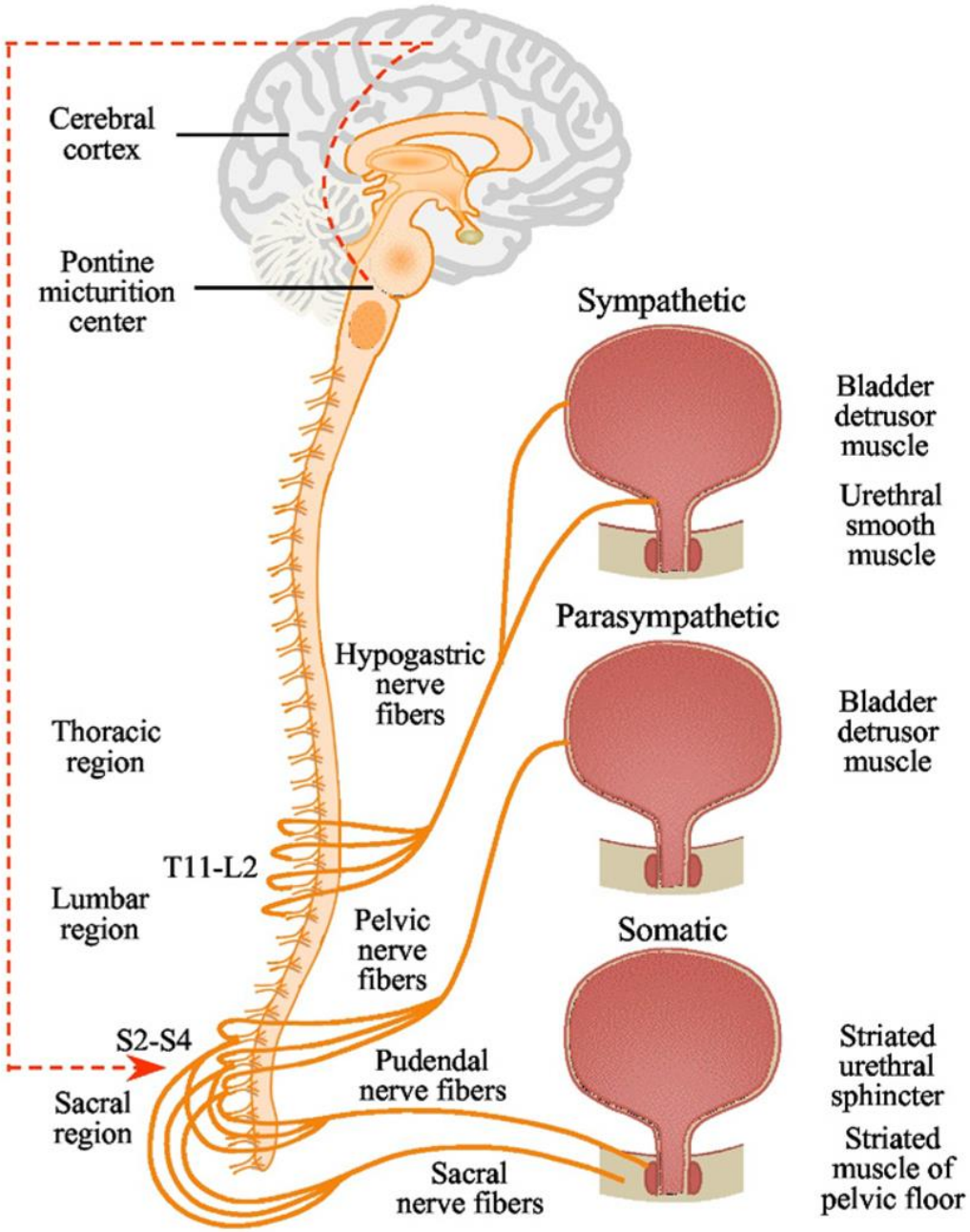

Figure 2-6 Human lower urinary tract innervation.

Coordination between bladder and outlet (bladder neck, urethra, and urethral sphincters) is mediated by sympathetic (hypogastric), parasympathetic (pelvic) and somatic (pudendal) nerves. Primary cell bodies of Aδ and C-fiber afferents of pelvic and pudendal nerves are contained in lower lumbar and sacral DRG, and afferent innervation in hypogastric nerve arises in rostral lumbar DRG (Kanai & Andersson, 2010).

is part of the peripheral nervous system associated with the voluntary control of body. The somatic nervous system consists of afferent nerves or sensory nerves, and efferent nerves or motor nerves.

The parasympathetic and sympathetic effector nerves to the bladder exit the sacral spinal cord in the anterior roots S2–S4 and T10–L2, respectively, and transit in the pelvic and hypogastric nerves to the major pelvic ganglion. The pelvic ganglia are unique in that both preganglionic and postganglionic parasympathetic and sympathetic neurons are localized within the same ganglion capsule. Their postganglionic processes extend into the bladder wall where they connect within intramural ganglia (Miftahof & Nam, 2013). The parasympathetic nerve fibres (i.e., Pelvic nerve) release adenosine 5'-triphosphate (ATP), acetylcholine (Ach) and nitric oxide (NO).

Elements of the sympathetic nervous system (The hypogastric nerve) transit via the T12-L2 region of the spinal cord. This nerve controls the tissue by releasing noradrenaline to act on the detrusor's β-adrenoceptors causing relaxation, or on urethral α-adrenoceptors to cause contraction.

Two chemical messengers (neurotransmitters) are used to communicate within the autonomic nervous system, acetylcholine, and norepinephrine. Nerve fibres that secrete acetylcholine are called cholinergic fibres. Fibres that secrete norepinephrine are called adrenergic fibres. Generally, acetylcholine has parasympathetic (inhibiting) effects and norepinephrine has sympathetic (stimulating) effects.

2.1.6 Neurotransmission

Autonomic input involves adrenergic (the main neurotransmitter is noradrenaline (NA)), cholinergic (the main neurotransmitter is acetylcholine (Ach), and NANC (Non-Adrenergic Non-Cholinergic) nerve fibres. These fibres spread about the entire bladder body and divide and spread throughout the numerous fascicles of the bladder. The distribution of nerve input is such that most of the adrenergic and cholinergic innervation is located at the base of the bladder in the trigone, with less innervation anteriorly and on the dome of the bladder body.

The storage and elimination of urine is dependent upon the coordinated interplay of mechanical reactions of the detrusor and the outflow region-the internal and external sphincters.

As the bladder fills there is no significant increase in intravesical pressure due to the relaxation of smooth muscle. The urothelium/lamina propria is stretched and the cells within this layer change their shape to accommodate an increasing volume. To accomplish this, mechanoreceptors on the urothelium respond to stretch by releasing chemical transmitters, specifically acetylcholine (Ach) (Hanna-Mitchell et al., 2007; Yoshida et al., 2006; Yoshida, Miyamae, Iwashita, Otani, & Inadome, 2004) and adenosine triphosphate (ATP) (Y. Cheng et al., 2011; Ferguson, Kennedy, & Burton, 1997; J. S. Young, Matharu, Carew, & Fry, 2012) are released. These promote the relaxation of the bladder wall. The cells of the urothelium secretes ATP and other macromolecules as wall tension increases, and high ATP concentrations contribute to nociception by binding purinergic receptors. These autocrine signals and their effects on receptors will be discussed below.

2.1.7 Pharmacology of Bladder Storage Function and Micturition

2.1.7.1 Adrenergic Nerves and Receptors- Bladder Storage

Sympathetic innovation to the bladder consists of androgenic nerves that originate from the paravertebral and prevertebral ganglia. Sympathetic and parasympathetic fibres form a plexus, the vesical plexus, which lies adjacent to the posterior and lateral walls of the urinary bladder. Similar ganglia occur through all regions of the bladder wall, both within and on the surface of the detrusor muscle (K. E. Andersson, 2017).

Both α_1 and β_2 subtypes of adrenoceptors are present in the urinary bladder. Their location varies with site, α-adrenoceptors predominantly in the trigone and β-adrenoceptors in the bladder body (Robert M Levin, Ruggieri, & Wein, 1988). It is known that stimulation of the α_1 receptor subtype induces a contraction in the detrusor of many species (K.-E. Andersson & Gratzke, 2007). It is also known that the α_2-adrenoreceptor receptor mediates the inhibition of both acetylcholine and noradrenaline release in the bladder of several

species including rat, rabbit and man (Mattiasson, Andersson, Elbadawi, Morgan, & Sjögren, 1987; Tobin & Sjögren, 1998).

Activation of β-adrenoceptors mediates the relaxation of the urinary bladder smooth muscle (Longhurst & Levendusky, 1999) however the specific β-adrenoceptor subtypes that do this vary between species. In the rabbit bladder, the relaxation seems to be mediated solely by β_2-adrenoceptors, while in the human bladder primarily by the β_3-adrenoreceptors (Igawa et al., 2001). However, the importance of the sympathetic input for human bladder function during the storage phase has not been established (K. E. Andersson, 2017).

In sum, it is generally considered, based on animal studies, that the activity in the adrenergic nerves keeps the bladder relaxed and the urethra contracted during filling (K.-E. Andersson & Arner, 2004; Igawa & Michel, 2013).

2.1.7.2 Cholinergic Nerves and Muscarinic Receptors- Bladder Micturition

Bladder storage function and micturition is a process in which neural circuits in the brain and spinal cord coordinate with lower urinary tract local processes to coordinate the activity of smooth muscle in the bladder and urethra. These circuits act as on-off switches to modulate the bladder between two modes of function: storage and elimination.

A cholinergic neuron is a nerve cell which mainly uses the neurotransmitter acetylcholine (ACh) to send its messages. In the urinary bladder of humans, cholinergic nerves are found around the bundles of smooth muscles cells of the bladder and are distributed in all regions of the bladder, forming a net-like plexa. Similarly, the urethra has a pattern of cholinergic nerve distribution as described for the urinary bladder (Ek, Alm, Andersson, & Persson, 1977).

Detrusor muscle of healthy human bladders are contracted by cholinergic nerves activating muscarinic receptors. Contractile responses can be completely abolished by atropine (Yoshimura & Chancellor, 2002), where this non-specific antagonist completely inhibits acetylcholine (Ach) at postganglionic muscarinic sites (Bhattacharjee, Pomponio, Evans, Pervitsky, & Gordon, 2013). Five subtypes of muscarinic receptors can be

identified by their molecular (m1–5) and pharmacological (M1–5) characteristics. The detrusor expresses the m2 and m3 subtypes, the m2 receptor being expressed three- to nine-times in excess to m3 receptors (P. Wang, Luthin, & Ruggieri, 1995). However, the functional affinity of the receptor is greatest for m3 (Fig 2-7.) compared to cells of m2 receptors (Chess-Williams, 2002). Currently it is thought that m3 receptors are mainly responsible for the normal rhythmic electromechanical activity of the bladder (C. H. Fry, Meng, & Young, 2010) and m2 receptors are thought to interfere in 're-contracting' bladder smooth muscle cells following their relaxation (Uchiyama & Chess-Williams, 2004; X. Zhang & DiSanto, 2011)

Their regulatory effects are achieved through direct stimulation of smooth muscle and ICCLC (K.-E. Andersson, 2002; K.-E. Andersson, Holmquist, Fovaeus, Hedlund, & Sundler, 1991; Hariss, Marsh, Birmingham, & Hill, 1995). When m3 receptors are activated, they create a cascade of cytosolic processes where intracellular calcium stores release Ca^{2+} for contraction. M2 receptors increase the Ca^{2+}-sensitivity of the contractile proteins. Further, muscarinic receptors can be influenced by inhibitors of Rho-kinase (RhoA). RhoA activation can stimulate phosphorylation of the regulatory light chain of myosin have been widely recognized to play an important role in the regulation of contractility and shortening in smooth muscle. Jezior et al., working with rabbit detrusor, found that bethanechol-induced contractions were practically abolished by inhibitors of Rho-kinase (Y27632, HA 1077) in combination with a nonselective cation channel inhibitor (LOE-908) (Jezior et al., 2001). They suggested that muscarinic receptor activation of detrusor muscle includes both nonselective cation channels and activation of Rho-kinase. Evidence suggests Rho-kinase has a role in the regulation of detrusor contraction and tone (Wibberley, Chen, Hu, Hieble, & Westfall, 2003).

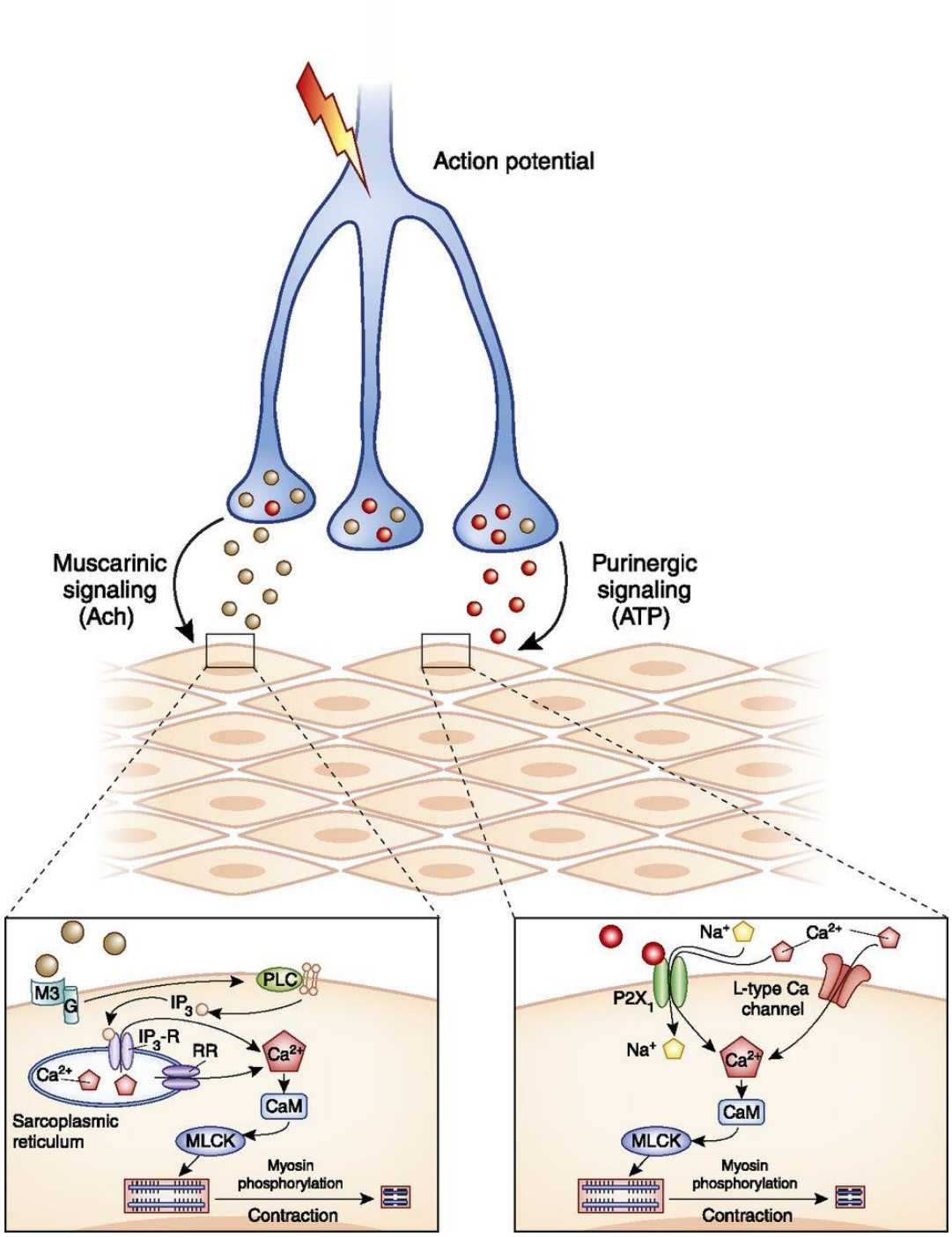

Figure 2-7 Molecular mechanisms leading to bladder smooth muscle contraction.

Parasympathetic neurons release primary neurotransmitters acetylcholine and ATP, which bind to the M_3 muscarinic receptor and $P2X_1$, respectively. This leads to several downstream effects, including membrane depolarization and increased cytosolic Ca^{2+} and ultimately myosin phosphorylation and myocyte contraction. CaM, calmodulin; G, G protein; IP_3, inositol trisphosphate; IP_3-R, inositol trisphosphate receptor; MLCK, myosin light chain kinase; PLC, phospholipase C; RR, ryanodine receptor (Hill, 2015).

2.1.7.3 Purinergic Nerves and Receptors- Nociception

The presence of a non-cholinergic, non-adrenergic component in the vertebrate autonomic nervous system is now well established (G Burnstock, 1980). In the bladder of most mammalian species, purinergic mechanosensory transduction occurs where ATP is released from urothelial cells during distension of bladder and ureter. Purinergic receptors on suburothelial sensory nerves are thought to be of two types. Firstly, a high threshold fibre that serves a nociceptive function, and a low threshold fibre which has a function in the voiding reflex. Therefore, there is a hypothesis that distension of the bladder leads to a release of ATP which then acts on receptors to modulate afferent firing that can lead to bladder voiding reflexes. Therefore, purinergic nerves react to hydrostatic pressure changes via epithelial cells and are speculated to be the basis of a sensory mechanism (Geoffrey Burnstock, 2014). Therefore, ATP appears as the most important among the non-adrenergic non-cholinergic (NANC) transmitters (Benham & Tsien, 1987; G Burnstock, 1980).

2.1.7.4 Interstitial Cells of Cajal Like Cells- Control of Bladder Modalities

ICCLC's act as mechanoreceptors and have a possible roll in accommodation i.e., activation of ICCs may brake ion flow between adjacent myocytes and thus influence their excitability. Moreover, imatinib mesylate (Glivec®), a c-kit tyrosine kinase inhibitor has been shown to influence spontaneous excitation and ion channel activity in detrusor smooth muscle (Kubota, Biers, Kohri, & Brading, 2006b). It has been suggested that c-kit-positive cells may play a role in modulating spontaneous electrical and mechanical activities in the bladder, both normally and after outflow obstruction (Kubota et al., 2006b). ICCLC's may be involved in signal transmission within the detrusor, coordinating the different contractile units (M. Drake et al., 2001). Evidence for such modulation by ICCLC's is growing (Johnston et al., 2008; McCLOSKEY, 2005, 2006; McCloskey & Gurney, 2002a).

Studies have also shown that ICCLC's can communicate between the complex tissue sheets within the bladder wall confirming they are able to signal within the complexity that is the bladder wall structure (Hikaru Hashitani, Yanai, & Suzuki, 2004b; Johnston et al., 2008). An application of carbachol to whole-sheet "*in situ*" preparations

increases the frequency of detrusor ICCLC's Ca^{2+}-transients suggesting that detrusor ICCLC's activity can be modulated by parasympathetic nerves (Johnston et al., 2008). However, the application of carbachol to enzymatically dispersed detrusor ICCLC's induced intracellular Ca^{2+}-transient which were not associated with contraction, in contrast to detrusor smooth muscle cells which are vigorously contractile under the same experimental conditions (Johnston et al., 2008). While carbachol generates an increase in Ca^{2+} in detrusor ICCLC's, there is no such response in ICCLC's-LP (C Wu, Sui, & Fry, 2004) and this difference may represent an important division of labour between two ICC subtypes in the bladder. This suggests that nerve released acetylcholine can activate detrusor myocytes directly, but also indirectly via activation of ICCLC's. How ICCLC's connect with myocytes remains to be established. In detrusor myocytes, the muscarinic receptor subtype involved in activation seems to be the M3 receptor (Johnston et al., 2008; McCloskey & Gurney, 2002a).

ICCLC's would be obvious candidates for such a role and there is ample evidence of their presence in the sub-urothelial region, in the lamina propria and on the peripheries of the muscle bundles of the detrusor(R. A. Davidson & McCLOSKEY, 2005; G. Sui et al., 2002; Wiseman, Fowler, & Landon, 2003). Spontaneous excitation in the bladder might be initiated by detrusor smooth muscle cells themselves with the main role of ICCLC's being to modulate the signal transmission. Clearly, ICCLC's are important in bladder physiology, but their exact influence and role is still yet to be defined.

2.2 The Uterus

2.2.1 Anatomy of the Uterus

In mammals, uteri vary in form: duplex, bipartite, bicornuate and simplex forms being seen (Lewitus & Soligo, 2011). Only duplex and simplex (Fig 2-8.) will be described and compared in this thesis.

Duplex uteri comprise two wholly separate uteri, each with a single fallopian tube. These are found in marsupials (e.g., kangaroos, Tasmanian devils, opossums, etc.), rodents (such as mice, rats, and guinea pigs), and lagomorphs (rabbits and hares).

Simplex uteri, in which two uterine elements are fused to form a single organ, are found in higher primates (including humans and chimpanzees). In some of these species (e.g., humans) the uterus is bicornuate where the two elements of the uterus are incompletely fused.

The non-pregnant human uterus is a small, pear-shaped organ located in the pelvis between the urinary bladder anteriorly and the rectum posteriorly. There is a gradual and steady increase in uterine size during pregnancy from 8 to 35 cm in length (Zara & Dupuis, 2017). This increase accompanies the increasing size of the developing foetus and the accommodation of amniotic fluid, the size of the cavity increasing from ≈34 mls (Sheth, Hajari, Lulla, & Kshirsagar, 2017) in the non-gravid uterus to ≈4,500 mls in the gravid uterus at term (Geirsson, Ogston, Patel, & Christie, 1985).

The relative increase in pregnant volume is greater in smaller mammals. Hence, the two horns of the uterus of the rabbit each increase to ≈390 ml at term (Arpad I. Csapo & Lloyd-Jacob, 1962), many times larger than its original volume.

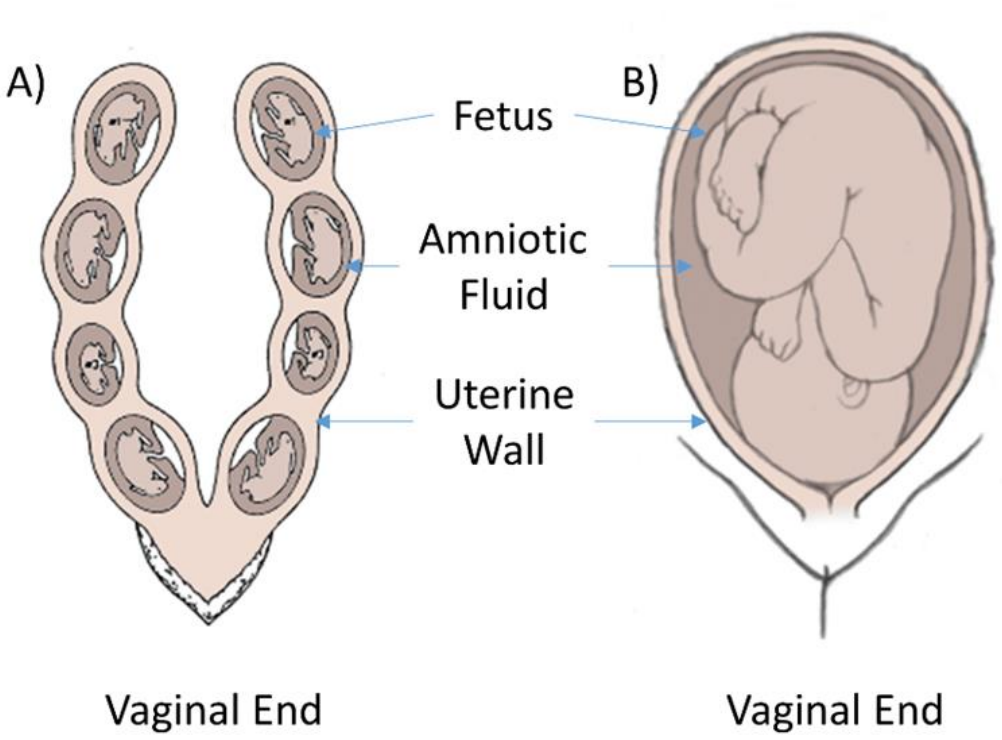

Figure 2-8 Schematic of the gravid rabbit duplex uteri A) and B) gravid human uterus.

Not to scale. (Adapted from (Buchmiller-Crair et al., 2001) and (Yeomans, Hoffman, Gilstrap, & Cunningham, 2017).

The uterus comprises three regions:

Fundus – the portion of the uterus lying cranial to the entry point of the fallopian tubes.

Body – the usual site of implantation of the blastocyst and placental development

Cervix – the distal part of uterus linking it with the vagina that has the capacity to greatly change in form during parturition.

The non-pregnant myometrium exhibits ongoing spontaneous and rhythmic contractions and relaxations (Heinricius, 1889; J. V. Kelly, 1962). These contractions are thought to facilitate the expulsion of menstrual debris at the time of menses, in the migration of spermatozoa, from the cervix to the distal ends of the fallopian

tubes (Birnholz, 1984; de Vries, Lyons, Ballard, Levi, & Lindsay, 1990; Heinricius, 1889; G Kunz et al., 1997; G Kunz, Herbertz, Noe, & Leyendecker, 1998; Toner & Adler, 1985; Wildt, Kissler, Licht, & Becker, 1998), and the return of oocyte/embryos to the uterine cavity (Bulletti et al., 2000).

The uterus is thick walled and muscular and grows to accommodate the products of conceptus. Histologically the uterus consists of three layers (Fig 2-9); a thin outer perimetrium, a thicker medial myometrium that consists principally of smooth muscle, and an inner epithelium termed the endometrium. The endometrium is the inner most layer and can be further subdivided into two regions; the deep stratum basalis which changes little throughout the menstrual cycle and is not shed at menstruation; and the superficial stratum functionalis which proliferates in response to oestrogens and becomes secretory in response to progesterone. The latter is shed during menstruation and regenerates from cells in the stratum basalis layer. The endometrial layer also contains extensive uterine glands that synthesize and secrete substances into the uterine lumen, including a complex array of enzymes, growth factors, cytokines, lymphokines, hormones, transport proteins and other substances, collectively termed histotroph (Bazer, 1975; Kane, Morgan, & Coonan, 1997).

The outer perimetrium consists of serous layers. It covers the outer surface of the uterus. Surrounding the uterus, this layer or band of fibrous and fatty connective connects the uterus to other tissues of the pelvis.

The middle layer, the myometrium, consists mainly of uterine smooth muscle cells (also called uterine myocytes), and a supporting stromal and vascular tissue. Its main function is to develop and control tone for accommodation and to expel the foetus at term.

The myometrium consists of bundles of interconnected myocytes that vary in orientation. Broadly speaking, they can be considered as layers in which particular orientations predominate. The outer longitudinal muscle layer consists of a network of bundles of smooth muscle cells that are generally orientated in the long axis of the uterus (AI Csapo, 1962; R. Garfield & Somlyo, 1985). The bundles connect to form a network that covers the entire the surface of the uterus (AI Csapo, 1962). Muscle cells of the inner circular layer are arranged mainly concentrically, at roughly right angles to the longitudinal axis of the uterus. The combined contraction of the

longitudinal and circular muscle constricts lumen volume, while contraction of the longitudinal muscle alone shortens the uterus (AI Csapo, 1962). The extracellular space between the muscle cells in both layers is occupied by collagen fibres and other types of cells including fibroblasts, blood and lymphatic vessels, and nerves (Chard, Grudzinskas, & Grudzinskas, 1994).

Enlargement of the uterus during pregnancy is thought to be primary accounted for by a combined increase in number of cells (hyperplasia) and size of muscle cells (hypertrophy) during gestation (Carsten, 1968). It is not known whether the number of interstitial cells similarly increase.

Blood is supplied by and drained via the uterine arteries and veins, respectively, with ancillary supply from the ovarian arteries and veins (Hurd & Falcone, 2007). The vasculature penetrates into the myometrium and the ascending branch travels in parallel along the side of the uterus and fallopian tubes, following a ‘U’ path from where the arterioles assume a circumferential course and spiral into the myometrium (Eroschenko, 2008). Hence, they have been termed helicine arterioles. However, they should not be confused with the spiral arteries, which are temporary, and penetrate the endometrium in the inner uterus. The radial arteries branch off from the arcuate artery through the myometrium (McKinley, O'loughlin, Pennefather-O'Brien, & Harris, 2006).

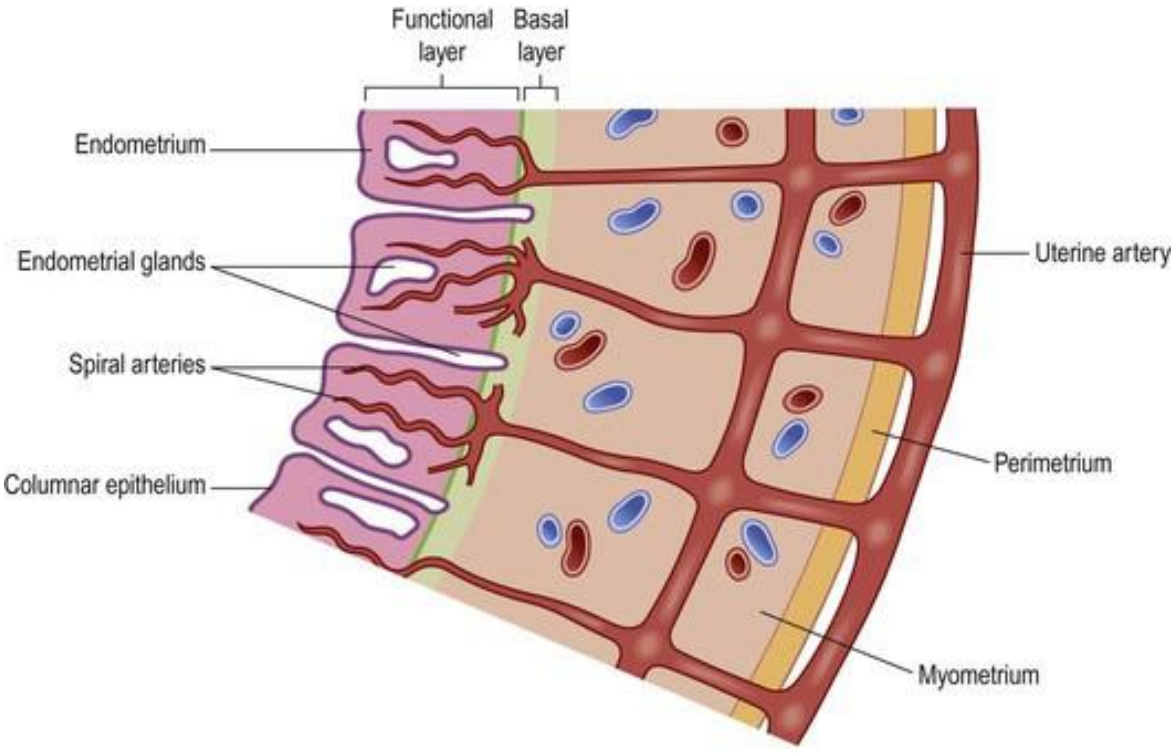

Figure 2-9 Functional structure of the uterine wall (Basicmedicalkey, 2022)

2.2.2 The Dual Purpose of the Uterus

The uterus plays a key role in reproductive health and function. It is where a fertilized egg implants during pregnancy and where the foetus gestates until birth. The uterus grows and stretches to accommodate the growth of the foetus, and similarly to the urinary bladder, ultimately switches from an accommodative organ to one of expulsion. The uterus muscle is maintained in a relatively quiescent state for the majority of normal pregnancy and then there is a series of events that that lead to powerful, rhythmic contractile activity at foetal maturity that leads to parturition. Initially, the switch from quiescence to labour was envisaged either as the loss of relaxant factors or the increased production of contractile factors. This simplistic view has been modified over recent years as it has become increasingly evident that foetal accommodation, and the initiation of labour, is not due to a single trigger but is the culmination of a cascade of complex cellular events that occur over days

or even weeks. It is now believed that a combination of cellular physiology, hormonal, chemical and mechanical signals interact to gradually down-regulate quiescent mechanisms and up-regulate contractile pathways as pregnancy approaches term (Tribe, 2001). The cellular components and modalities of control will be discussed in the preceding sections, examining their effect and influence of gestation and parturition.

2.2.3 The Myometrium

2.2.3.1 The Morphology of the Myometrial Smooth Muscle Cell

Uterine smooth muscle cells are spindle-shaped, occasionally branching cells ranging in size from 2 to 10 pm in diameter and 200-600 pm in length, depending on the species and hormonal state of the individual. Their hypertrophy during the later stages of gestation is thought to be induced by steroid secretions (to be discussed latter) along with the mechanical effects of distention caused by foetal growth (Bergman, 1968; Bo, Odor, & Rothrock, 1968; Ross & Klebanoff, 1967).

The internal morphology of myometrial cells is similar to that of other smooth muscle cells. However, the sarcoplasmic reticulum (SR) of myometrial smooth muscle of pregnant or oestrogen-treated animals is the more extensive (R. Garfield & Somlyo, 1985). In the latter case, sarcoplasmic tubules frequently establish structurally close couplings with the plasma membrane and also contacts with the caveolae and gap junctions of the plasma membrane(R. Garfield & Somlyo, 1985). (Bond, Kitazawa, Somlyo, & Somlyo, 1984; A. P. Somlyo, 1984)

The plasma membrane of myometrial smooth muscle cells is similar to that of other smooth muscle cells. Caveolae are abundant and create regular, longitudinally orientated arrays. As in the smooth muscle of the bladder, areas of the plasma membrane located between the longitudinal rows of caveolae are occupied by sites for the attachment of the cytoskeletal and contractile apparatus on the inner plasma membrane surface and cell-to-cell adhesion on the outer surface. Again, there are dense bands into which thin filaments of the contractile apparatus and intermediate filaments of the cytoskeleton are inserted. Further, myometrial cells

like other smooth muscle cells, form extensive cell to cell junctions with neighbouring myocytes and other cells termed gap junctions (Waelchli, 2007).

2.2.4 Control of Contractile Behaviour

The non-pregnant myometrium exhibits ongoing spontaneous and rhythmic contractions and relaxations (Heinricius, 1889; J. V. Kelly, 1962). These contractions are thought to facilitate the expulsion of menstrual debris at the time of menses, in the migration of spermatozoa, from the cervix to the distal ends of the fallopian tubes (Birnholz, 1984; de Vries et al., 1990; Heinricius, 1889; G Kunz et al., 1997; G Kunz et al., 1998; Toner & Adler, 1985; Wildt et al., 1998), and the return of oocyte/embryos to the uterine cavity (Bulletti et al., 2000). What is not well understood is the contractile change seen in the uterus that transforms the uterus from an organ of spontaneous contraction and tone, to one of coordinated function to expel the foetus. This developmental change occurs in a relatively short span of time (Hutchings, Williams, Cretoiu, & Ciontea, 2009).

It is important to note that further descriptions of the myometrium will be of the parturient organ and of the process that activates labour. Parturition is a complex event that includes such different steps as cervical ripening and dilation, augmentation of the action of uterine musculature and the correct presentation and posture of the foetus(es). The term labour may be regarded physiologically as a release from the inhibitory effects of pregnancy on the myometrium, rather than as an active process mediated by uterine stimulants. This is accompanied by an increase in myometrial activity or, more precisely, a change in the myometrial contractility pattern from “contractures” (long lasting, low frequency activity) to “contractions” (high intensity, high frequency activity (Thorburn, Challis, & Robinson, 1977). Viewed functionally these changes may be viewed as a change from tonal adjustment to passively accommodate the growing foetus, to active expulsion of the foetus at term.

2.2.4.1 Myocyte Control

Like the detrusor muscle in the bladder, uterus belongs to that group of muscles that are spontaneously active. Hence isolated myocytes of, gravid and non-gravid, uterus develop regular spontaneous contractions (SUSAN Wray, 1993).

The frequency, magnitude, and strength of myometrial contractions are dependent on the frequency and duration of action potentials, and the total number of cells that are simultaneously active (J. M. Marshall, 1962b). The myometrial resting potentials has been recorded to be between -35 and -80 mV (Aguilar & Mitchell, 2010). As with the resting membrane potential of other cell types, it is maintained by a Na+/K+ pump. This resting potential undergoes rhythmic oscillations, which may be related to the development of slow waves and reflect intrinsic activity of slow wave action potentials seen in smooth muscles of the gut (Aguilar & Mitchell, 2010).

2.2.4.2 Role of Gap Junctions

Myometrial gap junctions, which appear and increase in number at term, are believed to allow the flow of ions between myocytes thereby extending their area of contractions (Loch-Caruso, Criswell, Grindatti, & Brant, 2003).

The uterine myocyte has one of the most extensive sarcoplasmic reticulum of any smooth muscle (R. Garfield & Somlyo, 1985) which is concerned with Ca^{2+} regulation. Myometrial Ca^{2+} uptake is quantitively increased with oestrogen and progesterone suggesting that capacity of the internal store increases with gestation.

The second method is surface membrane Ca^{2+} transport. Under normal physiological conditions extracellular Ca^{2+} can enter the myometrial sarcolemma in a variety of ways, 1) there is a low passive resting leak of Ca^{2+} into the cell, 2) voltage dependent Ca^{2+} channels, and 3) receptor operated Ca^{2+} channels. These last two are important to the maintenance of contraction in the uterus (Sheldon, Shmygol, van den Berg, & Blanks, 2015).

Ca^{2+} can be removed from the cytoplasm by a Ca-ATPase pump and also by the SR Ca-ATPase pump, although the former may be quantitatively more important (SUSAN Wray, 1993). The myometrium also has a Na^{+}-Ca^{2+} exchanger, which in its normal mode of action will remove Ca^{2+} from the cell (Grover, Kwan, & Daniel, 1981). However, the contribution of this exchanger is probably small under most physiological conditions. Relaxation or the myocyte repolarisation results in a lowering of Ca^{2+} by extrusion across the plasma membrane and reuptake into internal stores.

It is possible that these diverse mechanisms can act together to modulate in concert to provide the smooth muscle cell with the ability to modulate the Ca^{2+}-force relationship in response to changing patterns of stimulation. This system would be advantageous to the uterus, whose contractile performance can be influenced by many factors, such as hormones, stretch, and metabolite concentrations, as will be discussed in the subsequent section on neuronal modulation and hormonal modulations. However, more importantly, gestation requires the inhibition of ordered contraction until the foetus is of enough maturity to survive outside the womb.

2.2.4.3 Role of Interstitial Cells of Cajal Like Cells

ICCLC's have been suggested to be involved in the regulation of spontaneous rhythmic contraction in the bladder (C. Collins et al., 2009). ICC's or 'myometrial Cajal-like interstitial cells' (m-ICLC) have also been observed in the myometrium (Duquette et al., 2005; A Shafik, El-Sibai, & Shafik, 2004; Yoshino, Wang, & Kao, 1997) and are intimately associated with oestrogen and progesterone receptors (Cretoiu, Ciontea, Popescu, Ceafalan, & Ardeleanu, 2006) (Fig 2-10). It is hypothesised that myometrial ICCs could act as hormonal "sensors", possibly participating in the regulation of human myometrial contractions via gap junctions and/or by hormone signalling (Cretoiu et al., 2006).

Studies in the rat and human have shown that m-ICC do not act as excitatory pacemakers or generators of slow waves within the myometrium (Duquette et al., 2005). However, m-ICC are closely associated with myometrial smooth muscle cells, and this close contact between the m-ICC's and myocytes suggests some degree of

communication or coupling between the two cell types. It has been hypothesized that m-ICC's have a modulating influence on smooth muscle like seen in the gut, where ICCs have also been associated with relaxation of gut smooth muscle by influencing neurotransmission (Burns, Lomax, Torihashi, Sanders, & Ward, 1996; Ward, Morris, Reese, Wang, & Sanders, 1998). Such a mechanism could provide the basis the generation of uterine tone, whilst the influence of neural (Wood, 1999) and hormonal (A.-R. Fuchs, 1978) signals adjust their magnitude and coordination during parturition (Olson, Mijovic, & Sadowsky, 1995).

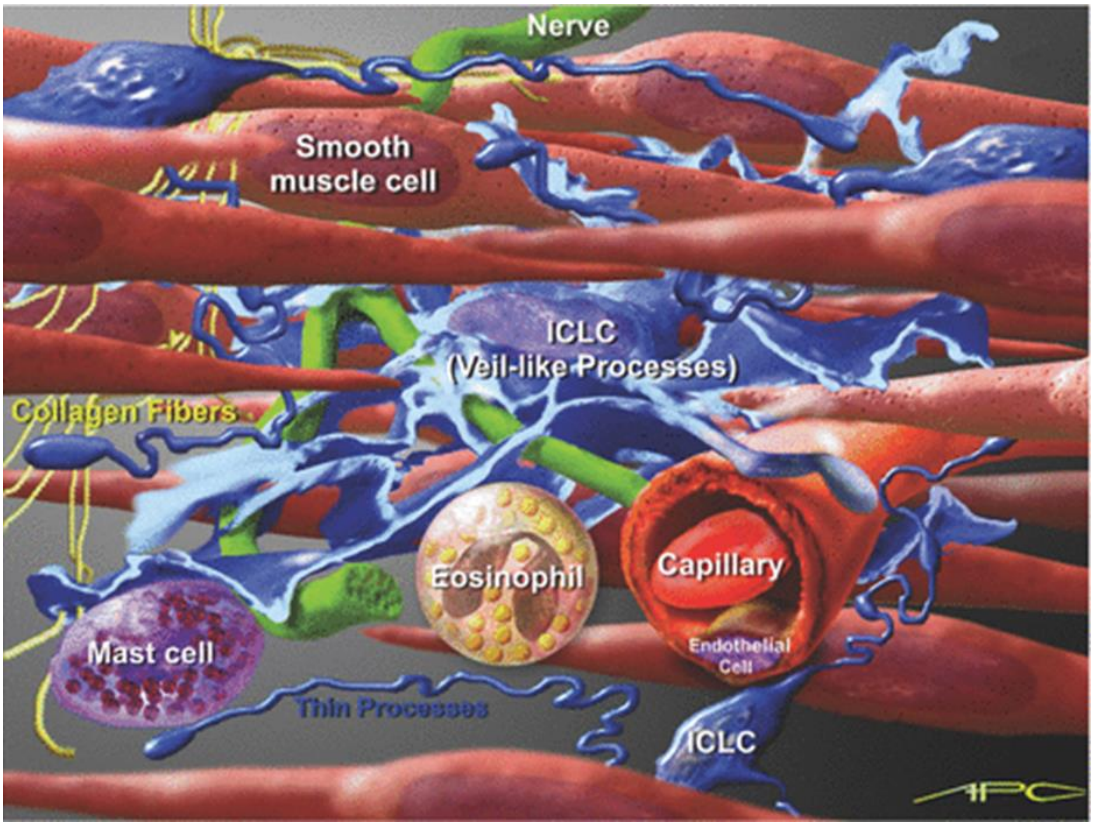

Figure 2-10 Artistic view of possible interconnectivity of m-ICLC in the uterine wall.

Close proximity of m-ICLC processes with smooth muscle cells, unmyelinated nerves, capillaries, collagen fibres and immunoreactive cells. Scale bar approximately 7 µm (erythrocyte's diameter). (Hutchings et al., 2009).

2.2.4.4 Electrophysiological Control

Spike action potentials of have been recorded in the isolated longitudinal muscle of sheep myometrium (Goto & Woodbury, 1958), and have been shown (*ex vivo*) to spontaneously fire at a steady rate of about 4 cycles per minute for several hours (H. C. Parkington, 1985). *In vivo* activity recorded prior in harvesting, revealed that spontaneous contractions occurred only 2–3 times per hour. Interestingly, a similar phenomenon occurs in human myometrium smooth muscle (H. C. Parkington, Tonta, Brennecke, & Coleman, 1999). Taken together, these observations suggest the existence of an endogenous inhibitor *in vivo* which would maintain relative quiescence by encouraging large negative membrane potential in the smooth muscle cells.

Action potentials in myometrium smooth muscles are complex in form, with simple spikes followed by a sustained plateau of depolarization, with the duration of the plateau dictating the duration of contraction. This form of action potential is most conspicuous in the inner, circular layer of the myometrium (Kawarabayashi & Marshall, 1981). Uterine stretch, and the levels of ovarian hormones can change the shape of an action potential, through their effects on the resting membrane potential (Bengtsson, Chow, & Marshall, 1984; Kawarabayashi & Marshall, 1981; Osa, Ogasawara, & Kato, 1983). A single spike can initiate a contraction, but coordinated spikes are needed for forceful and sustained contractions.

2.2.5 Neurophysiology of the Myometrium

Although there is enough information about both morphological and pharmacological characteristics of uterine autonomic nervous supply, the precise importance of the neurological component on uterine modulation, remains to be determined.

Uterine innervation has two components:

- One afferent which is responsible for transmitting information to the central nervous system (this component is not addressed for this thesis) *and*
- Efferent, autonomic type

In the myometrium (as in other smooth muscle types) there is no direct connection between axon endings and myocytes but rather neurotransmitters being released by exocytosis from efferent nerve endings in the perifascicular space to interact with receptors, situated on the smooth muscle cell membrane (Tica et al., 2011). Further, as limited branches of the axon end in the matrix that surrounds each muscle bundle, only smooth fibres on the outside of the bundle may be directly stimulated, the internal muscle bundles requiring a longer diffusion distance. However, these myocyte bundles further inside (which has no innervation) may be stimulated indirectly by action potentials from the outer fibres, especially via gap junctions.

Uterine innervation is strongly dependent, both morphologically and functionally, on hormonal influences. In humans, maternal oestrogen plasma concentration levels increase progressively during gestation, peaking at term (Olson et al., 1995). Contractility of the myometrium is dependent on oestrogen, which supports the synthesis of intracellular contractile proteins and sources of energy (ATP) (Corner & Csapo, 1953). Oestrogen also inhibits the development of uterine innovation (Tica et al., 2011). The mammalian uterus undergoes large sympathetic axon depletion in late pregnancy, possibly representing an adaptation to promote smooth muscle quiescence and sustained blood flow (Brauer & Smith, 2015). and also contributing to a decrease in myometrium activity until term, despite the very marked increase in its contractile capacity.

The uterus receives both sympathetic and parasympathetic innovation. Efferent sympathetic nerve fibres have their origins in the lumbar spine and axonal ending terminate in the musculature of the uterus, particularly in the cervical area. The terminal vesicles secrete noradrenaline (responsible for adrenergic affects, dopamine β-hydroxylase (the enzyme that converts dopamine to noradrenaline), adenosine triphosphate (ATP), chromogranin and other proteins (Tica et al., 2011)), which, beside the two main neurotransmitters, can modulate myometrial activity.

All four main types of adrenergic receptors (i.e., α1, α2, and β1 and β2) appear to be present in the uterine myocyte smooth muscle cells (Bottari, Vokaer, Kaivez, Lescrainier, & Vauquelin, 1985). In general, α-activation generates contraction whilst β-activation generates relaxation (Bulbring, 1987). Receptor type varies with

location. Type α1 adrenergic receptors predominate in uterine myocyte cells in circular bundles, , whilst, β2 adrenergic receptors predominate in myocytes of the uterine body (Adrian, Dun, Tica, & Cojocaru).

In general, high progesterone levels increase the relative proportions of β-receptors, in line with this agent's role in decreasing uterine contractile activity. Progesterone appears to induce a predominance of high-affinity state α-adrenoceptors. Hence at term there is a desensitization leading to a loss of myometrial responsiveness to β-agonists.

Efferent postganglionic parasympathetic fibres, that originate in the inferior hypogastric ganglion, are distributed almost exclusively to the cervix. Terminal vesicles contain acetylcholine, ATP, proteoglycans, and other proteins in their cholinergic endings. In myometrial smooth muscle, muscarinic receptors can be operationally and genomically classed into five different subtypes, M1, M2, M3, M4 and M5. Mixed populations of muscarinic receptors are present in many smooth muscle tissues, with both M2 and M3 receptors involved in contraction. Nonetheless, their precise function remains unknown (Eglen et al., 1997). Moreover, the nature of the muscarinic receptor subtype that mediates myometrial contraction has yet to be definitively classified. The rabbit uterus has not been extensively studied but M2, M3 and M4 receptors have been identified (Crankshaw, 1984; Dörje et al., 2012).

In vitro, acetylcholine induces an increase in frequency and intensity of myometrial contraction, without a significant change in tone (phasic-type effect) (Tica et al., 2011). Further, although M3 receptors are present on the membranes of all myometrial cells, cholinergic endings are found only in significant numbers in the cervical area and the uterus isthmus and in small numbers in the rest of the uterus (Tica et al., 2011). (Tica et al., 2011)

Although the adrenergic nerves in the uterine body degenerate by the end of pregnancy, those in the cervix do not (Elmer, Alm, & Thorbert, 1980). This could mean a withdrawal of neural inhibitory influences in the body allows spontaneous myogenic contractions to intensify in this region, while cervical relaxation is assured by tonic adrenergic inhibitory tone (J. Marshall, 1981). However, these theories have not been tested.

2.2.6 Hormonal Modulation of the Uterine Quiescence and Contractility

Changes in the hormonal milieu have an important effect on the force of uterine contractions. Oestrogens and progesterone have long been known to influence contractility (Bozler, 1941; A.-R. Fuchs, 1978). Effects of these hormones vary with gestation and thus their actions must be considered in relation to the period of gestation.

The hormonal regulation of uterine activity during pregnancy can be divided into four distinct physiological phases (Huber et al., 2005; Jenkin & Young, 2004);

Phase 1: Inhibitors active- During pre-parturient pregnancy, the uterus is maintained in a state of functional quiescence through the action of progesterone and other agents. Hence, administration of a progesterone receptor antagonist (Peyron et al., 1993; Spitz & Bardin, 1993) or removal of the corpus luteum in the ovary (Arpad I Csapo, Pulkkinen, & Wiest, 1973) readily induces abortion in early pregnancy (Before 7 weeks of gestation). Again, administration of exogenous progesterone after early lutectomy prevents abortion, indicating that ovarian progesterone is essential for the maintenance of early pregnancy. Placental production of progesterone increases between five and seven weeks, the placenta being the predominant source of progesterone thereafter (Norwitz, Lockwood, & Barss). Circulating levels of progesterone in the blood do not change significantly during pregnancy or prior to the onset of labour (A. R. Fuchs & Fuschs, 1984; Zeeman, Khan-Dawood, & Dawood, 1997).

Phase 2: Myometrial activation- As term approaches the uterus becomes increasingly sensitive to uterotrophins such as oestrogen. This phase is characterised by an increase in the expression of many contraction-associated proteins and myometrial receptors for prostaglandin and oxytocin. Prostaglandins have been implicated in the three events most related to the onset of labour (Garrioch, 1978; Karim & Hillier, 1979) i.e., the onset of synchronous uterine contractions, cervical ripening, and the increase in myometrial sensitivity to oxytocin from an increase the formation of myometrial gap junctions and oxytocin receptors.

Phase 3: Stimulatory phase- The "primed" uterus can be stimulated by uterotonic agonists such as oxytocin. Oxytocin is produced in the hypothalamus, and released from the pituitary in a pulsatile fashion (Norwitz et al.). It is also produced by the placenta.

Myometrial oxytocin receptor concentrations increase approximately 100-200-fold during pregnancy, reaching a maximum during early labour (A.-R. Fuchs, Fuchs, Husslein, Soloff, & Fernstrom, 1982; A. R. Fuchs & Fuschs, 1984; Nathanielsz et al., 1997; Zeeman et al., 1997). This is thought to account for the increased sensitivity of the myometrium to circulating levels of oxytocin during the second half of pregnancy (Norwitz et al.) Studies have shown that foetus also secretes oxytocin into the maternal circulation (A. R. Fuchs & Fuschs, 1984). Furthermore, the calculated oxytocin secretion rates from the fetus suggest an increase from a baseline of 1 mU/min prior to labour to approximately 3 mU/min after spontaneous labour (Dawood, Wang, Gupta, & Fuchs, 1978). The latter concentration is similar to the dose of oxytocin normally administered to women to induce labour at term 2-8 mU/min (Norwitz et al.).

Phase 4: Involution- Involution of the uterus after the delivery occurs during phase 3 and is mediated primarily by oxytocin.

Progesterone and oestrogen, as well as relaxin and prostaglandin also affect the extracellular matrix composition and mechanical strength of the cervix (Ekman-Ordeberg, Stjernholm, Wang, Stygar, & Sahlin, 2003; Ghulé, Gray, Galimberti, & Anumba, 2012; H. Ji, Long, Briody, & Chien, 2011; Simon & Einspanier, 2009). The consequence of their action results in four stages: softening (first trimester), ripening (second trimester), dilatation (third trimester) and reconstitution of the non-pregnant cervix post-partum (Read, Word, Ruscheinsky, Timmons, & Mahendroo, 2007). Each stage has a characteristic collagen and proteoglycan composition. Ultimately, the whole process can be characterized by a 60% decrease in collagen and proteoglycan levels that occurs in parallel with an increase in collagenase activity, which itself is involved in collagen catabolism and disturbance of collagen bundles (Ekman, Malmström, Uldbjerg, & Ulmsten, 1986; Norman, Ekman, & Malmström, 1993).

In summary, labour is a multifactorial physiological event within the tissues of the uterus which occur progressively over a period of days to weeks towards the end of gestation. These changes include, but are not limited to, an increase in prostaglandin release within the uterus, and increase in myometrial gap junction formation, and the upregulation of myometrial oxytocin receptors. Once the myometrium has matured, factors from the uterus and foetus bring about a switch in the pattern, coordination, and force of contractions. The foetus appears to control initiation of labour by coordinating the switch in myometrial activity via steroid hormone production, mechanical distension of the uterus and secretion of other stimulators. Labour results, increasing in intensity and frequency and the foetus negotiates out the birthing tract.

2.3 Factors that Contribute to the Modification of Tone in the Walls of the Urinary Bladder and Gravid Uterus

The biomechanical properties of capacious structures have been investigated directly in strips of smooth muscle (Arrowsmith, Keov, Muttenthaler, & Gruber, 2018; Borsdorf et al., 2019) and whole organs, the latter both *ex vivo* (Chakrabarty et al., 2019; Dodds, Travis, Beckett, & Spencer, 2021; Lentle et al., 2015a) and *in vivo* (K.-E. Andersson, Ingemarsson, & Persson, 1975; Lecci, Giuliani, Meini, & Maggi, 1995; Maggi, Santicioli, & Meli, 1984; Setekleiv, 1964b; L. Wilson & Kurzrok, 1938), using mechanical tests as well as a number of computational biomechanical studies (Dunford, Lutton, Atia, Blanks, & van den Berg, 2019; Roccabianca & Bush, 2016). All these investigations pertain to the physics that govern the relationships between wall tension and pressure (Laplace's Law), the regulation of compliance and shape, the structure of the smooth muscle myocyte and the application of mechanical principles to living structures. These contributing elements will be discussed below and specifically their relevance to the modulation of tone in the urinary bladder and gravid uterus.

2.3.1 The Mechanics of Dimension and the Law of Laplace

The derivation of the Law of Laplace is attributed to Pierre Simon de Laplace (1749 –1827). Simply stated the Law of Laplace says that the direction of the resultant stress in the walls of a hollow spherical structure, from the contents within, is orientated at right angles to its circumference and is termed hoop stress (Fig 2-11.). Further, that the magnitude of the hoop stress is dependent on both the pressure within the container's contents and the radius of the container.

Hence hoop stress (H) may be calculated using La Place's equation.

$H = PR/t$

where P is the pressure within the sphere, R is the radius of the sphere and t the thickness of the walls.

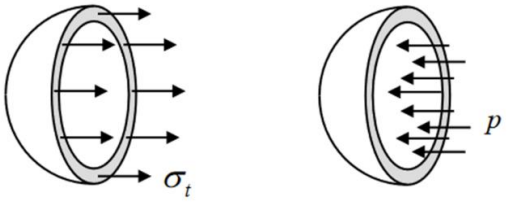

Figure 2-11 A free body diagram of one half of the spherical pressure vessel.

Hoop stress (σ_t) and Pressure (p) acting on the walls of a sphere. (P. Kelly, 2020)

In a perfect sphere the radius is the same at all points and the hoop stress is uniform in all planes of transection. Therefore, where the mechanical characteristics of the walls of similarly shaped anatomical structures are similarly uniform, the stimulation of any cellular or neural contained stress sensitive mechanoreceptors would be equal at all points on its surface provided they were able to sense tension in the appropriate direction. This would enable uniform global adjustments to be made to accommodate any increase in the volume of the contents. As discussed previously the situation becomes more complex when we consider the varying orientation of the mechanoreceptors situated along the long axes of smooth muscle cells. In addition to the active, mechanoreceptor controlled, compliance of smooth muscle cells, the cellular elements in the walls and the fibrous elements in the surrounding stroma also exhibit 'passive' compliance arising from the invariant mechanical properties of the tissue. Hence at any given moment hoop stress will result from a combination of active compliance in contracting areas of smooth muscle and passive compliance in other sites. The relative areas of mechanoreceptor-induced contraction or relaxation may differ along vertically and transversely orientated arcs, and thus the assumption of uniformity of hoop stress in a simple passively compliant symmetrical sphere (Fig 2-12) are violated.

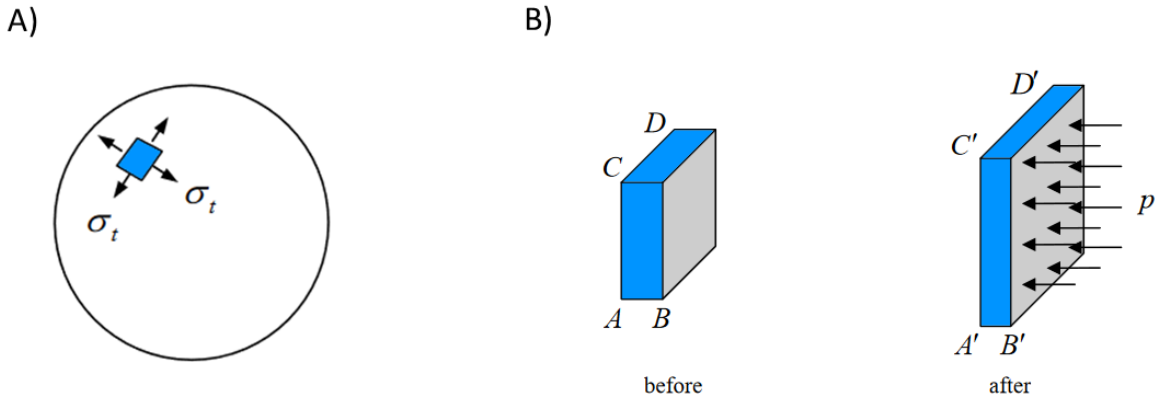

Figure 2-12 A thin walled spherical shell.

A) Because of the symmetry of the sphere and of pressure loading, the hoop stress (σ_t) at any location and in any tangential orientation must be the same. B) The thin-walled pressure vessel expands when it is internally pressurised. This results in stretching in two perpendicular in-plane directions causing thinning of the wall and an increase in tension (Adapted from (P. Kelly, 2020).

2.3.2 Theoretical Aspects of Compliance

Theoretical compliance can be explored and compared using relatively simple physical and mathematical models to demonstrate that wall tension and stress can vary significantly within the walls of incompressible spherical shells of non-living material (rubber balloon) (Fig 2-13A) and living spherical shells (urinary bladder (Fig 2-13B) and gravid uterus (Fig 2-13C) with a uniform internal pressure. The inflation of a typical spherical rubber balloon can be modelled using the nonlinear theory of elasticity. The nonlinear theory of elasticity suggests that elastic materials have nonlinear stress strain relationships even when at low strains. This relationship between the inflation pressure (*P*) and the deformation stretch λ (or volume *v*) can be presented in graphical form. Similar models of accommodation of volume in the urinary bladder and gravid uterus allows the effects of these materials to be compared and contrasted.

The physics of inflation and modelling of rubber shells introduces interesting phenomena and instabilities. In the case of the balloon, its initial inflation is more difficult than subsequent inflation owing to the change in

thickness of the wall Hence the rubber walls are initially thicker and thus harder to stretch given that, according to La Places Law, inflation pressure depends on the tension in the rubber divided by the radius of the curvature of the surface. Thus, the pressure that is required to inflate the balloon is dependent upon the elasticity of the balloon material and the rate at which the circumference increases. The pressure-deformation curve in spherical rubber shells quickly reaches a maximum pressure, which is referred to as the *limit-point instability.* Ultimately, further inflation after maximum pressure *limit point instability* results in stretch suddenly jumping to a larger value, called *inflation-jump instability*, on the *second ascending branch* (Anssari-Benam, Bucchi, & Saccomandi, 2021) and bursting point is reached.

In comparison to the rubber balloon, which is composed of a single material, capacious structures of the body are composed of living soft tissues are viscoelastic composites of cells and extracellular matrix. They are frequently arranged in complex geometries, and routinely experience large strains. Comparisons of the inflation of a passive structure such as the balloon and that of the urinary bladder and gravid uterus shows a similar early response to filling. Hence, inflation pressure initially rises rapidly in the same way as balloon, as the walls of the organs are thick and the tension high. However, unlike the balloon, in both the bladder and uterus the pressure stabilizes which is associated with the *filling phase* and gestation, respectively. The bladder and uterus have passive and active mechanical properties which allow physiological compliance, and these elements which will be described in detail latter. Plateaued pressure and tonic accommodation are commonly assumed to be dominated by the passive properties of the bladder i.e., unfolding of collagen and lengthening of elastin (elastic and plastic elongated stress respectively). However, recent work has found that accommodation of a volume is via myogenic tonic pressure, in equilibrium with passive elongations and active contractions (W. A. van Duyl, 2021). The voiding or parturition phase is controlled by the active properties which are attributed to the phasic contraction of detrusor and myometrial smooth muscle.

In conclusion in, pressure in both organs can be considered in terms of Laplace's law where pressure within the sphere is a function of T/r, where T is the wall tension and r the radius. Both organs accommodate volume by stretch (increasing r) on T. Therefore, the development of pressure reflects the relative change of T/r. The

weak sigmoid shaped pressure curve of the bladder and gravid uterus suggests that intravesical and intrauterine pressure, and thus T relative to r increases more rapidly at the start and end than in the storage phase. It can therefore be speculated that pressure and wall tone is mediated by compliance specific anatomical, neurological, and hormonal control on bladder and gravid uterine musculature.

2.3.3 Physiological Aspects of Compliance in the Walls of the Bladder and Gravid Uterus

As described in the previous section the relationship between volume and pressure determines compliance. Various biological tissue types making up the walls of the bladder and uterus have characteristic length/tension relationship that can be attributed to their physical and physiological characteristics. and physiological attributes that allow these capacious structures to accommodate a changing volume. Both organs adaptability is the aggregate result of the characteristics of individual cells and the collection of cells making up the tissue wall. The viscoelasticity of the wall is reported to vary (W. A. van Duyl, 2021) with rate of distension, and again changes in the structure of the walls can change over time with an increase in cell number from chronic irritation in the bladder or from hormonal stimulation in the uterus).

2.3.3.1 The Mechanics of the Smooth Muscle Myocyte

2.3.3.1.1 Contractile Mechanics

Muscles are the contractile tissues of the body. Smooth muscle cells contract to generate force for a particular movement by actively changing their dimension. The structure of smooth muscle is fundamentally unicellular and differs greatly from that of syncytial striated muscle and may vary between organs. The smooth muscle of the urinary bladder is termed detrusor muscle and that of the uterus is termed the myometrium.

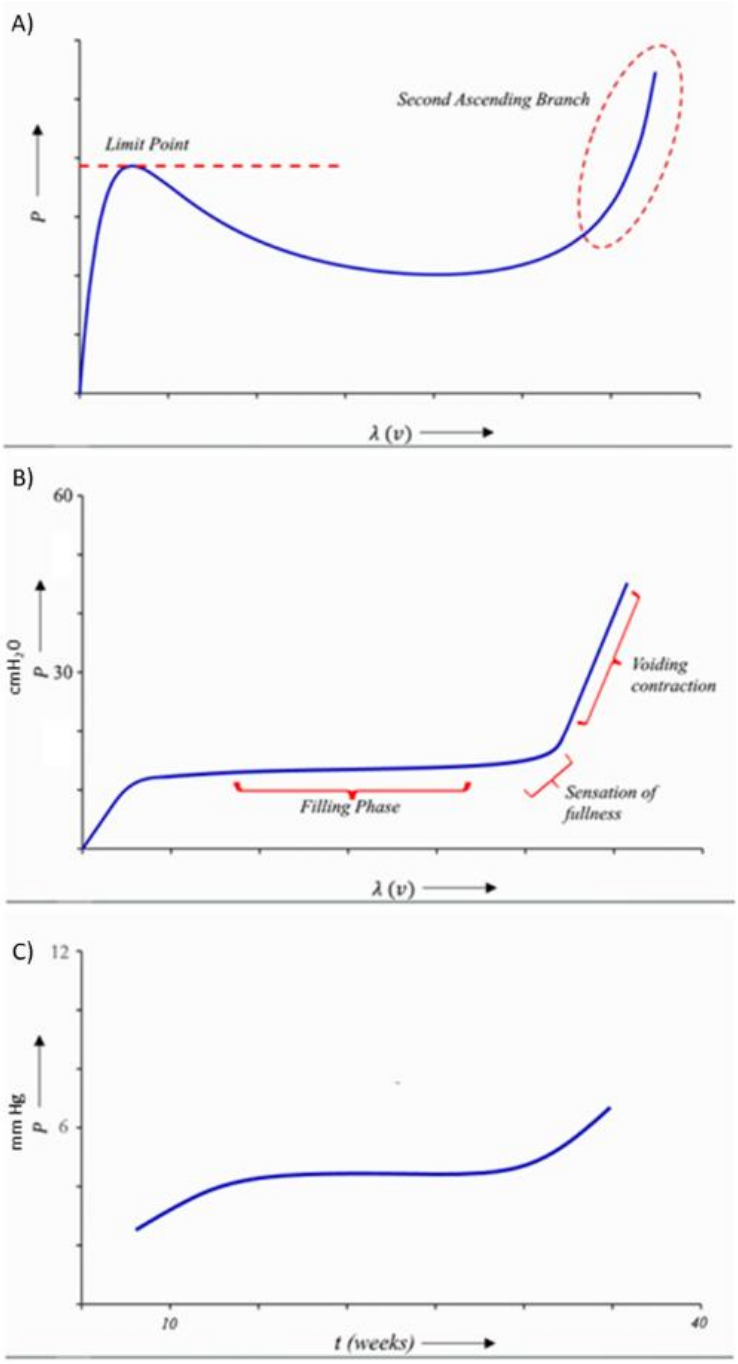

Figure 2-13 Diagrammatic relationships of inflation pressures.

A typical inflation pressure (P) versus stretch (λ) or volume (v) curve for a spherical rubber shell, exhibiting limit-point and inflation-jump instabilities (Adapted from (Anssari-Benam et al., 2021)) B) A normal cystometrogram study showing a large capacity, compliant bladder. Little change in bladder pressure is produced with filling until capacity is reached (Adapted from (Bannowsky & Juenemann, 2003)). C) Human amniotic pressure vs gestational age in singleton pregnancies. Amniotic pressure increases more rapidly in the first and third trimesters than in mid-pregnancy (Adapted from (Fisk et al., 1992)).

Smooth muscle cells are generally spindle shaped i.e., longitudinally tapered with their outer poles reducing in size. Human detrusor smooth muscle cells are approximately 300-400 µm in length (Tasian, Cunha, & Baskin, 2010). In contrast, an individual myometrial cell can enlarge almost 100-fold to around 500 µm in length at term (Hsu et al., 2014) as a response to both biochemical and biophysical stimuli during pregnancy. In all smooth muscle cells, a substantial proportion of the cytoplasm is occupied by longitudinally and geometrically orientated fibrous structures composed of myosin and actin. The actin fibres are able to chemically link to adjacent myosin fibres (Schwartz & Mecham, 1995) to initiate muscle shortening.

This process can be explained in the following stages (Habteyes, 2014):

a. Myosin head attaches to actin (high energy ADP + P configuration) forming a cross-bridge.
b. Power stroke: myosin head pivots pulling the actin filament toward the centre.
c. The cross-bridge detaches when a new ATP binds with the myosin.
d. Cocking of the myosin head occurs when ATP → ADP + P so another cross-bridge can form.

Smooth muscle tissues can be characterized as either 'tonic' (generating a slow maintained isometric contraction) or 'phasic' (generating a fast transient isometric contraction). In capacious structures like the urinary bladder and gravid uterus, the muscles have a 'tone'- by definition, a contraction that can be maintained without apparent fatigue.

Smooth muscle cells have a variable force-length relationship implying that the number of force generating cross-bridges is regulated, and vary velocity-load relationships implying that cross-bridge cycling rates are regulated (Strauss & Murphy, 1996).

When myosin light chain kinase (MLK) and myosin light chain phosphatase (MLP) enzymes are both strongly activated, the cycling frequency of myosin head movement and the velocity of contraction are great. However, as the activation of the enzymes decreases, the cycling frequency decreases, but at the same time, the

deactivation of these enzymes allows the myosin heads to remain attached to the actin filament for a longer and longer proportion of the cycling period. Therefore, the number of heads attached to the actin filament at a given time remains large. Because the number of heads attached to the actin determines the static force of contraction, tone is maintained, or 'latched', and little energy is used by the muscle, since ATP is not degraded to ADP except on the rare occasion when a head detaches. In contrast, 'phasic' contraction results in high energy expenditure during contraction, largely due to the ATP splitting associated with the continual cross bridge cycling between sliding actin and myosin filaments. Activation, sustained tension, or tone of any given smooth muscle may therefore be dependent on and defined by the rate of energy release to its contractile machinery (Rüegg, 1971). Summarized simply, the economy of tension maintenance is inversely related to the speed of contraction; thus 'tonic' contraction is more economical than fast muscle contraction and is uniquely suited to capacious structures accommodating a volume.

2.3.3.1.2 Locational and Directional Dependencies of Smooth Muscle Properties

2.3.3.1.2.1 The Urinary Bladder

The urinary bladder is distensible, allowing it to change shape as it accumulates, stores, and ultimately expels urine during micturition. The bladder wall consists of several sublayers of smooth muscle cells, which are predominantly arranged in longitudinal and circumferential orientation (Morales-Orcajo, Siebert, & Böl, 2018). Porcine bladders have been found to display anisotropism, having a physical property which has a different value when measured in different directions (Gilbert et al., 2008; Morales-Orcajo et al., 2018; Natali et al., 2015; Seydewitz, Menzel, Siebert, & Böl, 2017; Zanetti, Perrini, Bignardi, & Audenino, 2012) and a heterogeneous or unequal (Korossis, Bolland, Southgate, Ingham, & Fisher, 2009; Morales-Orcajo et al., 2018) passive behaviour. These terms mean that differences in the biomechanical properties of the bladder appear to be related to the direction (relative to the orientation of the whole organ) of the muscle strip being investigated. Higher active stress in the longitudinal direction can be explained by a more longitudinal arrangement of muscle fibres, i.e., approximately parallel with the long axis of the organ, with histological analyses showing a higher proportion of smooth muscle cells orientated in the longitudinal direction (Borsdorf

et al., 2019). Moreover, the trigone exhibits a greater passive stress than the body, and greater passive stress in the longitudinal than circumferential direction. The latter might be attributed to its microstructure (more longitudinally arranged muscle fibres) (Borsdorf et al., 2019), but Cheng et. Al. attribute the higher passive stress in the trigone to the proportionally higher collagen content, the latter being a major contributor to passive stress in the bladder at high stretch levels (F. Cheng et al., 2018). Other than the trigone, detrusor muscle shows no differences in contractile properties across the porcine bladder and studies imply that distribution between "phasic" and "tonic" muscle fibers are uniform across the bladder (Boberg, Szekeres, & Arner, 2018; Borsdorf et al., 2019).

2.3.3.1.2.2 The Gravid Uterus

In mammals, the uterus is a hollow, thick walled and contractile organ that receives the products of fertilization and supports their gestation, growth, and subsequent birth. Gravid human uterine data exist in early histologic (Danforth, 1947), and X-Ray studies (E. C. Gillespie, 1950). New technologies in ultrasound (Buhimschi, Buhimschi, Malinow, & Weiner, 2003; Buhimschi et al., 2005; Degani, Leibovitz, Shapiro, Gonen, & Ohel, 1998; Durnwald & Mercer, 2008; Sokolowski et al., 2010) and MRI (House, Bhadelia, Myers, & Socrate, 2009) have further described the uterine structure during gestation. These studies could only describe the relative magnitude and distribution of muscle growth, and analyses of stretch and distension remain unknown.

The exact orientation of smooth muscle fibres in the uterus remains controversial. Numerous *in vivo* and *in vitro* experimental findings suggest:

1. Two counter rotating spiral muscle fibre arrangement (Goerttler, 1968)
2. A circular fibre orientation in the stratum sub vasculature only with highly disordered fibres in the rest of the myometrium (Weiss et al., 2006b)
3. A largely interwoven continuous bundle type of organization without definite layers (Ramsey, 1994).

However, the above considerations are based on investigations of nonpregnant uteri and might be inappropriate in the pregnant state. Studies, involving magnetic resonance imaging, have clearly demonstrated the existence of distinct inner and outer muscular zones, with an intermediate zone between them in the case of the human myometrium. The fibres of the first inner layer are mostly longitudinal while those of the outer are mostly circular. The middle layer, which forms at least two-thirds of total uterine thickness, is sometimes called the "vascular stratum" (Testut, 1984). Here, the fibres are orientated around the numerous blood vessels, and are arranged in a system of plexiform sheaths that defies any order (Escalante & Pino, 2017). Recent three-dimensional structure analysis of the term-pregnant human (R. Young & Hession, 1999) and mouse (Kagami et al., 2020) have described a mesh-like layer within this stratum. Between the outer an inner smooth muscle layers, fibres merge, dichotomize, and intertwine with each other to form an interlacing network (R. Young & Hession, 1999). The presence of a such a novel mesh-like stratum that connects longitudinal and circular muscle layers, suggests a coordinating role in myometrial contractions.

The conditions under which uterine tissue must function are unique. During early pregnancy the myometrium is relatively passive and does not develop significant tension (Schofield & Wood, 1964). Studies have shown that one important development of uterine tissue is the relation of tension to the resting length of the muscle. Therefore, the myometrium has a resting length relating to the *in vivo* length at different stages of pregnancy. Thus in mid-pregnancy the myometrium is at such a length that it cannot develop maximum tension, but, as pregnancy advances, the length approaches the resting length and at term the muscle is able to develop the maximum tension required (Schofield & Wood, 1964).

The separation of the myometrium into definite layers strongly favours an anisotropic behaviour of the muscle. However, due to the intricate interlacing of the fibre bundles through the various layers, the myometrium may also show some isotropy, or uniformity in behaviour all directions.

Studies on human uterine kinetics have shown that during the early stages of labour the contractile deformations are still small, the different groups of muscle fibres, due to their interlacing, still act together,

and a close approximation isotropy prevails (Mizrahi, Karni, & Polishuk, 1980). With the advancement of labour, deviations from isotropy build up indicating that each group of fibres become more and more functionally independent of the others. They even exhibit different material properties (Fang et al., 2021). Thus, towards the last phase of labour, the active forces of contraction–relaxation produced by myometrial smooth muscle occur in a large number of small loci that are distributed throughout different anatomical locations and layers of the wall of the uterus (Fang et al., 2021). It can therefore be assumed, that like the bladder, the gravid uterus possesses similar anisotropic behaviour as a result of smooth muscle fibre mechanics and the elastic properties of the extra cellular matrix (ECM), which will be discussed next.

2.3.3.2 Viscoelasticity in the Tissue of the Bladder and Gravid Uterus

Tissue and organ-scale viscoelasticity are essential contributors to urinary bladder and uterine function. The extracellular matrix transmits external mechanical loads to smooth muscle cells and at the same time, the smooth muscle cells constantly remodel the ECM in response to the mechanical environment (Bonnans, Chou, & Werb, 2014). Thus, it response to an external load, living cells in biological tissues undergo deformation without compromising their integrity and behave as viscoelastic material (Kasza et al., 2007).

In materials science, the term viscoelasticity is the property of materials that exhibit both “viscous” (which refers the internal resistance of a fluid to flow) and “elastic” (able to be stretched and return to an original length) characteristics when undergoing deformation. Therefore term “viscoelasticity” combines both types of mechanical response, the response of elastic solids and viscous fluids. Consequently, a biological tissues viscoelastic ability enables it to maintain a fundamental architectural structure owing to their solid-like nature, but at the self-same time to dynamically rearrange themselves into various conformations and modes owing to their viscous nature (Mierke, 2022).

Viscoelastic materials display three prominent characteristics: Hysteresis, (a condition brought about by loading and unloading processes), stress relaxation, (which is the stress decreases with time), and creep (a constant stress with a decrease in strain with time).

In contrast to fully elastic materials, in which the strain is completely recoverable, the stress–strain curve is not the same for loading and unloading in materials exhibiting viscoelasticity. Owing to the presence of a viscous component in biological tissues, some energy is dissipated as molecular friction, leading to a phenomenon called hysteresis (Ajalloueian, Lemon, Hilborn, Chronakis, & Fossum, 2018). Conceptually, hysteresis represents the energy lost to the system as biomechanical or thermodynamic work(Cole, Shaffer, & Scott, 1987). Dynamic mechanical testing of tissues of both the bladder and uterus exhibit hysteresis whereby stress-strain plots clearly show energy is lost during the unloading stage. (A. E. Finkbeiner, 1999; Omari, Varghese, Kliewer, Harter, & Hartenbach, 2015). Studies have shown that the effect of frequency of preloading of bladder and uterine tissue and loading history creates significant changes in the mechanical behaviour of both tissues, with increasing numbers of cycles, the loss of linearity in the hysteresis loop and a more pronounced relaxation is described (Jelen, Lopot, Budka, Novacek, & Sedlacek, 2008; Zanetti et al., 2012).

Stress relaxation and creep are two other features that describe the viscoelastic behaviour of soft tissues (Winkelstein, 2012).

The bladder muscle wall exhibits a nonlinear relation between stretch and passive tension. Urodynamic studies, such as cystometry (whereby the bladder is slowly filled *in vivo*), has shown that when the bladder wall is stretched wall tension increases steeply. During fast stretch or extensive deformation, the bladder wall also exhibits viscous and plastic behaviour i.e., the material deforms irreversibly and does not return to its original shape and size, even when the load is removed. (Alexander, 1973; BL Coolsaet, Van Mastrigt, Van Duyl, & Huygen, 1976; Alex E Finkbeiner & O'Donnell, 1990; Kondo & Susset, 1973). This phenomenon is called “stress relaxation” or “strain softening” and is observed in the whole urinary bladder and isolated muscle strips. Strips of rabbit detrusor smooth muscle exhibit regulated bladder compliance characterized by “strain softening”, a loss of stiffness on after stretch to a new length (Speich et al., 2006).

Several studies have demonstrated that repeated stretches of “passive” rabbit or mouse bladder strips (Ratz & Speich, 2010; Speich, Borgsmiller, Call, Mohr, & Ratz, 2005; Speich et al., 2006) or repeated filling of isolated

mouse bladders (Speich et al., 2012) can strain-soften or increase the compliance of the bladder (Almasri, Ratz, & Speich, 2010; Speich, Almasri, Bhatia, Klausner, & Ratz, 2009; Speich et al., 2005; Speich et al., 2007; Speich et al., 2006), just as repeated stretches of a latex balloon make it easier to inflate. However, unlike a latex balloon, an increase in compliance due to strain softening can be reversed by active contraction at short muscle lengths (Almasri et al., 2010; Speich et al., 2009; Speich et al., 2005; Speich et al., 2007; Speich et al., 2006).

Less is known of the mechanical behaviour of the uterine wall and its changes during pregnancy because material tests of pregnant human tissue are extremely rare (Baah-Dwomoh, McGuire, Tan, & De Vita, 2016). However, *ex vivo* uterine tissue has been tested in uniaxial tension i.e., the specimen has been subjected to force acting in only one direction (Conrad, Johnson, Kuhn, & Hunter, 1966; Manoogian, Bisplinghoff, Kemper, & Duma, 2012; Mondragon, Yoshida, & Meyers, 2013; Pearsall & Roberts, 1978), and uniaxial compression (Pearsall & Roberts, 1978). Results of this study found that uterine tissue from pregnant patients exhibited a rate of stress relation that was higher than uterine tissue from nonpregnant patients under the same strain levels (Conrad et al., 1966). Non-pregnant uterus tissue is expected to have a less elastic stress–strain response than pregnant uterus tissue due to hormonal changes that remodel the gravid uterus tissue in preparation for labour. Further, myometrial stretch and tension during gestation plays an important role in preparing the uterus for increased excitability and responsiveness required for parturition at term (Lye et al., 2001). (Pearsall & Roberts, 1978)Mechanical compressive testing on the non-pregnant human uterine tissue response to loading describes, like the urinary bladder, viscoelastic tissue stiffening with increased loading or stretch frequency (Kiss et al., 2006; Omari, Varghese, Kliewer, Harter, & Hartenbach, 2015). Thus, as the uterine accommodates the foetus during gestation, the proteins of the extracellular matrix, particularly the interstitial collagens are responsible for this property of “firmness” and for the mechanical strength of the tissue. In biomechanical terms this property is referred to as stiffness.

In sum, bladder and uterine tissue is highly dynamic. Muscle strips of both organs are found to be stretch-rate dependant. The primary influence stretch rate and tension is ultimately the smooth muscle length; however, stretch and relaxation rates do influence the inherent smooth muscle properties of hysteresis, stress-

relaxation, and creep. Elasticity allows the tissue of the bladder/uterine wall to stretch to a certain degree without an increase in wall tension. Viscoelasticity allows stretch to induce a rise in muscle tension, followed by stress relaxation to the new muscle resting length. The storage function of the bladder and uterus is therefore very much a result of the ECM and passive smooth muscle properties of muscle length and tension which can, however, be altered by superimposed myogenic, neurologic, and hormonal influences.

2.3.3.3 Extracellular Matrix of the Bladder and Uterine Wall.

Slow stretching generates a relatively small increase in wall tension, compared to more rapid stretching. In the latter case, excess tension is dissipated shortly after termination of the stretch. In both the urinary bladder and gravid uterus, this is partly due to the surrounding environment of the cells, the extracellular matrix (ECM). The structural elements constituting the supporting tissue of the bladder and uterine wall, transmit external mechanical loads to smooth muscle cells, and at the same time, smooth muscle cells constantly remodel the ECM in response to the mechanical environment. As a result, the ECM evolves a complex profile with distinct mechanical properties in individual tissues. What follows will summarize the major components of the ECM of the bladder and gravid uterus. Finally, the viscoelastic behaviour of the ECM and smooth muscle of these capacious organs under normal physiological conditions will be described. In both the urinary bladder, and gravid uterus, accommodation is maintained by the close integration of tension generating or “active elements” (smooth muscle cells) with tension bearing and elastic elements (collagen and elastin), that are passive structural components.

2.3.3.3.1 The Urinary Bladder ECM

2.3.3.3.1.1 Anatomy and Mechanical Properties of Bladder Collagen

Collagen and elastin fibres, the major components of the connective tissue, are present throughout the wall of the urinary bladder (Cortivo, Pagano, Passerini, Abatangelo, & Castellani, 1981; Ewalt et al., 1992). Collagen is a structural protein which consists of amino acids bound together to form a triple helix of elongated fibril known as a collagen helix. In mammals there are five common types (Ashokkumar & Ajayan, 2021) of collagen

with only Type I (skin, tendon, vasculature, organs, bone (main component of the organic part of bone)) and Type III (reticulate (main component of reticular fibres), commonly found alongside type I) being found in the bladder.

Collagen fibres are found in mucosal, muscular, and serosa layers of the urinary bladder. In the mucosal layer collagen bundles are aligned in various directions so the structure can withstand tensile force from any direction. In the muscular layer, smooth muscle fascicles are separated from one another by collagen and elastin layers. This enables each fascicle to move independently as a contractile unit. The collagen sheets probably ensure the independent movement of the fascicles and protect them from over stretching and elastin fibres give further resilience. Further, wavy bundles of collagen connect muscle fascicles to one another. These collagen bundles probably maintain the original location of the of the fascicles irrespective of the contraction and distension of the bladder wall (Murakumo et al., 1995). Lastly, the serosa layer consists of wavy collagen bundles formed into a sheet. This arrangement probably allows the serosa layer to expand and contract in coordination with the motion of the muscular layer, while the layer may also, in some degree, protect the urinary bladder against overstretching.

When the bladder is empty, Type III collagen of the lamina propria and detrusor appears to be a meshwork of loose, wavy fibres without a specific orientation (Steven L Chang, Howard, Koo, & Macarak, 1998). However, during filling and when the bladder reaches capacity, the conformation of the fibres become altered. As the bladder fills, Type III fibres in the mucosa change in orientation becoming parallel to the urothelium while those in the detrusor orientate orthogonally to the urothelium and detrusor (Steven L Chang et al., 1998) (S. L. Chang, Chung, Yeung, Howard, & Macarak, 1999). It is hypothesized that the collagen fibres undergo conformational and/or orientation changes to accommodate an increasing intravesical volume. Fibres accommodate the volume change by first reorientating and then expanding its coiled structure as intravesical volume increase. Further, as the bladder reaches capacity and the walls of the bladder maximum strain, the tension is gradually transferred through the rest of the mucosa and toward the detrusor muscle bundles through the process of collagen uncoiling and reorientation of the type III fibres (Steven L Chang et al., 1998)

At bladder capacity, the collagen fibres that were once loose and wavy, become long, thin, taut fibres. Type III fibres of the completely filled bladder are tightly packed and are orientated parallel to the urothelium throughout the entire bladder wall (mucosa and detrusor) (Steven L Chang et al., 1998). Collagen fibres are resistant to stretch, as evidenced by their having a high stiffness modulus, and they probably provide support for the microstructure of the elements of the bladder wall (Freed & Doehring, 2005; Tang, Ballarini, Buehler, & Eppell, 2010) guarding them against undue tissue distension from excessively high hoop stress and strain. During progressive stretch the point where collagen fibres have been straightened, and are recruited into load bearing, is known as the "recruitment stretch" (Watton, Hill, & Heil, 2004). At this there is a dramatic stiffening of the tissue. This behaviour is reported to occur in the wall of the urinary bladder (Steven L Chang et al., 1998) (Fig 2-14). Moreover, at bladder capacity, the muscle bundles reorganize by sliding past one another as the collagen fibres between them bear increasing levels of tension. It can therefore be speculated that bladder accommodation is achieved by changes in collagen fibre orientation (direction) and conformation (loose coil to taught fibre) coupled with tonic contraction of the smooth muscle which transfers tension uniformly via the circular and longitudinal muscle layers of the bladder wall and accounts for the ability of the bladder to sustain large strains.

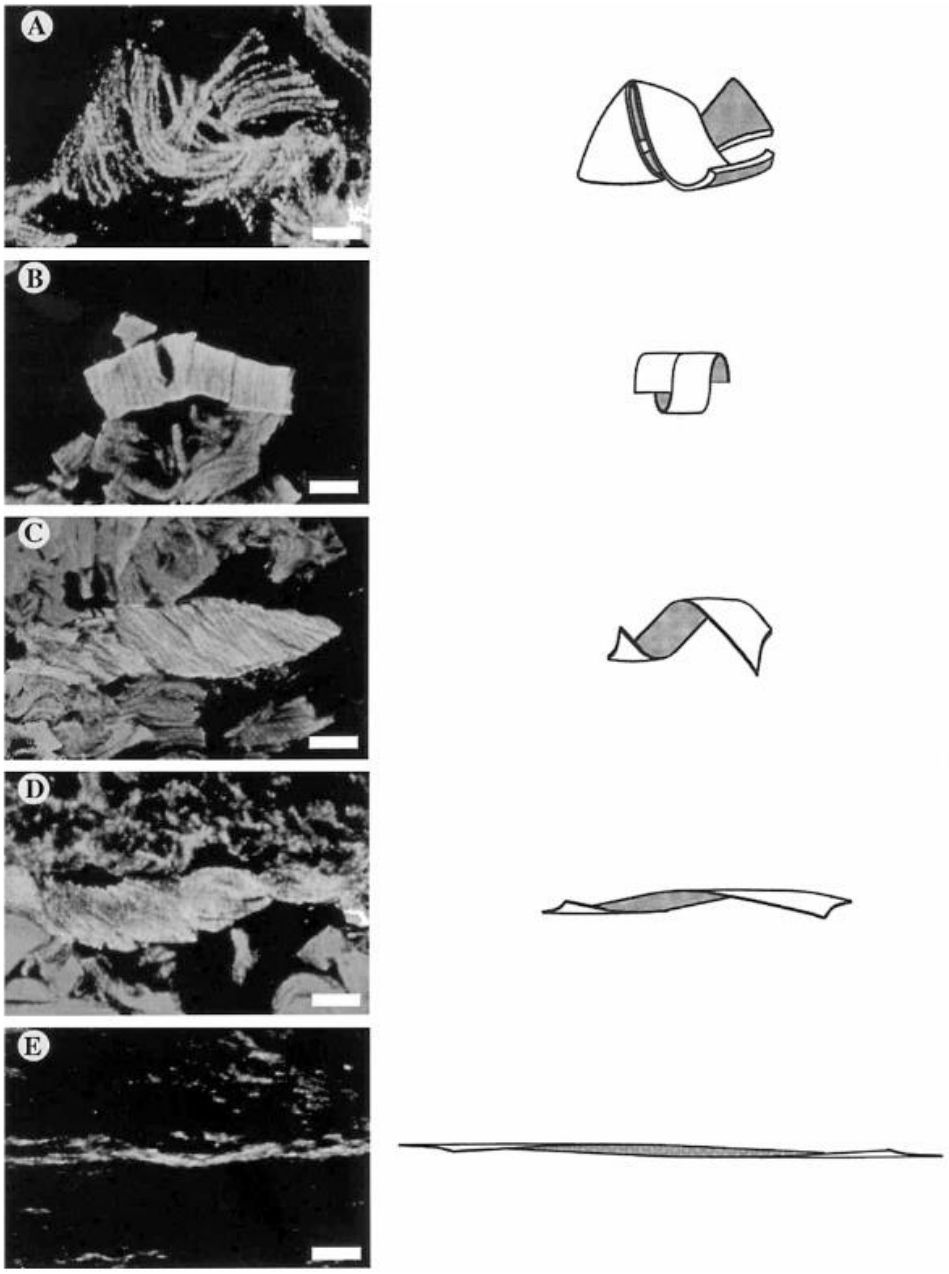

Figure 2-14 Confocal microscopy of type III collagen fibres in the detrusor layer of the bladder.

Section showing the random orientation of the relaxed, type III collagen fibre bundle in the 0% distended foetal bovine bladder. The fibre bundle possesses a "wavy" characteristic and coiling is evident. (b) Section showing the tightly coiled fibre bundle in the 25% distended foetal bovine bladder. (c) Section showing the early stages of type III collagen fibre expansion or extension in the 25% distended foetal bovine bladder. (d) Section showing the later stages of type III collagen fibre extension in the 25% distended foetal bovine bladder. (e) Section showing the linearization of type III collagen fibres in the 100% distended foetal bovine bladder (S. L. Chang et al., 1999).

2.3.3.3.1.2 Anatomy and Mechanical Properties of Bladder Elastin

Like collagen, elastin is a resilient connective tissue protein found in the ECM of most vertebrate tissues, and it is an important part of tissues that undergo repeated physical deformations in the human body (Swee, Parks, & Pierce, 1995).

Elastins are one of the main ECM elements in the urinary tract (Kaya & Şahin, 2016), however, in the bladder, elastic fibres are sparse, being found only in the muscular and serosal layers of the bladder.

In the muscular layer of the bladder, ECM coverings of the smooth muscle fascicles separate each from one another. It is hypothesized that collagen allows the fascicles to move independently of one another and that the elastic fibres surrounding the fascicles provide proper resilience and a capacity to recover from stretch (Murakumo et al., 1995). Further, the presence of collagen and elastin probably maintains the original location of the muscle irrespective of the contraction or distention of the bladder.

The serosal layer of the bladder has also been found to contain an elastic fibre network with accompanying collagen sheets (Monson et al., 1988; USHIKI & MURAKUMO, 1991). However, it appears that this arrangement of tissue allows for the serosal layer to expand and contract in coordination with the muscular layer. It is probably not a significant contributor to, or limiter of, bladder compliance (Murakumo et al., 1995).

2.3.3.3.2 The Gravid Uterus ECM

The cellular and fibrous components of the gravid uterus and their proportions change during pregnancy. Three phases in the expansile state of uterus may be recognised; a phase of uterine preparation, a phase in which uterine enlargement predominates, and a phase in which distension by the uterine contents predominates. The human uterus undergoes hyperplasia i.e., increase in myocyte volume in early pregnancy, followed by hypertrophy i.e., an increase in myocyte growth in later gestation. However, it is the connective tissue, which provides a supportive matrix for the bundles of smooth muscle, which is the predominant growth of the uterus during pregnancy via stretch-induced myometrial hypertrophy (Ramsey, 1994).

2.3.3.3.2.1 Anatomy and Mechanical Properties of Uterine Collagen

The predominant forms of collagen in the uterus are Type I and Type III. The human uterus shows a gradual and progressive increase in content of collagen during gestation. The collagen content at term is about 8 times total greater total content than the non-pregnant uterine value (Morrione & Seifter, 1962). In early pregnancy, collagen fibres are rather sparse in the uterine stroma, but by late pregnancy, the proportion of fine elastic fibres between smooth muscle cells has increased, and collagen extends continuously around smooth muscle cells (Nishinaka & Fukuda, 1991) forming a honeycomb-like structure (Leppert & Yu, 1991). The matrix of collagen reinforces smooth muscle cells. The thin structure of the uterine wall is freely stretchable in any direction. Thus, the uterine wall may provide a soft elastic structure that maintains the growing foetus without exerting undue pressure on the conceptus.

2.3.3.3.2.2 Anatomy and Mechanical Properties of Uterine Elastin

Like that of collagen, proportions of elastin increases within uterine tissue during pregnancy (Metaxa-Mariatou et al., 2002). Gunja-Smith and Woessner reported that a 4 to 5 fold increase occurs during pregnancy, and that in the non-gravid uteri elastin content increases with parity (Gunja-Smith & Woessner Jr, 1985). Further, elastin has been shown to vary regionally within the myometrium being greater in the outer myometrium and lower in the inner myometrium (Brosens, Barker, & deSouza, 1998; Chalubinski, Deutinger, & Bernaschek, 1993; de Vries et al., 1990; G Kunz, Beil, Deininger, Wildt, & Leyendecker, 1996; Lyons et al., 1991; Metaxa-Mariatou et al., 2002).

Elastin is very abundant in the endometrial arterioles (Metaxa-Mariatou et al., 2002). Farrer-Brown *et al*. have hypothesized that the tortuosity of the myometrial arteries is designed to allow expansion of the gravid uterus, which would otherwise be subject to excessive tension (Farrer-Brown, Beilby, & Tarbit, 1970). Further, spiral nature of the arteries is thought to reduce the force required to produce elongation. It is therefore suspected that elastin associated with the smooth muscle and vascular system, has a specific adaptation that facilitates stretch (Metaxa-Mariatou et al., 2002). In sum, elastin's proportional differences within the uterus could

provide a dynamic function during pregnancy by allowing the uterus to accommodate the physical strain within the uterine muscle.

2.3.3.4 Micturition, Parturition, and Spontaneous Contractile Activity of the Bladder and Uterus

The urinary bladder and gravid uterus have two important functions: accommodation and expulsion. The contractile processes of expulsion i.e., micturition and parturition are better understood than those of storage function.

2.3.3.4.1 Micturition and Parturition

Micturition, or urination, is initiated by a complex neural control system that is located in the brain, the spinal cord, and the peripheral ganglia (Fowler, Griffiths, & De Groat, 2008). Voiding in the bladder is initiated via the pontine micturition centre (PMC) of the brain, which activates descending pathways that causes urethral muscles and urethral sphincter to relax (Sam, Jiang, & LaGrange, 2021) , the detrusor muscles to contract and generate an increase in intravesical pressure to start the flow of urine down the urethra. In contrast, parturition is not voluntary but initiated via hormonal and mechanical stimuli. The principle hormones are progesterone, relaxin, oestrogen, oxytocin, and a number of the prostaglandins (J. Marshall, 1981; J. M. Marshall, 1962b).The excitability of the gravid uterus depends upon the balance between progesterone(which maintains quiescence) and prostaglandins, oxytocin ,oestrogen (Caspo, 1975; Arpad Csapo, 1956; A.-R. Fuchs, 1978; Keelan, Coleman, & Mitchell, 1997; Zakar & Hertelendy, 2007) (which activate smooth muscle). Moreover, uterine cavity expansion and contractile activity are also modulated by the static strain placed on the walls of the uterus imposed by the growing foetus and accommodation of amniotic fluid.

2.3.3.4.2 Accommodation

The processes that govern accommodation and storage function observed in the urinary bladder and gravid uterus are little understood. Moreover, urinary, and uterine muscle is not inactive during the storage/gestation phase with both organs' exhibiting accommodating smooth muscle contractions (Lentle et al., 2015a; McEvoy & Sabir, 2021). The process of accommodation allows the cavities of the bladder and gravid uterus to

accommodate significant increases in volume with a minimal rise in cystic (Homma et al., 2002) or amniotic intra-luminal pressure (Fisk et al., 1992), which implies the bladder and gravid uterus can modulate its muscular tone. Both organs exhibit ongoing spontaneous contractile activity termed “micromotions”. These contractions are seen not only *in vivo*, but in *ex vivo* muscle preparations. Thus, they are in part intrinsic to detrusor and myometrial tissue. The precise physiological role of spontaneous contractions in the bladder and uterus is not well understood but it is likely that their intensity, frequency, duration, and area may be modulated by locally or reflexively by mechanical stimulation. Such a hypothesis raises two subsidiary questions: what are the origins of spontaneous contractions; and how might they coalesce into larger ones?

2.3.3.4.3 Spontaneous Contractions in the Urinary Bladder

During the filling phase the bladder exhibits patches of spontaneous contractile activity during the filling phase, in isolated muscle strips, and during accommodation (A. F. Brading, 1997; Lentle et al., 2015a; Malkowicz et al., 1986). The spontaneous activity cannot be abolished by tetrodotoxin, atropine, phentolamine, propranolol, or hexamethonium, indicating that the activity is not dependent on neural influence (M. Wang et al., 2018). This activity was thought to be associated with abnormal bladder function, however, it is now understood that spontaneous contractions during filling and storage are evident in healthy human bladders (Robertson, 1999; Van Doorn, Remmers, & Janknegt, 1992).

The patchy distribution of spontaneous contractions could either result from propagation of contractile waves (Marcus J Drake et al., 2003) or from a potential occurrence at multiple sites across the bladder wall (Christopher H. Fry & McCloskey, 2019). Either type of contractile activity is likely to be augmented by stretch activation of mechanoreceptors. Hence filling causes the amplitude and frequency of spontaneous contractions (T. J. Heppner, Tykocki, Hill-Eubanks, & Nelson, 2016; Lagou, Drake, & Gillespie, 2004) to increase and it is hypothesized that spontaneous contractions generate additional, transient changes in wall tension. Increase in such activity is likely to influence bladder wall muscular tone and ultimately bladder compliance and thus lumen pressure. Thus, normal bladder accommodation and homeostasis may be accomplished by

acute muscle length adaptation, described previously, which theorises spontaneous rhythmic contractions modulate this ability.

2.3.3.4.3.1 Smooth Muscle Cells

The origin of bladder spontaneous activity is thought to originate from bladder detrusor muscle (DSM). There is evidence that the smooth muscle cells in the bladder wall develop spontaneous action potentials, spontaneous intracellular calcium transients, and spontaneous contractions (T. Heppner, Bonev, & Nelson, 1997; K. Lee, Mitsui, Kajioka, Naito, & Hashitani, 2016). The origin of this activity is not fully understood, but it appears to be an intrinsic property of the smooth muscle cells as the contractions are not extinguished by tetrodotoxin, confirming their non-neurogenic origin. The same activity is exhibited by isolated smooth muscle cells. (Anderson et al., 2013) Smooth muscle cells are coupled by gap junctions as is isolated tissue (Bramich & Brading, 1996; T. Heppner et al., 1997).

2.3.3.4.3.2 Interstitial Cells of Cajal

The observation that Interstitial cells of cajal (ICC) can act as pacemakers in the wall of the gut suggests that smooth muscle in other organs may also be modulated by ICC. ICC-like cells have been reported in the renal pelvis, ureter, bladder, and urethra of the urinary tract. In the bladder specifically, ICC-like cells are most numerous in the lamina propria (Fry, Nyirady, unpublished data) and are especially abundant near the urothelium where they often situated near afferent nerves (Wiseman et al., 2003). Moreover, such ICC-like cells are electrically excitable and are coupled by gap junctions to one another suggesting they form a functional electrical syncytium (G. Sui et al., 2002). It has been hypothesised that activating ICC-like cells initiate contraction of smooth muscle cells in the bladder (Christopher H Fry et al., 2012), possibly via direct electrical coupling through gap junctions. However, the frequency of spontaneous depolarisation of ICC-like cells is of markedly lower frequency than in neighbouring detrusor smooth muscle cells, suggesting that they are not acting as pacemakers, but may serve to modulate detrusor smooth muscle activity (Gray, McGeown, McMurray, & McCloskey, 2013; Hikaru Hashitani, Yanai, et al., 2004b). Therefore, the spread of non-micturition

activity is thought to be through the ICC-like cells, which form a network throughout the bladder wall, but this has yet to be definitively described.

2.3.3.4.4 Uterine Spontaneous Contractions and Labour

Spontaneous contractile activity is observed in the non-gravid and gravid state in the uterus. In the non-gravid state such patterns of motility vary through the menstrual cycle. Hence low amplitude, high frequency contractions occur during the follicular phase, and high amplitude, lower frequency contractions during the luteal phase. These non-pregnant contractions of the myometrial smooth muscle have been suggested to initiate a peristaltic-like in motion (Y. Zhang et al., 2019). Again, uterine peristalsis has been suggested to initiate a rapid and sustained directed sperm transport and high fundal implantation during conception, as well as evacuating products of menstruation (Georg Kunz & Leyendecker, 2002).

After fertilization, and in early pregnancy, uterine contractions are reduced or absent and it is proposed that this reduction may aid implantation of the fertilized egg into the endometrium, although the evidence is not extensive (Kuijsters et al., 2017).

The tissue of the wall of the uterus is unique among smooth muscle organs in that, during pregnancy, it undergoes a number, largely reversible, changes orchestrated by ovarian hormones, notably hypertrophy and hyperplasia of the uterine muscle cells (Riemer & Heymann, 1998). Again, changes in progesterone, oestrogen/progesterone ratio, prostaglandins, oxytocin, as well as in cellular oxytocin receptors seem to be responsible for relative uterine quiescence during gestation compared and subsequent heightened contractile activity during labour.

2.3.3.4.4.1 Smooth Muscle Cells

Smooth muscle cells within the uterus are able to contract without nervous or hormonal input (SUSAN Wray, 1993) i.e., exhibit spontaneous contractions. Sporadic spontaneous contractions and relaxations occur in the human uterine muscle from about 6 weeks of gestation but are not usually felt until the second or third trimester of pregnancy (Raines & Cooper, 2017). The latter palpable contractions are termed “Braxton Hicks”

contractions, prodromal or “false labour” pains. Braxton Hicks contractions are irregular in duration and intensity, occur periodically, but do not indicate that labour is imminent. Moreover, animal models support the concept of the gravid uterus reaching maturity before parturition with basal spontaneous myometrial contractions increasing but failing to exceed those observed during parturition (Y. Zhang et al., 2019). In sheep the force of basal contraction is reported to increase gradually some time before term (Apostolakis et al., 1993; Baguma-Nibasheka et al., 1998) and similarly in the rhesus macaque (Haluska & Novy, 1993; Honnebier et al., 1991). However, in both these animals, uterine contractile activity is augmented over 2-fold immediately preceding parturition.

Labour is viewed as a culmination of changes that have been progressing over many months and there is no one key event that initiates a switch to labour. Changes to the muscle cells themselves include increase in the size of myocytes, changes in ion channels, and also increase in gap junctions (described in proceeding chapters) ensure that muscle bundles and contractions are coordinated prior to the onset of labour. This is accompanied by a change in the endocrine environment, notably increased oxytocin release and increased number of oxytocin receptors.

2.3.3.4.4.2 Interstitial Cells of Cajal

The mechanisms used to coordinate contractions are not known. A large body of literature has addressed intracellular (S. Wray et al., 2003) and intercellular (Aslanidi et al., 2011) signalling in the gravid uterus, but only hypotheses exist on how contractions are ordered at the organ level . What is clear is that at the cellular level, similarly seen in the urinary bladder, electrical excitability properties control the signal to contract. Although action potential propagation recruits tissue for contraction over short distances, a single action potential sweeping through the uterus cannot explain organ level function (R. C. Young & Barendse, 2014). Therefore, the exacting functions of whole uterine contractile dynamics have yet to be explained in detail and are still debated.

One hypothesis suggests that, like the bladder, uterine contractions are initiated by stretch (R. C. Young & Barendse, 2014) and thus the adjustment of local tone by mechanoreceptors. Because the uterus is pressurized, contraction of the first region raises the intrauterine pressure slightly, which stretches the entire uterine wall. The stretch recruits another regional contraction, which generates more pressure. Higher pressure raises tension throughout the entire uterine wall, which initiates local contractions into those seen at organ-level. However, this hypothesis would work for the onset of labour but not for accommodation of the foetus during pregnancy. During gestational accommodation, more contractions would result in a higher muscle tone and lower wall compliance and an increase rather than decrease in intrauterine pressure. Uterine hypertonicity can cause abnormally high intrauterine pressure which can result in foetal distress and in some cases uterine perforation (Rood, 2012). Therefore, this theory of myometrial mechanical properties and mechanotransduction has only been described by computational biological simulation and has yet to be proven *in vivo*. Further, speculation of ICC-like intermediaries residing between cell and organ which may modulate afferent uterine smooth muscle function, have yet to be explored in detail.

2.3.4 The Control of Tone in Capacious Structures

In principle, normal spontaneous contractile activity of smooth muscle cells may arise from several, not mutually conflicting sites.

Smooth muscle cells are not pre-programmed to contract i.e., contract autonomously. Bladder and myometrial smooth muscle cells show spontaneous contractile activity which is influenced by the amount of strain placed on structural and anatomic parts of the organs wall. Characteristically, in single-unit smooth muscles, a contractile response can often be induced by stretching the muscle (K.-E. Andersson & Arner, 2004). Both the bladder and uterus are composed of multiunit, multifibre bundles of smooth muscle that are orientated in different layers and directions. The tissue walls are also densely innervated and functionally require nervous coordination to achieve micturition and parturition. As there is little evidence for a hypothesis of smooth

muscle cell pre-programmed contraction, it could be hypothesised that spontaneous smooth muscle activity in the walls of the bladder and uterus contract in response to mechanical stimuli i.e., are mechanoregulated. Moreover, there must be mechanoreceptors that relay extracellular stimuli to intracellular signal transduction in order to control or modulate tonicity and contractions within the walls of these accommodating structures. This section will consider the role of mechanoregulation in both the bladder and gravid uterus.

Most studies of bladder afferents *in vivo* have identified mechano-receptors that fire in proportion to intravesical pressure, reflecting the combination of passive distension and active contraction of the bladder wall (Daly, Rong, Chess-Williams, Chapple, & Grundy, 2007; Rong, Spyer, & Burnstock, 2002; Xu & Gebhart, 2008; V. P. Zagorodnyuk, I. L. Gibbins, M. Costa, S. J. Brookes, & S. J. Gregory, 2007). The gravid uterus also is reported to have not only mechanoreceptors influenced by stretch (A. G. Savitsky et al., 2013; Shelkovnikov, Savitskiĭ, & Abramchenko, 1986b), but also specialized hormone receptors up-regulated by wall tension (Terzidou et al., 2005). Therefore, in both the bladder and uterus, wall tension and tone are constantly modulated by these sensors.

The identification of mechanoreceptors in the wall of the bladder and uterus that encode a large range of mechanical stimuli (distension, storage, and contraction), raises the question of where these receptors are located specifically. Clearly, there is great complexity in the structural organization and sensory innervation of the bladder and uterine wall. However, the location of mechanoreceptors that can modulate and signal the mechanical environment of the bladder and uterus are speculated to be located in four specific sensory locations;

1. In the wall of the smooth muscle cell (Myocyte)
2. At the junction between smooth muscle cells and an interstitial cell of cajal (ICC)
3. In an ICC
4. In a nerve ending

Evidence supporting the location of mechanoreceptors at these specific locations will now be summarized briefly below.

2.3.4.1 Smooth Muscle Mechanoreceptors

The smooth muscle tissue of the bladder and gravid uterus are exposed to considerable mechanical stress and it has been long been known that changes in cell length and tension causes contraction of the myocyte (Bayliss, 1902). One process by which mechanical stress causes myocyte contraction is through the opening of mechanical and stress sensitive ion channels (Guharay & Sachs, 1984; Sigurdson, Ruknudin, & Sachs, 1992). These mechanoreceptors are often calcium activated potassium channels and calcium activated chloride channels located in the cell membrane. Increases or decreases in cell length associated with changes in luminal pressure in hollow organs such as the bladder and gravid uterus organs might be expected to affect Ca^{2+} release and result in coordinated changes in electrical activity.

Experiments *in vitro* have revealed three distinct classes of stretch-sensitive afferents that behave as tension receptors in the bladder: low threshold mechanoreceptors in the muscle layer; mechanoreceptors at the interface between muscle and mucosa (muscle-mucosal mechanoreceptors); and high threshold mechanoreceptors in the muscle layer (Daly et al., 2007; Rong et al., 2002; Xu & Gebhart, 2008; V. P. Zagorodnyuk et al., 2007). There also may be 'volume' receptors, which sense bladder distension irrespective of pressure (Morrison, 1999).

Gravid uterus myocytes also feature distinct membranous localizations of mechanoreceptors (Y. H. Lee, Hwang, Morgan, & Taggart, 2001). Such plasmalemmal regions are Ca^{2+} sensitive and extracellular signals such as stretch is likely to contribute to receptor-coupled contractile activation of uterine smooth muscle.

2.3.4.2 Muscle Gap Junction Mechanoreceptors

In the individual myocyte contractile activity is preceded and initiated by an action potential that is calcium driven (Hikaru Hashitani, Brading, & Suzuki, 2004). The bladder and gravid uterus have muscle tissue bundles in prescribed layers, and spontaneous contractile activity is observed during urine storage and gestation,

respectively. Intercellular connections may contribute to smooth muscle control but also act as locally generated mediators. Both the detrusor and myometrial smooth muscle cells are electrically coupled via gap junctions (Balducci et al., 1993; John, Wang, Wehrli, Hauri, & Maake, 2003).

In the human bladder, connexin (Cx) subtype 45 proteins (Cx45) in the cell membrane create intercellular pathways or gap junctions between detrusor myocytes (Geiger, Yehuda-Levenberg, & Bershadsky, 1995). In bladders that are obstructed, Cx45 protein expression is fundamentally altered (John, Walch, Lehmann, & Maake, 2009) suggesting that an over distended or stretched bladder develops gap junction pathology. Further, Kinder and Mundy found that spontaneous contractile activity developed more often in muscle strips from overactive than normal bladders (R. Kinder & Mundy, 1987). Therefore, some evidence does suggest that gap junctions are mechanosensitive and thus are an important factor when investigating bladder contractility and maintenance of tone.

In the human gravid uterus, twenty connexin isoforms have been identified in human tissue, with connexin 43 (Cx43) being the most abundant (Willecke et al., 2002). Stretch in combination with low levels of circulating oestrogen causes a significant increase in the number of gap junctions in the myometrium (Wathes & Porter, 1982) as well as frequent but non-propagating spike bursts (Ishikawa & Fuchs, 1978). However, near term, the myometrium exhibits "Ca^{2+} Sensitization" (A. Somlyo & Somlyo, 1998) where agonists such as oxytocin cause smooth muscle cells to coordinate and give stronger force of contraction. Thus, the mechanosensitivity of uterine gap junctions suggest molecules diffusing in the interstitial medium or through the gap junctions can spread activity from cell to cell and may modulate myometrial contractile excitability.

2.3.4.3 Interstitial Cells of Cajal-Like Mechanoreceptors

Interstitial cells interact with and form electrical connectivity with smooth muscle cells in many organs, and these cells provide important regulatory functions. In the gastrointestinal system for example, interstitial cells of cajal (ICC) are well described in detail, and represent distinct classes of cells with unique structure and functions such as pacemaker activity, propagation pathways for slow waves, transduction of inputs from motor

neurons, and mechanosensitivity (Sanders, Ward, & Koh, 2014). In the bladder and gravid uterus, ICC-like cells are also suspected to have a mechanosensory function.

One of the most substantial functions of ICCs in gut is the capability to respond to mechanical stimulation, and consequently modulate intestinal peristalsis (Kraichely & Farrugia, 2007a; K.-J. Won, K. M. Sanders, & S. M. Ward, 2005). Likewise, during bladder filling, smooth muscle cells relax and lengthen to help maintain constant intravesical pressure, perhaps in response to signals from ICCs that sense the increase in volume (M. Drake et al., 2003). Studies have shown that obstructed bladders show increased proliferation of ICC-like cells in the muscular layer and in close communication with Smooth muscle cells in response to long term mechanical stretch (Hikaru Hashitani & Lang, 2010). Further, it has been found that bladder ICC-like cells have calcium transients, or membrane depolarisation independent of those of smooth muscles (H. Hashitani, 2006). It has therefore been hypothesized that bladder ICC-like cells may coordinate the sensory response to bladder-wall stretch and passively change the excitability of nearby smooth muscle cells to coordinated patterns of mechanical activity (Hikaru Hashitani & Lang, 2010) and thus be responsible for accommodation and bladder wall tone.

ICC-like cells have also been reported throughout the myometrium on the borders of smooth muscle bundles (Hutchings et al., 2009). Again, these cells are similar to ICC in the gut but a precise role for myometrial ICC-like cells has not been identified. However, having been identified in the myometrium, it is suspected that they have the potential to fulfil a role similar to those cells found in the gastrointestinal tract and urinary bladder for signal generation and coordination. Studies have shown that prior to synchronous intracellular rises of calcium in myometrial smooth muscle bundles, there are fluctuations in intracellular calcium in ICC-like cells (A Shmygol, Blanks, Bru-Mercier, Astle, & Thornton, 2006). This finding is important in that the site of origin and subsequent spread of the signal supports the possibility that the myometrial contractions are modulated by myometrial ICC-like cells.

2.3.4.4 Neuronal Mechanoreceptors

Bladder distension activates urothelium-innervating neurons with low and high response thresholds (Xu & Gebhart, 2008), suggesting that increases in bladder volume evoke variable perceptions (from filling to discomfort to pain) by activating additional classes of sensory neurons and coupling to higher order neural circuits and ultimately the pontine micturition centre (PMC) in the brain (Umans & Liberles, 2018). Bladder wall stretch also triggers mechanical responses in the urothelium, leading to release of chemical transmitters that can activate afferent nerves. One of the major neurotransmitters is adenosine triphosphate (ATP which) response magnitude correlates closely with the extent of tissue stretch (Vlaskovska et al., 2001). ATP-mediated control of bladder accommodation involves purinergic receptors on muscles onto which ATP binds. This leads to several downstream effects, including membrane depolarization and increased cytosolic Ca2+ and ultimately myosin phosphorylation and myocyte contraction (Hill, 2015).

Muscarinic (M#) receptors are also found in the bladder smooth muscle and urothelium, and on parasympathetic and sympathetic nerve terminals regulating acetylcholine (Ach) and noradrenaline (NA) respectively. M2 and M3 are the dominate subtype in the human bladder and stretch of the bladder wall has been associated with release of acetylcholine which binds to muscarinic receptors, leading to Ca^{2+} influx via voltage-gated Ca^{2+} channels (Griffin, Thornbury, Hollywood, & Sergeant, 2018). Evidence suggest that M3 receptors mediate bladder contraction (Yamanishi, Chapple, & Chess-Williams, 2001), while M2 receptors regulate smooth muscle tone (Eglen & Nahorski, 2000).

The neuronal and molecular mechanisms responsible for myometrial activation from the quiescent gestating state to the active contractile state during labour is only partially understood. Myometrial stretch has been implicated, clinically, in the activation of the myometrium for labour, but the mechanisms involved are unclear (Li et al., 2009). What is known is that that the uterus becomes essentially denervated during gestation (Haase, Buchman, Tietz, & Schramm, 1997; Latini et al., 2008). During early pregnancy the uterus is innervated by postganglionic adrenergic and cholinergic fibres that form part of the autonomic nervous system (Owman, Rosengren, & Sjöberg, 1967; Thorbert, 1978), but most adrenergic and cholinergic nerves disappear at term

(R. Garfield, 1986; J. Marshall, 1981). As a result, it is unlikely that any coordinated nervous regulation of the myometrium is centrally orchestrated (Latini et al., 2008). However, it is speculated that what limited factors of neural control remain may have modulating effect (R. Garfield, Blennerhassett, & Miller, 1988). Acetylcholine remains an important factor in myometrial excitability throughout gestation, and noradrenaline an inhibiting factor at term (Bengtsson et al., 1984; Izumi, 1985; J. M. Marshall & Kroeger, 1973). Noradrenaline is present in the blood as a hormonal factor (Wuttke, 1989), but also suspected to be active in the uterus despite the absence of nerve fibres (Sheldon et al., 2015). Ultimately, regulation of myometrial functions during gestation, labour, and birth, is under considerable hormonal control.

2.3.5 Problems with Mechanoreception in Capacious Structures, and the Theory for Hierarchical Control of Tone.

If we observe the tissue of the detrusor and myometrium and ignore the many morphological and physiological complexities, collagen fibre crimps, interconnections between collagen fibres and the cell membrane, and spring-like elements within the muscle fibre, the individual myocyte can be described simply as a muscular-hydrostat. The most important feature of a muscular hydrostat is that it is a structure of constant volume. The myocyte is composed primarily of an aqueous liquid which is practically incompressible at physiological pressures (KIER & SMITH, 1985). In a muscular-hydrostat or other structure of constant volume, any change in one dimension will cause a compensatory change in at least one other dimension. This principle serves as the basis for the following analysis of structure and movement in muscular hydrostats.

As previously described, the bladder and myometrium stretch to accommodate a growing volume. Stretching causes thinning of the muscle wall and the elongation of the smooth muscle. Both the urinary bladder and gravid uterus organs are characterised by spontaneous muscle contractions (Maland, 1928; Charles S. Sherrington, 1892), therefore any contraction of a myocyte will result similarly result in orthogonal distension (Fig 2-15). If all the myocytes are similarly orientated in one direction i.e., longitudinally, and the organs

principal direction of propagation is in the longitudinal direction e.g., the terminal ileum, then any orthogonally orientated decrease in stress will not affect the organs principal direction of operation i.e., lengthwise shortening. However, capacious organs such as the urinary bladder and gravid uterus have their myocytes orientated both longitudinally and circularly, the result being that the myocytes have their axis orientated at a variety of angles to a given axis. Hypothetically, imagine a perfectly spherical organ whereby the long axis of the myocytes are randomly orientated over its surface. Given that contraction results in orthogonal expansion, when all the vectors of longitudinal contraction and width wise expansion are summed, the overall effects from width wise reduction will effectively decrease the effects of length wise accommodation. The net effect is that there would be the equal strain in all directions of the spherical structure because the relative contributions from longitudinally and orthogonally orientated myocytes are the same at all sites. In reality, this is not the case. The urinary bladder and gravid uterus are not completely spherical, both often being described as "pear" shaped, and nor are their muscle layers homogenous. The result will be that the stress will not be uniform over the entire organ and similarly hoop stress will differ in all 3 dimensions. Therefore, evidence suggests that the regulation of tone is not just a global phenomenon, but there must also be some adjustment at the local level.

Local adjustment of tone could be the result from the action of neural mechanoreceptors. There are typically considered to be two structurally distinct populations of bladder afferents; those with terminal receptive fields in the detrusor smooth muscle, and those in the vicinity of the urothelium (V. P. Zagorodnyuk, S. J. Brookes, & N. J. Spencer, 2010). The structural location of these two populations of afferents reflects the two current theories for how neurally mediated mechanosensation is triggered. The first theory is that initiation of afferent firing is caused by mechanical deformation of the urothelial layer and detrusor smooth muscle. This type of mechanosensitivity is dependent on the distortion of mechanically gated ion channels on peripheral varicosities innervating both the muscle layer and the sub-urothelial layer (Xu & Gebhart, 2008; V. P. Zagorodnyuk et al., 2007).

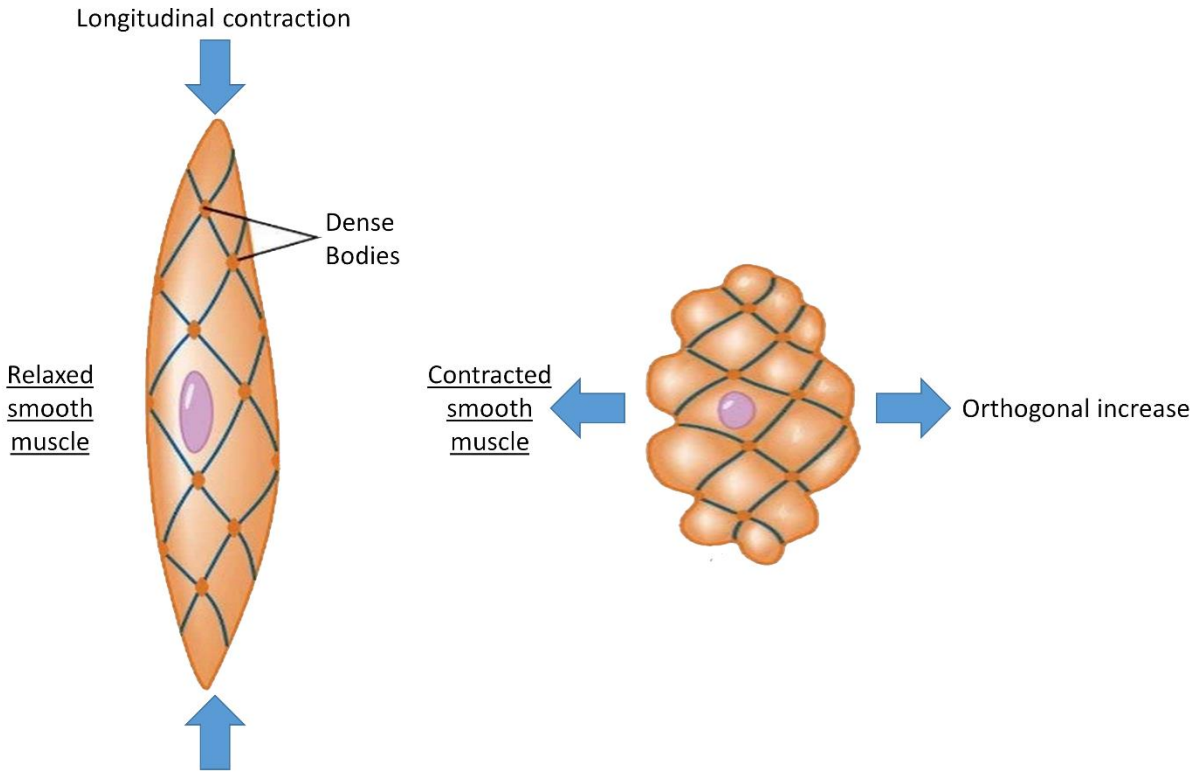

Figure 2-15 Change in myocyte morphology as a result of longitudinal contraction.

A myocyte contracting along its long axis will result in a corresponding increase in the orthogonal direction.

These respond to either muscle stretch and act as in-series or in-parallel tension receptors to distort the urothelium. In-parallel, mechanoreceptors respond to stimuli that elongate the organs wall while in series, mechanoreceptors respond to stimuli that increase the tension within the tissue wall. In series, mechanoreceptors are activated during distension and during contraction against a resistance; they are inactivated during relaxation. In parallel, mechanoreceptors are activated during distension and relaxation and are inactivated during contraction (Tack & Sifrim, 2000). Evidence suggests the bladder (Iggo, 1955) and myometrium (R. C. Young & Barendse, 2014) tend toward an in-series tension model.

The second theory is that of an indirect mechanosensation mechanism through the release of mediators from the urothelium which either directly activate sub-urothelial afferents or have a modulating influence over their mechanosensitivity.

In the myometrium, work has also shown there is a relationship between membrane excitability properties and intracellular mechanisms that leads to cellular contractions (S Wray et al., 2015). Myometrium is an excitable tissue in which contraction can be induced by an action potential in response to membrane depolarization that opens voltage-gated Ca^{2+} channels, especially the L-type Ca^{2+} channel, leading to an influx of extracellular Ca^{2+} that increases intracellular free Ca^{2+} and triggers the contractile machinery.

During gestation, the myometrium must remain quiescent but at term switch to a state capable of producing a series of forceful contractions so as to expel the foetus. This quiescent state usually is maintained until foetal development is sufficient for extrauterine life, at which point speculated mechanisms that were described above precipitate conversion to a highly contractile state. Frequent contractions that consistently generate high uterine pressures are necessary and sufficient for labour (Arpad Csapo, 1970). Therefore, in order to achieve high pressures, the uterus must somehow contract most areas at the same time. Therefore, a local increase in wall tension activates mechano-sensitive cells in the uterine wall. With contraction of another region, intrauterine pressure rises even more, wall tension throughout the uterus increases again, more mechanosensitive cells are activated, and more regions are recruited to participate in contraction. The process then repeats. This mechanism can be summarized as ‘pressure-tension-mechanotransduction’ (R. C. Young, 2016). Similarly, recent work has shown that there may be afferent modulating of contractility in the myometrium with the identification of a new population of ICC-like cells throughout the myometrium on the boarders of smooth muscle bundles (Hutchings et al., 2009).

Whatever the trigger, an adjustment of tone at one site will influence that in neighbouring sites. Hence, a mechanoreceptor mediated increase in myocyte length at one site will reduce tension and mechanoreceptor activation in longitudinally aligned sites whilst its associated decrease in width acts to increase tension and

mechanoreceptor activation in orthogonally orientated sites so that adjustment is patchy and circumscribed. Again, if the circumferential stress varies with dimension, any tension dependent propagation may take place in the dimension that is orthogonal to that of longitudinal relaxation.

We therefore hypothesise that the process of maintenance of tone in the described capacious structures generally involves a hierarchy of myogenic and neurogenic control systems and is more dynamic than previously thought. Hence during accommodation such structures exhibit frequent local, mechanoreceptor based tonal revision that can be modulated by various hierarchically higher mechanisms. The modulating action of the latter is generally more evident during voiding and is less well understood. Hence for example there is ongoing debate as to whether the intensification of local contractile activity during the voiding of uterine contents during labour results from the resetting of the mechanoreceptor threshold of tonal contractions or the instigation of peristaltic-like phasic contractile activity.

3 A Review of the Methodologies for the Measurement of Bladder and Uterine Contractility

Bladder spontaneous contractions or were first described in 1882 in human females and dogs (A Mosso & P Pellacani, 1882), and subsequently in a range of species including monkeys and cats (Charles S. Sherrington, 1892). Activity of the uterus was also described in the late 19th century with Friedrich Schatz being the first to measure *in vivo* uterine contractility during parturition in 1872 (Schatz, 1872). Since these early rudimentary recordings, many advances have been made to measure the contractile behavior of the bladder and gravid uterus. These methodologies will be briefly described below, highlighting their ability, advantages, and limitations when it comes to measuring detrusor and myometrial smooth muscle contractile activity.

3.1 Isolated Muscle Strips

Isolated tissue bath methodologies have been used to study smooth muscle contraction for over 100 years (Jespersen, Tykocki, Watts, & Cobbett, 2015). Tissue removed from an anaesthetized animal (or in the case of human uterine tissue post labour, or during biopsy), is placed in Krebs solution, and cut into strips. Strips are placed into a chamber filled with warm Krebs solution. One end is attached to an isometric tension transducer to measure contractile force, the other end is attached to a fixed rod. Tissue is stimulated by directly adding compounds to the bath or by electric field stimulation electrodes that activate nerves, similar to triggering contractions *in vivo*.

In the bladder, this experimental method can be used to evaluate spontaneous smooth muscle contractility, the nature of neurotransmission, factors involved in modulation of smooth muscle activity, and the role of bladder individual components. Similarly, uterine tissue can be used to investigate factors and molecules involved in the modulation of myometrial contractility and to determine their excitatory of inhibitory actions.

Moreover, the isolated tissue bath allows for the characterisation of novel pharmaceutical compounds on both tissues and concentration-dependant modulation of contraction frequency, force and duration can be measured.

The primary advantage of the isolated tissue bath technique is that the tissue is living, with a physiological outcome (contraction or relaxation) that is relevant to the body. Further, retaining tissue function allows calculation of important pharmacological variables that are more meaningful in a tissue vs. a cellular setting i.e., it comes closer to how drugs examined would work in the body as a whole.

Although this method is technically feasible and with good reproducibility, there are several limitations. This is an *in vitro* method of a reduced preparation; the tissue having been removed from its normal structural orientation i.e., its position within the organ as a whole. Further, the method cannot account for changes in blood flow, hormones, humeral substances, external mechanical forces, or extrinsic neural control. The tissue is also acutely decentralized; thus, injury and ischemia related responses need to be evaluated and considered. Further, data generated describes mostly tensile information on the tissue rather than detail on the contractile intricacies of the tissue.

3.2 Electromyography

Resting action potentials of bladder and uterine smooth muscle have been extracellularly recorded from isolated, viable smooth muscle cells via patch clamp electrodes (Hikaru Hashitani, Brading, et al., 2004; Klöckner & Isenberg, 1985; Montgomery & Fry, 1992; Roger C Young, Smith, & McLaren, 1993). This has shed important information on the resting potentials of smooth muscle cells, action potentials, and also propagation of membrane currents and other associated electrophysiological phenomena. In contrast, electromyography (EMG) is the clinical technique of recording the biological electrical activity generated during contractile

activation of a muscular organ *in situ*, using extracellular electrodes. The value of this method to measure whole organ electromyographic contractile phenomena in the bladder and uterus is controversial and varied.

The recording of a bladder (EMG) from the surface of the body would be useful as a relatively non-invasive measure of detrusor function, as well as provide more fundamental information about the electrical activity of this organ. Unfortunately, attempts to record EMG activity in the bladder has been very difficult. Studies have reported EMG activity (Cosgrove, LaJoie, & Jones, 1977; Craggs & Stephenson, 1976) but in contrast to the electromyography of skeletal and cardiac muscle, detrusor smooth muscle electromyography has remained in its infancy despite 50 years of scientific effort (Andrew Ballaro, 2008). Of the studies that have reported EMG activity, most have been criticized as the signals may have been contaminated by other electrical potentials, arising from pelvic floor musculature, other abdominal smooth muscles, and the electrocardiogram (ECG), as well as by mechanical artifacts from bladder and urethral contraction physically moving the recording electrodes (Jünemann et al., 1994). Therefore, there remains problems with bladder electromyograms with regard to their relevance, interpretation, and existence.

Uterine electromyography, also known as electrohysterograms (EHG), has proved to be one of the most valuable tools for the evaluation of uterine contractions and the electrophysiological state of the uterus (Escalante-Gaytán et al., 2019). The EHG allows for the measurement of the bioelectrical signal resulting from the propagation of action potentials in the myometrium. The uterine electrical activity is recorded through electrodes located in the abdominal wall. However, EHG measurement requires considerable computing power to attenuate signals such as skeletal muscle electromyogram, maternal electrocardiogram, breathing, and movement artifacts. Moreover, ECH also needs to incorporate data processing programs, which are used to perform frequency analysis, spectral filtering, or spectral temporal mapping functions to specifically quantify electrical signals produced by the uterine muscle (Devedeux, Marque, Mansour, Germain, & Duchêne, 1993). Ultimately the analysis of these electrical signals is complex and provides information on uterine contractility at a macro scale (i.e., contractile activity, propagation, and pacemaker insight) but very little detail elsewise on uterine wall contractile activity.

3.3 Pressure Based Sensors

Cystometry, also known as flow cystometry, is a clinical diagnostic procedure used to evaluate bladder function. Specifically, it measures contractile force of the bladder when voiding. The first experiments using pressure sensors to monitor the urinary bladder were conducted by Brindley (Brindley, 1977). A fluid-filled capsule was sewn onto the bladder wall, such than it invaginated the bladder. The method has now evolved to part of urodynamic study (UDS).

A urodynamic study involves the insertion of a catheter into the bladder. The catheter allows the bladder to be emptied completely. It is also used to measure the amount of urine in the bladder after micturition. The catheter measures the strength of the bladder by recording pressure. Another small catheter is inserted into the rectum and used to measure pressure on the outside of the bladder. The bladder is slowly filled with sterile saline and pressure within the bladder recorded. Pressure at micturition will also be measured as part of the test called Pressure Voiding Study (or pressure flow study).

UDS is a complex procedure and small modifications have a large impact on UDS data collection and only rigorous quality assessment allows for satisfactory interpretation (Rosier et al., 2017). The technique is vulnerable to such variables as bladder compliance, urine leakage, the total duration of the UDS effecting detrusor and sphincter activity. Patient pitfalls include voiding phase inhibition, movement, and positional artifacts. Therefore, UDS studies have long been resistant to easy standardisation, although some models have recently been proposed (Solomon et al., 2018). UDS is the only method that can objectively access function/dysfunction of the lower urinary tract (Blok et al., 2019; C. W. Collins & Winters, 2014) but offers little insight into changes in bladder anatomy and detrusor muscle function (Pewowaruk et al., 2020)

An intrauterine pressure catheter (IUPC) or transducer is a device placed inside a pregnant women's uterus to monitor uterine contractions during labour. The catheter measures the pressure within the amniotic space during contractions and estimates strength, frequency, and duration. Montevideo units (MVUs) are calculated by subtracting the baseline uterine pressure (resting tone) from the peak contraction pressure of each

contraction in a 10-minute window and adding the pressures generated by each contraction; this sum is the number of MVUs.

IUPCs are used when external monitoring is not sufficient, or when high-risk pregnancies necessitate highly accurate readings. However, IUPC is not recommended for routine use due to potential complications (Mandile, 2017). IUPC use is associated with increased risk for bacterial infection, maternal fever, and need for surgical delivery. Moreover, like the pressure data generated by urinary catheters, information gleaned from IUPC is prone to be erratic. This errant behaviour manifests as elevated baselines, decreased contraction maximum pressures, and incorrectly decreased contraction intensity (Beeson & Martens, 2004). Measurements of baseline and peak pressures in the uterus are not reproducible, even with properly calibrated equipment (W. R. Cohen, 2017). Pressures vary according to the position of the catheter/transducer within the uterus and with patient posture. Similarly, like urinary catheters, IUPC are only a measure of contractile pressure and do not give detail on myometrial smooth muscle contractile and accommodative dynamics.

3.4 Magnetic Resonance Imaging (MRI)

MRI and image based patient specific computational models have been extensively used for cardiovascular evaluation and personalized treatment planning (Baillargeon, Rebelo, Fox, Taylor, & Kuhl, 2014; Marsden & Feinstein, 2015; Taylor & Figueroa, 2009; Taylor & Steinman, 2010) as well as becoming a well-established tool for the study of pelvic morphology and function (Bø, Lilleås, Talseth, & Hedland, 2001). However, the use of non-invasive methods for the study of lower urinary tract anatomy and function has been limited (Pewowaruk et al., 2020) and only recently have pilot studies focussed on MRI as a tool for attempting to describing bladder contractile activity.

Studies have used real time MRI (rtMRI) as a means to measure anatomical changes in the bladder during fluid dynamic studies and voiding (Hocaoglu et al., 2012; Pewowaruk et al., 2020). They describe the interaction

between the bladder, urethra, and pelvic floor, but are absent is their capacity to describe in detail bladder wall contractile behaviour. MRI machines often used for clinical evaluation of patients with bladder or prostate-related diseases (Guneyli et al., 2017; Wasserman, Spilseth, Golzarian, & Metzger, 2015) are often of insufficient resolution thus requiring demanding additional assumptions when performing even volumetric measurements (Pewowaruk et al., 2020). In sum, bladder MRI studies, while providing insight into how changes in anatomy might affect urine storage and voiding, they are at this time unable to measure the subtleties of bladder wall compliance and contractile behaviour.

MRI is also seen as a promising technique for measuring and quantifying gravid uterine contractile activity in a non-invasive way. Unfortunately, like the rtMRI imaging of the bladder, the technology is in its infancy. Uterine rtMRI contractile measurement is confounded by intra-uterine factors such as foetal movement, and also extra-uterine factors including maternal respiration and other organ motion, such as bowel peristalsis (Coakley et al., 2004; Prayer, Brugger, & Prayer, 2004). As a result, studies using rtMRI to access human uterine contractility in during early gestation require captured data to be filtered with tracking algorithms (Martin et al., 2020). Subsequently, data presented described increased contractile frequency with increased gestation as well as a dominant direction of contraction (superior to inferior direction). Unfortunately, like seen in the bladder, limitations in uterine rtMRI fails to be able to describe uterine wall contractile activity in any substantive detail.

3.5 Ultrasound

Transabdominal ultrasound is non-invasive and well tolerated by patients. Nagle et. al. (2018) describe the novel use of ultrasound during urodynamic studies to measure several new biomedical properties of the bladder wall including wall tension, wall strain, wall stress, and dynamic elasticity (Nagle, Klausner, et al., 2017).

Described simply, the method uses theoretical models of bladder wall volume and strain and applies these models to clinical data collected including intravesical pressure (p_{ves}), analyses of sequenced two-dimensional (2D) ultrasound images of the bladder, and info from a patient controlled handheld sensation meter (Nagle, Speich, et al., 2017). The method uses advanced maths correlated with bladder wall measurements to estimate, rather than directly measure bladder wall parameters. Detrusor elasticity and stress were correlated with "patient sensation" (derived from the handheld receiver) and thus a mechanistic assessment of how the bladder wall functions was derived. Like other methods previously described, the method lacks the ability or detailed resolution to directly quantify detrusor smooth muscle contractile activity.

Ultrasonic demonstration of myometrial contractions in pregnancy have been observed since the 1970's (R. L. Wilson & Worthen, 1979). However, most ultrasonic techniques have focussed on assessing the welfare of the foetus *in utero* rather than the contractile behaviour of the uterus itself (L. H. Cohen, 1972; Kurjak, Latin, Mandruzzato, D'Addario, & Rajhvajn, 1984; Marsal, 1983; McHugh, McDicken, Bow, Anderson, & Boddy, 1978; Merkur, 1979; Willocks & Dunsmore, 1971). Some studies have however attempted to adapt the method of sonography to describe uterine contractile motility in the pregnant and non-pregnant uterus (Huang et al., 2018; Mischi, Rabotti, Kuijsters, & Schoot, 2015; Chiara Rabotti, de Lau, Haazen, Oei, & Mischi, 2013b; F Sammali et al., 2018; Federica Sammali et al., 2018).

Robotti et. al. described a method termed "mechanohysterogram" whereby observations of the mechanical properties of the uterus during pregnancy and during contractions were measured by transabdominal ultrasound (Chiara Rabotti et al., 2013b). Uterine movements were detected by 2D ultrasound and the effect of uterine movements on the abdominal surface was measured with a 3D accelerometer placed on the abdomen. The study is the first to continuously observe contractions in the pregnant uterus during pregnancy, but the results were limited in their scope. The mechanohysterogram revealed a change in thickness of the uterine wall during contraction, but results were confounded by placenta location, maternal obesity, and foetus position. Also, myometrial contractile velocity recorded was also lower than those reported in electrohysterogram studies (W. J. Lammers, 2013; Lucovnik et al., 2011; Chiara Rabotti, Mischi, Oei, &

Bergmans, 2010). Therefore, the viability of ultrasonic measurement of myometrial smooth muscle contractility is currently questionable and is certainly unsuitable for describing and measuring the complex contractile dynamics of the gravid uterus wall in any detail.

3.6 Whole Organ Animal Model Preparations

An ideal circumstance in the goal to investigate the mechanisms of detrusor and myometrial contractility would be having the ability to accrue all essential experimental details from human-derived tissue. However laudable, this goal is unrealistic. In animal models it usually is possible to get optimal experimental samples, and in regard to gestation samples, at precisely calculated time points. In contrast, collection of the most appropriate human samples is rigidly regulated by clinical, ethical, and even economic considerations (Mitchell & Taggart, 2009). Therefore, physiologists have turned to animal models, although because physiological differences between species exist, experiments on animal models must be carefully designed and interpreted.

Lower urinary tract function has been investigated in a variety of animal models (de Groat, Griffiths, & Yoshimura, 2015), mostly on cats and sheep in the past, whereas recent studies have focussed on rodents, rabbits and pigs (Balasteghin, Nardo, Amaro, & Padovani, 2003; Bijos & Drake, 2015; Chakrabarty et al., 2019; Lentle et al., 2015a; B. A. Parsons, M. J. Drake, A. Gammie, C. H. Fry, & B. Vahabi, 2012; Sartori, Kessler, & Schwab, 2021). *In vivo* urodynamic studies have been performed in anesthetised, restrained, and freely moving animals allowing for the collection of such data as bladder pressure, bladder compliance, intravesical pressure (Pves), flow rate and voiding frequency (Sartori et al., 2021). Although these observations are important, only until recently has *ex vivo* direct measurement of detrusor activity been observed and quantified.

Several studies in the *ex vivo* rat, guinea pig, and pig bladder have directly visualised detrusor contractility and attempted to quantify its activity (Bijos & Drake, 2015; Chakrabarty et al., 2019; M. Drake et al., 2003; Marcus J Drake et al., 2003; B. A. Parsons et al., 2012). The method involved isolated bladders, and using multiple-point

motion analysis, it was shown that the bladders of these various species exhibited micromotions which could be observed with and without changes in intravesical pressure. However, the above studies were unable to describe the intricacies of detrusor contractile activity. This was due to the technique having limited ability to delineate the area of tissue that is contracting, or its rate and direction, as a large number of marker points are required to identify and track the area of contraction. Therefore, measurements of contractile muscle activity including velocity, duration, propagation, and area of contraction were unable to be quantified.

Rats are widely used in biomedical research of gestation and parturition because of their physiological and anatomical similarity with humans (Malik, Roh, & England, 2021). On the other hand, many studies related to parturition, stress, and pain in other mammals such as mares, cows, and mice, have helped to understand neurobiological characteristics of parturition such as the parasympathetic predominance during the expulsion of the foetus (Martínez-Burnes et al., 2021). Scientific descriptions of direct myometrial contractile activity in animals are few and are even rarer in gravid uteri.

Most *ex vivo* analyses of whole organ uterine contraction consists of maintaining the organ in organ baths. Moreover, many e*x-vivo* uterine preparations are restricted to rodent models where the tissue is able to survive in oxygenated Krebs or PBS by simple diffusion (Dodds et al., 2021; Liang, Bursova, Lam, Chen, & Obukhov, 2019; Refuerzo et al., 2016). In larger specimens e.g., human and porcine uteri, the tissue can be perfused to maintain viability (Geisler et al., 2012; Richter et al., 2006). The main advantage of the whole organ model is that the reproductive tract is intact, preserving all intrinsic intrauterine cellular interactions. However, organ bath preparations have several limitations. Since the myometrium is very sensitive to compressions or pulls, this complicates the dissection process of the reproductive tract. If the horns are damaged during dissection, no spontaneous contractility will be observed. This is a major limitation of the protocol because it is uncertain whether the contractile smooth muscle cells were unknowingly damaged despite the use of proper care and caution or whether they lacked motility due to natural causes (Liang et al., 2019).

Various studies have been able to characterise *ex vivo* contractile motility using a single method or a combination of methods. Contractile frequency, amplitude, direction and velocity, action potentials and intraluminal pressure have been recorded using a combination of spatiotemporal mapping, pressure, and electromyography recordings (Dodds et al., 2021; Geisler et al., 2012; Richter et al., 2006). Further, motion tracking algorithms have been used to measure spontaneous contractile motility between the proximal part of the vagina and the middle segment of a uterine horn (Liang et al., 2019). Although the description of all these contractile phenomena is important, results are limited to the non-pregnant uterus. Moreover, there is a failure to measure the timing and propagation of tonic and phasic contractions that result from these events and the manner of their progression through and over the surface of the uterus.

Preface: Chapter 4

Chapter 4 introduces the primary methodology used in this thesis, that being spatiotemporal mapping. The proceeding review chapter defines what spatiotemporal mapping is, describes the evolution of various techniques, their strengths, weaknesses, and limitations. In sum, spatiotemporal mapping is a powerful tool for the measurement of activity at one or multiple locations on the tissue surface of a smooth muscle organ. Spatiotemporal maps can provide data on motility direction (i.e., stationary, peristaltic, anti-peristaltic), velocity, duration, frequency, and strength of contractile motility patterns. Moreover, spatiotemporal mapping enables the analysis of interaction or simultaneous development of different motility patterns in different regions of the same organ, visualization of motility pattern changes over time, and analysis of how activity in one region influences activity in another region.

Copy of Paper- Quantifying Patterns of Smooth Muscle Motility in the Gut and Other Organs with New Techniques of Video Spatiotemporal Mapping

The following pages contain a copy of the published journal article with the following bibliography-

Lentle, R. G., & Hulls, C. M. (2018). Quantifying patterns of smooth muscle motility in the gut and other organs with new techniques of video spatiotemporal mapping. Frontiers in Physiology, 9, 338.

The main format of the publish peer-reviewed article is reproduced in this chapter section with its format and content maintained. All references cited are listed in a separate sub-section after the main body of the article. These references would be reproduced in the main bibliography of this thesis (i.e., after the thesis appendix) only should they be used elsewhere beyond this section (i.e., of this published article). All further work beyond this section will be citing the work presented in this section where appropriate.

4 Quantifying patterns of smooth muscle motility in the gut and other organs with new techniques of video spatiotemporal mapping.

4.1 Abstract

The uses and limitations of the various techniques of video spatiotemporal mapping based on change in diameter (D-type ST maps), change in longitudinal strain rate (L-type ST maps), change in area strain rate (A-type ST maps) and change in luminous intensity of reflected light (I-maps) are described, along with their use in quantifying motility of the wall of hollow structures of smooth muscle such as the gut. Hence ST-methods for determining the size, speed of propagation and frequency of contraction in the wall of gut compartments of differing geometric configurations are discussed. We also discuss the shortcomings and problems that are inherent in the various methods and the use of techniques to avoid or minimise them. This discussion includes the inability of D-type ST maps to indicate the site of a contraction that reduces the diameter of a gut segment, the manipulation of axis (the line of interest) of L-maps to determine the true axis of propagation of a contraction, problems with anterior curvature of gut segments and the use of adjunct image analysis techniques that enhance particular features of the maps.

Definitions

Compliance of the wall: the ability of the wall of a hollow structure to undergo deformation from increase in luminal pressure. The reciprocal of stiffness.

D-map; A spatiotemporal (ST) map based on changes in the diameter i.e., number of pixels between the upper and lower border at an array of locations along the length of a hollow tubular structure over time.

Phase; The position of a point in time on a waveform measured in degrees.

Phase difference or offset; Difference in in degrees of phase between two waveforms at a particular point in time

R-map; An ST map based on a longitudinal sequence of changes in the distance in pixels from either the upper or lower border of a tubular structure to the edge of a marker or structure that is positioned longitudinally along the centre of the profile e.g., a colonic taenia,

Strain; degree of deformation induced by an application (or removal) of a force to a tissue such as the gut wall. Positive strain i.e., an increase in distance between two markers, occurs with a tensile force and negative strain i.e., an increase in the distance between two markers, occurs with a compressive force

Strain rate; the rate at which positive or negative deformation takes place

Area strain; the deformation in along the diametric side of square of a tissue in the gut wall multiplied by the degree of deformation of the longitudinal side consequent on the application of a (contractile or other) force.

Area strain rate; Rate of change in the area of a square of tissue in the gut wall consequent on the application of a (contractile or other) force.

4.2 Introduction

The use of video spatiotemporal maps to define the timing and site of smooth muscle contraction has rapidly increased over the last decade, such that over 1,500 reports have been published since the late 1990s. Until recently the techniques had been used to quantify movements in various components of the gut. In this context the technique has provided valuable insights into the genesis and control of contractile activity in the gut as well as providing a source of reciprocal illumination in which to view electro-physiological findings. Hence, spatiotemporal mapping has proven useful in determining how specific receptors (Abdu, Hicks, Hennig, Allen, & Grundy, 2002) microflora (J. Collins, Borojevic, Verdu, Huizinga, & Ratcliffe, 2014) genetic mutations (R. R. Roberts, Bornstein, Bergner, & Young, 2008) or pharmacological interventions (Bogeski, Shafton, Kitchener, Ferens, & Furness, 2005; Schreiber et al., 2014; Nicholas John Spencer et al., 2013) alter motor activity in the relevant organ. Moreover, the concurrent use of longitudinal and radial mapping allows for resolution of the contributions of the circular and longitudinal muscle (Lentle et al., 2008) and the spatial resolution of the outputs of the neural circuitry (Lynn, Zagorodnyuk, Hennig, Costa, & Brookes, 2005). Further, the use of recently developed area ST mapping techniques can allow the pattern of growth and propagation of fronts or areas of smooth muscle contraction across the surface of large hollow organs such as the bladder to be mapped (Lentle et al., 2015b) and their effects of tone to be surveyed (R. G. Lentle, G. W. Reynolds, C. M. Hulls, & J. Chambers, 2016).

A particular advantage of the spatiotemporal mapping method is that it avoids the insertion or application of monitoring devices into, or onto, the surface under study. This avoids the generation of artefacts such as those that may result from movement of electrodes relative to the tissue and the ensuing debates as to the validity of the observations (O. Bayguinov, Hennig, & Sanders, 2011). Hence, for example, the debate as to whether electrical changes recorded during contraction have a real physiological basis or result from relative movement between the smooth muscle cells and the electrode (A Ballaro, Mundy, Fry, & Craggs, 2003). Again, the lack of any requirement for surface contact during ST mapping and consequent low risk of contamination could make the technique potentially useful during laparoscopy provided that small video cameras with sufficient image

definition are available. Hence, ST mapping of laparoscopic video sequences could be useful in mapping the contractile outcome of conditions such as diabetic gastroparesis that are known to be accompanied by adverse electrophysiological states such as slow wave dysrhythmias and re-entrant rhythms (J. Chen & McCallum, 1992). Spatiotemporal mapping can provide a stream of real time data regarding the frequencies, speeds and directions of propagation, amplitudes and durations during progression of a contraction through the walls of a hollow tubular or sacculate structures (Fig 4-1) that can subsequently be incorporated into computational fluid dynamic models to assess their effect on the mixing and on flow of their contents (Clément de Loubens et al., 2014).

Whilst alternative methods such as water perfused (Di Lorenzo et al., 2002) and fibreoptic (P. Dinning et al., 2014b) catheters and barostats (Ohe, Hanson, & Camilleri, 1994) can be used to directly assess changes in the pressure within the lumen of such structures and thus to infer motility, they generally do not provide sufficient spatial or dimensional resolution to enable the mixing regime to be accurately defined. Thus, the use of high resolution fibreoptic catheters that record local changes in lumen pressure at intervals of around one centimetre along the lumen (P. Dinning et al., 2014b), have similar limitations to those of early spatiotemporal mapping methods based on widely spaced markers (G. W. Hennig, Costa, Chen, & Brookes, 1999), notably being prone to aliasing. Hence, a number of types of contraction have short territories and frequencies that are not amenable to resolution with such spacing e.g. haustral boundary contractions in the colon which occupy less than 0.25 cm of the wall (J.-H. Chen et al., 2013). Again, the radial positioning of fibreoptic catheters within the gut lumen cannot be precisely defined or controlled. The current differences in the nomenclature of colonic contractions described by this (P. Dinning et al., 2014a) and by water perfused catheter techniques (Camilleri et al., 2008; Rao, Sadeghi, Beaty, Kavlock, & Ackerson, 2001) from that described by D-type spatiotemporal mapping (J.-H. Chen, Yang, Yu, & Huizinga, 2016; Costa, Dodds, et al., 2013; Philip G Dinning, Costa, Brookes, & Spencer, 2012; Lentle et al., 2008) is testament to such limitation.

4.3 The development of video spatiotemporal mapping techniques

In this section we describe the development of the various types of video spatiotemporal map and the advantages and disadvantages of each method. The progenitors of video spatiotemporal mapping techniques, described 18 years ago (G. W. Hennig et al., 1999) were based on changes in the outline of the organ (Fig 4-1A and B), and in the positions of regularly spaced markers, generally in the longitudinal dimension, which latter can be regarded as the mapping of strain (G. W. Hennig et al., 1999).

Ultimately, video spatiotemporal mapping comprises the comparison through time of the spatial position of an object or of distinctive features of the object. In this sense Edward Muybridge was the first to employ the technique to determine patterns of leg movement and of footfall in the galloping horse (Muybridge, 1887) . Later workers, notably Cannon (W. B. Cannon, 1898), compared the profiles of a succession of images that were drawn, filmed (W. C. Alvarez & Zimmermann, 1927; Tasaka & Farrar, 1969) or X-rayed (Bowditch, 1897; W. B. Cannon, 1898) to characterise the contractile behaviour of various segments of the gut.

The advent of video recording permitted the motion of distinctive features in an area under investigation to be followed through a stream of successive images taken at a uniform intervals whilst the development of image analysis techniques (Russ, 2006), allowed search algorithms to be successively applied to each frame to identify edges (Sobel, 1970), with subsequent plotting of the distances between them at successive points along the length of the segment of gut, a technique termed diameter or D-type mapping. This technique was originally applied to the small intestine of the rat maintained *ex vivo* (Benard, Bouchoucha, Dupres, & Cugnenc, 1997) and subsequently to the stomach (Berthoud, Hennig, Campbell, Volaufova, & Costa, 2002; Lentle, Janssen, Goh, Chambers, & Hulls, 2010), small (G. W. Hennig et al., 1999; Lentle et al., 2007) and large (P.G Dinning, Szczesniak, & Cook, 2008; Gwynne, Thomas, Goh, Sjovall, & Bornstein, 2004; G.W Hennig, Gregory, Brookes, & Costa, 2010; Lentle et al., 2008) intestine from a range of species maintained *ex vivo* as well as *in vivo* (P.W.M Janssen et al., 2014).

Whilst these video spatiotemporal mapping techniques allowed changes in the diameter and length of the walls of hollow tubular structures such as the gut to be quantified, the subsequent development of strain rate

mapping i.e., L-type ST maps (Lentle et al., 2007) and area strain rate (Lentle et al., 2015b) i.e., A-type ST maps allowed local changes in length and in area to be determined and plotted over time with higher resolution. This allowed the site of contraction of circular and longitudinal components of the *tunica muscularis* to be directly identified at all points within the borders of the image. Further, the rhythmic sequence of longitudinal and circumferential components could be simultaneously mapped along a user-defined line of interest located at a particular site on the intestinal wall (P.W.M Janssen et al., 2014).

4.3.1 D-type video spatiotemporal maps

4.3.1.1 Method and interpretation

D-type spatiotemporal maps are based on changes in the diameter of a segment or organ over time (Fig 4-1 A, B, C and D). Typically, edge detection algorithms (Russ, 2006) are used to search for and delineate the upper and lower edges of a tubular length of gut that is positioned with its long axis parallel to the upper and lower borders of the video frame (Fig 4-1). Edge detection algorithms, such as those described by Sobel (Sobel, 1970), Kirsch (Kirsch, 1971), and Frei and Chen (Frei & Chen, 1977) work well with ST mapping of preparations that are maintained *ex vivo* in a situation when there is good contrast between the optical characteristics of the preparation and the background (indeed many operators ensure that there is a uniform black or white colouration on the background surface of the organ bath). The total distances in pixels between the two edges are determined for every pixel column along the visible length of the preparation (Fig 4-1). The totals for successive columns are each then plotted as a shade or colour coded total per column so as to form a pixel row across the D-map (P.W.M Janssen & Lentle, 2013).

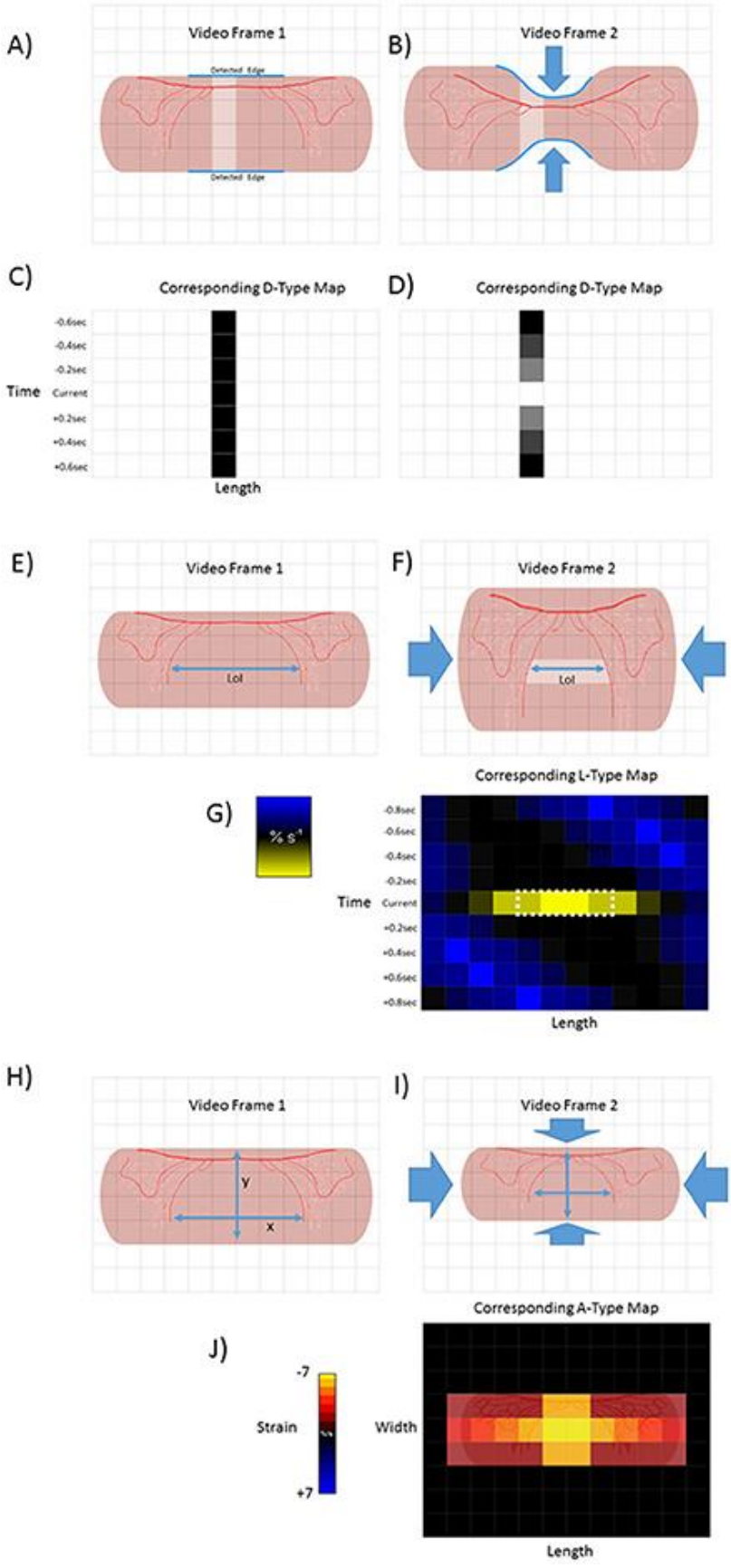
A)
Video Frame 1
Detected Edge
Detected Edge
B)
Video Frame 2
C)
Corresponding D-Type Map
-0.6sec
-0.4sec
-0.2sec
Time
Current
+0.2sec
+0.4sec
+0.6sec
Length
D)
Corresponding D-Type Map
E)
Video Frame 1
LoI
F)
Video Frame 2
LoI
G)
% s⁻¹
Corresponding L-Type Map
-0.8sec
-0.6sec
-0.4sec
-0.2sec
Time
Current
+0.2sec
+0.4sec
+0.6sec
+0.8sec
Length
H)
Video Frame 1
y
x
I)
Video Frame 2
Corresponding A-Type Map
J)
-7
Strain
+7
Width
Length

Figure 4-1 Basic methodologies of D-type, L-type, and A-Type video-spatiotemporal mapping techniques.

D-type ST maps A), B), C) and D). The upper and lower edges of a structure (in this case a pink tubular segment of gut) are detected (blue line) and the number of pixels counted between the edges of successive columns (pale area). The totals are then colour coded for each column within each frame (dark square in time series of D-type map below) (C). Circumferential contraction (frame 2) causes reduction in diametric profile and corresponding pixel total (light square in time series of D-type map below) (D).

L-Type ST maps E), F), and G). The line of interest (LOI) that is to be used as a datum point for quantification of lengthwise movement in successive frames is chosen (blue line). The colour coded magnitudes of changes in distance (strain) between distinctive features (in this case red vascular markings) on successive video frames (strain rate) are plotted for each pixel along the length of the LOI (in this case shown only for one set of distinctive features between video frame 1 and 2).

A-type ST maps H), I) and J). The diametric and lengthwise changes in distances between distinctive features (in this case red vascular markings) in successive frames are determined over each component pixel over a defined area within the edges of the structure. The derived diametric and lengthwise changes within each pixel in successive frames for are then multiplied to give area strain rate. The colour coded values for strain rate then overlaid onto the corresponding pixels of the video frame to produce a map of area strain. Hence map J), shows the hypothetical two-dimensional result of a contraction at a single point.

Thus, any site along the length of the gut where the diameter is relatively reduced will have a lower low pixel sum and be of a lighter (or darker) shade on the D-map than one at a site that is distended which will have a higher pixel sum. On such a map a propagating peristaltic contraction will generate a band of lighter (or darker) pixels of the D-map that shows lengthwise progression in successive rows (Fig 4-2). The duration of the contraction at any given point will be shown by its breadth on the time axis and its lengthwise extent by its breadth on the distance axis. Similarly, the speed of its lengthwise propagation will be directly proportional to the angle of the (lighter or darker) band to the time axis, greater angles indicating faster progression. Further, when a regular succession of contractile events occurs, their frequency can be determined at any point on the length of the gut component from the number of lighter bands that transect a line of known duration drawn from that point on the ST map parallel to the time axis. Again D-type ST maps are useful in identifying points along the length of the intestine at which the frequencies of contractions change (phase dislocations), which are seen on the D-map as points of fusion or bifurcation of individual propagating contractions. The sites and timings of these changes have been related to the coupled oscillator theory of propagation (Parsons & Huizinga, 2015) which hypothesises that the spontaneous oscillations in neighbouring interstitial cells of Cajal

(ICC's) become entrained within the limits of their respective inherent frequencies. Hence when the difference in the inherent oscillation frequencies of neighbouring ICCs reaches its limit there is a sudden change in the frequencies of their slow waves and corresponding contraction frequencies.

Currently there is no consensus regarding which axis of ST maps is displayed vertically and which is displayed horizontally. However, the convention used by a number of workers in which the length axis is vertical axis and time horizontal (J.-H. Chen et al., 2016; Costa, Dodds, et al., 2013; Philip G Dinning et al., 2012) may make the visualisation of rate easier as the slope described by the contractile event is more readily seen to be proportional to its rate of propagation and is similar in orientation to that used in most reports of catheter studies.

Darker areas on D-type ST maps, signifying relative distension of the lumen, can provide information regarding the movement of contents and their influence on the pattern of radial constriction. Hence, in the colon, a darkened zone propagating in advance of a diametric constriction may indicate displacement or accumulation of contents (Fig 4-3) (Lentle et al., 2008). Further, the triangular configuration of the (white) area of diametric constriction on the D-map indicates that the constriction persists at all sites until it has propagated along the entire length of the preparation whereupon relaxation, signified by the darker area, progresses from the distal to the proximal end. Such a contractile configuration would likely maximise the emptying of the viscid contents of the colon by preventing backflow.

A)

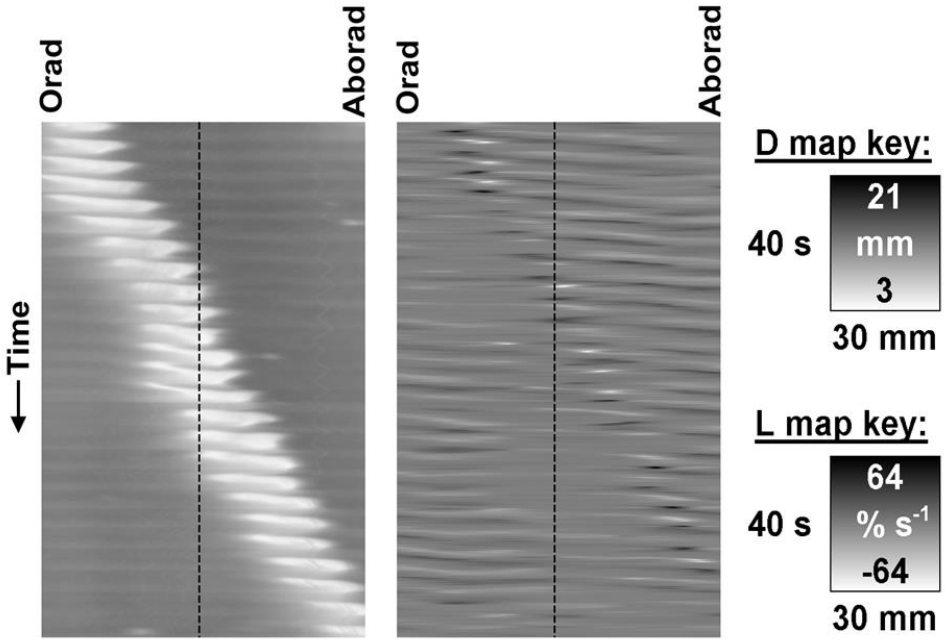

B)

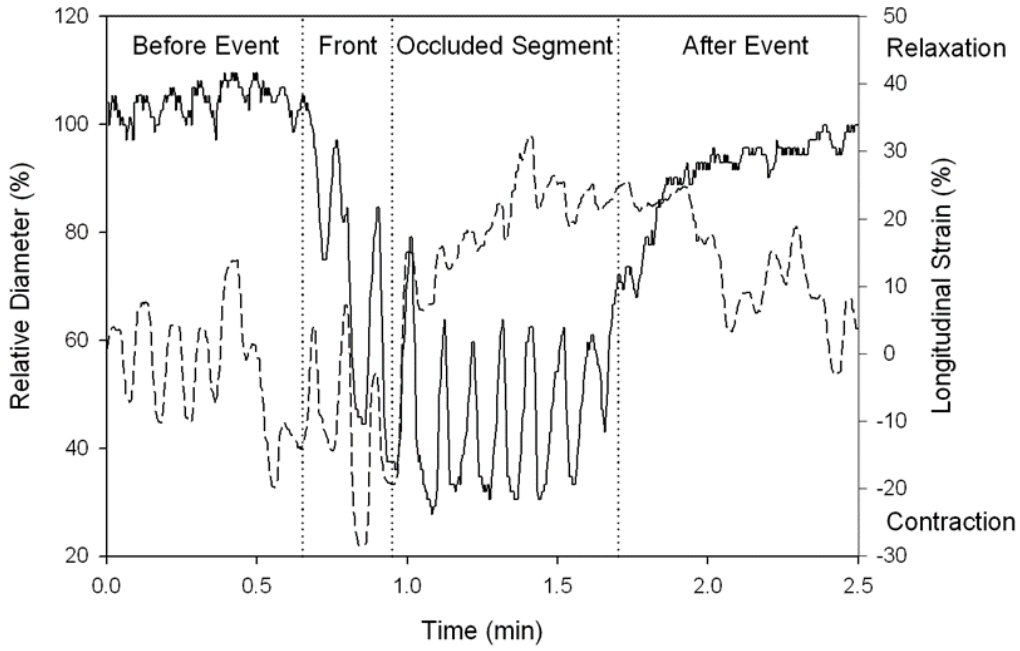

Figure 4-2 Synchronous (A) D-type (diameter type) ST map (left) and L-type (right) (linear strain rate) ST maps and graph of transects (B) showing progression of a peristaltic contraction though a segment of possum ileum.

A) Lighter areas on the D-map indicate sites along the length of the organ where the diameter is reduced and lighter areas sites where the diameter is increased. The thickness of the band measured vertically is the duration of the contraction. The thickness of the band measured horizontally is the length of the organ that is undergoing contraction at any given time. The angulation of the band to the vertical (time) axis is proportional to the velocity of propagation of the constricted area. Note the component horizontal 'stripes' on the D map which indicate rapid activation of successive regions of smooth muscle occurring at the slow wave frequency. Also note the darker shading i.e., distension in advance of the propagating lighter band than that in the rear showing that lumen contents are being propelled in advance of the constriction.

Lighter areas on the L map indicate sites of negative longitudinal strain rate i.e., constriction in the longitudinal dimension. Events at the vertical dotted line, placed at the same site in the two maps (fig 2B below), indicate that longitudinal shortening occurs in advance of the circular constriction.

Fig. 2B Coordination between D (solid line) and L (dashed) maps during a peristaltic event. Values were taken from the vertical line delineating a particular site on the synchronous D and L maps. Contractions are seen to be 180^0 out of phase prior to the peristaltic contraction and in phase during the contraction. The amplitude of circular contraction on the D map increased during the peristaltic event. *Figures adapted from (Lentle et al., 2007).*

4.3.1.2 Drawbacks

D-type spatiotemporal maps have several shortcomings. Firstly, in summing the total number of pixels at a given point along the length of the gut, D-maps sum the cumulative effects of smooth muscle contractions that occur at all of the sites across the diametric transect and do not describe the relative contribution of any localized contractions at particular points across the diameter. Hence, for example, while it is reported that there is anisotropy in the degree of contraction between the mesenteric and ab-mesenteric sides of the small intestine (Lentle et al., 2012), D-maps cannot identify the sites of such differences. This shortcoming is a particular problem at sites where the muscles associated with the upper and lower edges behave autonomously so that the edge profiles of the upper and lower edges do not correspond, for example during ripple contractions in the haustrated colon (Lentle et al., 2008). Hence, for example, at any given point on its length, the pixel sum on a D-map that reflects the overall reduction in diameter will be influenced by the extent to which the changes in edge profiles, which reflect ripple contractions in the upper and lower halves, are synchronised. This problem cannot be circumvented by incorporating an algorithm that determines the midpoint between the upper and lower borders of the gut and determines changes in each separate half (radial segment) as, if the two edges are moving independently or differently, both will affect the position of the midpoint at that instant. However, this problem may be countered in cases where there is a distinctive

longitudinally disposed structure on the cylindrical surface of the gut wall. With appropriate rotation, the edges of such a structure can positioned along the midline between the upper and lower edges of the image and used to subdivide the diametric dimension of the structure. Hence, for example, when the *taenia libra* is positioned midway between the upper and lower borders of the colon this structure provides a consistent basis on which to subdivide the image into upper and lower radial halves allowing a separate 'R'-map' to be plotted for each (Lentle et al., 2008). The use of this technique can allow the movements of colonic haustrae in each radial half of the preparation to be separately examined and subsequently compared (Lentle et al., 2008).

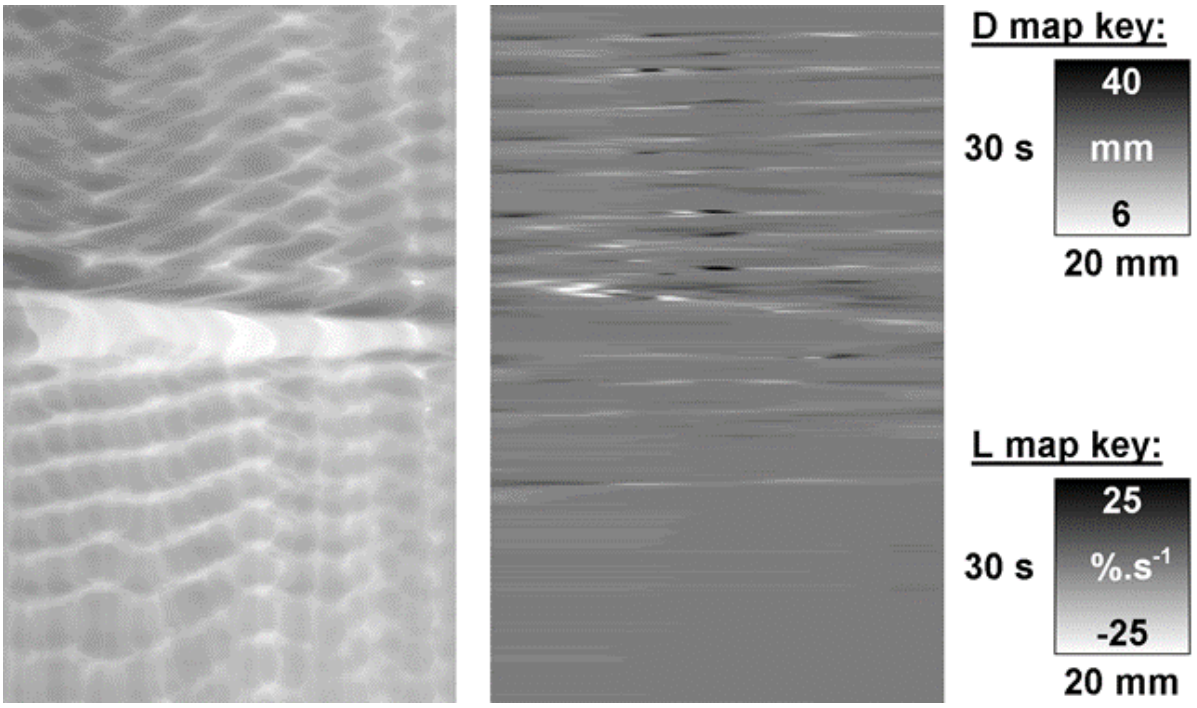

Figure 4-3 D-type ST map (left) and L-type ST maps (right) of a mass peristaltic event traversing the proximal colon perfused with saline.

The triangular white area on the D-map indicates a diametric constriction from mass peristalsis rapidly propagating from proximal to distal along the organ with a darker area from distension of the lumen by distally displaced contents travelling in advance. Note that the constriction propagates from proximal to distal, but relaxation progresses from distal to proximal as can be seen by the differences in the slopes of the onset and offset of the event and the consequent triangular configuration.

The angled track of narrow white areas (-ve strain rate) on the L map (right) indicate a sequence of short-lived longitudinal constrictions occurring in advance of the diametric constriction of peristalsis. Note that more regular and more rapidly and extensively propagating longitudinal constriction (likely fast phasic contractions) and column of episodic localised radial constriction (likely ripple contractions) occur at times when there are no peristalses. *Figure adapted from (Lentle et al., 2008).*

Even in situations where contractions within the diameter of a tubular element of the gut, such as the small intestine, arise synchronously in the upper and lower halves, problems can arise with assessing such characteristics as its speed of propagation. As stated hitherto, the velocity with which a contractile front propagates along a tubular length of gut is generally considered to be proportional to the angle of the track of the contraction with the axis defining time. However, if the contraction involves only a limited region of the visible intestinal wall, it is possible that it can propagate over a number of possible curved trajectories that are not aligned with the lengthwise axis of the organ, for example in a spiral course (Laforet, Rabotti, Mischi, & Marque, 2013; Z. S. Wang, He, & Chen, 2004). Hence, the true velocity of propagation will be greater than that shown on the D-map as the distance covered will be greater than the overall length of the segment.

A similar problem arises when assessing the direction in which contractions propagate through gut components that are not tubular in shape. Hence, when the passage of antral contraction waves through the stomach of the guinea pig is mapped across its three constituent sections (the proximal, middle and distal components of the stomach), with the pixel columns orientated at right angles to the longitudinal axes of symmetry in each section, the trajectory of the contraction on the D-map is of a sigmoidal configuration with respect to time and of varies in duration (thickness) (Berthoud et al., 2002). On the other hand, in another analyses of the transit of antral contraction waves in the rat stomach, when the pixel columns for the D-maps were positioned orthogonal to an arcuate axis of symmetry cantered on at the anterior limit of the junction of the oesophagus with the cardia (Fig 4-4A), the trajectory of propagation of antral contractions on the ST map was a straight line of near uniform breadth (Lentle et al., 2010) indicating that the velocity of propagation was constant as was the duration (Fig 4-4B). The principal of parsimony (Occam's razor) would favour the latter situation where the velocity of propagation is invariant and duration constant. Hence, plots of D-type ST maps based on principal axes of various geometries can thus be used iteratively to determine the direction of propagation of contractions across the surface of a non-tubular organ, assuming that the map will be linear when the geometry is aligned with the principal axis of propagation. Note that this method is broadly akin to the use of different LOI on which to base L-maps (see below).

A)

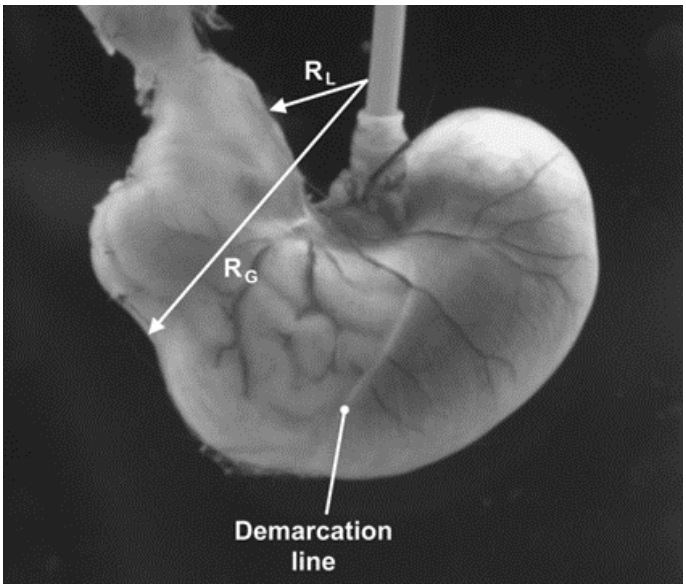
R_L
R_G
Demarcation line

B)

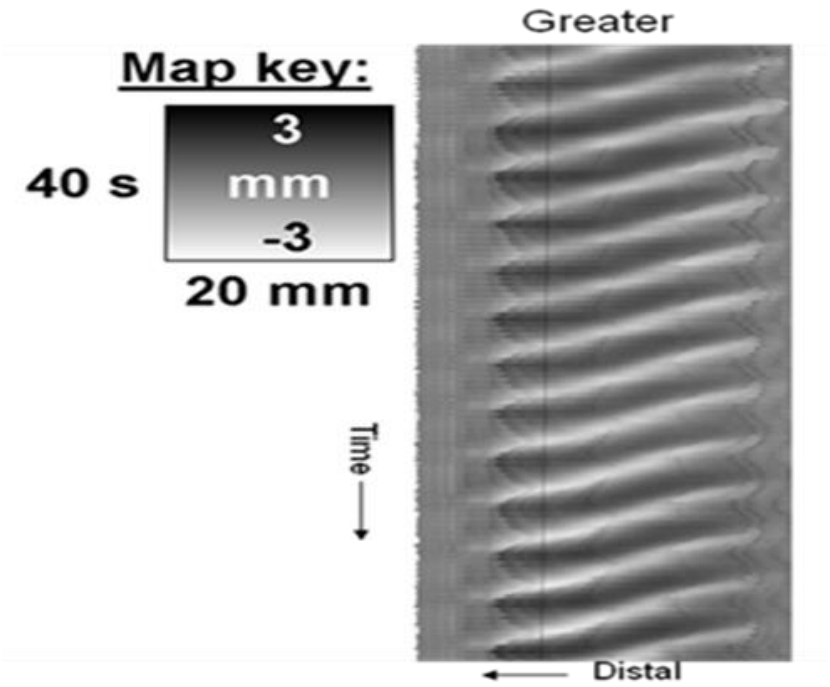
Greater
Map key:
3
mm
-3
40 s
20 mm
Time
Distal

Figure 4-4 D-type ST map of transit of gastric peristalses along an arc based near the greater curvature (abscissa) and centred at the anterior limit of the oesophageal junction.

A) Diagram showing the basis of the arc of curvature. Spatiotemporal maps are derived with the cumulative angle of deviation on the horizontal axis with the intensity proportional to the distance along the line to the lesser (RL) or greater (RG) curvature with lighter shading for longer and darker shading for shorter distances. The scaling of the raw maps can be converted to linear distance from the pylorus to enable linear velocity to be quantified.

B) D-type ST map showing the rhythmic sequence of angled lighter bands of radial constriction from regular antral peristaltic events. The uniform thickness of the bands indicates they are of constant duration regardless of their position with respect to the pylorus. The uniformly linear trajectory angled toward the pylorus (on the left) indicates that their velocity of propagation is uniform along the arc of the LOI. Note that the darker area lying to the right of each propagating contraction is from dilatation from retropulsion of contents and that the extent of this distension decreases near the pylorus presumably from increased thickness and decreased compliance of the distal walls. *Figure adapted from (Lentle et al., 2008).*

A third problem with D-type ST mapping arises from the effects of a contraction on the adjacent gut wall. Hence, a localised contraction of circular or longitudinal muscle occurring at a given site on a length of gut may cause the adjacent wall to be drawn toward it or to be pushed away. This may be due in part to the incompressibility of the tissue that is undergoing contraction. Hence, the contraction of the long axes of circularly orientated myocytes in the circular muscle layer of the gut wall will cause a simultaneous increase in their width as their fluid contents are incompressible, generating a lengthwise expansion that will displace adjacent uncontracted circumferentially orientated myocytes. Similarly, myocytes that are orientated longitudinally will expand circumferentially whilst contracting. Conversely, the inherent elasticity of the gut wall may draw any tissue that is undergoing active relaxation or accommodation towards it. At either event, a phasic contraction occurring in a length of gut will generate a change in the longitudinal disposition of the constituent and adjacent pixel columns in relation to the proximal and distal ends of the gut causing their column 'address' within the video frame to change, a process that we term 'shunting'. These problems can occur both *in situ* and *ex vivo* but can become particularly severe when lengthy sections of gut are mapped, for example an entire colon. In *ex vivo* preparations these problems may be exacerbated by sagging i.e., a tendency for the central region of a segment to sink within the organ bath during relaxation and rise during contraction. Whilst it is not

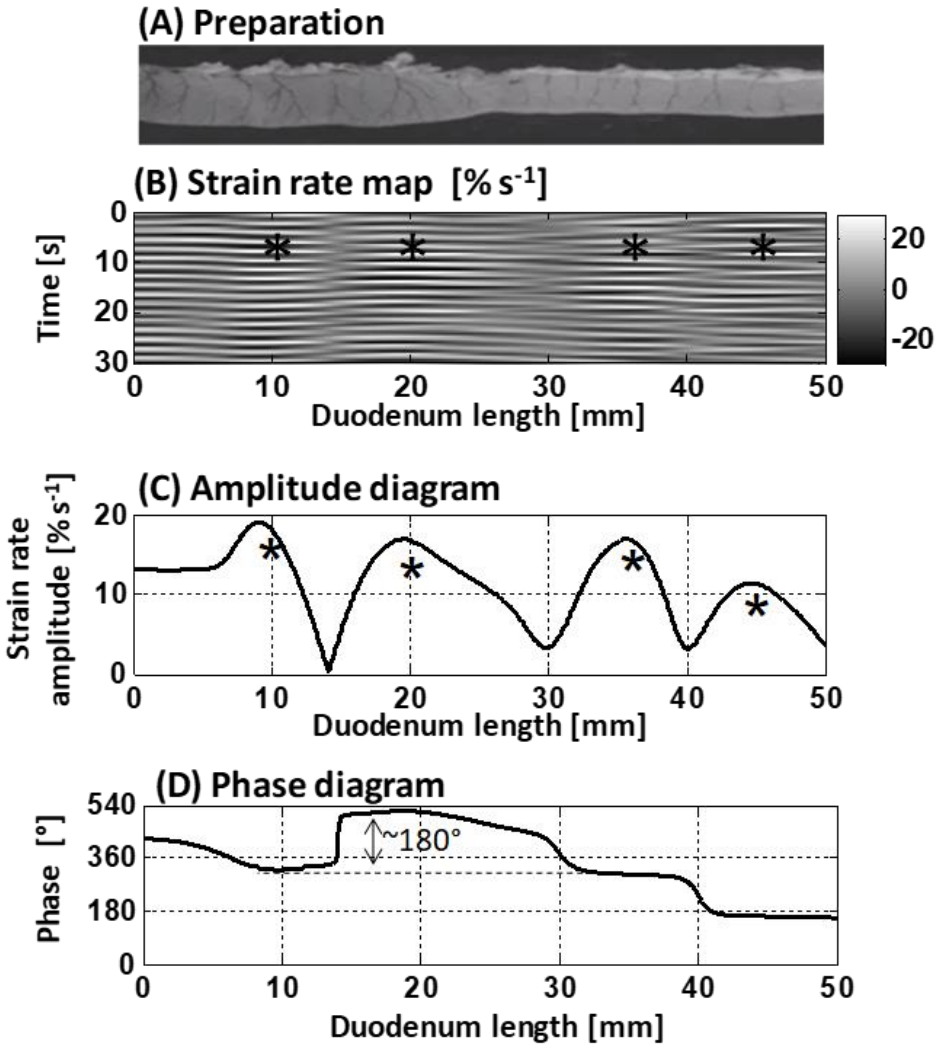

Figure 4-5 L-type ST Map (B) showing temporal variation in longitudinal components of segmentative contractions in the proximal duodenum (A) of the rat with concomitant variation in amplitude (C) and phasic relationship (D) over successive contractions.

The regular sequences of (white) short-lived (limited vertical thickness) rapidly propagating (near horizontal) longitudinal contractions and following (dark) short-lived dilatation recur at similar sites along the duodenum thus forma series of columns of varying length on the L map.

The asterisks show the regions in which contractions tend to recurrently peak within each column which the authors term 'domains' and the phase diagram the temporal relationship between the cyclic longitudinal contractions within each domain. Hence for example, the peak in amplitude (expressed as a percentage increase in the minimum strain in that domain) of the first marked column occurs during relaxation in the second marked column i.e., is 180^{0} out of phase with the second. *Figure adapted from (Clément de Loubens et al., 2014).*

possible to entirely eliminate such sagging, its magnitude may be reduced either by positioning a lengthwise plastic rod within the intestinal lumen or by supporting the intestine on a shallow cradle termed a kit-kat (Parsons & Huizinga, 2015). Alternatively, where practicable, such sagging may be reduced by limiting the length of the *ex vivo* segment that is mounted in the organ bath.

The generation of D-type ST maps from segments of gut that are maintained *in situ* within the abdominal cavity is often complicated by impairment of the detection of the edges of the section under study. Hence, for example, when studying the intestine at laparotomy, the partial overlaying of one loop of gut upon another reduces the surrounding area of contrast compared to that in an organ bath. Whilst viable loops can be isolated and maintained on (white or green) saline moistened swabs at laparotomy (P.W.M. Janssen, Lentle, Hulls, Ravindran, & Amerah, 2009), this procedure may generate additional tension on each end of an isolated segment that may exacerbate shunting.

A particular advantage of D-type over L-type ST maps is that they avoid problems that arise from anterior curvature of the surface under study. This curvature results in a gradation of the angle at which the surface is viewed within the video frame which influences the magnitude of any surface displacement caused by a given contraction. When gut segments such as the small intestine are mapped on a basis of surface displacement i.e., undergo L- or A-type mapping (see sections below), the curvature is generally insufficient to produce significant reduction in the apparent magnitude of a contraction except at the extreme periphery. However, when larger structures such as the urinary bladder are mapped using L- or A- techniques, the sites where there is significant reduction in magnitude will extend for greater distances from the edges. Hence, D-type maps are better able to accurately determine the magnitudes of movements around the edges of such structures than are L-type or A-type ST maps.

4.3.2 Video spatiotemporal maps of strain and strain rate

4.3.2.1 Method and interpretation

A number of workers have used a method for assessing local changes in length based on the distances between sets of evenly spaced markers i.e., strain (G. W. Hennig et al., 1999; Schreiber et al., 2014). However, as with D-type ST maps, the distance between any two markers will be that from shortening of smooth muscle at various sites, minus that from lengthening at other sites from active relaxation and from passive elastic stretching. However, the plotting of the rate of change in strain i.e., strain rate, between multiple randomly and finely distributed marker points, along a user defined LOI (Fig 4-1 E, F and G) can distinguish local areas of negative strain rate that result either from contraction of smooth muscle, or from recovery after stretching from areas of positive strain rate that result from muscular relaxation or from passive stretching, and from sites where neither contraction or elastic changes are occurring where strain rate is zero.

Anatomical markers that are distributed along the LOI, such as distinctive junction points in vascular arcades, can be used as reference points along the LOI. Alternately, at sites where such natural markers do not occur, a variety of particulate inert substances such as India ink (Melville, Macagno, & Christensen, 1975), silk knots (G. W. Hennig et al., 1999), dots of soot (W. J. E. P. Lammers, Dhanasekaran, Slack, & Stephen, 2001) and 100 μm flecks of glitter (G. W. Hennig et al., 2010) have been applied to the gut wall as artificial markers.

Early researchers used changes in the distances between successive artificial markers that had been placed at regular intervals along the LOI to estimate longitudinal shortening or lengthening (G. W. Hennig et al., 1999; Melville et al., 1975). Recently, more sophisticated algorithms based on cross-correlation (P.W.M Janssen & Lentle, 2013) have been developed that do not depend on determination of changes in distance between equally spaced markers. Briefly, the movement of a reference point within a characteristic pattern of randomly distributed markers is detected in a 21 × 21 pixel square surrounding it. This dimension is adequate for use with vascular markers when these are evident e.g. in the small intestine *in vivo* (Lentle et al., 2007) or when particles of carbon black are applied to the surfaces of less vascular structures (Lentle et al., 2015b). The

function describing the relationship between the position of a reference point on the image pattern within that square, and that within a displaced square in the subsequent frame, is given by:

$$C(x,y)=\sum_{i=-10}^{+10}\sum_{j=-10}^{+10}\left(\left(P(i,j)-\mu_P\right)-\left(Q(i+x,j+y)-\mu_Q\right)\right)^2 \quad (1)$$

where C (x, y) corresponds to a displacement of x & y pixels between the current and subsequent frames. P & Q are individual pixel intensities from the current and subsequent frames respectively, while μ_P & μ_Q are mean pixel intensities for the 21 × 21 pixel squares in these frames. A simpler function based on the sum of the absolute difference in pixel intensities has also been used (J. D. Huizinga, Lammers, Mikkelsen, Zhu, & Wang, 2010) but our experience is that this is not a critical factor.

The function is evaluated over a range of integer x and y values that are selected to cover the maximum displacements observed between frames, typically with gastrointestinal smooth muscle around -15 to +15 pixels. The minimum of this function represents the movement in pixels of a point at the centre of the square between the successive frames, and hence the local velocity, as the frames are captured at regular time intervals, typically 15 per second (Jähne, 2004). Earlier work simply searched for the pixel displacement with the lowest function value (J. D. Huizinga et al., 2010; Lentle et al., 2007). However, the author and co-workers have refined the technique to determine the minimum value by fitting a 2D cubic spline to the cross-correlation data and calculating the minimum value on the fitted spline so as to give the displacement in real numbers, i.e., fractions of a pixel.

Importantly, these methods defeat shunting as the identity of a particular region of the wall is marked by a distinctive local pattern of randomly distributed marker points. However the cross-correlation mapping technique can have difficulty evaluating slow tonal changes such as the increase in caecal length associated with receptive relaxation (Lentle et al., 2007). This is due to the algorithm determining long term change by cumulatively summing the many small changes that occur between sequential images over that time, a process

that tends to accumulate errors over long periods of time. This can be avoided by less frequent sampling of the video frames so that the time interval between successive frames is increased.

The fact that strain rate mapping is able to distinguish contractile states within surfaces gives it several practical advantages over D-mapping. Firstly, the fact that it does not depend on the identification of edges, allows it to be used to map localised sites that are distant from the edges of the organ, obviating the need to visualise the entire organ. This attribute could be particularly useful in analysis of laparoscopic video data so as to detect propulsive dysrhythmias in sites where loops of bowel adjacent to the area under study would confound edge detection. Secondly, given that the site of the LOI can be chosen by the operator, a number of L maps based on a sequence of longitudinal LOIs that are positioned longitudinally at various points across the radial dimension of the segment, can be prepared from the same video and the patterns of longitudinal contraction along the various LOIs quantified and compared. The use of this technique has allowed the pattern, amplitude and timing of longitudinal (pendular) contractions at mesenteric and ab-mesenteric sites on the duodenum to be compared and sites of differences identified (Lentle et al., 2012). Again, as with D-type ST maps, the preparation and comparison of a range of L-maps based on linear and non-linear LOIs orientated at various angles is useful in determining the principal direction of propagation of a patch contraction on the surface of a sacculate structure such as the bladder (Lentle et al., 2015b). As discussed hitherto, the LOI yielding the greatest amplitude and most consistent slope will generally be aligned with the true direction of propagation (Lentle et al., 2015b).

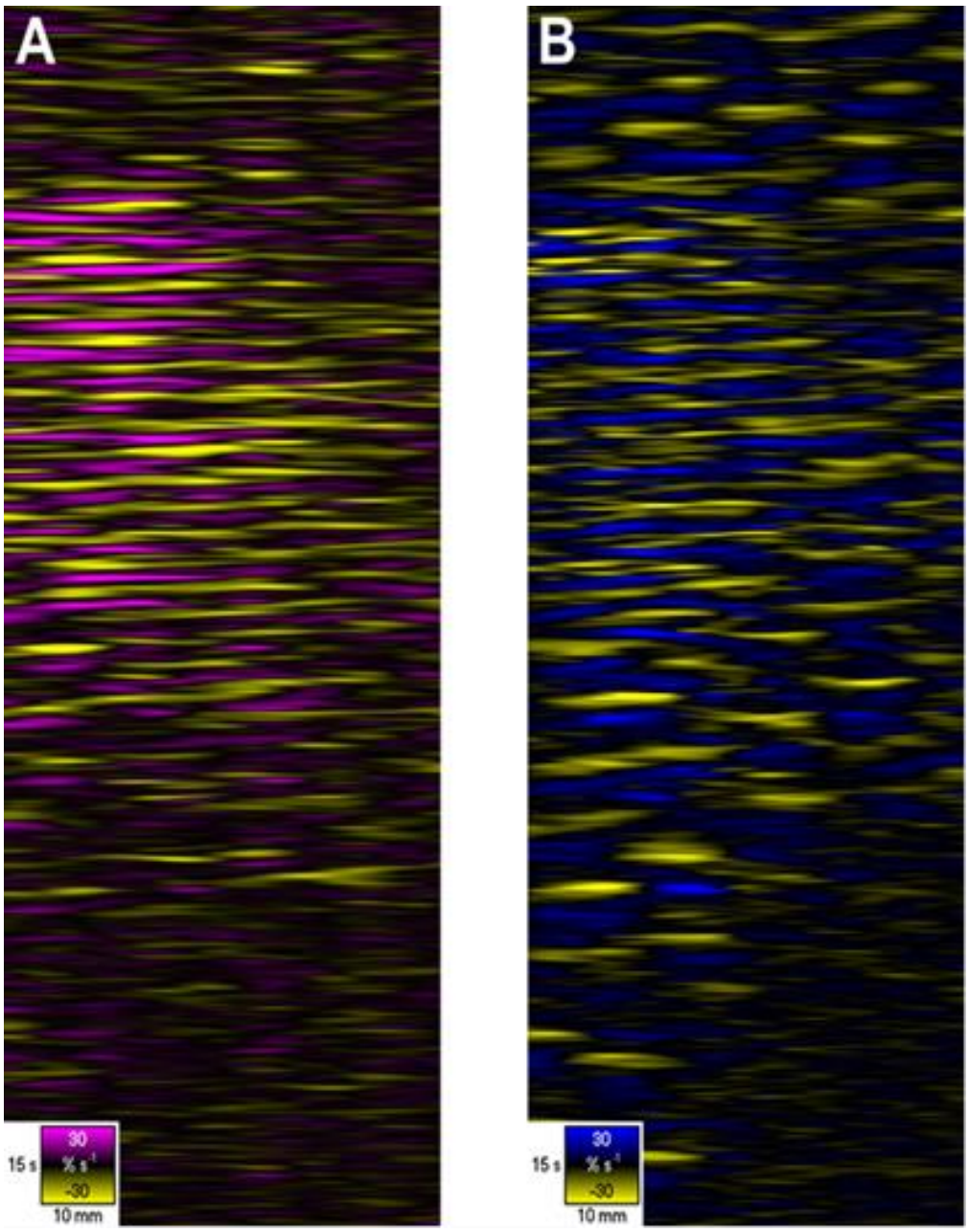

Figure 4-6 D- and L-type ST Maps showing variation in circumferential (A) and longitudinal (B) strain rate in the terminal ileum of the pig *in situ* at laparotomy, before and after dosage with remifentanyl.

The markers are the vascular arcades which are prominent *in vivo*. Areas of circular (A) and longitudinal (B) contraction (negative strain rate) are shown in yellow and areas of circular and longitudinal relaxation in purple and blue respectively note colour codes and magnitudes at the base of each map. Note that the contractions i.e., the discrete patterns of negative circular (a) and longitudinal (b) strain rate typical of segmentation (Fig 5 and the upper region of the D- and L-type ST maps) briefly become aligned i.e., in staggered phase, during the period after the administration of remifentanyl. Hence the contraction appears to propagate along the length of the ileum. *Figure adapted from (P.W.M Janssen et al., 2014).*

The high degree of resolution obtained when mapping strain rate along an LOI allows minor changes in the pattern of contraction through time to be distinguished. Hence, the use of L-type ST maps has allowed the temporal changes in the disposition of small areas of stationary longitudinal contraction that occur during pendular movements and their phasic relationship to each other to be distinguished, both in the duodenum (Lentle et al., 2012) (Fig 4-5) and in the ileum (P.W.M Janssen et al., 2014). Further, the technique is capable of distinguishing subtle changes in the pattern of contraction *in vivo*, such as the commencement of coherent distal propagation in a static array of segmentative or pendular contractions when pro-kinetic agents such as remifentanyl are given (P.W.M Janssen et al., 2014) (Fig 4-6). Similarly, those effects of pharmacological agents which aid in the distinction of myogenic from neurogenic contractions (Lentle et al., 2012).

The ability of strain rate mapping to accurately determine the site, speed of propagation, duration and frequency of cycles in strain rate in a succession of events over a set period of time enables sequences of real time data to be incorporated into mathematical models that assess their effects on wall movement and mixing and transport of the lumen contents (Clément de Loubens et al., 2014; C. de Loubens, Lentle, Love, Hulls, & Janssen, 2013). Moreover, the veracity of the model may subsequently be checked by comparing the predicted mixing outcome with that determined from dilution of a bolus of tracer dye perfused through the preparation over the same time period during which the map was derived (Clément de Loubens et al., 2014).

4.3.2.2 Drawbacks

L-type ST maps may underestimate the amplitude of strain when LOIs are orientated on curved surfaces, for example when the LOI is orientated at right angles to the long axis of a tubular structure such as the intestine. In areas at the periphery of a large spherical structure where angulation of the surface is high, strain rate may be significantly underestimated. In such situations the problem of distortion at the edges of the image can be avoided by the use of multiple cameras, located in such positions that the central parts of the various images cover all aspects of the organ. Alternatively, it may be possible to determine the curvature of the surface on

which the LOI is located directly with a laser profiler (Hennessy, Kinsella, & Waddington, 2002; Strobl et al., 2004) and mathematically weight the strain rates along the LOI accordingly.

4.3.3 Composite plots and plots derived from video spatiotemporal maps

The positioning of a vertical line at a given lengthwise point on D- or L-type ST maps, and the recruitment of pixel data from the column coincident with that line, can provide quantitative information regarding component frequencies. Fast Fourier transformation of the ST data is commonly used to identify and quantify these frequencies (Neal, Parry, & Bornstein, 2009) and enable their quantitative comparison before and after the application of various pharmaceutical agents (R.R. Roberts et al., 2010).

Where a contractile pattern such as peristalsis contains both longitudinal and circumferential components, the judicious use of synchronous vertical ST transects to show the phasic relationship between the two components at a particular point along the length of the preparation (Fig 4-2B) can shed addition light on their causation. Hence, in synchronous D-type and L-type ST maps of peristalsis, a forerunning band of negative longitudinal strain rate and a following region of circumferential contraction can be distinguished (Lentle et al., 2007). Comparison of their synchronous vertical (temporal) transects taken at the same site (Fig 4-2B) showed that the onset of the longitudinal shortening component was synchronous with that of circular contraction presumably reflecting synchronous neural signalling.

Again, where L-type ST maps of cylindrical structures such as the small intestine show longitudinally distributed arrays of stationary contractions within successive domains, similar comparisons of a sequence of vertical map transects can distinguish their phasic relationships and relative amplitudes (Fig 4-5) (Clément de Loubens et al., 2014; C. de Loubens et al., 2013).

In respect of D-maps, it is noteworthy that, if the arrays of longitudinal strain rate values obtained from the cross correlation techniques used in the preparation of L-type ST maps are integrated with respect to time, they can be used to derive displacement maps that track the lengthwise position of fixed points on the gut

segment. While such maps are of little physiological interest *per se*, they can be used to systematically correct a D-map so that a column of the D-map corresponds to a fixed point on the segment surface rather than a certain distance along the segment i.e., to defeat shunting in D-maps.

Whilst both D- and L-maps give an incomplete picture of the mechanical state of the muscle, recent work has identified local changes in the mechanical states of the intestinal wall during intestinal contraction on a basis of the relationship between local changes in length distinguished on D-maps and concurrent local pressure within the lumen determined by fibreoptic catheters (Costa, Wiklendt, et al., 2013). These workers were able to distinguish sites of isovolumetric and isobaric contraction and relaxation, passive shortening and elongation and auxotonic contraction and relaxation (where the muscle changes force and length simultaneously). Areas of passive dilatation and shortening contributed to less than 4% of the map and two dimensional plots of active muscle contraction vs active relaxation were of broadly the same configuration as the corresponding D-maps (Costa, Wiklendt, et al., 2013). Given that the interpretation of the mechanical states of areas that abut regions of active contractile shortening was likely to be confounded to some extent by shunting, and that fine pressure resolution would be to some extent compromised by the low density of pressure sensors (one per cm), these results indicate that, despite of their shortcomings, ST-maps can provide a useful overview of contractile patterns.

A number of parameters can be mathematically derived from D- or L-maps by application of a suitable algorithm e.g. to derive maps of frequency and velocity (G.W Hennig et al., 2010). A number of conventional image processing operations can be applied to the ST maps including high, low and band pass filters, mathematical operations with scalars or other images, autocorrelation and 2D Fourier transforms (Jähne, 2004; Russ, 2006).

The difference between two maps may be mapped by simple subtraction of arrays of values on one map from the corresponding values of the other. This technique has been used to highlight the limited coordination of

the ripple contractions that occur in adjacent intertaenial domains in the haustrated proximal rabbit colon (Lentle et al., 2008).

Again the correlation of a particular D-type or L-type ST image, with itself when it is displaced over an array of known distances in an array of known directions (i.e., autocorrelation), or with the synchronous ST image of contraction in another dimension (cross correlation), can be useful in identifying and quantifying repeating features within the map (Russ, 2006) (Fig 4-7). The operation has the effect of averaging the individual repeating features and removing noise. The central event in the autocorrelation image represents the distance that the second image can be displaced before the features no longer lie on top of each other, and thus provides the best measure of the size of the repeating elements in the two images. Other less bright repeating events at particular angles and distances from the centre of the autocorrelation image indicate correlation between the points in the original image with those that are displaced by a particular distance and direction i.e., rhythmicity. The form of the repeating elements on the auto correlograms of ST maps can also be used to better distinguish hydraulic distension induced by regular contractions at other sites, from the direct effects of propagating contractions. Hence the repeating points generated by (instantaneous) hydraulic distension appear as parallel horizontal lines whilst those formed by (more slowly) propagating phasic contractions appear as parallel angled lines, the speed of their propagation being inversely proportional to their slope.

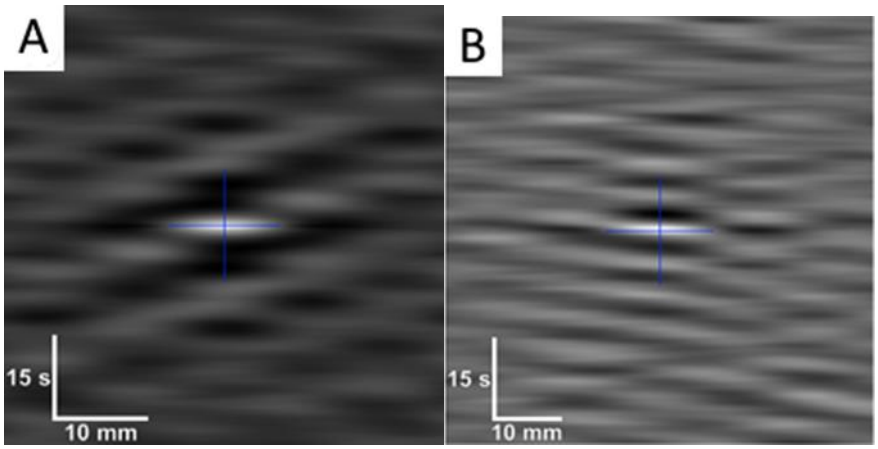

Figure 4-7 Auto-correlogram (A) and cross-correlogram (B) of data from D-type and L-type ST maps during pendular/segmentative activity in the terminal ileum of an anesthetised pig.

White indicates high levels of correlation and darker shades lower correlation. The cross indicates the geometric centre of each correlogram.

The auto-correlogram (A), which is from a subsection of an L map of ileal motility, shows a pattern in which a longitudinal contraction at a particular point along the gut occurs with every second or third wave of the base frequency (centre). Hence, the variability in the spacing between lighter (contraction) bands at all points around the single central band of the base frequency, indicates local variability in contractile responses to slow waves.

The cross correlogram (B) (bottom) is derived from synchronous subsections f of D-type and L-type ST maps of ileal motility. It shows an underlying pattern of regular spacing between contractile events at all points around the central band of the base frequency indicating that the two events likely result from a common initiating signal. *Figure adapted (P.W.M Janssen et al., 2014).*

4.3.4 Spatiotemporal maps of luminous intensity (I-maps)

A further technique that is useful for tracking movements that are not necessarily related to contraction or strain is based on the detection of movement of light, reflected from or transmitted through, the tissue under study. The rows of the I-type ST map therefore correspond to the light intensities along a user-specified LOI.

The mapping of changes in patterns of light intensity is useful for the detection of the incidental movement of passive structures such as the displacement of mucosal folds as a result of changes in the internal dimensions of the lumen (Lentle, Janssen, et al., 2013). I-mapping can also be used to track light that is generated within the preparation. Hence, the intensity map methodology can be used to track the movement of local florescence

associated with contractile activity (Park et al., 2006) and the migration of electrophysiological phenomena (W. J. E. P. Lammers et al., 2001; Seerden, Lammers, De Winter, De Man, & Pelckmans, 2005) notably activation of myogenic cells such as ICCs (P. O. Bayguinov, Hennig, & Smith, 2010a, 2010b; Nick J Spencer et al., 2007).

Where practicable, concurrent L-type ST mapping can be used to determine whether the movement detected by I-maps is spatiotemporally coincident with the region of contraction (Roger Graham Lentle et al., 2016).

Whilst the I-mapping technique has been used to estimate the frequency and propagation velocity of contractions (Fig 4-8) (C Hulls et al., 2012), their quantification is not as reliable as that from D- and strain rate maps. Where a preparation is illuminated by light from a fixed direction, displacement of the gut wall may cause the direction in which light is reflected from its surface into the camera to change. Hence light may initially be reflected from the apex of a propagating distension and subsequently from its side so that the rate of progression of the brightest region in the intensity map will not provide a true estimate of the rate at which the distended area is propagating. Again, local variation in the thickness of the gut wall through which light must propagate may influence its intensity so that it is not consistently proportional to the amplitude of the source that generates it. Hence it is always advisable to check the values obtained from intensity maps against those obtained by other means.

4.3.5 Two-dimensional (area) video spatiotemporal mapping

4.3.5.1 Method and use

The strain rate mapping technique may be extended from mapping changes in a linear dimension, i.e., along a single LOI, to map changes in areas between groups of markers that are orientated at right angles to each other, i.e., between local longitudinally and radially orientated LOIs, on successive frames (Fig 4-1 H, I and J). Such a ‘rate of change in area’ or A-type ST mapping technique is broadly similar to the ‘rate of change in volume’ technique used in three dimensional mapping of contraction in the wall of the heart (Tops et al., 2005) save that it operates on the surface of the organ rather than the volume of the tissue. The derived maps of

changes in area strain rate (A-type maps), can subsequently be overlaid onto the corresponding video image so as to provide real time record of changes in the sites of contraction (negative area strain rate) and expansion (positive area strain rate) (Fig 4-9).

Direct synchronous overlays real time of A-type maps also enable the shapes and extents of areas of contraction (or relaxation) on the surface of an organ or compartment e.g. the body of the stomach, (Lentle et al., 2010) to be determined. Again, comparison of overlays on successive frames, allows the principal direction of propagation of patches of contraction to be directly visualised and an appropriately orientated linear or curved LOI to be identified for subsequent unidimensional (L-type) strain rate mapping. This can also allow circular (re-entrant) paths of contraction that may follow from disturbances in slow wave propagation associated with conditions such as gastroparesis (O'Grady et al., 2012) to be identified. The dynamics of the development and involution of contractions may also be quantified by appropriate use of algorithms that compute mean number of contractile sites, patch area and CV , perimeter to area ratio, shape index and perimeter area fractal dimension (McGarigal, 2014) on successive frames. Again, the use of algorithms that sum the total areas of contraction within successive frames (core area%) can be used to assess cyclic contractile behaviour and its co-variation with lumen pressure on an organ scale (Lentle et al., 2015b).

The use of an algorithm that stacks successive A-type ST maps over a given period of time and sums the number of occasions that contractions, i.e., periods of negative area strain rate, occur at each pixel location allowing the effect of time to be directly incorporated into a single map (Fig 4-10). The resulting stacked A-type contraction density plots with colour coded rates of occurrence of contractions at each pixel (Fig 4-10D) may be viewed as similar to the stacked sequence of the lengthwise location of contractions over time seen on D-type ST maps (Fig 4-2) save that the direction of propagation is visualised over 360^0.

A)

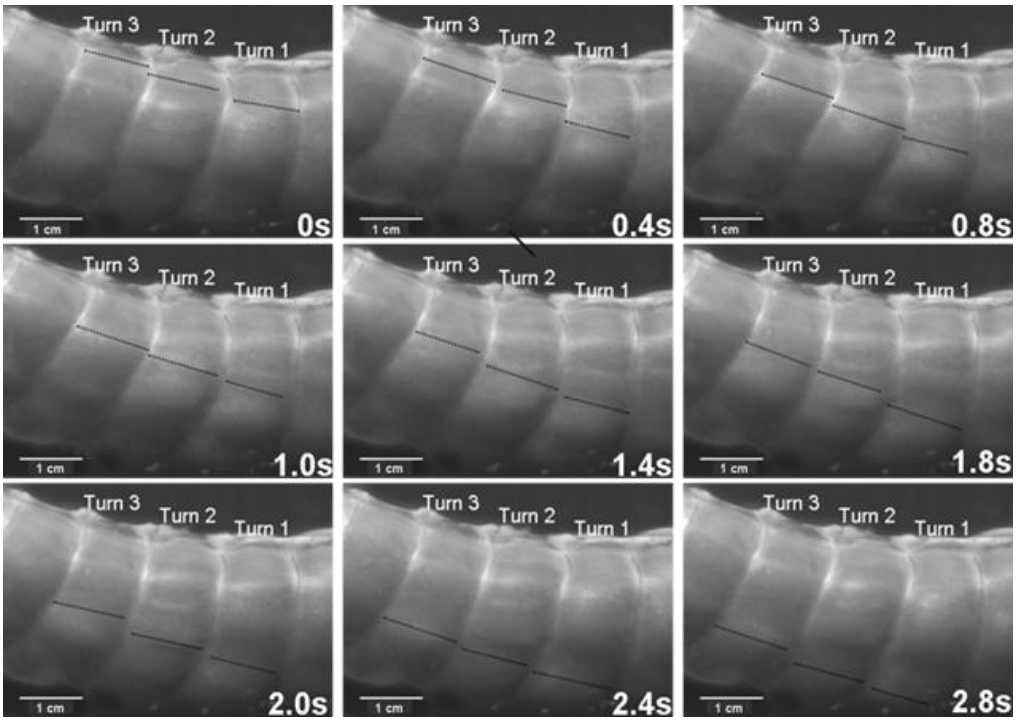

B)

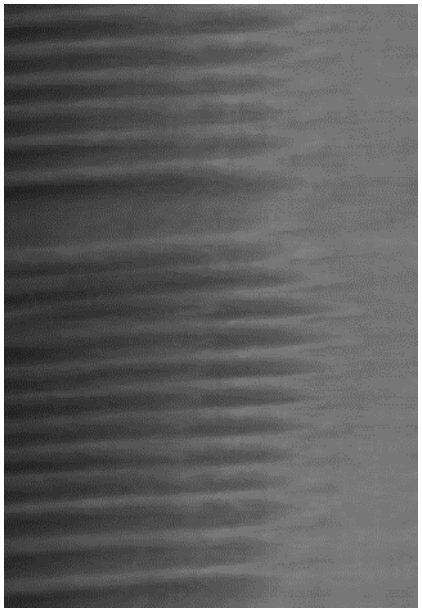

Figure 4-8 The use of I-maps in determining the frequency of ladder contractions in the rabbit caecum.

Photo sequence (A) shows a sequence of video frames of lengthwise ladder contractions (dark lines) in three successive spiral turns of the mid caecum at 0.4 s intervals.

The I-type ST map (B) is taken from of a single spiral turn during the transit of ladder contractions. The X axis represents the width of the turn (Turn number 2 on the photo sequence) with the proximal end of preparation to the right. Note that the arrays of contractions do not occupy the proximal third of the turn and that the slope of the largely regular sequence of contractions indicates that they are propagating from the proximal to the distal end of the turn. *Figure adapted from (Corrin Hulls et al., 2012).*

Hence the highest number of contractile pixels will occur at sites where contractions repeatedly propagate or originate, the number decreasing in the surrounding zones according to the direction of propagation. Such maps can also be useful in factoring out lateral expansion and determining the mean direction of propagation of a patch of contraction across a surface and hence in identifying an appropriate LOI (Roger Graham Lentle et al., 2016; Lentle et al., 2015b).

4.3.5.2 Disadvantages

A-type strain rate area maps and stacked A-type ST contraction density plots suffer from similar disadvantages to those of linear strain rate maps i.e., L-type ST maps, in that they record only the strain rate and cannot distinguish the negative strain rate of contraction from that of elastic recovery.

4.3.6 Other technical matters

The principal arbiter of high-quality video spatiotemporal mapping is definition. Hence wherever possible the use of colour video cameras should be avoided as the local grouping of sensor cells in arrays of three different colour sensitivities decreases the overall level of resolution.

The contraction rates of gastrointestinal, arterial, and urinary smooth muscle are relatively slow. Thus, sampling rates of 15 frames per second, are adequate for the mapping of most phasic contractions in the GI tract. However, studies of certain neurogenic contractions such as the fast phasic contractions found in the colon (Lentle et al., 2008) may require faster rates. Again, mapping algorithms may fail to detect changes in

distances between surface markers in successive frames when the rate of change is low. Hence, the mapping of tonal contractions may require appropriate down sampling of the stream of video frames.

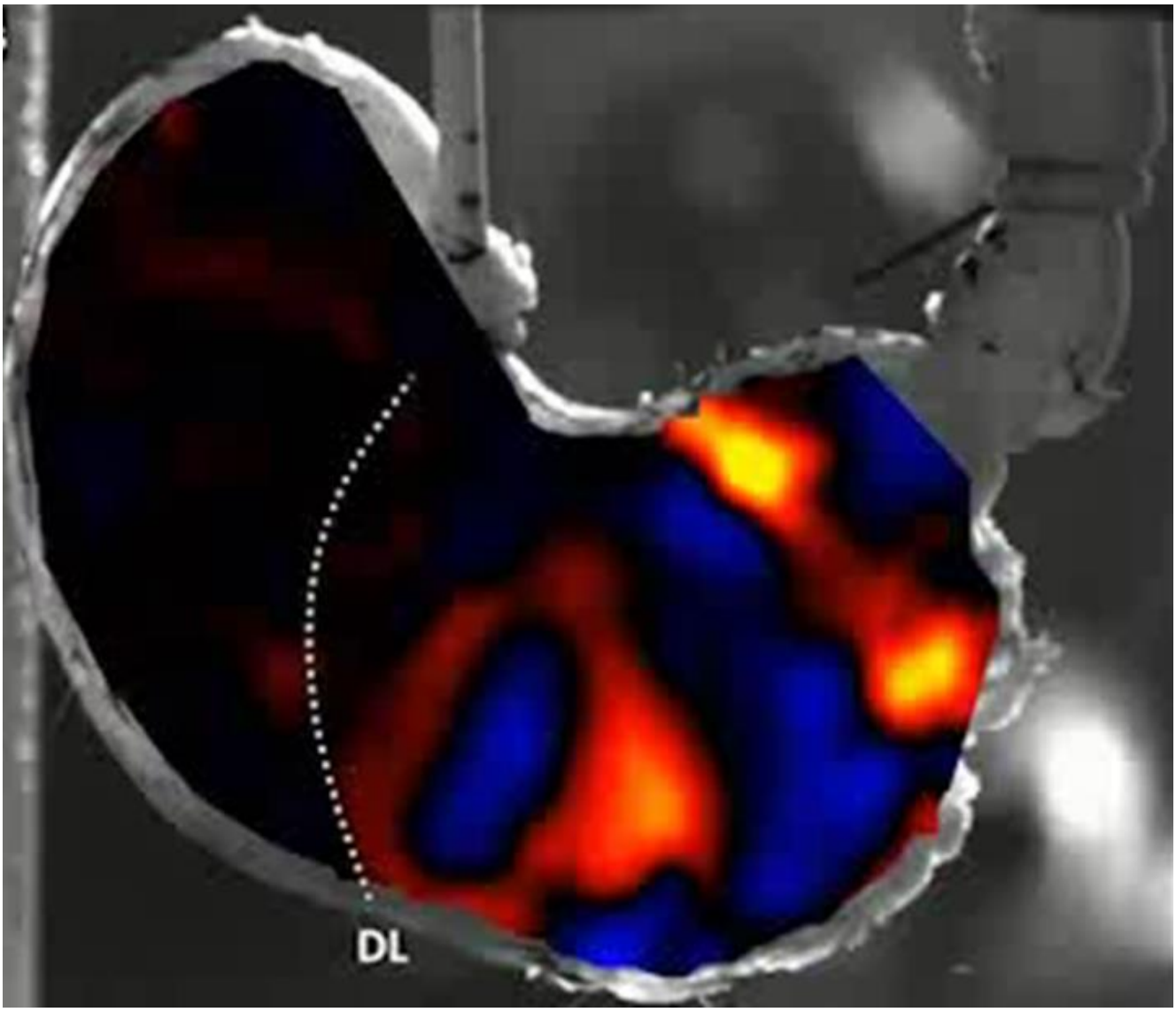

Figure 4-9 An A-type ST map of area strain rate from antral peristalsis in the stomach of the rat.

The pylorus lies on the right and the (cannulated) oesophagus is situated at the top slightly to right of the midpoint. The area strain rate map is overlaid onto, and synchronous with, the image from which it is derived. Note the randomly dispersed carbon particles on the areas to the side of the A-map which are also in the area under the map and were used as reference points. The succession of areas of high negative strain rate (yellow and red) are sites undergoing antral peristalses. The areas of positive strain rate (blue) correspond to areas of relaxation. The dotted line marked DL indicates the position of the line of demarcation between the fundus and body, which is anatomically evident in rats. Note the increase in the magnitude of area strain as the contractions near the pylorus and the failure of antral peristalses to extend to the lesser curve in the proximal corpus and antrum. *Modified figure from (R. G. Lentle, G. W. Reynolds, C. M. Hulls, & J. P. Chambers, 2016).*

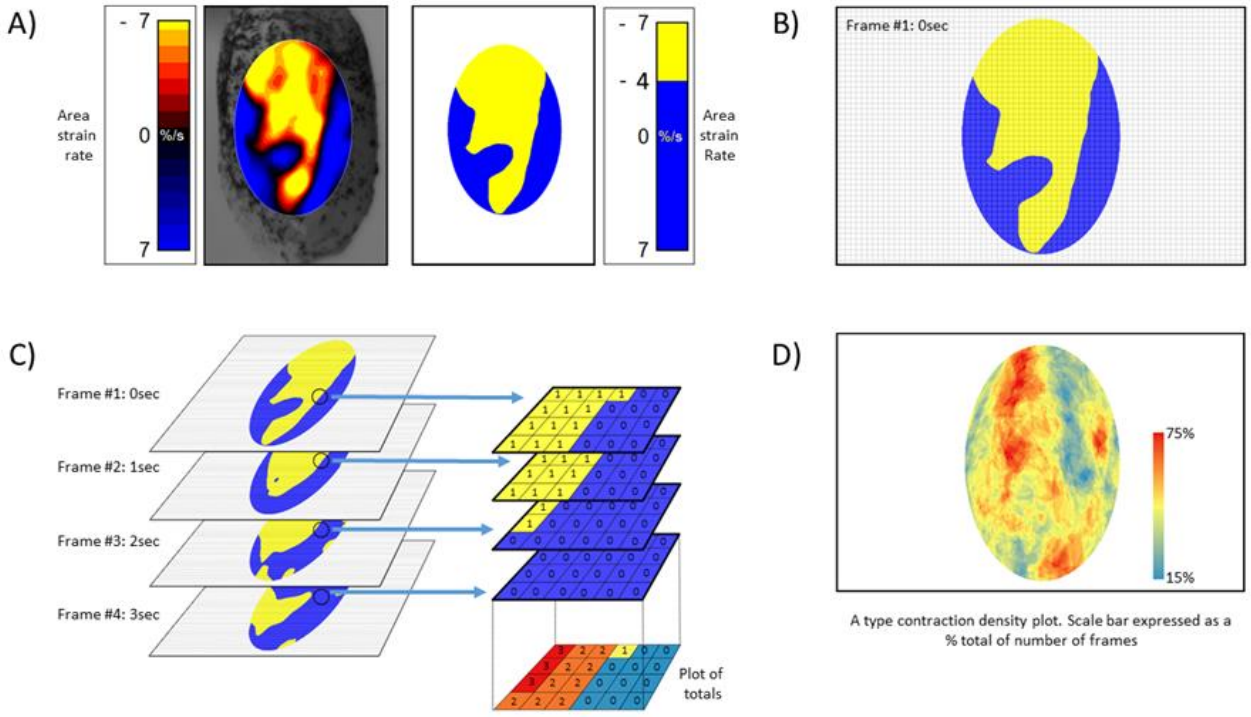

Figure 4-10 Method of construction of A-type contraction density plots.

A) Successive Area Spatiotemporal maps were thresholded to include all sites at which strain rate exceeds a chosen value (in this case less than -4 % strain s^{-1}).

B) Frames were suitably subsampled at chosen time intervals.

C) The subsampled frames, taken over a chosen time span, were stacked and the number of frames within each pixel of the stack with strain rates in excess of the chosen threshold counted. The results were then plotted as a colour coded percentage total to produce a stacked A-type contraction density plot.

D) Typical stacked A-type contraction density plot covering over 45% of the anterior surface of the bladder.

Adapted from (C M Hulls, Lentle, King, Reynolds, & Chambers, 2017).

4.4 Conclusion

The judicious use of video spatiotemporal mapping techniques has, and will, enable significant advances in our understanding of the physiological basis of contractile activity in the various compartments of the gut and the effects of these on the mixing and propulsion of their contents. There are nevertheless a number of limitations with which the operator should be familiar so as to avoid incorrect interpretation. The technique has great

potential for the diagnostic assessment of motility during laparoscopic examination when suitable small, high definition video cameras become available.

Acknowledgements

Grateful thanks to Dr Patrick Janssen who wrote the software for the new methods of analysis.

References

Abdu, F., Hicks, G. A., Hennig, G., Allen, J. P., & Grundy, D. (2002). Somatostatin sst2 receptors inhibit peristalsis in the rat and mouse jejunum. *American Journal of Physiology-Gastrointestinal and Liver Physiology, 282*(4), G624-G633.

Alvarez, W. C., & Zimmermann, A. (1927). The absence of inhibition ahead of peristaltic rushes. *American Journal of Physiology, 83*(1), 52-59.

Ballaro, A., Mundy, A., Fry, C., & Craggs, M. (2003). Bladder electrical activity: the elusive electromyogram. *BJU International, 92*(1), 78-84.

Bayguinov, O., Hennig, G., & Sanders, K. (2011). Movement based artifacts may contaminate extracellular electrical recordings from GI muscles. *Neurogastroenterology and Motility, 23*(11), 1029-e1498.

Bayguinov, P. O., Hennig, G. W., & Smith, T. K. (2010a). Ca2+ imaging of activity in ICC-MY during local mucosal reflexes and the colonic migrating motor complex in the murine large intestine. *The Journal of Physiology, 588*(22), 4453-4474.

Bayguinov, P. O., Hennig, G. W., & Smith, T. K. (2010b). Calcium activity in different classes of myenteric neurons underlying the migrating motor complex in the murine colon. *The Journal of Physiology, 588*(3), 399-421.

Benard, T., Bouchoucha, M., Dupres, M., & Cugnenc, P. H. (1997). In vitro analysis of rat intestinal wall movements at rest and during propagated contraction: a new method. *American Journal of Physiology, 273*(4), G776-784.

Berthoud, H. R., Hennig, G., Campbell, M., Volaufova, J., & Costa, M. (2002). Video-based spatio-temporal maps for analysis of gastric motility in vitro: effects of vagal stimulation in guinea-pigs. *Neurogastroenterology and Motility, 14*(6), 677-688.

Bogeski, G., Shafton, A. D., Kitchener, P. D., Ferens, D. M., & Furness, J. B. (2005). A quantitative approach to recording peristaltic activity from segments of rat small intestine in vivo. *Neurogastroenterology and Motility, 17*(2), 262-272.

Bowditch, H. (1897). Movements of the alimentary canal. *Science, 5*, 901-902.

Camilleri, M., Bharucha, A. E., Di Lorenzo, C., Hasler, W., Prather, C., Rao, S., & Wald, A. (2008). American Neurogastroenterology and Motility Society consensus statement on intraluminal measurement of gastrointestinal and colonic motility in clinical practice. *Neurogastroenterology and Motility, 20*(12), 1269-1282.

Cannon, W. B. (1898). The movements of the stomach studied by means of the Röntgen rays. *American Journal of Physiology, 1*(3), 359-382.

Chen, J.-H., Yang, Z., Yu, Y., & Huizinga, J. D. (2016). Haustral boundary contractions in the proximal 3-taeniated rabbit colon. *American Journal of Physiology, 310*(3), G181-192.

Chen, J.-H., Zhang, Q., Yu, Y., Li, K., Liao, H., Jiang, L., . . . Chen, S. (2013). Neurogenic and myogenic properties of pan-colonic motor patterns and their spatiotemporal organization in rats. *PloS one, 8*(4), e60474.

Chen, J., & McCallum, R. W. (1992). Gastric slow wave abnormalities in patients with gastroparesis. *American Journal of Gastroenterology, 87*(4)

Collins, J., Borojevic, R., Verdu, E., Huizinga, J., & Ratcliffe, E. (2014). Intestinal microbiota influence the early postnatal development of the enteric nervous system. *Neurogastroenterology and Motility, 26*(1), 98-107.

Costa, M., Dodds, K. N., Wiklendt, L., Spencer, N. J., Brookes, S. J., & Dinning, P. G. (2013). Neurogenic and myogenic motor activity in the colon of the guinea pig, mouse, rabbit, and rat. *American Journal of Physiology-Gastrointestinal and Liver Physiology, 305*(10), G749-G759.

Costa, M., Wiklendt, L., Arkwright, J. W., Spencer, N. J., Omari, T., Brookes, S. J., & Dinning, P. G. (2013). An experimental method to identify neurogenic and myogenic active mechanical states of intestinal motility.

de Loubens, C., Lentle, R. G., Hulls, C., Janssen, P. W., Love, R. J., & Chambers, J. P. e. (2014). Characterisation of Mixing in the Proximal Duodenum of the Rat during Longitudinal Contractions and Comparison with a Fluid Mechanical Model Based on Spatiotemporal Motility Data. *PloS one, 9*(4), e95000.

de Loubens, C., Lentle, R. G., Love, R. J., Hulls, C., & Janssen, P. W. M. (2013). Fluid mechanical consequences of pendular activity, segmentation, and pyloric outflow in the proximal duodenum of the rat and the guinea pig. *Journal of the Royal Society Interface, 10*(83), 20130027.

Di Lorenzo, C., Hillemeier, C., Hyman, P., Loening-Baucke, V., Nurko, S., Rosenberg, A., & Taminiau, J. (2002). Manometry studies in children: minimum standards for procedures. *Neurogastroenterology and Motility, 14*(4), 411-420.

Dinning, P., Wiklendt, L., Maslen, L., Gibbins, I., Patton, V., Arkwright, J., . . . Brookes, S. (2014a). Quantification of in vivo colonic motor patterns in healthy humans before and after a meal revealed by high-resolution fiber-optic manometry. *Neurogastroenterology and Motility, 26*(10), 1443-1457.

Dinning, P., Wiklendt, L., Maslen, L., Gibbins, I., Patton, V., Arkwright, J., . . . Brookes, S. (2014b). Quantification of in vivo colonic motor patterns in healthy humans before and after a meal revealed by high-resolution fiber-optic manometry. *Neurogastroenterology and Motility, 26*(10), 1443-1457.

Dinning, P. G., Costa, M., Brookes, S., & Spencer, N. J. (2012). Neurogenic and myogenic motor patterns of rabbit proximal, mid, and distal colon. *American Journal of Physiology-Gastrointestinal and Liver Physiology, 303*(1), G83-G92.

Dinning, P. G., Szczesniak, M. M., & Cook, I. J. (2008). Twenty four hour spatiotemporal mapping of colonic propagating sequences provides pathophysiological insight into constipation. *Neurogastroenterology and Motility, 20*(9), 1017-1021.

Frei, W., & Chen, C.-C. (1977). Fast Boundary Detection: A Generalizationand New Algorithm. *IEEE Transactions on Computers, 26*(10)

Gwynne, R. M., Thomas, E. A., Goh, S. M., Sjovall, H., & Bornstein, J. C. (2004). Segmentation induced by intraluminal fatty acid in isolated guinea-pig duodenum and jejunum. *Journal of Physiology, 556*(2), 557-569.

Hennessy, R. J., Kinsella, A., & Waddington, J. L. (2002). 3D laser surface scanning and geometric morphometric analysis of craniofacial shape as an index of cerebro-craniofacial morphogenesis: initial application to sexual dimorphism. *Biological Psychiatry, 51*(6), 507-514.

Hennig, G. W., Costa, M., Chen, B. N., & Brookes, S. J. H. (1999). Quantitative analysis of peristalsis in the guinea-pig small intestine using spatio-temporal maps. *Journal of Physiology, 517*, 575-590.

Hennig, G. W., Gregory, S., Brookes, S. J. H., & Costa, M. (2010). Non-peristaltic patterns of motor activity in the guinea-pig proximal colon. *Neurogastroenterology and Motility, 22*, e207–217.

Hennig, G. W., Spencer, N. J., Jokela-Willis, S., Bayguinov, P. O., Lee, H., Ritchie, L. A., . . . Sanders, K. M. (2010). ICC-MY coordinate smooth muscle electrical and mechanical activity in the murine small intestine. *Neurogastroenterology and Motility, 22*(5), e138-151.

Huizinga, J. D., Lammers, W. J. E. P., Mikkelsen, H. B., Zhu, Y., & Wang, X. Y. (2010). Toward a Concept of Stretch Coupling in Smooth Muscle: A Thesis by Lars Thuneberg on Contractile Activity in Neonatal Interstitial Cells of Cajal. *Anatomical Record, 293*(9), 1543-1552.

Hulls, C., Lentle, R. G., de Loubens, C., Janssen, P. W., Chambers, P., & Stafford, K. J. (2012). Spatiotemporal mapping of ex vivo motility in the caecum of the rabbit. *Journal of Comparative Physiology B, 182*(2), 287-297.

Hulls, C., Lentle, R. G., de Loubens, C., Janssen, P. W. M., Chambers, P., & Stafford, K. J. (2012). Spatiotemporal mapping of ex vivo motility in the caecum of the rabbit. *Journal of Comparative Physiology. B, Biochemical, Systemic, and Environmental Physiology, B182*, 287-297. 10.1007/s00360-011-0610-2

Hulls, C. M., Lentle, R. G., King, Q. M., Reynolds, G. W., & Chambers, J. (2017). Spatiotemporal analysis of spontaneous myogenic contractions in the urinary bladder of the rabbit: timing and patterns reflect reported electrophysiology. *American Journal of Physiology-Renal Physiology, 313*(3), F687-F698.

Jähne, B. (2004). *Practical Handbook on Image Processing for Scientific and Technical Applications* (2nd ed.). Boca Raton: CRC Press.

Janssen, P. W. M., & Lentle, R. G. (2013). Spatiotemporal Mapping Techniques for Quantifying Gut Motility. In L. K. Cheng & G. Farrugia (Eds.), *New Advances in Gastrointestinal Motility Research* (pp. 219-241). New York: Springer.

Janssen, P. W. M., Lentle, R. G., Chambers, P., Reynolds, G. W., De Loubens, C., & Hulls, C. M. (2014). Spatiotemporal organization of standing postprandial contractions in the distal ileum of the anesthetized pig. *Neurogastroenterology and Motility, 26*(11), 1651-1662.

Janssen, P. W. M., Lentle, R. G., Hulls, C., Ravindran, V., & Amerah, A. M. (2009). Spatiotemporal mapping of the motility of the isolated chicken caecum. *Journal of Comparative Physiology. B, Biochemical, Systemic, and Environmental Physiology, B179*(5), 593-604.

Kirsch, R. A. (1971). Computer determination of the constituent structure of biological images. *Computers and Biomedical Research, 4*(3), 315-328.

Laforet, J., Rabotti, C., Mischi, M., & Marque, C. (2013). Improved multi-scale modeling of uterine electrical activity. *Irbm, 34*(1), 38-42.

Lammers, W. J. E. P., Dhanasekaran, S., Slack, J. R., & Stephen, B. (2001). Two-dimensional high-resolution motility mapping in the isolated feline duodenum: methodology and initial results. *Neurogastroenterology and Motility, 13*(4), 309-323.

Lentle, R. G., De Loubens, C., Hulls, C., Janssen, P. W. M., Golding, M. D., & Chambers, J. P. (2012). A comparison of the organization of longitudinal and circular contractions during pendular and segmental activity in the duodenum of the rat and guinea pig. *Neurogastroenterology and Motility, 24*(7), 686-e298.

Lentle, R. G., Janssen, P. W. M., Asvarujanon, P., Chambers, P., Stafford, K. J., & Hemar, Y. (2007). High definition mapping of circular and longitudinal motility in the terminal ileum of the brushtail possum *Trichosurus vulpecula* with watery and viscous perfusates. *Journal of Comparative Physiology. B, Biochemical, Systemic, and Environmental Physiology, B177*(5), 543-556.

Lentle, R. G., Janssen, P. W. M., Asvarujanon, P., Chambers, P., Stafford, K. J., & Hemar, Y. (2008). High definition spatiotemporal mapping of contractile activity in the isolated proximal colon of the rabbit. *Journal of Comparative Physiology. B, Biochemical, Systemic, and Environmental Physiology, B178*, 257-268.

Lentle, R. G., Janssen, P. W. M., DeLoubens, C., Lim, Y. F., Hulls, C., & Chambers, P. (2013). Mucosal microfolds augment mixing at the wall of the distal ileum of the brushtail possum. *Neurogastroenterology and Motility, 25*(11), 881-e700.

Lentle, R. G., Janssen, P. W. M., Goh, K., Chambers, P., & Hulls, C. (2010). Quantification of the Effects of the Volume and Viscosity of Gastric Contents on Antral and Fundic Activity in the Rat Stomach Maintained *Ex Vivo*. *Digestive Diseases and Sciences, 55*(12), 3349-3360.

Lentle, R. G., Reynolds, G. W., Hulls, C. M., & Chambers, J. (2016). Advanced spatiotemporal mapping methods give new insights into the coordination of contractile activity in the stomach of the rat. *American Journal of Physiology-Gastrointestinal and Liver Physiology*, ajpgi. 00308.02016.

Lentle, R. G., Reynolds, G. W., Hulls, C. M., & Chambers, J. P. (2016). Advanced spatiotemporal mapping methods give new insights into the coordination of contractile activity in the stomach of the rat. *American Journal of Physiology-Gastrointestinal and Liver Physiology, 311*(6), G1064-G1075. 10.1152/ajpgi.00308.2016

Lentle, R. G., Reynolds, G. W., Janssen, P. W. M., Hulls, C. M., King, Q. M., & Chambers, J. (2015). Characterisation of the contractile dynamics of the resting ex vivo urinary bladder of the pig. *BJU International, 116*(6), 973-983.

Lynn, P., Zagorodnyuk, V., Hennig, G., Costa, M., & Brookes, S. (2005). Mechanical activation of rectal intraganglionic laminar endings in the guinea pig distal gut. *The Journal of Physiology, 564*(2), 589-601.

McGarigal, K. (2014). Fragstats v4: Spatial Pattern Analysis Program for Categorical and Continuous Maps-Help manual. *Amherst: University of Massachusetts. Recuperado de http://www. umass. edu/landeco/research/fragstats/fragstats. html*

Melville, J., Macagno, E., & Christensen, J. (1975). Longitudinal contractions in the duodenum: their fluid-mechanical function. *American Journal of Physiology, 228*(6), 1887-1892.

Muybridge, E. (1887). Complete human and animal locomotion. *New York*

Neal, K. B., Parry, L. J., & Bornstein, J. C. (2009). Strain specific genetics, anatomy and function of enteric neural serotonergic pathways in inbred mice. *Journal of Physiology, 587*(3), 567-586.

O'Grady, G., Angeli, T. R., Du, P., Lahr, C., Lammers, W. J., Windsor, J. A., . . . Cheng, L. K. (2012). Abnormal initiation and conduction of slow-wave activity in gastroparesis, defined by high-resolution electrical mapping. *Gastroenterology, 143*(3), 589-598. e583.

Ohe, M. R., Hanson, R. B., & Camilleri, M. (1994). Comparison of simultaneous recordings of human colonic contractions by manometry and a barostat. *Neurogastroenterology and Motility, 6*(3), 213-222.

Park, K. J., Hennig, G. W., Lee, H. T., Spencer, N. J., Ward, S. M., Smith, T. K., & Sanders, K. M. (2006). Spatial and temporal mapping of pacemaker activity in interstitial cells of Cajal in mouse ileum in situ. *American Journal of Physiology, 290*(5), C1411-1427.

Parsons, S. P., & Huizinga, J. D. (2015). Effects of gap junction inhibition on contraction waves in the murine small intestine in relation to coupled oscillator theory. *American Journal of Physiology-Gastrointestinal and Liver Physiology, 308*(4), G287-G297.

Rao, S. S., Sadeghi, P., Beaty, J., Kavlock, R., & Ackerson, K. (2001). Ambulatory 24-h colonic manometry in healthy humans. *American Journal of Physiology-Gastrointestinal and Liver Physiology, 280*(4), G629-G639.

Roberts, R. R., Bornstein, J. C., Bergner, A. J., & Young, H. M. (2008). Disturbances of colonic motility in mouse models of Hirschsprung's disease. *American Journal of Physiology, 294*(4), G996-G1008.

Roberts, R. R., Ellis, M., Gwynne, R. M., Bergner, A. J., Lewis, M. D., Beckett, E. A., . . . Young, H. M. (2010). The first intestinal motility patterns in fetal mice are not mediated by neurons or interstitial cells of Cajal. *Journal of Physiology, 588*(7), 1153-1169.

Russ, J. C. (2006). *The Image Processing Handbook* (5th ed.). Boca Raton: CRC Press.

Schreiber, D., Klotz, M., Laures, K., Clasohm, J., Bischof, M., & Schäfer, K.-H. (2014). The mesenterially perfused rat small intestine: A versatile approach for pharmacological testings. *Annals of Anatomy-Anatomischer Anzeiger, 196*(2), 158-166.

Seerden, T. C., Lammers, W., De Winter, B. Y., De Man, J. G., & Pelckmans, P. A. (2005). Spatiotemporal electrical and motility mapping of distension-induced propagating oscillations in the murine small intestine. *American Journal of Physiology, 289*(6), G1043-1951.

Sobel, I. (1970). *Camera models and machine perception*. DTIC Document.

Spencer, N. J., Bayguinov, P., Hennig, G. W., Park, K. J., Lee, H.-T., Sanders, K. M., & Smith, T. K. (2007). Activation of neural circuitry and Ca2+ waves in longitudinal and circular muscle during CMMCs and the consequences of rectal aganglionosis in mice. *American Journal of Physiology-Gastrointestinal and Liver Physiology, 292*(2), G546-G555.

Spencer, N. J., Nicholas, S. J., Sia, T., Staikopoulos, V., Kyloh, M., & Beckett, E. A. (2013). By what mechanism does ondansetron inhibit colonic migrating motor complexes: does it require endogenous serotonin in the gut wall? *Neurogastroenterology and Motility, 25*(8), 677-685.

Strobl, K. H., Sepp, W., Wahl, E., Bodenmuller, T., Suppa, M., Seara, J. F., & Hirzinger, G. (2004). *The DLR multisensory hand-guided device: The laser stripe profiler.* Paper presented at the Robotics and Automation, 2004. Proceedings. ICRA'04. 2004 IEEE International Conference on.

Tasaka, K., & Farrar, J. T. (1969). Mechanics of small intestinal muscle function in the dog. *American Journal of Physiology, 217*(4), 1224-1229.

Tops, L. F., Bax, J. J., Zeppenfeld, K., Jongbloed, M. R., Lamb, H. J., van der Wall, E. E., & Schalij, M. J. (2005). Fusion of multislice computed tomography imaging with three-dimensional electroanatomic mapping to guide radiofrequency catheter ablation procedures. *Heart Rhythm, 2*(10), 1076-1081.

Wang, Z. S., He, Z., & Chen, J. D. (2004). Chaotic behavior of gastric migrating myoelectrical complex. *IEEE Transactions on Biomedical Engineering, 51*(8), 1401-1406.

DRC 16

MASSEY UNIVERSITY
TE KUNENGA KI PŪREHUROA
UNIVERSITY OF NEW ZEALAND

GRADUATE RESEARCH SCHOOL

STATEMENT OF CONTRIBUTION
DOCTORATE WITH PUBLICATIONS/MANUSCRIPTS

We, the candidate and the candidate's Primary Supervisor, certify that all co-authors have consented to their work being included in the thesis and they have accepted the candidate's contribution as indicated below in the *Statement of Originality*.

Name of candidate:	Corrin Hulls
Name/title of Primary Supervisor:	Prof RG Lentle
In which chapter is the manuscript /published work:	Chapter 4

Please select one of the following three options:

(●) The manuscript/published work is published or in press

- Please provide the full reference of the Research Output:

Front. Physiol., 09 April 2018
Sec. Gastrointestinal Sciences
https://doi.org/10.3389/fphys.2018.00338

( ) The manuscript is currently under review for publication – please indicate:

- The name of the journal:

Frontiers in Physiology

- The percentage of the manuscript/published work that was contributed by the candidate: 70%
- Describe the contribution that the candidate has made to the manuscript/published work:

Conducted experiment (practical work)
Process of writing of results
Statistic procedure

( ) It is intended that the manuscript will be published but it has not yet been submitted to a journal

Candidate's Signature:	
Date:	3.10.22.
Primary Supervisor's Signature:	Professor Roger LENTLE
Date: 2/10/22	

This form should appear at the end of each thesis chapter/section/appendix submitted as a manuscript/ publication or collected as an appendix at the end of the thesis.

Preface Chapter 5

The proceeding chapter describes the normal myogenic activity of the *ex vivo* tetrodotoxinzed rabbit bladder. Applied spatiotemporal mapping techniques describe the motility of contractions including frequency, duration, velocity, area, and origin of activity. Further, the chapter provides a quantitative evaluation of bladder contractile motility. Ultimately, two types of contractile phenomenon are identified which are broadly similar to those based on published electrophysiological recordings but provide additional insight into the organisation of contractile behaviour in the whole organ and ultimately tonal accommodation.

Copy of Paper- Spatiotemporal analysis of spontaneous myogenic contractions in the urinary bladder of the rabbit: timing and patterns reflect reported electrophysiology

The following pages contain a copy of the published journal article with the following bibliography-

Hulls, C. M., Lentle, R. G., King, Q. M., Reynolds, G. W., & Chambers, J. P. (2017). Spatiotemporal analysis of spontaneous myogenic contractions in the urinary bladder of the rabbit: timing and patterns reflect reported electrophysiology. *American Journal of Physiology-Renal Physiology*, *313*(3), F687-F698.

The main format of the publish peer-reviewed article is reproduced in this chapter section with its format and content maintained. All references sited are listed in a separate sub-section after the main body of the article. These references would be reproduced in the main bibliography of this thesis (i.e., after the thesis appendix) only should they be used elsewhere beyond this section (i.e., of this published article). All further work beyond this section will be citing the work presented in this section where appropriate.

5 Spatiotemporal analysis of spontaneous myogenic contractions in the urinary bladder of the rabbit; timing and patterns reflect reported electrophysiology.

5.1 Abstract

The temporal and spatial dynamics of propagating myogenic contractions in the wall of the resting *ex vivo* urinary bladder of the rabbit were characterised by spatiotemporal maps of area strain rate and of linear strain rate and A-type contraction density plots and related to cyclic variation in intravesical pressure (p_{ves}).

Patches of propagating contractions (PPCs) enlarged and involuted with a frequency of 6.33 ± 0.67 cycles per minute (cpm), in near synchrony with peaks in intravesical pressure (p_{ves}) (3.85 mean ± 0.3 cpm). PPCs were generally preceded by regions of positive strain i.e., stretch. The maximum percentage of the anterior surface of the bladder undergoing contraction (55.28 ± 2.65 %) and the sizes of individual PPCs (42.61 ± 1.65 mm^2) also coincided with the peak in p_{ves}.

PPCs, originated and propagated within temporary patch domains (TPDs) and comprised groups of near synchronous cyclic individual contractions (PICs). The TPDs were located principally along the vertical axis of the anterior surface of the bladder, either to the left or the right of midline and changed in location from one side to side and from side to tip or base. The sites of origin of PICs within PPCs were inconsistent, consecutive contractions often propagating in opposite directions along linear maps of strain rate. Similar patterns of movement of PPCs within TPDs of the same form occurred in areas of the anterior bladder wall that had been stripped of mucosa.

Intravesical pressure (p_{ves}) varied cyclically with total area of contraction and with the indices of the size and aggregation of PPCs, indicating that PPCs grew and involuted by a combination of peripheral enlargement or shrinkage and by coalescence or fission with other PPCs, their areas being maximal at or around the peak in p_{ves}.

The synchronisation and extended propagation of PICs within PPCs and the concurrent variation in p_{ves} were sometimes lost or diminished, uncoordinated PICs then occurred irregularly (between 4 and 20 cpm), propagated shorter distances, and had little effect on p_{ves}. There was no evidence that any influence of bladder shape on stress influenced the principal direction of propagation of either PCCs or PICs or the disposition of TPDs.

Hence the authors postulate that that the formation and involution of PPCs within a TPD resulted from cyclic variation of excitation, likely from excitation of a field of intramuscular ICCs, that increased the incidence and distance over which component PICs propagated but did not influence their inherent frequency or direction of propagation.

5.2 Introduction

The bladder acts as a temporary repository for the intermittent inflow of urine by appropriate and ongoing adjustment of wall compliance to mitigate any consequent rise in luminal pressure (A. Brading, 2006). Hence, the bladder wall exhibits rhythmic spontaneous phasic contractions or 'micromotions' (Bo Coolsaet, 1985) that are superimposed on (Poley et al., 2008) and may reset (Lentle et al., 2015b) baseline tone.

Micromotions or patch contractions were first described in 1882 in human females and dogs (Angelo Mosso & P Pellacani, 1882), and subsequently in a range of species including monkeys, cats (Charles S Sherrington, 1892a), guinea pigs (M. Drake et al., 2003), rats (Sugaya & de Groat, 2000), and pigs (B. L. Coolsaet, Van Duyl, Os-Bossagh, & De Bakker, 1993). Subsequent work showed that such activity was not inhibited by denervation (Plum & Colfelt, 1960) and occurred in bladders that were maintained *ex vivo* (M. Drake et al., 2003) as well as in isolated strips of bladder muscle (A. F. Brading, 1997). Further, the failure of atropine or tetrodotoxin to inhibit these contractions (ROBERT M Levin et al., 1986) lead to the conclusion that the rhythmic activity and tone were primarily myogenic (Turner & Brading, 1997) but could be influenced by parasympathetic and sympathetic nervous input (J. Gillespie, 2004a). Whilst much is known regarding the cellular activity of the myogenic cellular components that generate patch contractions, the mechanisms that underlie their genesis and pattern of development are poorly understood.

The smooth muscle of the bladder (Hikaru Hashitani, Brading, et al., 2004) is capable of undergoing activation by an endogenous membrane oscillator (Berridge, 2008) leading to the generation of action potentials (Hikaru Hashitani, Brading, et al., 2004). These action potentials can occur singly (frequency 8-27 cpm) or in bursts (mean frequency 4.2 ± 2.2 cpm), the latter grouping being thought to occur under normal physiological conditions (Hikaru Hashitani, Brading, et al., 2004). The frequency of spontaneous patch contractions in the intact pig bladder (3 cpm) (Lentle et al., 2015b) lies below that of repeated single action potentials in the guinea pig bladder (14.5 ± 6.2 cpm) (Hikaru Hashitani, Brading, et al., 2004) but is close to the mean frequency of 'burst patterns' of action potentials (4.2 ± 2.2 cpm) (Hikaru Hashitani, Brading, et al., 2004). Again the frequency of spontaneous Ca^{2+} transects generated in smooth muscle cells from the guinea pig bladder (4.5 ± 1.7 cpm)

(McCloskey & Gurney, 2002b) is greater than those from C-kit positive cells (0.66 ± 0.27 cpm) (McCloskey & Gurney, 2002b) (Hikaru Hashitani, Yanai, & Suzuki, 2004a) the former being closer to the frequency of spike patches (W. J. E. P. Lammers & Slack, 2001).

The areas of patches of propagating contractions (PPC) in the bladder (Bo Coolsaet, 1985; M. Drake et al., 2003; Lentle et al., 2015b) are generally larger than those of the sites in the intestine termed 'spike patches' or 'electrical patches' (W. J. E. P. Lammers & Slack, 2001), that delineate the area through which an action potential can radiate among neighbouring myocytes (Ikeda et al., 2007). However, the electrical coupling between adjacent detrusor smooth muscle cells is relatively poor, particularly in the transverse direction i.e., at right angles to the long axes of the myocytes (Hikaru Hashitani & Alison F Brading, 2003a) being lower than that of smooth muscle in most other tissues (Tomita, 1990). Hence, it has been hypothesised that, these properties would impair spread of an action potential through large numbers of myocytes (Hikaru Hashitani & Alison F Brading, 2003a). It therefore appears that the spread of patch contractions may be facilitated by other means.

C-kit positive (Johnston et al., 2010) and PDGFR positive (Koh et al., 2012; Monaghan, Johnston, & McCloskey, 2012) ICCs have been identified in the detrusor. Whilst it is generally accepted that these ICC do not generate slow waves (A. Brading, 2006), they may modulate (Hikaru Hashitani, Yanai, et al., 2004a) the spread of action potentials along the bundles of smooth muscle to allow concerted contraction within a patch (Ikeda et al., 2007). Whilst calcium imaging studies showed that ICC located at the periphery of muscle bundles, and in the interstitial tissue between them, generate slow rising spontaneous calcium transients that may facilitate myogenic contraction within bundles, there was little evidence of inter-bundle conduction and facilitation (Hikaru Hashitani, Yanai, et al., 2004a).

It is possible that the spontaneous electrical waves that propagate through limited numbers of gap junctions (Hammad, Stephen, Lubbad, Morrison, & Lammers, 2014; W Lammers, Morrison, Lubbad, Stephen, & Hammad, 2013) maintain their impetus by biomechanical activation (Elbadawi, 1995; G. Ji, Barsotti, Feldman,

& Kotlikoff, 2002), local contraction engendering stretch (+ve strain) that activates either ICCs or adjacent myocytes (Elbadawi, 1995; G. Ji et al., 2002). It is known that myogenic contraction (-ve strain) may be elicited in isolated strips of detrusor in response to quick stretch (Geoffrey Burnstock & Prosser, 1960). Further, it is known that stretch influences cytosolic Calcium levels via L-type calcium channels (Davis & Hill, 1999) and non-selective ion channels (M.-C. Wellner & G. Isenberg, 1993), notably stretch dependent ryanodine receptors (G. Ji et al., 2002) and Rho kinase activity (Poley et al., 2008). Again, a 20% stretch of C-kit positive interstitial cells cultured from the guinea pig bladder evoked calcium transients in addition to the regular baseline frequency (1.22 ± 0.52 cpm) indicating that ICC may facilitate the response to stretch (Y. Wang et al., 2010). Further, similar cells cultured from partially obstructed bladders displayed significantly more lateral branching and a higher frequency of calcium transects than those cultured from unobstructed bladders (Y. Wang et al., 2010).

Thus, coordination of contraction within a patch, and expansion or migration of a patch, could result from a local increase in strain in the bladder wall (Poley et al., 2008) in a similar manner to that in the distended gastric fundus (Roger Graham Lentle et al., 2016), or may locally augment the growth of a patch once contraction and surrounding tension are established (Elbadawi, 1995; G. Ji et al., 2002). However, it is noteworthy that the overall vectoring of strain, and the local response to it, may be influenced by other factors, notably the orientation of myocytes within the bladder wall, the mechanical properties of the bladder wall and the shape of the bladder.

Given the ellipsoidal shape of myocytes, the total strain that accrues in each cell will be greater when a given stress is applied along their longitudinal axes. The distribution of the orientation of myocytes, in the rat bladder at least, is biased with a predominance of myocytes having their long axes orientated parallel with the vertical axis of the bladder (Nagatomi, Toosi, Grashow, Chancellor, & Sacks, 2005). Given the greater longitudinal than transverse electrical coupling, propagation between adjacent myocytes (Hikaru Hashitani & Alison F Brading, 2003a) will be similarly biased.

Biomechanical studies indicate that normal bladder tissue is isotropic when loaded, with equal stress in both radial and vertical directions (Gloeckner et al., 2002), but can behave in an anisotropic manner under unequal stress loading i.e., exhibit differing mechanical properties according to the direction in which the stress is applied (Gloeckner et al., 2002).

The overall shape of the bladder may also influence the magnitudes of the stresses in the various dimensions. Hence, if the bladder is viewed as an inverted solid cone, stress in the horizontal (circular) dimension i.e., hoop stress, will be greater than that in the vertical dimension (Thompson & Little, 1970). Further, hoop stress will be greater toward the dome where the radius is greatest (Thompson & Little, 1970). If tension receptors are equally sensitive to tension throughout the bladder wall, then the likelihood of stress induced activation will similarly increase, and contraction will be more likely to commence in the upper half of the bladder. Alternatively, the distribution of ICCs and the possibility of their forming an interconnected network or responding to local stretch in a coordinated manner may vary regionally with local stress (Y. Wang et al., 2010) so that contractions will tend to be initiated and their propagation facilitated at sites where the density of ICC is high (Ahmed Shafik, El-Sibai, Shafik, & Shafik, 2004) or where their morphology is elongated in a particular dimension.

The current work applies the two-dimensional spatiotemporal mapping of strain rate and adjunct techniques, developed by our unit, to map spontaneous contractions in the bladder of the rabbit maintained *ex vivo* by super-perfusion. This was undertaken to evaluate the patterns of genesis and propagation of patches of myogenic contractions (PPCs) and their co-ordination with cyclic changes in intravesical pressure, with a view to identifying any effects of local or general wall tension on the behaviour of these patterns and on the level of coordination between contractions at various sites in the wall of the bladder.

5.3 Materials and Methods

All the experimental procedures were approved by the Massey University Animal Ethics Committee (MUAEC approval number 14/50) and complied with the New Zealand Code of Practice for the Care and Use of Animals for Scientific Purposes. Ten New Zealand White rabbits were obtained from a commercial breeder and

maintained on commercial feed, which was available *ad libitum* with water until immediately prior to the procedure.

5.3.1 Experimental procedures

5.3.1.1 Intact bladder

Once the animal had been anaesthetised with halothane, the abdomen was opened with a midline ventral incision and the symphysis pubis divided at the midline. The bladder was freed from its mesenteric and basal attachments, the ureters transected and tied approximately 0.5cm from the trigone, the urethra transected approximately 2 cm distal to the neck, and then removed from the peritoneal cavity. Immediately following its removal, the bladder was immersed in ice cold oxygenated Earle's HEPES buffer solution (HBS) prior to installation in an organ bath. The animal was subsequently euthanized with intracardiac pentobarbitone (125 mg/kg).

The urethra was cannulated with a curved metal cannula (2 mm OD) and secured in position with a ligature 5 mm distal to its junction with the bladder base. The cannula had been prefilled with saline as was a length of tubing that connected the cannula to a port on a three-way valve with the other two ports connected to a pressure transducer and a syringe pump, respectively. The syringe pump allowed physiological saline to be instilled into or removed from the cavity of the bladder. The output from the pressure transducer (Spectramed P23XL, Oxnard, CA, USA) was connected to a PowerLab 8SP computer interface (AD Instruments, Sydney, Australia) and pressure readings were acquired at 100 Hz.

The anterior and lateral surfaces of the bladder were sprinkled with carbon black. The bladder was then then suspended, apex downward, from the urethral cannula in an organ bath with its anterior surface facing the video camera (Fig 1A) and immersed in oxygenated (95% O_2, 5% CO_2) HBS solution of pH 7.35, comprising 124.0 mM NaCl, 5.4 mM KCl, 0.8 mM $MgSO_4$, 1.0 mM NaH_2PO_4, 14.3 mM $NaHCO_3$, 10.0 mM HEPES, 1.8 mM $CaCl_2$ and 5.0 mM glucose maintained at 37°C and continuously recirculated at a flow rate of 160 ml/min.

A typical filling protocol consisted of adding 15 ml aliquots of saline to a maximum of 30ml, waiting 15 minutes between additions.

Tetrodotoxin 0.5 mg (to give a concentration of 0.005 mmol l^{-1}) was added directly to the superperfusate of each preparation 10 minutes prior to the commencement of video and transducer recordings to ensure that only myogenic activity was evaluated.

5.3.1.2 Bladder with mucosa removed

In an additional three bladders an area of bladder mucosa of around 155 mm^2 was removed from the internal surface of the anterior wall before it was mounted in the organ bath for spatiotemporal analysis in a similar procedure to that described above.

Immediately after removal from the rabbit the bladder was immersed in ice cold Earle's HEPES solution and a vertical full thickness incision extended upwards over the lower third of the posterior wall of the bladder from the bladder base. The bladder was then evaginated and the rectangle of transitional mucosa dissected from the bladder wall. The bladder was then invaginated, the vertical incision sutured with continuous chromic gut, and installed in an organ bath.

At the conclusion of the experiments, representative samples of the bladder wall were taken at the site of removal of the bladder mucosa and at adjacent sites where it was preserved and preserved in 10% Formol-saline for subsequent embedding transverse sectioning and staining with haematoxylin and eosin.

5.3.1.3 Image acquisition and processing

Image sequences were captured on a video camera mounted to the side of the organ bath and saved as an uncompressed AVI video file for off-line processing.

The motility pattern over the bladder surface was evaluated by extending cross-correlation techniques (P.W.M Janssen & Lentle, 2013) to two dimensions. In this method, the local movement of the distinctive visual textural features between successive frames was used to quantify the displacements of reference points on a grid of

equally spaced points within a rectangular region of interest (ROI). The area strain rate (ASR) for each reference point was determined from the local displacement rates using the same technique that was described in a previous paper (Lentle et al., 2015b). Briefly, ASRs were expressed as the percentage change in muscle area per unit time, i.e., % s^{-1}. The sensitivity of the ASR mapping method is well established. ASR maps derived from myocardial MRI has been shown to provide better discrimination between normal and ischemic zones than other indices of strain (Azhari, Weiss, Rogers, Siu, & Shapiro, 1995).

Two dimensional maps of local ASRs i.e., successive A-type ST maps were each superimposed on corresponding video images of the bladder to enable the patterns of motility on its surface to be visualised. The area of superimposition was limited by a user-specified ellipsoidal mask which occupied 45% of the anterior surface and excluded sites that were close to the edge of the organ profile where artefacts from minor rotation of the organ and foreshortening from angulation of the surface could occur (Fig 5-1). The ASRs were colour-coded such that rapidly contracting areas appeared yellow (-ve ASR), more slowly contracting areas appeared red and expanding areas appeared blue (+ve ASR).

L-type Spatiotemporal maps i.e., plots of the variation in linear strain rate at all points along a line of interest (x axis) over time (y axis) were also generated from the video (Figs 5-1A and B). Hence LOIs were positioned vertically, traversing the right- and left-hand sides of the bladder, and horizontally, traversing the upper (lowermost in frame) and lower (uppermost in frame) halves of the bladder.

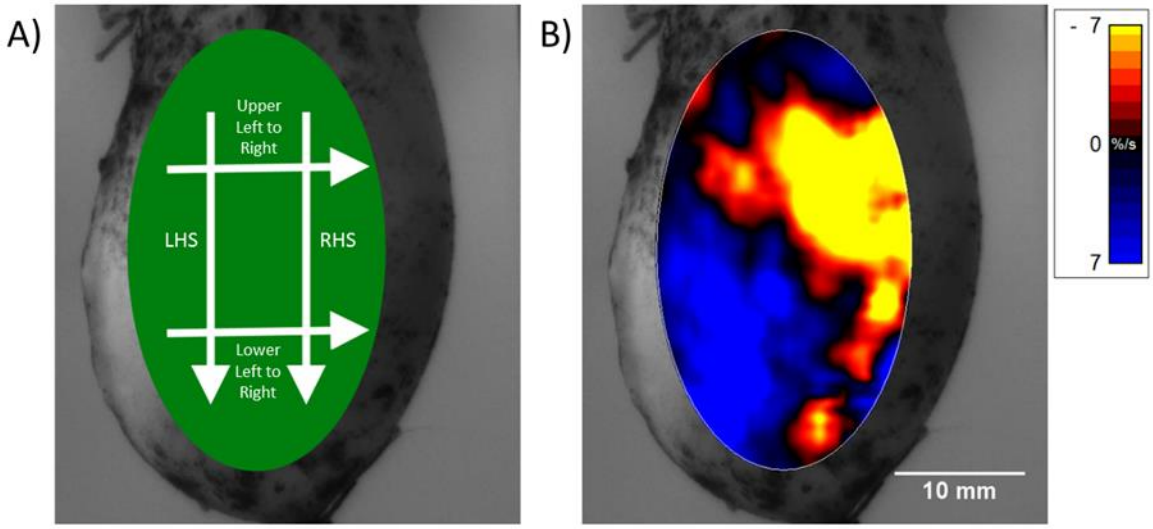

Figure 5-1 Methods for ST mapping of the bladder.

The position of the bladder in the organ bath with urethra uppermost after carbon black has been randomly applied to the anterior face. A) the ellipse applied to cover a defined percentage of the anterior surface (green). The positions and directions of analysis of the vertical LOIs in the left and right halves of the bladder and the horizontal LOIs in the uppermost (lower half) and lowermost (upper half) halves of the bladder. B) showing overlay of area (A) type ST map onto the image of the bladder with positions of transects for L map ST maps as in A.

The speed and direction of propagation of a contraction or group of contractions could be directly determined from these maps as it was inversely proportional to the angle of the contraction stripe to the horizontal axis. This technique also allowed for identification of the propagating individual contractions (PICs) that made up PPCs by their varying (minor) degrees of deviation from the LOIs. Cyclic variation in strain rate over time was assessed by Fast Fourier transforms of vertical transects of the L-type ST maps, derived in Excel.

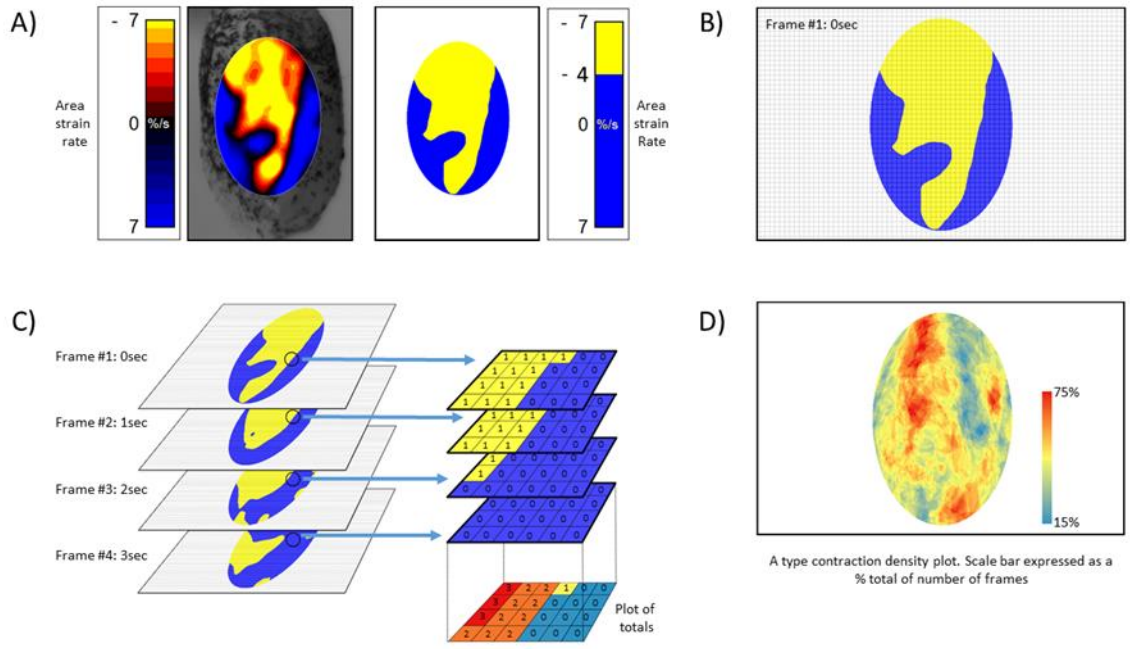

Figure 5-2 Showing method of construction of A-type contraction density maps.

A) Successive Area Spatiotemporal maps are thresholded to include all sites at which strain rate exceeds a chosen value (less than -4 % strain s^{-1}). B) Frames are suitably subsampled at chosen intervals; C) Subsampled frames are stacked over a chosen time span and the number of frames within the stack with strain rate in excess of the chosen threshold counted for each pixel stack and plotted as a colour coded total i.e., stacked A-type contraction density plot. D) Typical stacked A-type contraction density plot covering over 45% of the anterior surface of the bladder.

5.3.1.4 Further data processing and Statistics

To facilitate the determination of the locations of groups of propagating patches of contraction (PPCs) we stacked A-type ST maps from video frames taken at one second intervals over successive minutes and plotted the frequency that area strain rate in each component pixel decreased below -4% s^{-1} during that minute, on a yellow to colour blue scale, to produce a graphic that we term an A-type contraction density plot (Fig 5-2). The resulting graphic allowed us to determine the size, shape, and position of sites on the anterior surface of the bladder at which PPCs occurred most frequently during a set time interval (60 s), which we termed a temporary patch domain (TPD). Thus, the lines of interest (LOIs) of the L-type spatiotemporal maps that were used to determine the rates of propagation of PPCs traversed the TPDs in the vertical and horizontal dimensions. The variation in mean total areas of PPCs and in P_{ves} over time were explored in Curve Expert Professional® V2.62

(D.G. Hyams @curve expert.net). Regressions of the two variables were conducted in SYSTAT version 11 (*http://www.systat.com*).

We used parameters that have been developed to describe the spatial structure of patches of vegetation in landscapes (McGarigal, Cushman, Neel, & Ene, 2002; McGarigal & Marks, 1995) in conjunction with the FRAGSTATS software suite (McGarigal et al., 2002) to quantify the changes in shape and size of PPCs during their development and involution. Hence this software was used on successive A-type ST maps of video frames, taken at one second intervals, to determine:

1) The mean total areas of all PPCs occurring in a given A-type ST map as a percentage of the total area viewed (PMTA) (McGarigal et al., 2002).

2) The area of the largest PPC as a percentage of the total area of the viewed (LPI) (McGarigal et al., 2002).

3) The aggregation index (*AI*) an expression describing the number of patches that are adjacent to the largest patch in the field of view.

$$AI = \left[\frac{g}{\max \rightarrow g}\right]$$

Where g = number of like adjacencies between patches of pixels delineating a contraction and $(\max \rightarrow g)$ is the maximal number of possible adjacencies when patches are clumped to form a single patch. Hence, where all patches are disaggregated $AI = 0$ and when all patches are aggregated into a single patch $AI = 100$.

The normalised values for PMTA and for LPI in successive A-type ST maps taken at one second intervals were plotted in SYSTAT against the percentage of the mean period of the cyclic variation in p_{ves} for that preparation with a LOWESS (running weighted average of local y values) smoother. Curve fits for each of the two parameters were obtained using the 'Curve fit' software (D. G. Hyams @curve expert.net). The covariation between the two parameters was explored by regression in SYSTAT. The three indices each required conversion in the Johnson algorithm of Minitab (Minitab Pty Ltd Sydney Aust.) to render them suitable for parametric

analyses. The converted values were subject to two-way ANOVA (contractile state and animal) to determine the effect of contraction (values taken during the peak in p_{ves}) i.e., during the period between 25 and 75% of the cycle in P_{ves} and values taken at times between these peaks i.e., in excess of 75% and below 25% of the cycle in P_{ves} and for the effect of preparation i.e., between animals.

Unless otherwise stated, all results are presented as the mean ± SE of the mean observation for each animal.

5.4 Results

5.4.1 Intact bladder

5.4.1.1 Pressure traces

Cyclic changes in p_{ves} continued throughout the bulk of observations in the bladder in all 10 rabbits (Fig 5-3). The mean frequency of p_{ves} cycles in the resting bladder was 3.85 ± 0.3 cpm (n = 7 rabbits, 3 observations), the mean amplitude was 0.353 ± 0.01 mm Hg (n = 7 rabbits, 3 observations). The large standard deviations in both of these parameters resulted from spontaneous changes from time to time in the amplitude and frequency of peaks in p_{ves}. The amplitudes but not the frequencies of cycles in P_{ves} temporarily increased after the insertion of further 15 ml aliquots of fluid into, and fell after removal of fluid from, the cavity of the bladder.

The amplitudes of p_{ves} cycles were generally greatest, and their frequency most stable, during periods when PPCs were in a quasi-stable rhythm and were lowest during periods of inconstancy in the grouping and pattern of propagation of PICs (see below) within PPCs (Fig 5-3). Hence, from time to time, the cyclic changes in p_{ves} ceased whereupon the mean pressure fell and fluctuated in a random manner (Fig 5-3).

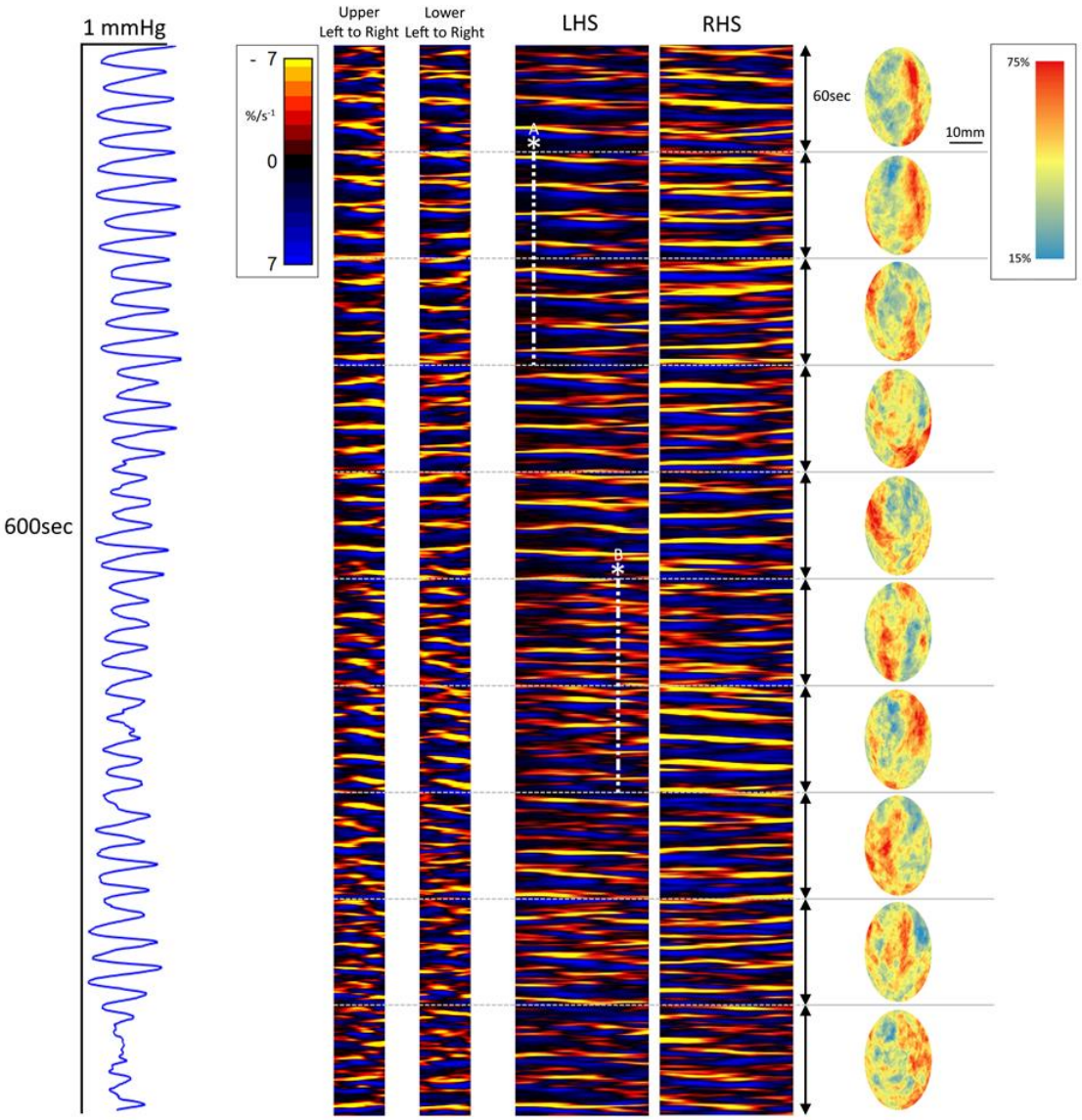

Figure 5-3 Composite of variation in intracystic pressure, A-type contraction density maps and L-type ST maps during propagation of PPCs across the anterior surface of a single preparation of rabbit bladder.

Left column; variation in intra-cystic pressure (p_{ves}); right column; A-type contraction density plots taken over consecutive 60 second periods (marked with horizontal dotted lines). The plots indicate the colour coded number of frames in which -ve strain rate is less than -4 % strain s^{-1} at a given pixel in a given 60 second sequence with yellow indicating highest count and blue lowest count expressed as a percentage of sixty frames.

Centre right pair of columns vertically L maps taken along vertically orientated LOIs on the left-hand side (LHS) and the right-hand side (RHS) of the bladder.

Centre left pair of columns L maps taken along horizontally orientated LOIs on the upper (upper left to right) and lower (lower left to right) halves of the bladder The slopes of the stripes on the L maps that mark PPCs, or PICs are inversely proportional to their propagation speed. Vertical dotted lines are positions of transects shown in Fig 6.

Note that these positions are with respect to the organ in its position in the bath not its anatomical position.

5.4.2 Spatiotemporal mapping

5.4.2.1 A-type maps of contraction density

Stacked A-type ST maps (Fig 5-3) showed that propagation of PPCs appeared to be restricted largely to vertically orientated sites, which we term temporary patch domains (TPDs), located on one or the other side of the anterior face of the bladder. Hence, the TPDs contained points at which high numbers of contractions commenced and subsequently propagated largely vertically whilst expanding laterally. The TPDs shifted in position spontaneously and erratically over time to other locations. The timing and locations of these shifts varied between preparations (Fig 5-4).

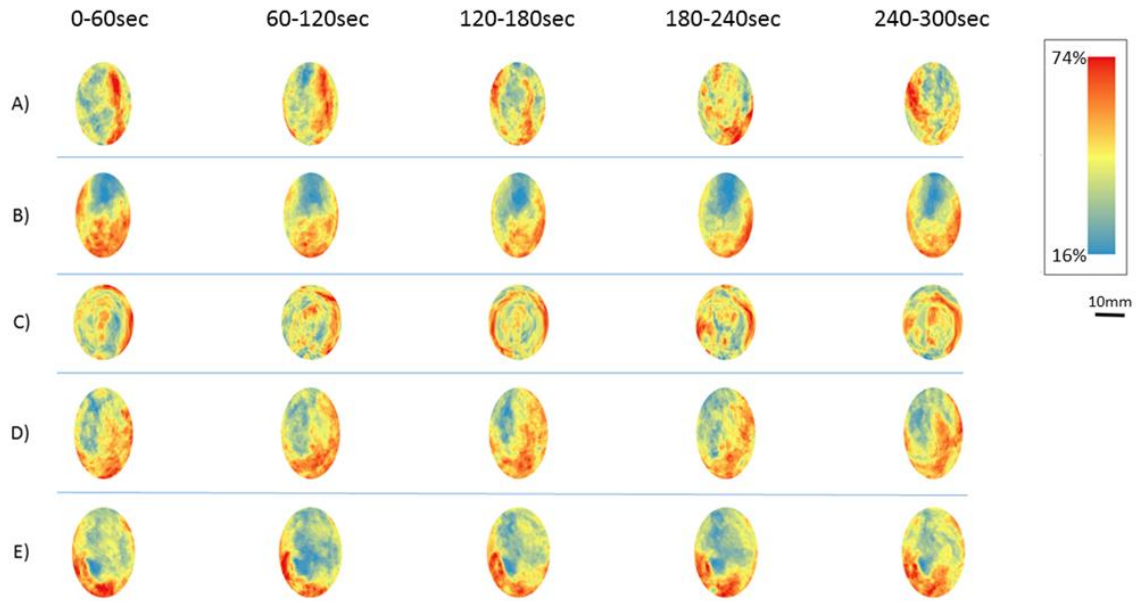

Figure 5-4 Serial A-type contraction density maps of five preparations of rabbit bladders.

Red areas of high frequency of contraction occur in distinct regions i.e., temporary patch domains (TPDs) and do not occupy the entire anterior surface of the bladder. TPDs spontaneously change in position from left to right and from top to bottom of the anterior surface with reciprocal changes in areas where contraction density is low (blue).

5.4.2.2 A-type ST maps

The number of pixels under negative strain on the anterior surface of the bladder varied sinusoidally over time (mean 55.28 ± 2.65% of area analysed; 6 rabbits, 3 replicates) rising to a maximum of 66.17 ± 1.63% and falling to a minimum of 18.7 ± 0.89% (2 rabbits, 30 observations each rabbit) of the total available area. Spontaneous rhythmic propagating patches of contraction (PPCs) (mean patch size 42.61 ± 1.65 mm^2) were visible in the anterior and anterolateral regions of the bladder wall when the bladder contained in excess of 15 ml of liquid (Fig 5-5 and Film 1). Their amplitudes increased with increase in volume of fluid rising to a maximum at a volume of 45 mls. No static PPCs were seen.

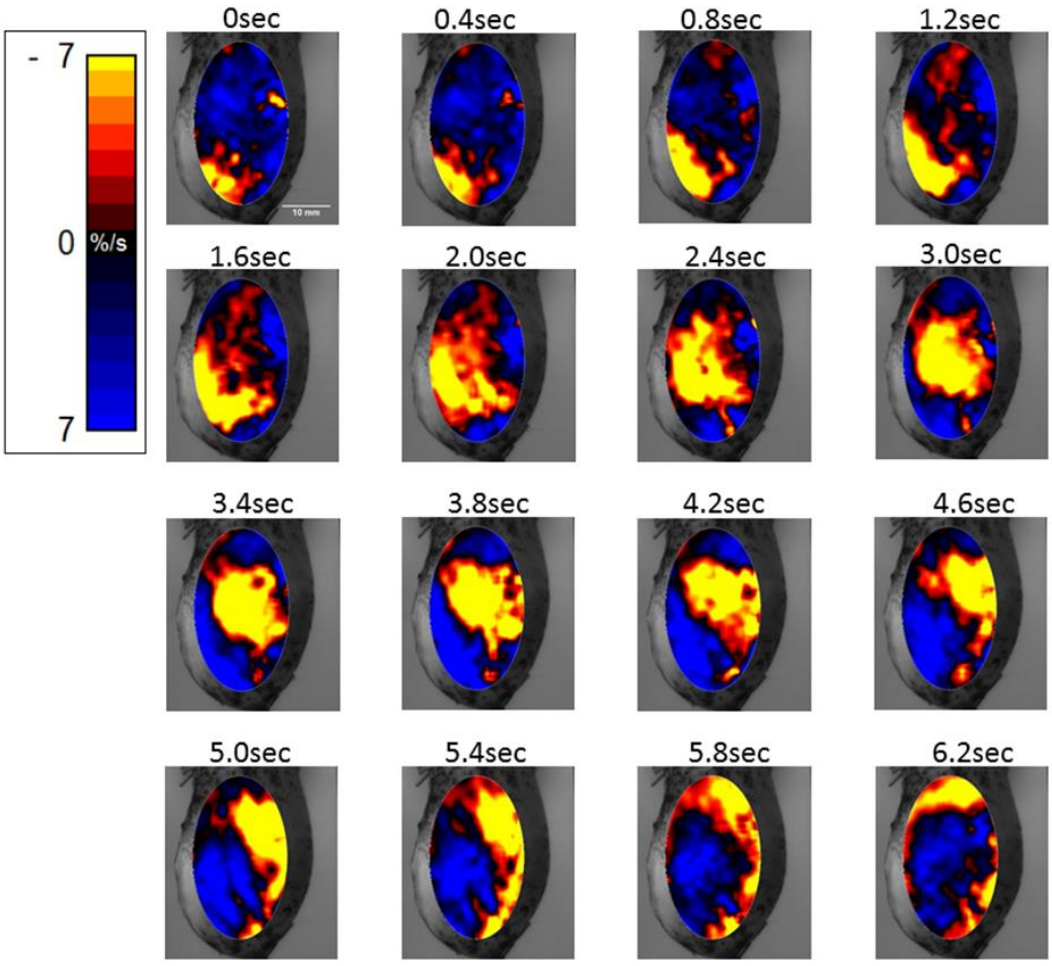

Figure 5-5 Sequence of A-type ST maps overlaid onto the anterior surface of the bladder during the transit of a PPC. During their transit across the surface of the bladder PPCs increase in size by peripheral growth and by aggregating with smaller PPCs and decrease in size by the reverse process.

The PPCs varied in size, the largest occupying up to 80.2% of the anterolateral surface of the bladder within the ellipsoidal mask. Whilst there was some variation between preparations in the speed at which PPCs propagated, there was no significant variation in the speeds of propagation according to their site of origin or their direction of propagation.

5.4.2.3 L maps based on vertical and horizontal transects through TPDs

PPCs propagated through axes that vertically transected TPDs in cyclic quasi-stable paths (Fig 5-3) at a mean frequency of 6.33 ± 0.67 cpm (7 rabbits 3 observations). The mean velocity of propagation of PPC measured along an LOI orientated on the long axis of TPDs was 4.5 ± 0.27 mm s^{-1} (5 rabbits, 5 observations) and the mean duration was 1.66 ± 0.06 s (5 rabbits, 5 replicates).

The cyclic bands of the PCCs on the L-maps each consisted of groups of propagating individual contractions (PICs) that, judging by the lack of angulation of these events to the horizontal axis, propagated at a higher velocity (in excess of 40 mm/s) than that of the PPC (Fig 5-3). Hence, the durations of PPCs (mean 1.66 ± 0.06 s; 5 rabbits 5 observations) varied according to the number of component PICs The mean duration of PICs was 0.64 ± 0.06 s (5 rabbits 5 replicates) hence, the average PPC would contain around 3 PICs. The timing and direction of propagation of the component PICs within a TPD varied locally along the LOI of the L-map so that they sometimes sloped in concert with the overall direction of propagation of the PPC i.e., travelled in the same direction, and sometimes sloped in the other i.e., travelled in the opposite direction (Fig 5-3).

On occasion the grouping of PICs into PPCs broke down, single PICs then occurring irregularly at higher frequencies (4-20 cpm) (Fig 5-6) than PPCs, each propagating over shorter distances than those within PPCs. Hence while the majority of PPCs propagated over the entire length of the vertical LOI, isolated PICs propagated between the mean distance of propagation (18.43 ± 1.05% of the length of the vertical LOI) (5 rabbits, 5 replicates) (Fig 5-3). Fast Fourier transforms of vertical transects though regions of the L-type maps where regular PPCs occurred, showed a dominant frequency of around 4 cpm with harmonics arising from variable grouping of component PICs within PPCs.

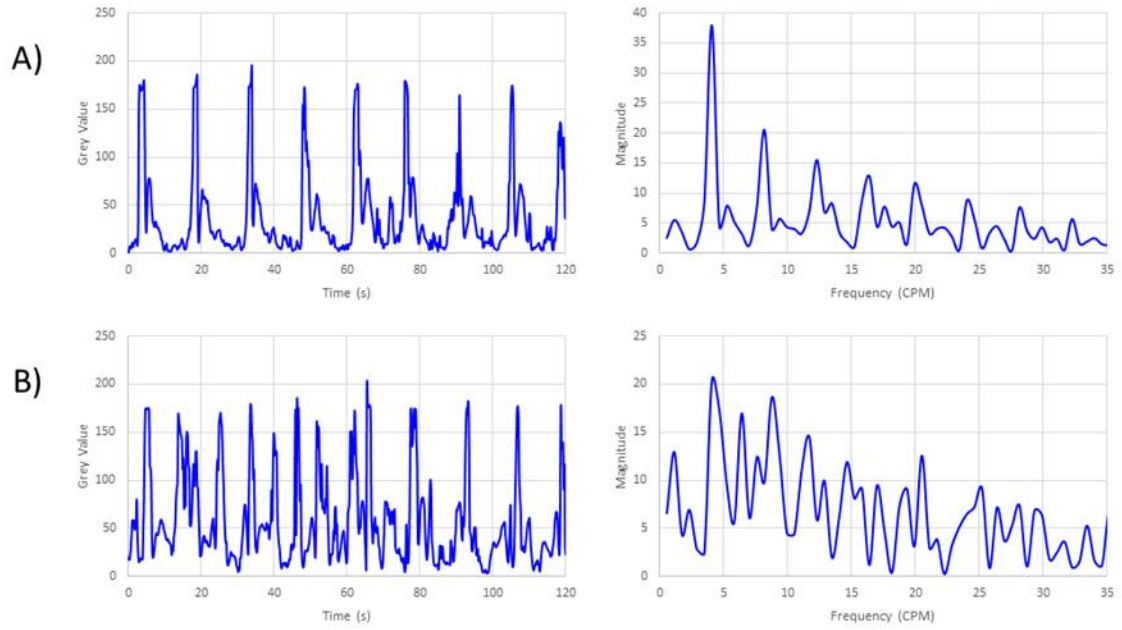

Figure 5-6 Vertical transects (right) and corresponding fast Fourier transforms (left) of L-type strain rate maps (right) taken along vertical LOIs at times and locations where PICs were grouped into PPCs (A) and during a period when PPCs were not evident (B).

The sites of the two L-type maps are marked as vertical lines on Figure 3. Note the sequence of harmonic frequencies starting at 4 cpm in A) results from the varying patterns of successive groups of PICs within each PPC and that the regular progression of harmonics is lost at times and locations where PICs were not grouped into PPCs.

Conversely those of vertical transects through regions in which PPCs broke down, gave an array of larger peaks at less regular frequencies that varied between 4 and 20 cpm.

Similar patterns of grouping of PICs into PPCs, and areas with loss of grouping of PICs into PPCs, were seen on L-type ST maps taken along LOIs on horizontal axes orthogonal to the main vertical axis of the TPD (Fig 5-3). However, whilst the propagation of the PPCs was sometimes maintained over the entire length of the vertically orientated LOIs, it was generally more limited on the horizontal LOIs (Fig 5-3). Similarly, the distance over which PICs propagated was relatively reduced on L-type ST maps with horizontal LOIs compared to those with vertical LOIs, both in the lower and upper halves of the bladder (Fig 5-3). Hence, the width wise spread of PPCs was reduced in the transverse axis compared with that along the main axis of the TPD. During periods on horizontal

LOIs, when the organisation into PPCs was lost, the distances that PICs propagated were reduced in a similar manner to those that occurred in the vertical LOIs.

Band like regions of local increase in strain rate i.e., rapid stretching, preceded but did not immediately follow, the PPCs (Fig 5-3). This arrangement tended to break down in sites where coordination of PICs into PPCs did not occur, thin i.e., short bands of relaxation sometimes preceded, sometimes followed, and sometimes occurred both before and after bands of contraction formed by PICs (Fig 5-3). Hence, PPCs tended to propagate into sites where stretching had recently occurred but without generating local stretch in their immediate wake whilst isolated PICs that were not within PPCs tended to propagate into, and to generate areas of stretch both in front of them and in their wake.

5.4.2.4 The development and involution of PPCs

Plots of variation of p_{ves}, of the % total area undergoing contraction and of the LPI over time with LOWESS smoothing showed that both parameters varied broadly sinusoidally. Best curve fits were p_{ves} = a + b cos (c*time + d), where a = 5.29E+01, b = 3.47E+01, c = 6.87E-02 and R^2 = 0.64 total area of contraction = a + b*cos (c*time + d), where a = 1.74E+01, b = 8.7E+00, c = 6.50E-02 and R^2 = 0.19 (Fig 5-7A and B). Those of the % total area undergoing contraction being almost identical to those of LPI.

Regression of P_{ves} against LPI was highly significant (df 1,184, F = 89.5; p <0.0005) though correlation was low (R= 0.32) presumably from high levels of random variation in the data.

The mean total areas of PPCs were significantly higher during the peak in p_{ves} (49.14 ± 0.87 mm^2) on two-way ANOVA of Johnson converted values (df 1,805, f= 23.7, p<0.0005) compared with those during in the trough in p_{ves} (34.55 ± 0.86 mm^2). Likewise, LPI values during the peak in the sinusoidal variation (19.29 ± 0.79%) in p_{ves} were significantly higher than those during the trough in p_{ves} (14.48 ± 0.65%) on two-way ANOVA (df 1,805, f = 45.14; p<0.0005) of Johnson converted values.

The total edges of PPCs that occurred during the peak in p_{ves} (59.86 ± 0.15 mm) were significantly longer on two-way ANOVA (df 1,804, f = 45.14; p<0.0005) of Johnson converted values than those that occurred during

the trough in p_{ves} (54.80 ± 0.15 mm) indicating that the PPCs were either increasing in size or in complexity of shape aggregation index scores during the peaks in p_{ves} (98.86 ± 0.05%) were significantly higher than those during the troughs in p_{ves} (98.51 ± 0.105) on two-way ANOVA (df 1,805, f= 14.76; p<0.0005) of Johnson converted values. Hence, it is likely that aggregation and subsequent fragmentation of PPCs, as well as simple increases in their total areas, both contributed to the increase in edge length during the rise in p_{ves}.

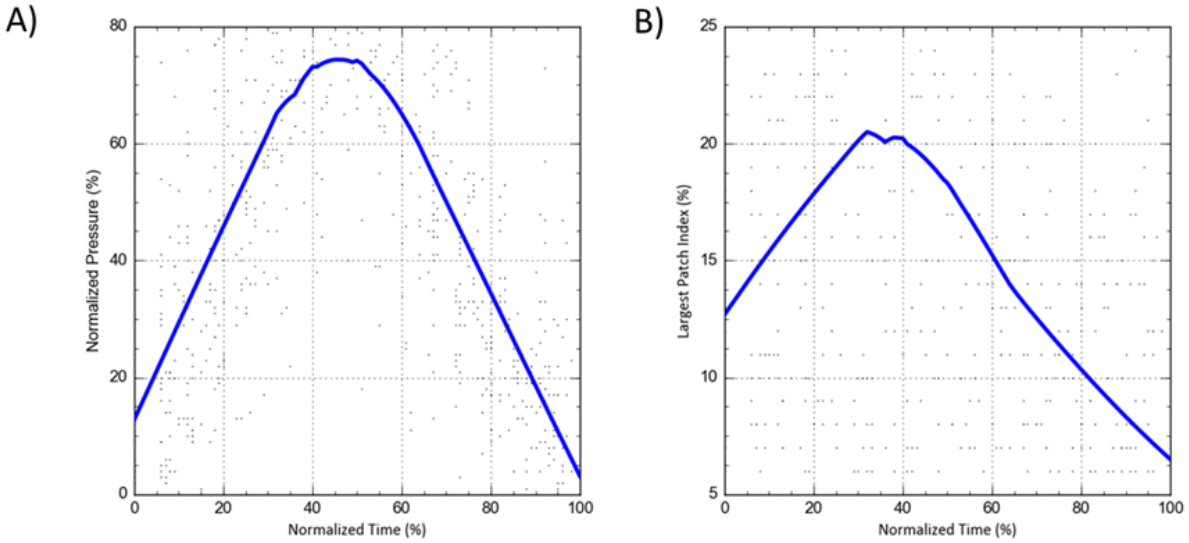

Figure 5-7 Variation with time of the largest patch index (LPI) and of P_{ves} during periods when PICs were synchronised within PPCs. The lines are from LOWESS smoothing of plots of normalised P_{ves} and LPI against the percentage of mean cycle time of P_{ves}.

5.4.2.5 Bladder with mucosa removed

Spontaneous PPCs commenced shortly after warming to 37°C in the organ bath in all three bladder preparations. Spatiotemporal mapping showed that the PPCs propagated across the rectangular defect in the of the mucosa at the same rate and amplitude as in the adjacent intact bladder wall (Fig 5-8).

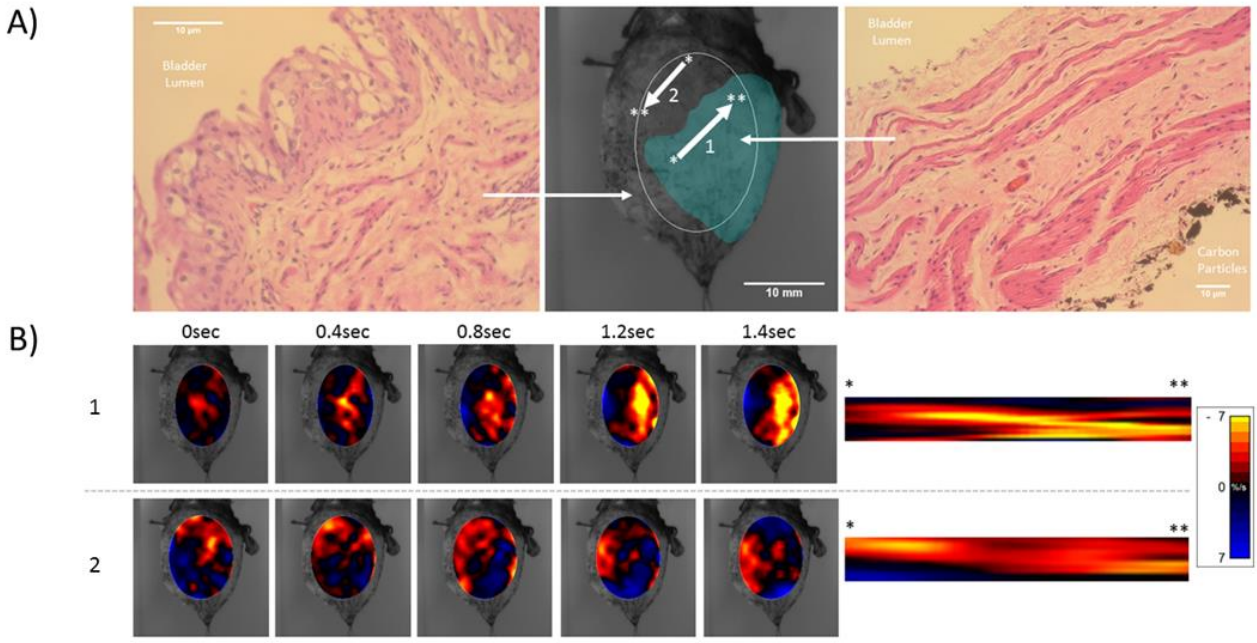

Figure 5-8 A-type A) and L-type B) spatiotemporal maps of PPCs traversing a region from which the bladder mucosa had been excised.

The central frame in A) shows the site of origin (marked *), termination (marked **) and direction of propagation of a PPC (1) transiting left to right across a site on anterior surface of the bladder overlying the rectangular defect (shown in blue) in the mucosa (lower arrow) and the site of a PPC (2) transiting right to left across an area that overlies intact mucosa (upper arrow).

The upper five frames in row B) are overlays of successive A-type ST maps of the PPC (1) at the site of the mucosal defect and the lower five overlays (B2 left five panels) are of PPC (2) at a site with intact mucosa (right to left upper arrow). The two panels on the right in row B) are 2.2 second segments of L-type ST maps along LOIs that traversed the principal direction of propagation of the two PPCs (upper panel PPC1, rate of propagation 7.5 mm s^{-1} ; lower panel PPC2 rate of propagation 7.66 mm s^{-1}).

The side panels in A) show Haematoxylin and Eosin stained sections of bladder wall with intact mucosa (Left) and stripped of mucosa (right) taken from the indicated sites at the conclusion of the experiment. Note the dark masses on the (anterior) serosal surface of the section which were carbon particles applied as markers for ST mapping. Scale bars indicate 10 µm.

Haematoxylin and Eosin stained sections confirmed that the mucosa and much of the underlying interstitial tissue had been removed from the rectangular site of microdissection (Fig 5-8).

5.5 Discussion

Whilst the general characteristics and disposition of patches of propagating contractions (PPCs) on the surface of the bladder have been described in previous publications (Lentle et al., 2015b), quantitative evaluation of their genesis and involution and accompanying changes in their area and distribution have not. The frequency and speed of propagation of PPC in the intact urinary bladder of the rabbit maintained *ex vivo* are broadly similar to those reported in the intact bladders of pigs *in vivo* and *ex vivo* (Lentle et al., 2015b). Further, the results from ST mapping are broadly similar to those based on published electrophysiological recordings (Hammad et al., 2014) but provide additional insight into the organisation of contractile behaviour in the whole organ. Hence, like the PPCs and PICs, the occurrence, and amplitudes of patches of spontaneous variation in electrical potential i.e., electrical waves, increased with stretch of the bladder wall. Further, as in this study the predominant direction of propagation of the changes in electrical potential was along the vertical axis, in line with the predominant orientation of myocytes and associated ICCs (Hammad et al., 2014). Similarly, TTX had little if any effect, either on the propagation of PICs and PPCs, or on electrical propagation (Hammad et al., 2014). Again, the mean frequencies of PPCs found in transversely and vertically orientated L-maps were close to those reported for bursts of action potentials and synchronous grouped contractions in sheets of guinea pig bladder wall denuded of mucosa (4.2 ± 2.2 min $^{-1}$) (Hikaru Hashitani & Alison F Brading, 2003a; Hikaru Hashitani, Brading, et al., 2004), moreover, the numbers of separate action potentials and accompanying contractions reported within each burst (5-20 events) was similar to that of PICs within PCCs on transverse and vertical ST maps. However, the characteristics of PPCs differed from those of electrical waves in a number of respects. Hence, as PPCs propagated vertically, they simultaneously enlarged in the transverse dimension whereas electrical waves were reported to rarely propagate in the transverse dimension (Hammad et al., 2014). Although the rates at which PPCs propagated in the rabbit bladder (4.5mm $\pm$ 0.27 s^{-1}) were similar to those reported in a previous ST study of the pig bladder (6.4 mm s^{-1}) (Lentle et al., 2015b) they were significantly slower than those of electrical waves in the guinea pig bladder (between 3 and 5 cm s^{-1}) (Hammad et al., 2014). However, the latter workers observed that electrical activity could occur either in single isolated spikes or in associated bursts and their estimates of the propagation velocity were based on propagation of the former, no

estimates being given for latter (Hammad et al., 2014). It was also reported that, whilst individual electrical waves propagated only a few centimetres before spontaneously disintegrating, repeated propagation could occur (Hammad et al., 2014). Correspondingly, in our work, the spatiotemporal configuration within PPCs, with their component PICs each propagating at a faster rate than the overall rate of propagation of the PPC, suggest that the slow rate of propagation of PPCs may result either from delays in the establishment of linkage between successive arrays of ICCs (the latter acting in a 'permissive' manner) (McCloskey, 2010b) or from delays in the activation of successive myocyte syncytia within electrical patches of excitation generated by ICCs. The former hypothesis is supported by the fact that electrophysiological 'patches' of excitation, which were also reported by these workers and hypothesised to be established by ICCs, (Hammad et al., 2014) were much smaller in size i.e., around 7.46 mm^2 or around 0.2% of the anterior surface, than the areas occupied by PPCs in the current study, which can cover as much as 80% of the elliptical area of analysis on the anterior surface of the bladder. Hence PPCs would be likely to contain many such electrophysiological 'patches'.

The occasional breakdown of organisation of regular PPCs on transverse and vertical ST maps, and their replacement by desynchronised bouts of irregularly timed PICs that propagated over more limited distances than those in PPCs (Fig 3) fits with reported findings (Hikaru Hashitani, Brading, et al., 2004; Kubota, Biers, Kohri, & Brading, 2006a) that action potentials and synchronous contractions could occur either in bursts or singly and irregularly in sheets of smooth muscle from guinea pig bladder, the latter at frequencies between 8 and 27 cpm which were the same broad range as the frequencies of PICs during these desynchronised bouts. It also fits with the observation that ongoing propagation of electrical waves via ICC may readily break down (Hammad et al., 2014). The finding that the administration of drugs such as Imatinab, which are reported to disrupt the function of ICC, also caused regular bursts of action potentials to revert to faster and irregular successions of single action potentials (Kubota et al., 2006a), whose frequency was again within the range exhibited by PICs in the desynchronised sections of the L-maps, further supports the hypothesis that ICCs are responsible for the synchronisation of PICs within PPCs.

However, the fact that the overall frequency of PPCs found in the current work was higher than the electrical frequency reported in individual ICC (0.66 ± 0.27 cpm) (Hikaru Hashitani, Yanai, et al., 2004a) supports the hypotheses that the predominant frequency of patch contractions results from the action of inherent pacemakers within the myocytes (Berridge, 2008) and that ICCs may aid propagation by inducing patches of change in potential in or around successive myocyte syncytia (A. Brading, 2006) that increase coordination and distance of propagation but do not subvert the inherent frequency.

The occurrence of TPDs, and of PPCs and PICs within them, has not been previously reported. The sudden shifts in the locations of TPDs and changes in the direction of propagation of PICs within PPCs lead us to postulate that such behaviour is more likely to result from changes in the organisation and linkage of spontaneous oscillation in chains of loosely coupled ICCs (Jan D Huizinga et al., 2015; Specht & Bortoff, 1972) than from linkage with permanent sites where populations of ICCs or myocytes have an inherently more rapid rhythm i.e., pacemakers (W. J. E. P. Lammers & Stephen, 2008).

The finding that the forms, frequencies, and rates of propagation of PPCs were identical in areas of the bladder that had been stripped of mucosa, with those in adjacent areas in which the mucosa was intact, suggests that PPCs and their component PICs are mediated by populations of ICCs within the detrusor muscle rather than by ICC within the lamina propria of the mucosa. This conclusion is also in line with the fact that the synchronised and desynchronised patterns of PICs seen in our work on bladders with intact mucosa match the two patterns of contractions reported in sheets of guinea pig detrusor that had similarly been stripped of mucosa (Hikaru Hashitani, Brading, et al., 2004). It is noteworthy in this regard that two types of intramuscular ICC have been identified, those positioned along the longitudinal axes of smooth muscle bundles, that do not form interconnected networks, and more stellate ICCs typically found in interstitial spaces between SM bundles (Johnston et al., 2010). It is tempting to speculate that the latter may be involved with cyclic regional activation leading to PPCs whilst the former activate individual PICs.

Whilst transverse (hoop) stress is generally higher than vertical stress in conical structures, the extent of propagation of PICs within PPCs was lower in the transverse than in the vertical dimension. Again, PICs within PPCs could originate either at the base or the apex of vertically orientated TPDs rather than being limited to the uppermost region, the site that would be expected to have the greatest hoop stress. Further, the rates of lateral spread of PPCs did not differ in the top half of the bladder from that in the bottom half of the bladder. Hence it appears that the overall geometry of the bladder, and any consequent gradation in hoop stress, had little effect on the disposition of PPCs. Rather, the propensity for PPC and their component PICs to originate and propagate along the right or left vertex, and the corresponding reported predominance of propagation of electrical waves along the vertical axis (Hammad et al., 2014) may result from morphological or physiological rather than mechanical bias i.e., the orientation of the long axes of myocytes (Nagatomi et al., 2005) and the processes of ICCs in the vertical dimension (Johnston et al., 2010) and the greater resistance of smooth muscle to conduction in a direction orthogonal to the long axis of myocytes (Hikaru Hashitani & Alison F Brading, 2003a). Nevertheless, areas of transient strain adjacent to local contraction may have a role in promoting excitation via local mechanoreceptors (Elbadawi, 1995; G. Ji et al., 2002). Localised bands of positive strain rate were found to precede PPCs on L-maps based on vertical LOIs through TPDs and thus could promote their formation. However, the pattern of disposition of strain around isolated PICs is more difficult to explain as bands of positive strain occurred both before and after these events.

Our observations on the morphology of developing and involuting PPCs (Fig 5-5) and our quantitative studies of the variation in area and shape of PPCs during cycles in intracystic pressure indicate that the sizes of PPCs increase and decrease by a combination of peripheral enlargement and agglomeration. Hence, that an increase in excitation within TPCs may lead to growth of PPCs by incremental extension of chains of coupled oscillators and to interlinking of such chains when smaller PCs approximate and fuse, whilst the reverse processes occur at times when the excitation and size of PPCs are declining.

In sum, analyses of the origin and transit of macroscopic patches of negative strain rate (PPCs) across the anterior surface of the bladder supports a hypothesis that PPCs result from the facilitation of the inherent

rhythmicity and frequency of contraction of myocytes by patches of ICC that become synchronised in the manner of coupled oscillators (Jan D Huizinga et al., 2015). This loose coupling is prone to break down allowing myocytes to contract at their own inherent frequency. A further paper will detail the effects of various pharmacological agent on the disposition and timing of TPDs, PPCs and PICs.

Acknowledgements

Andrew J Neverman, Institute of Agriculture and Environment, Massey University.

Thomas Cushnahan, Institute of Agriculture and Environment, Massey University.

Dr Dan E Patterson, Department of Geography and Environmental Studies, Carlton University, Ontario, Ottawa, Canada.

References

Azhari, H., Weiss, J. L., Rogers, W. J., Siu, C. O., & Shapiro, E. P. (1995). A noninvasive comparative study of myocardial strains in ischemic canine hearts using tagged MRI in 3-D. *American Journal of Physiology, 268*(5), H1918-1926.

Berridge, M. J. (2008). Smooth muscle cell calcium activation mechanisms. *Journal of Physiology, 586*(21), 5047-5061.

Brading, A. (2006). Spontaneous activity of lower urinary tract smooth muscles: correlation between ion channels and tissue function. *The Journal of Physiology, 570*(1), 13-22.

Brading, A. F. (1997). A myogenic basis for the overactive bladder. *Urology, 50*(6, Supplement 1), 57-67. https://doi.org/10.1016/S0090-4295(97)00591-8

Burnstock, G., & Prosser, C. (1960). Responses of smooth muscles to quick stretch; relation of stretch to conduction. *American Journal of Physiology--Legacy Content, 198*(5), 921-925.

Coolsaet, B. (1985). Bladder compliance and detrusor activity during the collection phase. *Neurourology and Urodynamics, 4*(4), 263-273.

Coolsaet, B. L., Van Duyl, W. A., Os-Bossagh, V., & De Bakker, H. V. (1993). New concepts in relation to urge and detrusor activity. *Neurourology and Urodynamics, 12*(5), 463-471.

Davis, M. J., & Hill, M. A. (1999). Signaling mechanisms underlying the vascular myogenic response. *Physiological Reviews, 79*(2), 387-423.

Drake, M., Harvey, I., & Gillespie, J. (2003). Autonomous activity in the isolated guinea pig bladder. *Experimental Physiology, 88*(1), 19-30.

Elbadawi, A. (1995). Pathology and pathophysiology of detrusor in incontinence. *The Urologic clinics of North America, 22*(3), 499-512.

Gillespie, J. (2004). The autonomous bladder: a view of the origin of bladder overactivity and sensory urge. *BJU international, 93*(4), 478-483.

Gloeckner, D. C., Sacks, M. S., Fraser, M. O., Somogyi, G. T., De Groat, W. C., & Chancellor, M. B. (2002). Passive biaxial mechanical properties of the rat bladder wall after spinal cord injury. *The Journal of urology, 167*(5), 2247-2252.

Hammad, F. T., Stephen, B., Lubbad, L., Morrison, J. F., & Lammers, W. (2014). Macroscopic electrical propagation in the guinea pig urinary bladder. *American Journal of Physiology-Renal Physiology, 307*(2), F172-F182.

Hashitani, H., & Brading, A. F. (2003). Electrical properties of detrusor smooth muscles from the pig and human urinary bladder. *British Journal of Pharmacology, 140*(1), 146-158.

Hashitani, H., Brading, A. F., & Suzuki, H. (2004). Correlation between spontaneous electrical, calcium and mechanical activity in detrusor smooth muscle of the guinea-pig bladder. *British Journal of Pharmacology, 141*(1), 183-193.

Hashitani, H., Yanai, Y., & Suzuki, H. (2004). Role of interstitial cells and gap junctions in the transmission of spontaneous Ca^{2+} signals in detrusor smooth muscles of the guinea-pig urinary bladder. *Journal of Physiology, 559*(2), 567-581.

Huizinga, J. D., Parsons, S. P., Chen, J.-H., Pawelka, A., Pistilli, M., Li, C., . . . Tong, M. (2015). Motor patterns of the small intestine explained by phase-amplitude coupling of two pacemaker activities: the critical importance of propagation velocity. *American Journal of Physiology-Cell Physiology, 309*(6), C403-C414.

Ikeda, Y., Fry, C., Hayashi, F., Stolz, D., Griffiths, D., & Kanai, A. (2007). Role of gap junctions in spontaneous activity of the rat bladder. *American Journal of Physiology-Renal Physiology, 293*(4), F1018-F1025.

Janssen, P. W. M., & Lentle, R. G. (2013). Spatiotemporal Mapping Techniques for Quantifying Gut Motility. In L. K. Cheng & G. Farrugia (Eds.), *New Advances in Gastrointestinal Motility Research* (pp. 219-241). New York: Springer.

Ji, G., Barsotti, R. J., Feldman, M. E., & Kotlikoff, M. I. (2002). Stretch-induced calcium release in smooth muscle. *The Journal of General Physiology, 119*(6), 533-543.

Johnston, L., Woolsey, S., Cunningham, R. M., O'Kane, H., Duggan, B., Keane, P., & McCloskey, K. D. (2010). Morphological expression of KIT positive interstitial cells of Cajal in human bladder. *The Journal of urology, 184*(1), 370-377.

Koh, B. H., Roy, R., Hollywood, M. A., Thornbury, K. D., McHale, N. G., Sergeant, G. P., . . . Koh, S. D. (2012). Platelet-derived growth factor receptor-α cells in mouse urinary bladder: a new class of interstitial cells. *Journal of Cellular and Molecular Medicine, 16*(4), 691-700.

Kubota, Y., Biers, S. M., Kohri, K., & Brading, A. F. (2006). Effects of imatinib mesylate (Glivec®) as ac-kit tyrosine kinase inhibitor in the guinea-pig urinary bladder. *Neurourology and Urodynamics, 25*(3), 205-210.

Lammers, W., Morrison, J., Lubbad, L., Stephen, B., & Hammad, F. (2013). *Electrical propagation in the guinea pig urinary bladder.* Paper presented at the Proceedings of The Physiological Society.

Lammers, W. J. E. P., & Slack, J. R. (2001). Of slow waves and spike patches. *News in physiological sciences, 16*, 138-144.

Lammers, W. J. E. P., & Stephen, B. (2008). Origin and propagation of individual slow waves along the intact feline small intestine. *Experimental Physiology, 93*(3), 334-346.

Lentle, R. G., Reynolds, G. W., Hulls, C. M., & Chambers, J. (2016). Advanced spatiotemporal mapping methods give new insights into the coordination of contractile activity in the stomach of the rat. *American Journal of Physiology-Gastrointestinal and Liver Physiology*, ajpgi. 00308.02016.

Lentle, R. G., Reynolds, G. W., Janssen, P. W. M., Hulls, C. M., King, Q. M., & Chambers, J. (2015). Characterisation of the contractile dynamics of the resting ex vivo urinary bladder of the pig. *BJU International, 116*(6), 973-983.

Levin, R. M., Ruggieri, M. R., Velagapudi, S., Gordon, D., Altman, B., & Wein, A. J. (1986). Relevance of spontaneous activity to urinary bladder function: an in vitro and in vivo study. *Journal of Urology, 136*(2), 517-521.

McCloskey, K. D. (2010). Interstitial cells in the urinary bladder—localization and function. *Neurourology and Urodynamics, 29*(1), 82-87.

McCloskey, K. D., & Gurney, A. M. (2002). Kit positive cells in the guinea pig bladder. *Journal of Urology, 168*(2), 832-836.

McGarigal, K., Cushman, S. A., Neel, M. C., & Ene, E. (2002). FRAGSTATS: spatial pattern analysis program for categorical maps.

McGarigal, K., & Marks, B. J. (1995). Spatial pattern analysis program for quantifying landscape structure. *Gen. Tech. Rep. PNW-GTR-351. US Department of Agriculture, Forest Service, Pacific Northwest Research Station*

Monaghan, K. P., Johnston, L., & McCloskey, K. D. (2012). Identification of PDGFRα positive populations of interstitial cells in human and guinea pig bladders. *The Journal of urology, 188*(2), 639-647.

Mosso, A., & Pellacani, P. (1882). Sur la fonction de la vessie. *Archives Italiennes de Biologie, 1*, 291–324.

Nagatomi, J., Toosi, K. K., Grashow, J. S., Chancellor, M. B., & Sacks, M. S. (2005). Quantification of bladder smooth muscle orientation in normal and spinal cord injured rats. *Annals of biomedical engineering, 33*(8), 1078-1089.

Plum, F., & Colfelt, R. H. (1960). The genesis of vesical rhythmicity. *Archives of Neurology, 2*(5), 487-496.

Poley, R. N., Dosier, C. R., Speich, J. E., Miner, A. S., & Ratz, P. H. (2008). Stimulated calcium entry and constitutive RhoA kinase activity cause stretch-induced detrusor contraction. *European journal of pharmacology, 599*(1-3), 137-145.

Shafik, A., El-Sibai, O., Shafik, A. A., & Shafik, I. (2004). Identification of interstitial cells of Cajal in human urinary bladder: concept of vesical pacemaker. *Urology, 64*(4), 809-813.

Sherrington, C. S. (1892). Notes on the arrangement of some motor fibres in the lumbo-sacral plexus. *Journal of Physiology, 13*(6), 621–772.

Specht, P. C., & Bortoff, A. (1972). Propagation and electrical entrainment of intestinal slow waves. *The American journal of digestive diseases, 17*(4), 311-316.

Sugaya, K., & de Groat, W. C. (2000). Influence of temperature on activity of the isolated whole bladder preparation of neonatal and adult rats. *American Journal of Physiology, 278*(1), R238-246.

Thompson, T. R., & Little, R. W. (1970). End effects in a truncated semi-infinite cone. *The Quarterly Journal of Mechanics and Applied Mathematics, 23*(2), 185-196.

Tomita, T. (1990). Spread of excitation in smooth muscle. *Progress in Clinical and Biological Research, 327*, 361.

Turner, W., & Brading, A. (1997). Smooth muscle of the bladder in the normal and the diseased state: pathophysiology, diagnosis and treatment. *Pharmacology and Therapeutics, 75*(2), 77-110.

Wang, Y., Fang, Q., Lu, Y., Song, B., Li, W., & Li, L. (2010). Effects of mechanical stretch on interstitial cells of Cajal in guinea pig bladder. *Journal of Surgical Research, 164*(1), e213-e219.

Wellner, M.-C., & Isenberg, G. (1993). Stretch Activated Nonselective Cation Channels in Urinary Bladder Myocytes: Importance for Pacemaker Potentials and Myogenic Response. *EXS, 66*, 93-99.

DRC 16

MASSEY UNIVERSITY
TE KUNENGA KI PŪREHUROA
UNIVERSITY OF NEW ZEALAND

GRADUATE RESEARCH SCHOOL

STATEMENT OF CONTRIBUTION
DOCTORATE WITH PUBLICATIONS/MANUSCRIPTS

We, the candidate and the candidate's Primary Supervisor, certify that all co-authors have consented to their work being included in the thesis and they have accepted the candidate's contribution as indicated below in the *Statement of Originality*.

Name of candidate:	Corrin Hulls
Name/title of Primary Supervisor:	Prof RG Lentle
In which chapter is the manuscript /published work:	Chapter 5

Please select one of the following three options:

(●) The manuscript/published work is published or in press

- Please provide the full reference of the Research Output:

Spatiotemporal analysis of spontaneous myogenic contractions in the urinary bladder of the rabbit: timing and patterns reflect reported electrophysiology
C. M. Hulls
. R. G. Lentle

( ) The manuscript is currently under review for publication – please indicate:

- The name of the journal:

American Journal of Physiology: Renal Physiology

- The percentage of the manuscript/published work that was contributed by the candidate: 70%
- Describe the contribution that the candidate has made to the manuscript/published work:

Conducted experimental work, planning of evaluation & data with statistical procedures

( ) It is intended that the manuscript will be published, but it has not yet been submitted to a journal

Candidate's Signature:	
Date:	3.10.22
Primary Supervisor's Signature:	Professor Roger LENTLE
Date:	2/10/22

This form should appear at the end of each thesis chapter/section/appendix submitted as a manuscript/ publication or collected as an appendix at the end of the thesis.

Preface Chapter 6

The disposition and dynamics of contractile behaviour in the *ex vivo* tetrodotoxinized bladder was described in the previous chapter. Chapter 6 investigates the level of myogenic and neuronal control of contractile motility using various pharmacological agents. Having previously identified two patterns of contraction on two-dimensional spatiotemporal mapping of the untreated tetrodotoxinized bladder (PPC's and PIC's), this chapter seeks to shed light on the contributions of ICCs and myocytes to the initiation, local spread and the propagation of contractions and the formation of microcontractions. Further, parasympathetic and sympathetic agonists are used to elucidate the relative proportions of the two contractile patterns over the surface of the bladder and whether they may be influenced by autonomic nervous input.

Copy of Paper- Pharmacological modulation of the spatiotemporal disposition of micromotions in the intact resting urinary bladder of the rabbit; their pattern is under both myogenic and autonomic control

The following pages contain a copy of the published journal article with the following bibliography-

Hulls, C. M., Lentle, R. G., King, Q. M., Chambers, J. P., & Reynolds, G. W. (2019). Pharmacological modulation of the spatiotemporal disposition of micromotions in the intact resting urinary bladder of the rabbit; their pattern is under both myogenic and autonomic control. *BJU international*, *123*, 54-64.

The main format of the publish peer-reviewed article is reproduced in this chapter section with its format and content maintained. All references sited are listed in a separate sub-section after the main body of the article. These references would be reproduced in the main bibliography of this thesis (i.e., after the thesis appendix) only should they be used elsewhere beyond this section (i.e., of this published article). All further work beyond this section will be citing the work presented in this section where appropriate.

6 Pharmacological modulation of the spatiotemporal disposition of micromotions in the resting urinary bladder of the rabbit; their pattern is under both myogenic and autonomic control.

6.1 Abstract

The disposition and dynamics of microcontractions i.e., propagating patches of contraction (PPCS) and their component individual myogenic contractions (propagating individual contractions - PICs) in the wall of the resting *ex vivo* tetrodotoxinized urinary bladder of the rabbit were characterised by spatiotemporal maps and related to cyclic variation in intravesical pressure (p_{ves}) before and after the administration of carbachol, isoprenaline, carbenoxolone, and the RhoA inhibitor Y-27632.

The results confirm that the bladder wall can exhibit two contractile states that are of similar frequencies to those of the two types of electrophysiological discharge described by previous workers. In the first of these large low frequency cyclic PPCs predominate. In the second, small irregular, higher frequency PICs predominate. The addition of carbachol increased the size, frequency, and speed of propagation of PPCs, causing the total area undergoing contraction and intravesical pressure to increase, whereas the addition of isoprenaline temporarily halted the incorporation of PICs into PPCs, reduced patch size, total area undergoing contraction and intravesical pressure. Comparison of the effects of the gap junction blocker carbenoxolone and the RhoA inhibitor Y27632 on the timing and disposition of contraction indicated that the local spatial spread of contractions in PPCs was governed largely by myocytes, whilst the propagation, frequency, and duration of PPCs was likely governed via gap junctions between ICC-IM and myocytes.

6.2 Introduction

The bladder acts as a temporary repository for inflowing urine by appropriate and ongoing adjustment of wall compliance i.e., baseline tone, to mitigate any consequent rise in luminal pressure (A. Brading, 2006). Bladder urine storage is regulated by local mechanoreceptors in conjunction with elements of the autonomic nervous system (K.-E. Andersson & Arner, 2004).

Myogenic contraction (-ve strain) induced by quick stretch in isolated strips of detrusor (Geoffrey Burnstock & Prosser, 1960) likely results from mechanosensitivity of a number of their cellular components. Hence, both myocytes (Bülbring, 1955; Kirber, Walsh, & Singer, 1988) and the recently identified (Johnston et al., 2010) C-kit positive interstitial cells (IC) have been shown to be mechanosensitive (Kraichely & Farrugia, 2007b; Strege et al., 2003; K. J. Won, K. M. Sanders, & S. M. Ward, 2005), a 20% stretch being sufficient to augment the regular baseline frequency (1.22 ± 0.52 cpm) of calcium transients in the latter (Y. Wang et al., 2010). The cellular sites of such mechanosensitivity (Setoguchi, Ohya, Abe, & Fujishima, 1997; X. Wu & Davis, 2001) are thought to be at or near gap junctions that link ICC (Rasmussen, Rumessen, Hansen, Smedts, & Horn, 2009) and myocytes (Thuneberg & Peters, 2001). Moreover, a body of work indicates that mechanosensitivity ultimately results from the mechanical disruption of certain ion channels within the plasma membranes. Hence, stretch of myocytes is reported to effect L-type calcium channels and calcium levels within the cytosol (Davis & Hill, 1999) as well as non-selective ion channels (M.-C. Wellner & G. Isenberg, 1993), notably stretch dependent ryanodine receptors (G. Ji et al., 2002; Poley et al., 2008).

Such mechanosensitivity and baseline tone may by modulated by beta adrenergic (Frazier, Peters, Braverman, Ruggieri, & Michel, 2008), and M_2 (Braverman, Tibb, & Ruggieri, 2006) and M_3 (Kories et al., 2003) mediated cholinergic as well NANC (purinergic, nitrergic and peptidergic) neurotransmitters (K.-E. Andersson & Arner, 2004). Further, bladder wall compliance may be modulated intracellularly via phosphatidyl inositol phospholipase C (Makhlouf & Murthy, 2006), and Rho kinase (ROCK), inhibitors of the latter causing a reduction in the potency of the muscarinic response (Braverman, Doumanian, & Ruggieri, 2006).

The bladder wall exhibits rhythmic spontaneous phasic contractions variously termed 'micromotions' (Bo Coolsaet, 1985) or non-voiding activity (NVA) (J. I. Gillespie et al., 2012b). These were first described in 1882 in human females and dogs (Angelo Mosso & P Pellacani, 1882), and subsequently in a range of species including monkeys, cats (Charles S Sherrington, 1892a), guinea pigs (M. Drake et al., 2003), rats (Sugaya & de Groat, 2000), and pigs (B. L. Coolsaet et al., 1993). Subsequent work showed that micromotions were not inhibited by denervation (Plum & Colfelt, 1960) and occurred in bladders that were maintained *ex vivo* (M. Drake et al., 2003) as well as in isolated strips of bladder muscle (A. F. Brading, 1997). Further, the failure of atropine or tetrodotoxin to inhibit these contractions (ROBERT M Levin et al., 1986) led to the conclusion that the rhythmic activity and tone were primarily myogenic (Turner & Brading, 1997), although studies of oscillation in the amplitude of intravesical pressure suggested that micromotions could be influenced both by parasympathetic and sympathetic nervous input (J. Gillespie, 2004a, 2004b; J. I. Gillespie et al., 2012b).

Recent work has shown that the spatiotemporal organisation of microcontractions is more complex than was originally described and not always reflected by synchronous change in the amplitude of oscillation in intravesical pressure (C M Hulls et al., 2017). Hence, in the rabbit bladder, there are periods when regular, vertically propagating, relatively prolonged, synchronised contractions of large areas of the bladder wall - i.e., PPCs - occur, which are generally accompanied by significant changes in intravesical pressure. These periods are interspersed with periods when shorter-lived, small, localised contractions - i.e., PICs - predominate, the latter having relatively little effect on intravesical pressure (C M Hulls et al., 2017). Further, the temporal characteristics of these two patterns are similar to those of electrophysiological events in tissue from the bladder wall. Hence, the frequencies of regular 'burst' patterns of multiple APs (mean 4.2 ± 2.2 cpm) reported by Hashitani (Hikaru Hashitani & Alison F Brading, 2003a; Hikaru Hashitani, Brading, et al., 2004) are similar to those of propagating coordinated patches of contraction (PPCs) we observed in the intact pig bladder (3 cpm) (Lentle et al., 2015b) and in the rabbit bladder (3.85 ± 0.3 cpm) (C M Hulls et al., 2017), whilst the frequency range in patterns of randomly spaced single APs (14.5 ± 6.2 cpm) (Hikaru Hashitani & Alison F Brading, 2003a; Hikaru Hashitani, Brading, et al., 2004) is similar to that of isolated patches of myogenic contraction (PICs)

(frequency 4 - 20cpm) (C M Hulls et al., 2017). Hence, we postulated that ICC may periodically coordinate PICs into PPCs (C M Hulls et al., 2017). This hypothesis was indirectly supported by reports that the agent imatinib (Glyvec®), a c-Kit tyrosine kinase inhibitor that inactivates c-kit positive ICs in strips of bladder muscle, progressively reduced the amplitudes of concerted bursts of action potentials, ultimately converting them into arrays of randomly firing single action potentials (Kubota et al., 2006a).

Currently, it is not known whether micromotions result from spontaneous, stretch-induced myogenic activity unrelated to the control of tone i.e., bystander activity (Lentle et al., 2015b), or whether they are a product of regulation of bladder tone (Lentle et al., 2015b). The observed progressive decline in *overall* intravesical pressure associated with a simultaneous increase in the amplitude and frequency of *excursions* in intravesical pressure, after a sudden increase in the fill of the isolated bladder (J. I. Gillespie et al., 2012b; Klevmark, 1974; Charles S Sherrington, 1892a; Streng, Hedlund, Talo, ANDERSSON, & Gillespie, 2006) suggests the latter. Similarly, morphological, and biomechanical considerations suggest that tone is likely to be maintained in hollow, roughly spherical structures, such as the bladder, by localised rather than global contraction. Hence, the maintenance of tone is complicated by the fact that myocytes, like other cells, are incompressible i.e., cannot change in volume as they consist largely of water. Hence, lengthwise contraction of a myocyte in response to a given strain will be accompanied by width-wise expansion which latter could relieve such strain in laterally adjacent tissue and inhibit stimulation of any contained mechanoreceptors. Such an effect could persist in the resting bladder, even if autonomic nervous elements globally adjusted the mechanoreceptor threshold, and magnitude of contractile response.

To date little is known of the way autonomic neurotransmitters, and agents that interfere with smooth muscle contraction at a cellular level, influence the patterns of contraction in the bladder wall and the consequent adjustment of tone and compliance. The current work investigates the direct effects of several such agents on the timing and disposition of the various patterns of micromotions, with a view to further elucidating their role in the maintenance of bladder tone and capacity.

6.3 Materials and Methods

All the experimental procedures were approved by the Massey University Animal Ethics Committee (MUAEC approval number 14/50) and complied with the New Zealand Code of Practice for the Care and Use of Animals for Scientific Purposes. Twenty New Zealand White rabbits were obtained from a commercial breeder and maintained on commercial feed, which was available *ad libitum* with water until immediately prior to the procedure.

6.3.1 Experimental procedures

Once the animal had been anaesthetised with halothane, the abdomen was opened with a midline ventral incision and the symphysis pubis divided at the midline. The bladder and urethra were mobilized, the ureters were transected and tied approximately 0.5cm from the trigone. The urethra was transected approximately 2 cm distal to the bladder neck. The bladder was then removed from the animal and immediately immersed in ice cold oxygenated Earle's HEPES buffer solution (HBS) prior to installation in an organ bath. The animal was subsequently euthanized with intracardiac pentobarbitone (125 mg/kg).

The urethra was cannulated with a curved metal cannula (2 mm OD), drained, and secured in position with a ligature 5 mm distal to the bladder neck. The cannula had been prefilled with saline as was a length of tubing connecting it to a port on a three-way valve. The other two ports were similarly connected to a pressure transducer and a syringe pump, respectively. The syringe pump allowed physiological saline to be infused into or removed from the lumen of the bladder. The output from the pressure transducer (Spectramed P23XL, Oxnard, CA, USA) was connected to a PowerLab 8SP computer interface (AD Instruments, Sydney, Australia) and pressure readings were acquired at 100 Hz. Pressure readings were synchronised with spatiotemporal maps and incorporated into composite diagrams (see below).

The anterior and lateral surfaces of the bladder were sprinkled with carbon black. The bladder was then suspended, fundus downward, from the urethral cannula in an organ bath with its anterior surface facing the

video camera (Fig 1a) and immersed in oxygenated (95% O_2, 5% CO_2) HBS solution of pH 7.35, comprising 124.0 mM NaCl, 5.4 mM KCl, 0.8 mM $MgSO_4$, 1.0 mM NaH_2PO_4, 14.3 mM $NaHCO_3$, 10.0 mM HEPES, 1.8 mM $CaCl_2$ and 5.0 mM glucose maintained at 37°C and continuously recirculated at a flow rate of 160 ml/min.

The bladder was immersed in the organ bath with the point at which the urethral cannula emerged from the bladder and the pressure transducer positioned at the level of the surface of the fluid in the organ bath. The pressure transducer was also connected, via the three-way tap, with length of fluid filled tubing to the cannula. Thus, all bladders were positioned such that the hydrostatic pressure of the connecting system was zero at the neck.

The filling protocol consisted of adding two consecutive 15 ml aliquots of saline, each over 2 minutes, to a total of 30 ml, with a period of 15 minutes between each. Hence, the measurement of the patterns of motility was carried out at a total bladder content volume of 30 ml.

Tetrodotoxin 0.5 mg (Alomone Labs Jerusalem) was added directly to the superperfusate of each preparation 10 minutes prior to the commencement of video and transducer recordings to give a concentration of 0.005 mM bath concentration. Thus, only myogenic activity was evaluated.

Various drugs were added to the preparation following stabilisation of their contractile (micromotional) activity. Carbachol (Sigma-Aldrich) was used as a broad-spectrum cholinergic agonist. Isoprenaline (Isuprel™ 1:5000. Hospira Pty Ltd) was chosen as the β_2 agonist because adrenoreceptor agonist mediated relaxation is mediated in the rabbit mainly by β_2 rather than β_3 agonists (Yamazaki et al., 1998). We also used carbenoxolone (18β-GA-0-hemisuccinate)(Sigma-Aldrich), a water soluble (Tare, Coleman, & Parkington, 2002) gap junction blocker (J. S. Davidson & Baumgarten, 1988) as it had been shown to influence the genesis of calcium transients in the guinea pig bladder (Hikaru Hashitani, Yanai, et al., 2004a) and Y-27632 a Rho kinase (ROCK) (Sigma-Aldrich) inhibitor reported to attenuate contraction in rat bladder smooth muscle (Jezior et al., 2001; Wibberley et al., 2003), given that both ROCK1 and ROCK2 have been detected in high levels in the urinary bladder of the rat and are thought to be involved in the regulation of smooth muscle contraction (Wibberley et al., 2003).

6.3.2 Image acquisition and processing

In all cases case the bladder was positioned with its anterior surface facing the camera with the point of junction of the (1 cm) ureteric remnants with the posterior surface (which could be seen projecting to each side of the anterior surface) positioned 1/3 of the way from the top of the video frame.

Image sequences were captured on a video camera mounted to the side of the organ bath and saved as an uncompressed AVI video file for off-line processing.

The pattern of motility over the bladder surface was evaluated by extending cross-correlation techniques (P.W.M Janssen & Lentle, 2013) to two dimensions. In this method, the local movement of the distinctive visual textural features or spatially distinct arrays of carbon particles between successive frames were used to quantify the displacements of reference points on a grid of equally spaced points within a rectangular region of interest (ROI). The area strain rate (ASR) for each reference point was determined from the local displacement rates using the same technique that was described in a previous paper (Lentle et al., 2015b). Briefly, ASRs were expressed as the percentage change in muscle area per unit time, i.e., % s^{-1}. The sensitivity of the ASR mapping method is well established. ASR maps derived from myocardial MRI has been shown to provide better discrimination between normal and ischemic zones than other indices of strain (Azhari et al., 1995).

Successive two-dimensional spatiotemporal maps of local ASRs (*A-type ST maps*) were each superimposed on corresponding video images of the bladder to enable the patterns of motility on its surface to be visualised. The area of superimposition was limited by a user-specified ellipsoidal mask which occupied 45% of the anterior surface and excluded sites that were close to the edge of the organ profile where artefacts from minor rotation of the organ and foreshortening from angulation of the surface could occur (Fig 1C). The ASRs were colour-

coded such that rapidly contracting areas appeared yellow (-ve ASR), more slowly contracting areas appeared red and expanding areas appeared blue (+ve ASR).

L-type ST maps i.e., linear plots of the variation in strain rate at all points along (x axis) a line of interest (LOI) over time (y axis), were also generated from the video. Analyses were conducted over two LOIs that were positioned vertically so as to traverse the right- and the left-hand sides of the bladder, as this is the reported principal direction of propagation (C M Hulls et al., 2017). The vertical speeds and directions of propagation of a contraction, or group of contractions, could be directly determined from these maps as it was inversely proportional to the angle of the contraction stripe to the horizontal axis. This technique also allowed for identification of the propagating individual contractions (PICs) that made up PPCs on a basis of their varying (minor) degrees of deviation from the LOIs. The magnitude of other parameters of PPCs at a particular time e.g., their duration and frequency (see below) were determined from vertical transects of the L-maps (see below).

The transducer recordings of variation in intravesical pressure were synchronised with the spatiotemporal maps. Mean values for baseline pressure over the 180 second periods designated on the ST maps (see below) were determined before and after each treatment for each preparation (Table 1).

Composite figures were prepared for suitable periods before and after treatment with each drug. These each showed the variation in intravesical pressures at the extreme right i.e., 1st column, variation in strain rate over vertical LOIs 2nd (left hand side) and 3rd (right hand side) columns and cumulative contraction over successive periods of 180 seconds (see below) 4th column.

6.3.3 Further data processing and Statistics

The following general indices of contraction were used. The mean percentages of the anterior surfaces of the bladders undergoing contraction (PMTA) (McGarigal et al., 2002), the mean number of patches of contraction occupying the anterior surfaces of the bladders (NP) and the mean patch size, the mean of the sizes of the

largest patches of contraction in each frame as a percentage of the total area (LPI) (McGarigal et al., 2002). Each was determined in FRAGSTAT (McGarigal, K., SA Cushman, and E Ene. 2012. FRAGSTATS v4: Spatial Pattern Analysis Program for Categorical and Continuous Maps) from 180 video frames taken at successive one second intervals at points before and after the time of administration of the various pharmaceutical agents that are marked on the various composite diagrams.

The following parameters of PPCs were derived directly from relevant L-type spatiotemporal maps taken along the right vertical transects (3rd column of composite figures) i.e., the principal (right) axis of their propagation

- the mean vertical rates of propagation determined from the mean of the slopes of all PPCs on L maps during the designated 180 second period.
- the distance of propagation i.e., the percentages of events that propagated over greater than half the lengths of the L maps.

The following parameters of PPCs were derived from vertical transects of L-type spatiotemporal maps taken along the right vertical transects (3rd column of composite figures)

- the mean duration of all PPCs during the 180 second period of the transect i.e., the mean of the widths of the peaks at 10% of the peak value,
- the dominant frequencies of cyclic variation in strain rate were determined from fast Fourier transforms of variation in strain rate taken over the 180 second period of the transect.

All these values were determined for each of the three animals before and after the various treatments and were subsequently compared by repeated measures ANOVA in the SYSTAT statistical suite (SYSTAT Software Inc.© SYSTAT 13 v13.1)). Unless otherwise stated, all results are presented as the mean ± SEs of the means of three separate preparations.

To aid in the visualisation of the principal locations and sizes of areas of negative strain rate i.e., contraction on the anterior surface of the bladder, we stacked A-type ST maps from 60 video frames taken at successive

one-second intervals and plotted the frequencies that the area strain rate in each component pixel decreased below -4% s^{-1} during that minute, on a yellow to blue colour scale. We termed the resulting graphic an “A-type contraction density plot”.

		Over-all Contraction Metrics				PPC Metrics				Baseline Pressure (mmHg)
		PMTA	NP	LPI	Mean Patch Size (mm^2)	Frequency (CPM) (ST Map)	Duration (s) (ST Map)	Velocity (mm/s) (ST Map)	Distance of Propagation (% of PPC's traversing >50% of ST Map)	
Carbachol	Baseline	16.56 ±0.88	3.99 ±0.16	13.80 ±0.88	30.29 ±2.80	3.90 ±0.40	3.24 ±0.06	4.52 ±0.69	77 ±2.31	0.72 ±0.15
	Treatment	25.99 ±0.87**	3.96 ±0.16	21.06 ±0.96**	52.88 ±4.03*	16.47 ±0.07***	2.02 ±0.03***	12.03 ±2.64*	93 ±2.31*	1.66 ±0.10*
Isoprenaline	Baseline	18.90 ±0.89	2.76 ±0.11	16.23 ±0.90	58.54 ±4.54	3.9 (±0.40)	3.47 ±0.06	4.04 ±0.72	80 ±1.52	0.61 ±0.08
	Treatment	5.65 ±0.6***	2.64 ±0.14	4.48 ±0.56***	15.98 ±2.41**	NIL	NIL	NIL	NIL	0.16 ±0.01*
Carbenoxolone	Baseline	20.98 ±0.94	3.72 ±0.15	17.63 ±0.95	53.22 ±4.63	3.70 (±0.20)	3.28 ±0.04	4.04 ±0.42	85 ±2.31	1.62 ±0.07
	Treatment	20.88 ±0.90	3.84 ±0.15	17.08 ±0.90	46.07 ±3.67	11.70 (±0.12)***	2.56 ±0.04***	6.48 ±0.13*	72 ±1.73	1.82 ±0.12
RhoA	Baseline	23.03 ±1.21	3.55 ±0.15	18.33 ±1.17	57.37 ±5.46	3.90 ±0.31	3.33 ±0.06	4.15 ±0.88	77 ±4.04	1.46 ±0.02
	Treatment	15.46 ±0.72*	4.25 ±0.16	11.49 ±0.72**	28.68 ±2.57*	5.37 ±0.12*	1.15 ±0.04**	6.28 ±0.99	61 ±1.73*	0.91 ±0.01***

*** < p 0.001, ** < p 0.005, * < p 0.05

Table 1 Comparison of various parameters of overall contraction and parameters of PPCs derived from L maps for rabbit bladders maintained *ex vivo* before and after the administration of various agents.

6.4 Results

6.4.1 Carbachol

The addition of 0.1 μM (bath concentration) of Carbachol caused the total area of contraction, largest patch size, and mean patch size to increase significantly (Fig 6-1 and Table 1). Similarly, it caused the frequency, speed, and distance of vertical propagation of PPCs to increase significantly (Table 1) with concomitant reduction in the occurrence of PICs (Fig 6-1). However, the mean duration of PPCs was significantly reduced and the number of contractile patches was unchanged (Table 1). These changes in spatiotemporal characteristics were accompanied by a significant rise in baseline intravesical pressure (Fig 6-1). Thus, at any given time, the overall area of myocytes undergoing contraction was greater than those in the resting bladder. It is noteworthy that, at the dose used, carbachol did not, at any time, cause generalised sustained contraction of the entire detrusor.

Dosage with 1 μM (bath concentration) of atropine (n=2) had no significant effect on the spatiotemporal organisation of either PPCs or PICs in the tetrodotoxin-dosed bladder, or on mean intravesical pressure, showing that tetrodotoxin had completely inhibited any cholinergic drive from elements of the parasympathetic or endogenous nervous tissue, and that there were no pre-existing changes from residual endogenous cholinergic transmitters. Hence, any effects of cholinergic agents on motility of the tetrodotoxin-dosed bladder would have resulted solely from their direct stimulation of tissue cholinergic receptors.

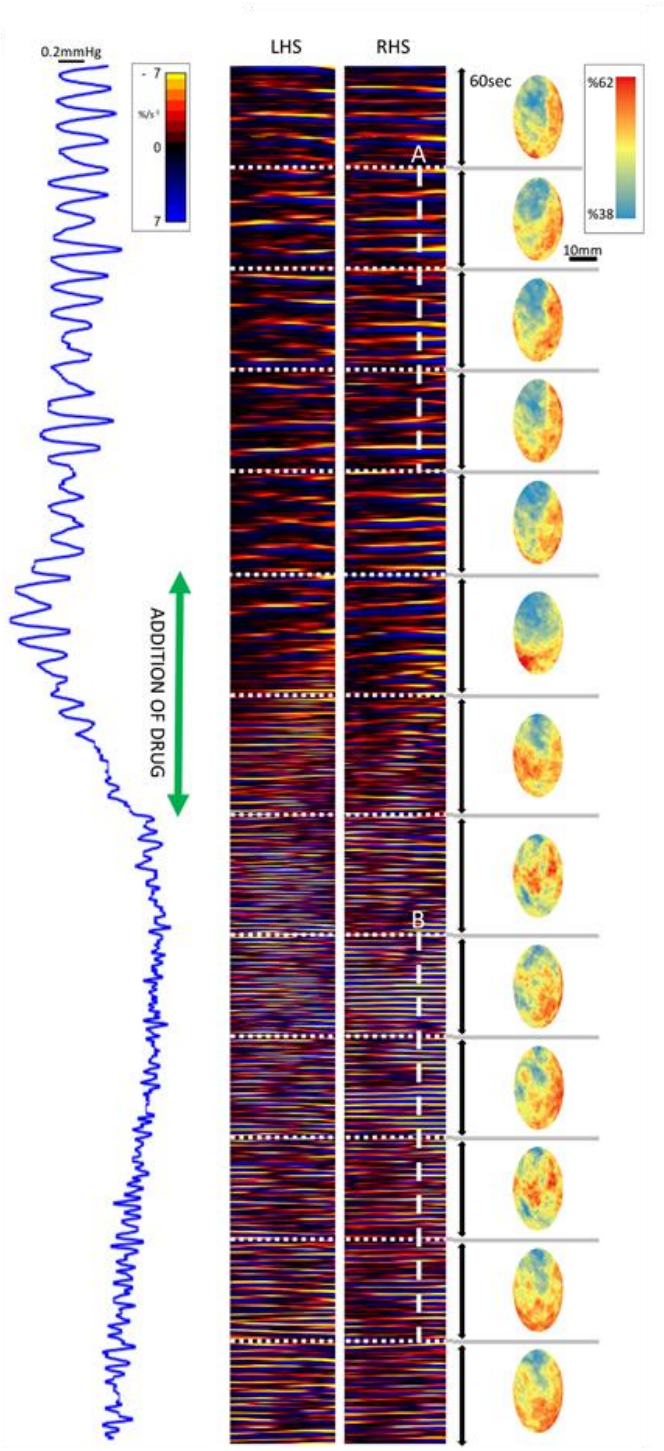

Figure 6-1 Composite of spatiotemporal maps showing the effect of carbachol (0.1 µM bath concentration) on resting contractile activity of the tetrodotoxinized ex-vivo rabbit bladder.

First (left) column, intravesical pressure; second column, L-map on the left vertical transect; third column, L-map on the right vertical transect; fourth column serial spatiotemporal two-dimensional maps of cumulative changes in strain rate over sixty seconds. Vertical white lines show regions used for extracting quantitative data prior to, and after, administration of the agent.

6.4.2 Isoprenaline

The addition of 1 μM (bath concentration) of isoprenaline caused prompt and marked reduction of PPCs with PICs then predominating (Fig 6-2). Hence, the percentage mean total area of contraction, mean patch size and largest patch index all decreased significantly (Table 1) whilst the number of patches was unchanged. Similarly, the propagation of remaining larger areas of contraction appeared to cease (Table 1). These changes were accompanied by a general decrease in mean basal intravesical pressure and a prompt decrease in the amplitude of its oscillation (Fig 6-2) (Table 1). Fragmentation of PPCs into component PICs was evident on vertical L-maps (Fig 6-2) shortly after dosage, as was re-association of PICs into PPCs at the commencement of recovery (180-300 minutes).

Dosage with 100 μM (bath concentration) of propranolol had no effect on the organisation of PPCs or PICs in the tetrodotoxin dosed bladder, showing that tetrodotoxin had completely inhibited any adrenergic drive from elements of the sympathetic or endogenous nervous tissue and that there were no pre-existing changes from residual endogenous adrenergic transmitters. Hence, any effects of adrenergic agents on the motility of the tetrodotoxin-dosed bladder would have resulted solely from their direct stimulation of tissue adrenergic receptors.

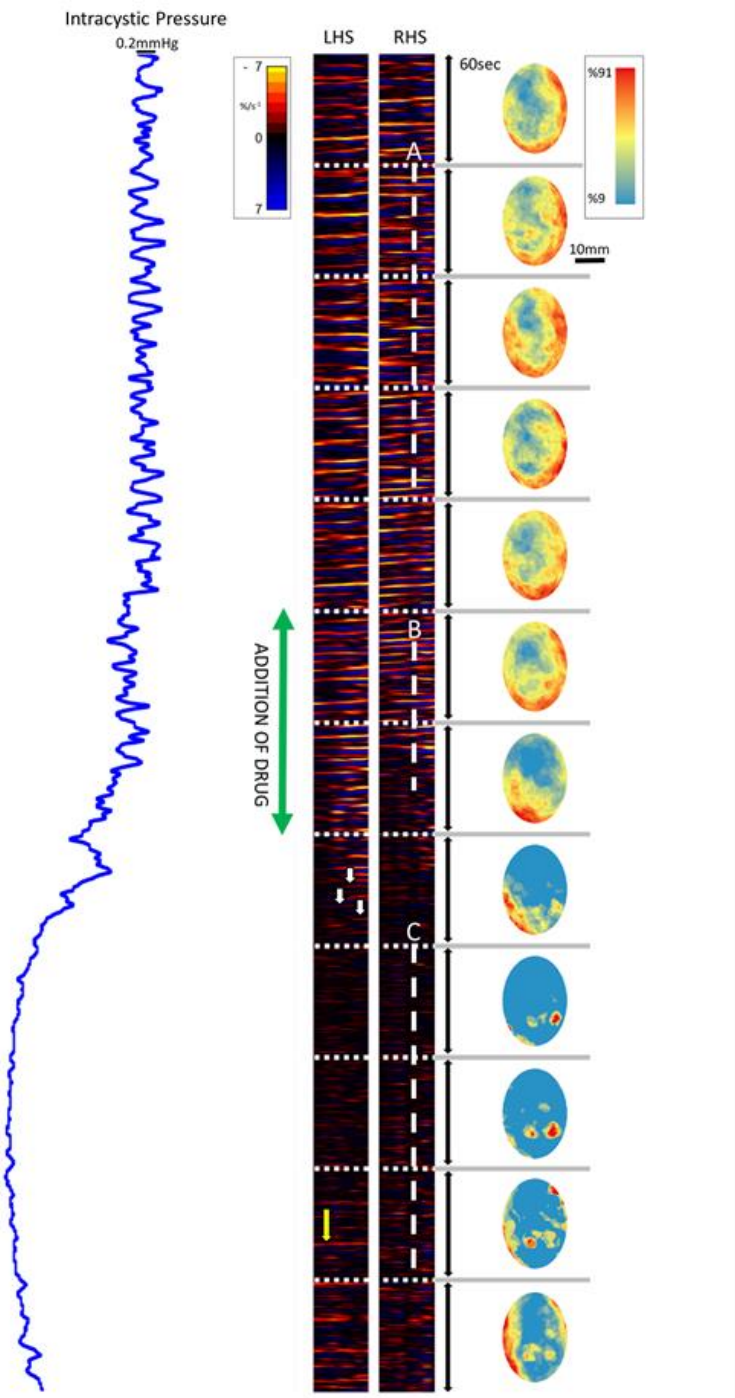

Figure 6-2 Composite of spatiotemporal maps showing the effects of Isoprenaline (1 µM bath concentration) on resting contractile activity of the ex-vivo tetrodotoxinized rabbit bladder.

First (left) column, intravesical pressure; second column, L-map on the left vertical transect; third column, L-map on the right vertical transect; fourth column serial spatiotemporal two-dimensional maps each of cumulative changes in strain rate over sixty seconds. Vertical white lines show regions used for extracting quantitative data prior to, and after, administration of the agent. White arrows on left vertical transect show point fragmentation of PPCs into PICs, yellow arrow point of re-association into PPCs.

6.4.3 Carbenoxolone

The addition of 0.05 mM (bath concentration) of carbenoxolone caused no change in either the PMTA, the number of contractile patches, the largest patch index, or the mean patch size. However, the durations of PPCs decreased significantly whilst both their frequency and velocity of propagation increased significantly (Table 1). There was no discernible increase in the numbers of PICs nor was there any significant change in baseline pressure, although one preparation showed a transient low-grade increase (Fig 6-3).

Thus, whilst the gap junction blocker did not influence any of the general characteristics of contraction or inhibit the organisation of PICs into PPCs, it reduced the duration of PPCs and increased their frequency and velocity of propagation.

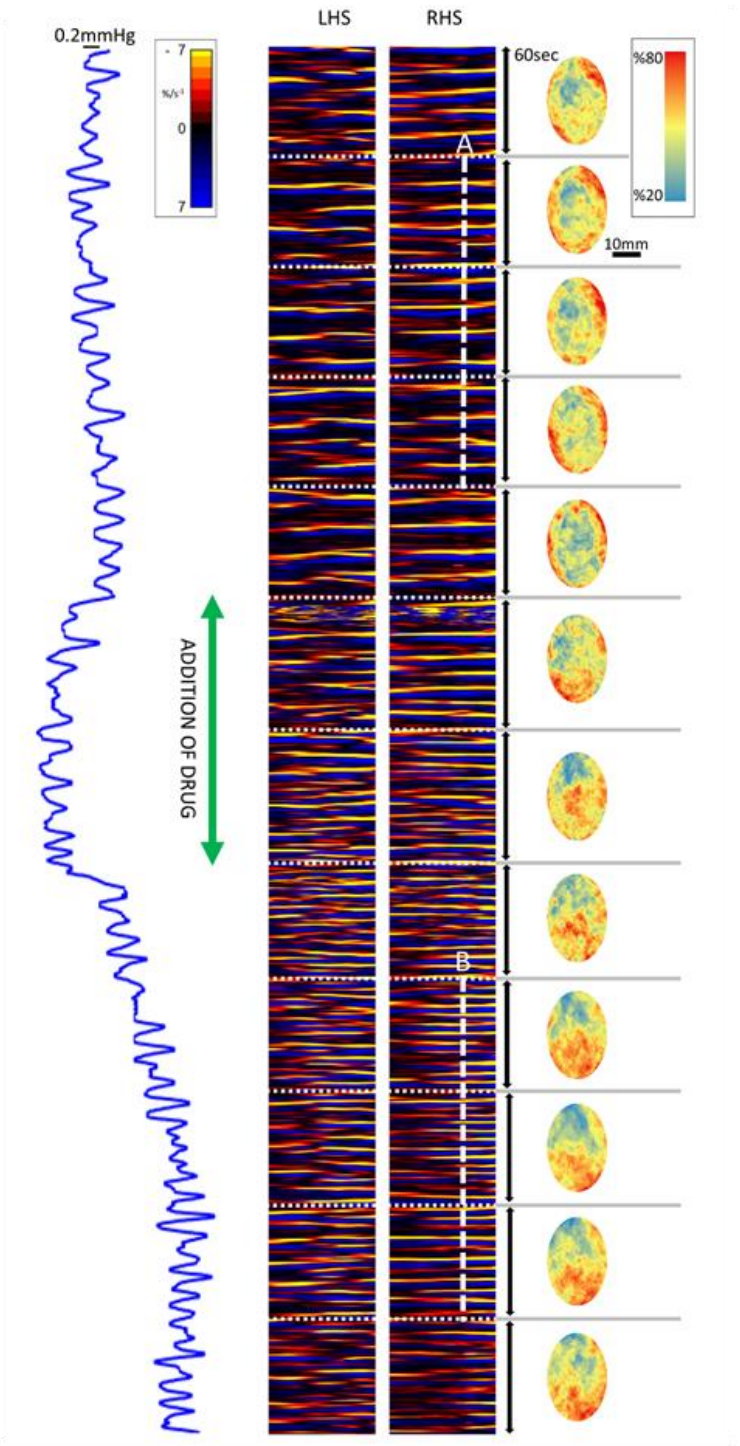

Figure 6-3 Composite of spatiotemporal maps showing the effects of the gap junction blocker carbenoxolone (0.05 mM bath concentration) on resting contractile activity of the tetrodotoxinized ex-vivo rabbit bladder.

First (left) column, intravesical pressure; second column, L-map on the left vertical transect; third column, L-map on the right vertical transect; fourth column serial spatiotemporal two-dimensional maps each of cumulative changes in strain rate over sixty seconds. Vertical white lines show regions used for extracting quantitative data prior to, and after, administration of the agent.

6.4.4 Rho A blockade

The addition of 1 mg RhoA Y-27632 (10μM bath concentration) caused a significant decrease in PMTA, mean patch size and largest patch index (Table 1). Correspondingly there was a decrease in the durations of PPCs, a reduction in their distance of propagation, an increase in their frequency (Table 1) and an increase in the numbers of PICs (Fig 6-4). The baseline intravesical pressure was significantly decreased (Table 1).

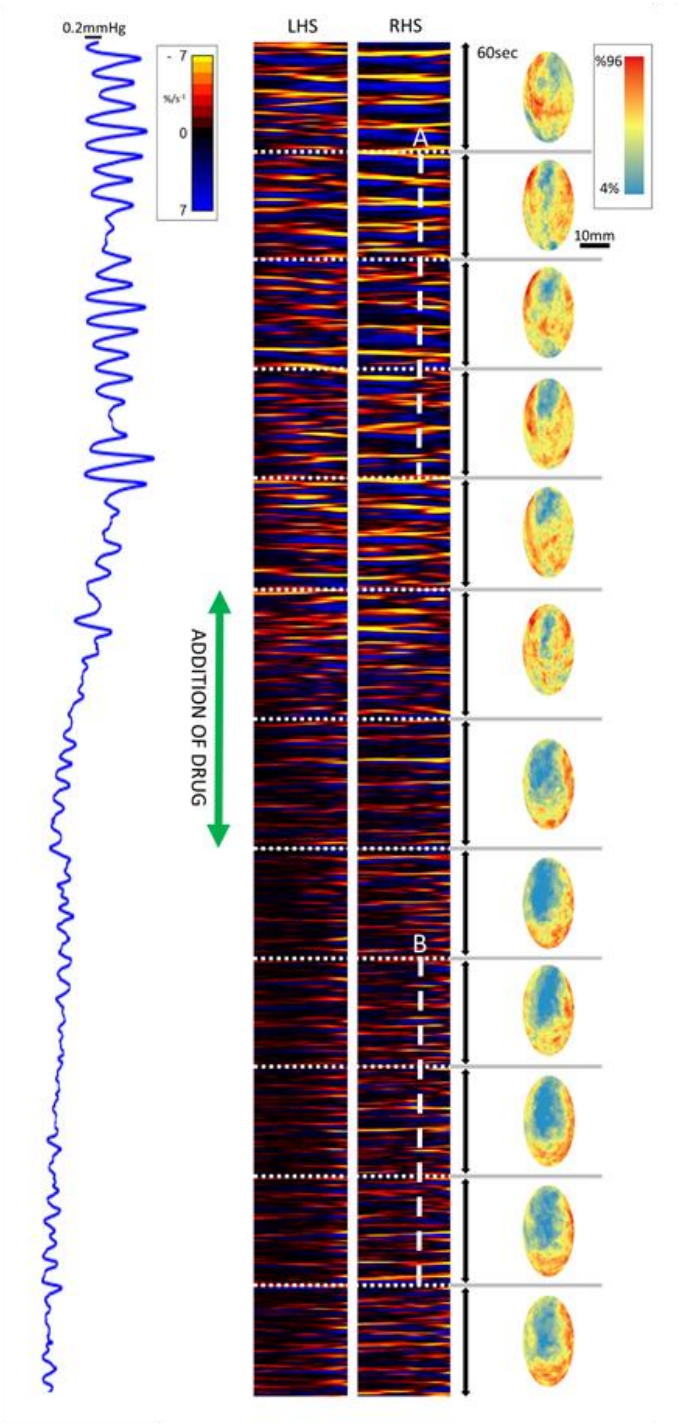

Figure 6-4 Composite of spatiotemporal maps showing the effects of Rho A inhibition (10 µM bath concentration of Y-27632) on resting contractile activity of the tetrodotoxinized ex-vivo rabbit bladder.

First (left) column, intravesical pressure; second column, L-map on the left vertical transect; third column, L-map on the right vertical transect; fourth column serial spatiotemporal two-dimensional maps each of cumulative changes in strain rate over sixty seconds. Vertical white lines show regions used for extracting quantitative data prior to, and after, administration of the agent.

6.5 Discussion

As in our previously published work (C M Hulls et al., 2017), two patterns of contraction were identified on two-dimensional spatiotemporal mapping of the untreated tetrodotoxinized bladder, the first consisting of large patches of propagating contraction (PPC) and the second consisting of irregularly-distributed small, localised contractions (PIC). These contractions and the responses to the various pharmaceutical agents that globally influenced the excitability and ease of transmission between the cellular components of the bladder wall, were not globally uniform, indicating that at any given time the distribution of compliance across the surface of the bladder was similarly inhomogeneous. The pattern of this inhomogeneity, with greater vertical than width wise propagation of PPCs, is in line with the reported predominance of vertically-orientated myocytes (Nagatomi et al., 2005), the bias in orientation of the processes of ICCs along the long axes of myocytes (Johnston et al., 2010) and the possible width wise expansion of contracting myocytes and consequent reduction of circumferential strain. Hence, regardless of any neurally mediated release of transmitters, volumetric accommodation to inflowing urine likely results from *dynamic localised*, rather than *static global* changes.

The results from dosage with parasympathetic and sympathetic agonists indicate that the relative proportions of the two contractile regimes over the surface of the bladder may be influenced by autonomic nervous input. Hence, the rate of formation of PPCs i.e., their frequency and the distance of their propagation, and the consequent general increase in the area of myocytes undergoing contraction at any given time, are promoted by cholinergic receptors, presumably the M_2 type in the rabbit (Schneider, Fetscher, Krege, & Michel, 2004). Similar increases in contractile activity with cholinergic agonists have been reported in thin sheets of bladder muscle (Hikaru Hashitani, Brading, et al., 2004) and in entire bladders maintained *ex vivo* that had not been treated with tetrodotoxin (Gevaert, Ost, & De Ridder, 2006; Brian A Parsons, Marcus J Drake, Andrew Gammie, Christopher H Fry, & Bahareh Vahabi, 2012) where it may have resulted from a combination of activation of myogenic and intrinsic neurogenic receptors. The result demonstrated that any rise in intravesical pressure or wall compliance was a consequence of an increase in overall areas and numbers of PPCs at a given time as well

as any augmentation in their amplitudes. The fact that dosage with 0.1 μM of carbachol did not cause a uniform contraction of the entire surface of the bladder may be attributed to the reported variation in the sensitivity of myocytes to cholinergic stimulation, and concomitant variation in cholinergic binding sites, according to their location within the bladder (ROBERT M Levin, Shofer, & Wein, 1980). Given that the contraction was determined in tetrodotoxinized bladder, and with very low doses of carbachol, it is also possible that areas in which contraction did not occur had higher thresholds to cholinergic stimulation. This effect is likely to be better shown in the tetrodotoxin-treated bladder. However, there may be additional dimensions of variation in the extent of innervation, given that denervation is reported to affect some muscle bundles in the bladder wall more severely than others (M.J Drake, Gardner, & Brading, 2003). At all events it appears that global cholinergic contraction is unlikely in the resting bladder given that resting activity is also modulated by NANC agonists and levels of cholinergic stimulation are low (J. Gillespie, 2004b).

The effects of isoprenaline in promoting the second type of contractile regime, by reducing or eliminating PPCs but not randomly sited PICs, is in line with reports that β-adrenergic agonists reduce the amplitude and frequency of oscillation in intravesical pressure as well as baseline intravesical pressure in rats with outflow obstruction (J. I. Gillespie et al., 2012b). Similarly, the findings are in line with work showing that the β_3 agonist mirabegron reduces the amplitude and frequency of pressure oscillations in the obstructed rat bladder (J. I. Gillespie et al., 2012b).The selective suppression of PPCs, with persistence of PICs after dosage with isoprenaline, suggests that adrenergic agonists either decrease the excitability of ICCs i.e., their ability to coordinate myocyte contraction to form large PPCs, or directly reduce the excitability of myocytes rendering ICCs unable to fire them. At all events, it appears that when low grade cholinergic signalling is present, PPCs predominate and PICs are reduced; and when adrenergic signalling is dominant, PPCs are reduced whilst PICs continue. This hypothesis is supported by reports that microcontractions are prominent in the bladders of neonatal rats (Ikeda et al., 2007; Sugaya & de Groat, 2000; Széll, Somogyi, de Groat, & Szigeti, 2003), given that parasympathetic development precedes other pathways in 2-12 day old rats (Sugaya, Roppolo, Yoshimura, Card, & de Groat, 1997). Again, these results support recent experiments based on the work of Barrington,

showing that sympathetic activity regulated the timing of voiding (Barrington, 1915), and the consequent hypothesis that the setting of the mechanosensitive circuitry within the wall of the urinary bladder (Charles S Sherrington, 1892b) involved micromotions and that this process was influenced particularly by the sympathetic nervous system (Eastham & Gillespie, 2013). Furthermore, sympathetic activity may be important in reducing motor-sensory 'noise' engendered by micromotions and the consequent sensation of bladder fullness, enabling micturition to be postponed (Eastham & Gillespie, 2013). Indeed, the concomitant lowering of intravesical pressure which was seen following dosage with isoprenaline may further aid such postponement. Thus, in the state where there is low grade cholinergic signalling, the intravesical pressure is higher, but frequent PPCs allow the elasticity of the wall to be continually 'dynamically' assessed and 'anticipatory' adjustment of bladder capacity made; whereas in the state where PPCs are reduced, a combination of diffuse un-coordinated contraction and passive mechanical properties of the tissue (Gregersen, 2003) allow more limited reactive adjustment of wall compliance, backed by a general lowering of intravesical pressure so that storage can continue in the short term. Hence the capacity to switch between these two states may be important for continence and impairment of either adrenergic or cholinergic response may lead to incontinence, as has been similarly concluded by other workers (K.-E. Anderson, 1993; K.-E. Andersson & Arner, 2004). It is noteworthy in this respect that this study did not examine the effects of NANC/purinergic agonists which may also influence the balance between the two states (J. Gillespie, 2004b).

Whilst it is known that ICC-IM can directly induce electrotonic change in groups of myocytes via gap junctions (Berridge, 2008) and hence initiate contraction via a 'spike patch' (W. J. E. P. Lammers & Slack, 2001; W. J. E. P. Lammers, Ver Donck, Schuurkes, & Stephen, 2003) in associated myocytes that may be equivalent to a PIC (C M Hulls et al., 2017), the spatiotemporal aspects of this role have not been elucidated. Hence, one or more ICC-IM could either initiate local spike patches and consequent PICs, synchronise local PIC contractions of groups of myocytes to form PPCs, or expedite directional propagation i.e., the direction of successive spike patches and consequent PICs, perhaps via coupled oscillation (Parsons & Huizinga, 2015, 2016). The differences in the contractile responses to the gap junction blocker carbenoxolone, which may blockade gap junctions

between ICC-IM and myocytes that bear connexin -43 (Hikaru Hashitani, Fukuta, Takano, Klemm, & Suzuki, 2001) and those between myocytes that bear connexin-45 (Christopher H Fry et al., 2004), and the responses to RhoA antagonists, which act directly on bladder myocytes attenuating their contraction (Wibberley et al., 2003), sheds some light on these three spatiotemporally distinct processes.

If we consider that

1) the overall duration of a PPC is proportional to the number of PICs that are successively incorporated into it,

2) that mean patch size is an index of synchronous local spread,

3) that the velocity of the PPC is an index of directional facilitation of propagation,

if ICC-IM associated gap junctions were responsible for all three actions, then they would all decrease on blockade of connexin-43 mediated gap junction. Conversely if the three actions were solely due to the electrotonic behaviour of myocytes, we would expect that the actions of gap junction blockers (which block connexin-45 mediated gap junctions) and RhoA antagonists (which generally decrease excitability of myocytes) would both cause these parameters to *decrease*. Again, if the three actions were solely due to the electrotonic behaviour of myocytes, and if the gap junction blocker acted only on connexin-43 mediated gap junctions, we would expect that RhoA antagonists *alone* would cause all three parameters to decrease. Hence the results showing that carbenoxolone had no significant effect on largest patch index or patch size, whilst RhoA significantly reduced both these parameters, suggest that, at the dose used, this agent had little effect on connexin-45 mediated gap junctions and that the synchronous local spread of contraction was governed solely by myocytes. Conversely, the fact that both carbenoxolone and the RhoA inhibitor Y-27632 decreased the durations of PPCs suggests that the former agent influenced connexin-43 mediated gap junctions, and that the electrotonic action of ICC-IM contributed to the successive incorporation of PICs into PPCs. This finding is in line with work showing that carbenoxolone reduced the coherence of propagation of ICC-MY engendered electrotonic effects in the terminal ileum (Park et al., 2006) and impaired the synchronicity of calcium (Ca^{2+})

wave transit across smooth muscle bundles (Hikaru Hashitani, Yanai, et al., 2004a) from the urinary bladder of the guinea pig. Hence in the intact bladder carbenoxolone appears to act on connexin-45 mediated gap junctions. The resultant dyssynergia could account for its effect in increasing the apparent overall frequency of ICC-IM engendered PPCs. It could also account for the increase in their velocity of propagation given that the likelihood of coupled oscillation (Parsons & Huizinga, 2015) may increase when a number of signals of similar frequency but differing coherence are present.

The failure of carbenoxolone to influence LPI and mean patch size (Table 1) at the dose used suggests that, in spite of its reported action in impairing the transit of dye between myocytes via gap junctions in muscle strips (Hikaru Hashitani et al., 2001), it has relatively little effect on electrotonic coupling between adjacent myocytes in intact bladders. A similar lack of myogenic effect has been reported in the isolated bladder of the adult rat (Ikeda et al., 2007). It is noteworthy in this respect that some of the prior work was conducted on muscle strips rather than the intact organ and used insoluble glycyrrhetinic acid derivatives that were dissolved in DMSO (Hikaru Hashitani et al., 2001) an agent known to induce pore formation in cell membranes (Gurtovenko & Anwar, 2007; Notman, Noro, O'Malley, & Anwar, 2006).

The suggestion that carbenoxolone has different effects on connexin-43 and connexin-45 mediated gap junctions fits in with evidence from strips of gallbladder smooth muscle, that contains numbers of ICCs (Lavoie, Balemba, Nelson, Ward, & Mawe, 2007), although the effects were opposite to those reported here. Hence, carbenoxolone interfered with the development of Ca^{2+} waves in smooth muscle but not within ICC (Lavoie et al., 2007).

Again, the finding that the disposition of contractions on A-type contraction density plots (Fig 5-3 column 4) changed markedly on addition of carbenoxolone suggests that different regions of the bladder may vary in their sensitivity to the agent. This is supported by findings that 18-beta-glycyrretinic had differing effects on trigonal and detrusor muscle strips taken from the guinea pig bladder (Roosen et al., 2009).

The finding that that the Rho A inhibitor Y27632 generally inhibited local spread of myocyte contraction fits in with its reports of inhibition of electrical field stimulation induced, bethanechol-induced (Jezior et al., 2001; Wibberley et al., 2003) and stretch-induced (Poley et al., 2008) contraction in isolated strips of smooth muscle from the rabbit bladder. Again its effect on the duration of PPCs fit in with its reported effect in reducing the amplitude and the regularity of burst type contractions in strips of guinea pig detrusor (Hikaru Hashitani, Brading, et al., 2004).

In summary: the results of this study shed further light on the manner in which adrenergic and cholinergic agents reciprocally influence the different types of contractile activity in the resting whole bladder. They also shed light on the contributions of ICCs and myocytes to the initiation, local spread and the propagation of contractions and the formation of microcontractions. The ability of two-dimensional spatiotemporal mapping to highlight subtle differences in the pathways and timings of contractions in the isolated bladder following treatment with pharmaceutical agents, offers good prospects for its use in further functional pharmacological assays.

References

Anderson, K.-E. (1993). Pharmacology of lower urinary tract smooth muscles and penile erectile tissues. *Pharmacological Reviews, 45*(3), 253-308.

Andersson, K.-E., & Arner, A. (2004). Urinary bladder contraction and relaxation: physiology and pathophysiology. *Physiological Reviews, 84*(3), 935-986.

Azhari, H., Weiss, J. L., Rogers, W. J., Siu, C. O., & Shapiro, E. P. (1995). A noninvasive comparative study of myocardial strains in ischemic canine hearts using tagged MRI in 3-D. *American Journal of Physiology, 268*(5), H1918-1926.

Barrington, F. (1915). The effect of division of the hypogastric nerves on frequency of micturition. *Experimental Physiology, 9*(3), 261-264.

Berridge, M. J. (2008). Smooth muscle cell calcium activation mechanisms. *Journal of Physiology, 586*(21), 5047-5061.

Brading, A. (2006). Spontaneous activity of lower urinary tract smooth muscles: correlation between ion channels and tissue function. *The Journal of Physiology, 570*(1), 13-22.

Brading, A. F. (1997). A myogenic basis for the overactive bladder. *Urology, 50*(6, Supplement 1), 57-67. https://doi.org/10.1016/S0090-4295(97)00591-8

Braverman, A. S., Doumanian, L. R., & Ruggieri, M. R. (2006). M2 and M3 muscarinic receptor activation of urinary bladder contractile signal transduction. II. Denervated rat bladder. *Journal of Pharmacology and Experimental Therapeutics, 316*(2), 875-880.

Braverman, A. S., Tibb, A. S., & Ruggieri, M. R. (2006). M2 and M3 muscarinic receptor activation of urinary bladder contractile signal transduction. I. Normal rat bladder. *Journal of Pharmacology and Experimental Therapeutics, 316*(2), 869-874.

Bülbring, E. (1955). Correlation between membrane potential, spike discharge and tension in smooth muscle. *Journal of Physiology, 128*(1), 200-221.

Burnstock, G., & Prosser, C. (1960). Responses of smooth muscles to quick stretch; relation of stretch to conduction. *American Journal of Physiology--Legacy Content, 198*(5), 921-925.

Coolsaet, B. (1985). Bladder compliance and detrusor activity during the collection phase. *Neurourology and Urodynamics, 4*(4), 263-273.

Coolsaet, B. L., Van Duyl, W. A., Os-Bossagh, V., & De Bakker, H. V. (1993). New concepts in relation to urge and detrusor activity. *Neurourology and Urodynamics, 12*(5), 463-471.

Davidson, J. S., & Baumgarten, I. M. (1988). Glycyrrhetinic acid derivatives: a novel class of inhibitors of gap-junctional intercellular communication. Structure-activity relationships. *Journal of Pharmacology and Experimental Therapeutics, 246*(3), 1104-1107.

Davis, M. J., & Hill, M. A. (1999). Signaling mechanisms underlying the vascular myogenic response. *Physiological Reviews, 79*(2), 387-423.

Drake, M., Harvey, I., & Gillespie, J. (2003). Autonomous activity in the isolated guinea pig bladder. *Experimental Physiology, 88*(1), 19-30.

Drake, M. J., Gardner, B. P., & Brading, A. F. (2003). Innervation of the detrusor muscle bundle in neurogenic detrusor overactivity. *BJU International, 91*(7), 702-710.

Eastham, J. E., & Gillespie, J. I. (2013). The concept of peripheral modulation of bladder sensation. *Organogenesis, 9*(3), 224-233.

Frazier, E. P., Peters, S. L., Braverman, A. S., Ruggieri, M. R., & Michel, M. C. (2008). Signal transduction underlying the control of urinary bladder smooth muscle tone by muscarinic receptors and β-adrenoceptors. *Naunyn-Schmiedeberg's Archives of Pharmacology, 377*(4-6), 449-462.

Fry, C. H., Sui, G.-P., Severs, N. J., & Wu, C. (2004). Spontaneous activity and electrical coupling in human detrusor smooth muscle: implications for detrusor overactivity? *Urology, 63*(3), 3-10.

Gevaert, T., Ost, D., & De Ridder, D. (2006). Comparison study of autonomous activity in bladders from normal and paraplegic rats. *Neurourology and Urodynamics, 25*(4), 368-378.

Gillespie, J. (2004a). The autonomous bladder: a view of the origin of bladder overactivity and sensory urge. *BJU international, 93*(4), 478-483.

Gillespie, J. (2004b). Modulation of autonomous contractile activity in the isolated whole bladder of the guinea pig. *BJU International, 93*(3), 393-400.

Gillespie, J. I., Palea, S., Guilloteau, V., Guerard, M., Lluel, P., & Korstanje, C. (2012). Modulation of non-voiding activity by the muscarinergic antagonist tolterodine and the β3-adrenoceptor agonist mirabegron in conscious rats with partial outflow obstruction. *BJU International, 110*(2b)

Gregersen, H. (2003). *Biomechanics of the gastrointestinal tract: new perspectives in motility research and diagnostics*. New York: Springer Verlag.

Gurtovenko, A. A., & Anwar, J. (2007). Modulating the structure and properties of cell membranes: the molecular mechanism of action of dimethyl sulfoxide. *The journal of physical chemistry B, 111*(35), 10453-10460.

Hashitani, H., & Brading, A. F. (2003). Electrical properties of detrusor smooth muscles from the pig and human urinary bladder. *British Journal of Pharmacology, 140*(1), 146-158.

Hashitani, H., Brading, A. F., & Suzuki, H. (2004). Correlation between spontaneous electrical, calcium and mechanical activity in detrusor smooth muscle of the guinea-pig bladder. *British Journal of Pharmacology, 141*(1), 183-193.

Hashitani, H., Fukuta, H., Takano, H., Klemm, M. F., & Suzuki, H. (2001). Origin and propagation of spontaneous excitation in smooth muscle of the guinea-pig urinary bladder. *Journal of Physiology, 530*(2), 273-286.

Hashitani, H., Yanai, Y., & Suzuki, H. (2004). Role of interstitial cells and gap junctions in the transmission of spontaneous Ca^{2+} signals in detrusor smooth muscles of the guinea-pig urinary bladder. *Journal of Physiology, 559*(2), 567-581.

Hulls, C. M., Lentle, R. G., King, Q. M., Reynolds, G. W., & Chambers, J. (2017). Spatiotemporal analysis of spontaneous myogenic contractions in the urinary bladder of the rabbit: timing and patterns reflect reported electrophysiology. *American Journal of Physiology-Renal Physiology, 313*(3), F687-F698.

Ikeda, Y., Fry, C., Hayashi, F., Stolz, D., Griffiths, D., & Kanai, A. (2007). Role of gap junctions in spontaneous activity of the rat bladder. *American Journal of Physiology-Renal Physiology, 293*(4), F1018-F1025.

Janssen, P. W. M., & Lentle, R. G. (2013). Spatiotemporal Mapping Techniques for Quantifying Gut Motility. In L. K. Cheng & G. Farrugia (Eds.), *New Advances in Gastrointestinal Motility Research* (pp. 219-241). New York: Springer.

Jezior, J. R., Brady, J. D., Rosenstein, D. I., McCammon, K. A., Miner, A. S., & Ratz, P. H. (2001). Dependency of detrusor contractions on calcium sensitization and calcium entry through LOE-908-sensitive channels. *British Journal of Pharmacology, 134*(1), 78-87.

Ji, G., Barsotti, R. J., Feldman, M. E., & Kotlikoff, M. I. (2002). Stretch-induced calcium release in smooth muscle. *The Journal of General Physiology, 119*(6), 533-543.

Johnston, L., Woolsey, S., Cunningham, R. M., O'Kane, H., Duggan, B., Keane, P., & McCloskey, K. D. (2010). Morphological expression of KIT positive interstitial cells of Cajal in human bladder. *The Journal of urology, 184*(1), 370-377.

Kirber, M. T., Walsh, J. V., & Singer, J. J. (1988). Stretch-activated ion channels in smooth muscle: a mechanism for the initiation of stretch-induced contraction. *Pflügers Archiv European Journal of Physiology, 412*(4), 339-345.

Klevmark, B. (1974). Motility of the Urinary Bladder in Cats during Filling at Physiological Rates: I. Intravesical Pressure Patterns Studied by a New Methods of Cystometry. *Acta Physiologica, 90*(3), 565-577.

Kories, C., Czyborra, C., Fetscher, C., Schneider, T., Krege, S., & Michel, M. C. (2003). Gender comparison of muscarinic receptor expression and function in rat and human urinary bladder: differential regulation of M2 and M3 receptors? *Naunyn-Schmiedeberg's Archives of Pharmacology, 367*(5), 524-531.

Kraichely, R., & Farrugia, G. (2007). Mechanosensitive ion channels in interstitial cells of Cajal and smooth muscle of the gastrointestinal tract. *Neurogastroenterology and Motility, 19*(4), 245-252.

Kubota, Y., Biers, S. M., Kohri, K., & Brading, A. F. (2006). Effects of imatinib mesylate (Glivec®) as ac-kit tyrosine kinase inhibitor in the guinea-pig urinary bladder. *Neurourology and Urodynamics, 25*(3), 205-210.

Lammers, W. J. E. P., & Slack, J. R. (2001). Of slow waves and spike patches. *News in physiological sciences, 16*, 138-144.

Lammers, W. J. E. P., Ver Donck, L., Schuurkes, J. A. J., & Stephen, B. (2003). Longitudinal and circumferential spike patches in the canine small intestine in vivo. *American Journal of Physiology, 285*(5), G1014-1027.

Lavoie, B., Balemba, O. B., Nelson, M. T., Ward, S. M., & Mawe, G. M. (2007). Morphological and physiological evidence for interstitial cell of Cajal-like cells in the guinea pig gallbladder. *The Journal of Physiology, 579*(2), 487-501.

Lentle, R. G., Reynolds, G. W., Janssen, P. W. M., Hulls, C. M., King, Q. M., & Chambers, J. (2015). Characterisation of the contractile dynamics of the resting ex vivo urinary bladder of the pig. *BJU International, 116*(6), 973-983.

Levin, R. M., Ruggieri, M. R., Velagapudi, S., Gordon, D., Altman, B., & Wein, A. J. (1986). Relevance of spontaneous activity to urinary bladder function: an in vitro and in vivo study. *Journal of Urology, 136*(2), 517-521.

Levin, R. M., Shofer, F. S., & Wein, A. J. (1980). Cholinergic, adrenergic and purinergic response of sequential strips of rabbit urinary bladder. *Journal of Pharmacology and Experimental Therapeutics, 212*(3), 536-540.

Makhlouf, G. M., & Murthy, K. S. (2006). Cellular physiology of gastrointestinal smooth muscle. In L. R. Johnson (Ed.), *Physiology of the Gastrointestinal Tract* (4th ed.). New York: Raven Press.

McGarigal, K., Cushman, S. A., Neel, M. C., & Ene, E. (2002). FRAGSTATS: spatial pattern analysis program for categorical maps.

Mosso, A., & Pellacani, P. (1882). Sur la fonction de la vessie. *Archives Italiennes de Biologie, 1*, 291–324.

Nagatomi, J., Toosi, K. K., Grashow, J. S., Chancellor, M. B., & Sacks, M. S. (2005). Quantification of bladder smooth muscle orientation in normal and spinal cord injured rats. *Annals of biomedical engineering, 33*(8), 1078-1089.

Notman, R., Noro, M., O'Malley, B., & Anwar, J. (2006). Molecular basis for dimethylsulfoxide (DMSO) action on lipid membranes. *Journal of the American Chemical Society, 128*(43), 13982-13983.

Park, K. J., Hennig, G. W., Lee, H. T., Spencer, N. J., Ward, S. M., Smith, T. K., & Sanders, K. M. (2006). Spatial and temporal mapping of pacemaker activity in interstitial cells of Cajal in mouse ileum in situ. *American Journal of Physiology, 290*(5), C1411-1427.

Parsons, B. A., Drake, M. J., Gammie, A., Fry, C. H., & Vahabi, B. (2012). The validation of a functional, isolated pig bladder model for physiological experimentation. *Frontiers in pharmacology, 3*

Parsons, S. P., & Huizinga, J. D. (2015). Effects of gap junction inhibition on contraction waves in the murine small intestine in relation to coupled oscillator theory. *American Journal of Physiology-Gastrointestinal and Liver Physiology, 308*(4), G287-G297.

Parsons, S. P., & Huizinga, J. D. (2016). Spatial Noise in Coupling Strength and Natural Frequency within a Pacemaker Network; Consequences for Development of Intestinal Motor Patterns According to a Weakly Coupled Phase Oscillator Model. *Frontiers in neuroscience, 10*

Plum, F., & Colfelt, R. H. (1960). The genesis of vesical rhythmicity. *Archives of Neurology, 2*(5), 487-496.

Poley, R. N., Dosier, C. R., Speich, J. E., Miner, A. S., & Ratz, P. H. (2008). Stimulated calcium entry and constitutive RhoA kinase activity cause stretch-induced detrusor contraction. *European journal of pharmacology, 599*(1-3), 137-145.

Rasmussen, H., Rumessen, J. J., Hansen, A., Smedts, F., & Horn, T. (2009). Ultrastructure of Cajal-like interstitial cells in the human detrusor. *Cell and Tissue Research, 335*(3), 517.

Roosen, A., Wu, C., Sui, G., Chowdhury, R. A., Patel, P. M., & Fry, C. H. (2009). Characteristics of spontaneous activity in the bladder trigone. *European Urology, 56*(2), 346-354.

Schneider, T., Fetscher, C., Krege, S., & Michel, M. C. (2004). Signal transduction underlying carbachol-induced contraction of human urinary bladder. *Journal of Pharmacology and Experimental Therapeutics, 309*(3), 1148-1153.

Setoguchi, M., Ohya, Y., Abe, I., & Fujishima, M. (1997). Stretch activated whole cell currents in smooth muscle cells from mesenteric resistance artery of guinea pig. *Journal of Physiology, 501*(2), 343-353.

Sherrington, C. S. (1892a). Notes on the arrangement of some motor fibres in the lumbo-sacral plexus. *Journal of Physiology, 13*(6), 621–772.

Sherrington, C. S. (1892b). Notes on the Arrangement of some Motor Fibres in the Lumbo-Sacral Plexus. *The Journal of Physiology, 13*(6), 621-772.

Strege, P. R., Ou, Y., Sha, L., Rich, A., Gibbons, S. J., Szurszewski, J. H., . . . Farrugia, G. (2003). Sodium current in human intestinal interstitial cells of Cajal. *American Journal of Physiology, 285*(6), G1111-1121.

Streng, T., Hedlund, P., Talo, A., ANDERSSON, K. E., & Gillespie, J. I. (2006). Phasic non-micturition contractions in the bladder of the anaesthetized and awake rat. *BJU International, 97*(5), 1094-1101.

Sugaya, K., & de Groat, W. C. (2000). Influence of temperature on activity of the isolated whole bladder preparation of neonatal and adult rats. *American Journal of Physiology, 278*(1), R238-246.

Sugaya, K., Roppolo, J. R., Yoshimura, N., Card, J. P., & de Groat, W. C. (1997). The central neural pathways involved in micturition in the neonatal rat as revealed by the injection of pseudorabies virus into the urinary bladder. *Neuroscience Letters, 223*(3), 197-200.

Széll, E. A., Somogyi, G. T., de Groat, W. C., & Szigeti, G. P. (2003). Developmental changes in spontaneous smooth muscle activity in the neonatal rat urinary bladder. *American Journal of Physiology-Regulatory, Integrative and Comparative Physiology, 285*(4), R809-R816.

Tare, M., Coleman, H., & Parkington, H. C. (2002). Glycyrrhetinic derivatives inhibit hyperpolarization in endothelial cells of guinea pig and rat arteries. *American Journal of Physiology-Heart and Circulatory Physiology, 282*(1), H335-H341.

Thuneberg, L., & Peters, S. (2001). Toward a concept of stretch-coupling in smooth muscle. I. Anatomy of intestinal segmentation and sleeve contractions. *Anatomical Record, 262*(1), 110-124.

Turner, W., & Brading, A. (1997). Smooth muscle of the bladder in the normal and the diseased state: pathophysiology, diagnosis and treatment. *Pharmacology and Therapeutics, 75*(2), 77-110.

Wang, Y., Fang, Q., Lu, Y., Song, B., Li, W., & Li, L. (2010). Effects of mechanical stretch on interstitial cells of Cajal in guinea pig bladder. *Journal of Surgical Research, 164*(1), e213-e219.

Wellner, M.-C., & Isenberg, G. (1993). Stretch Activated Nonselective Cation Channels in Urinary Bladder Myocytes: Importance for Pacemaker Potentials and Myogenic Response. *EXS, 66*, 93-99.

Wibberley, A., Chen, Z., Hu, E., Hieble, J. P., & Westfall, T. D. (2003). Expression and functional role of Rho-kinase in rat urinary bladder smooth muscle. *British Journal of Pharmacology, 138*(5), 757-766.

Won, K. J., Sanders, K. M., & Ward, S. M. (2005). Interstitial cells of Cajal mediate mechanosensitive responses in the stomach. *Proceedings of the National Academy of Sciences of the United States of America, 102*(41), 14913-14918.

Wu, X., & Davis, M. J. (2001). Characterization of stretch-activated cation current in coronary smooth muscle cells. *American Journal of Physiology, 280*(4), H1751-1761.

Yamazaki, Y., Takeda, H., Akahane, M., Igawa, Y., Nishizawa, O., & Ajisawa, Y. (1998). Species differences in the distribution of β-adrenoceptor subtypes in bladder smooth muscle. *British Journal of Pharmacology, 124*(3), 593-599.

DRC 16

MASSEY UNIVERSITY
TE KUNENGA KI PŪREHUROA
UNIVERSITY OF NEW ZEALAND

GRADUATE RESEARCH SCHOOL

STATEMENT OF CONTRIBUTION
DOCTORATE WITH PUBLICATIONS/MANUSCRIPTS

We, the candidate and the candidate's Primary Supervisor, certify that all co-authors have consented to their work being included in the thesis and they have accepted the candidate's contribution as indicated below in the *Statement of Originality*.

Name of candidate:	Corrin Hulls
Name/title of Primary Supervisor:	Prof RG Lentle
In which chapter is the manuscript /published work:	Chapter 6

Please select one of the following three options:

(●) The manuscript/published work is published or in press

- Please provide the full reference of the Research Output:

Pharmacological modulation of the spatiotemporal disposition of micromotions in the intact resting urinary bladder of the rabbit; their pattern is under both myogenic and autonomic control
Corrin Murray Hulls, Roger Graham Lentle, Quinten Michael King, John Paul Chambers, Gordon Willoughby Reynolds

( ) The manuscript is currently under review for publication – please indicate:

- The name of the journal:

BJU International

- The percentage of the manuscript/published work that was contributed by the candidate: 70%
- Describe the contribution that the candidate has made to the manuscript/published work:

Conducted experimental work
Processing of video & results
Statistical procedures

( ) It is intended that the manuscript will be published, but it has not yet been submitted to a journal

Candidate's Signature:	
Date:	3.10.22
Primary Supervisor's Signature:	PROFESSOR ROGER LENTLE
Date:	2/10/22

This form should appear at the end of each thesis chapter/section/appendix submitted as a manuscript/ publication or collected as an appendix at the end of the thesis.

Preface Chapter 7

Chapter 7 is comparative in nature and investigates another smooth muscle capacious structure- the *in vivo* gravid uterus. The urinary bladder is a repository for the storage of urine secreted by the kidneys, and similarly the uterus must act as a repository for the growing foetus. This chapter investigates the smooth muscle contractile behaviour of the uterus and examines whether there are similarities with the urinary bladder that underlie an 'accommodative' modulation of tone and to also characterise the onset and progression of labour dependent upon the development of rhythmic, synchronous, and powerful contractions of the myometrium.

Copy of Paper- Spatiotemporal Mapping of the Contracting Gravid Uterus of the Rabbit Shows Contrary Changes with Increasing Gestation and Dosage with Oxytocin

The following pages contain a copy of the published journal article with the following bibliography-

Hulls, C. M., Lentle, R. G., Chua, W. H., Suisted, P., King, Q. M., Chagas, J., Chambers, J. P., & Stewart, L. (2019). Spatiotemporal mapping of the contracting gravid uterus of the rabbit shows contrary changes with increasing gestation and dosage with oxytocin. *Frontiers in Endocrinology*, *10*, 802.

The main format of the publish peer-reviewed article is reproduced in this chapter section with its format and content maintained. All references sited are listed in a separate sub-section after the main body of the article. These references would be reproduced in the main bibliography of this thesis (i.e., after the thesis appendix) only should they be used elsewhere beyond this section (i.e., of this published article). All further work beyond this section will be citing the work presented in this section where appropriate.

7 Spatiotemporal mapping of the contracting gravid uterus of the rabbit shows contrary changes with increasing gestation and dosage with oxytocin.

7.1 Abstract

Spontaneous and oxytocin induced contractile activity was quantified in the bicornuate uteri of pregnant rabbits maintained *in situ,* using data from two- and uni- dimensional video spatiotemporal maps (VSTM) of linear and area strain rate and compared statistically. Spontaneous contractions occurred over a range of frequencies between 0.1 and 10 cpm (cycles per minute), in gravid animals at 18-21 and at 28 days of gestation and propagated both radially and longitudinally over the uterine wall overlying each foetus. Patches of contractions were randomly distributed over the entire surface of the cornua and were pleomorphic in shape. No spatial coordination was evident between longitudinal and circular muscle layers nor temporal coordination that could indicate the activity of a localised pacemaker. The density and duration of contractions decreased, and their frequency increased with the length of gestation in the non-labouring uterus. Increasing intravenous doses of with oxytocin had no effect on the mean frequencies, or the mean durations of contractions in rabbits of 18-21 days gestation but caused frequencies to decrease and durations to increase in rabbits of 28 days gestation, from greater spatial and temporal clustering of individual contractions. This was accompanied by an increase in the distance of propagation, the mean size of the patches of contraction, the area of the largest patch of contraction and the overall density of patches. Together these results suggest that progressive smooth muscle hypertrophy and displacement with increasing gestation is accompanied by a decrease in smooth muscle connectivity causing an increase in wall compliance and that oxytocin restores connectivity and decreases compliance, promoting volumetric expulsion rather than direct propulsion of the foetus by peristalsis. The latter effects were reversed by the β2 adrenergic receptor agonist salbutamol thus reducing area of contraction, duration, and distance of propagation.

7.2 Introduction

The principal mechanical functions of the mammalian uterus are to act as a repository in which foetal growth can take place and to provide a means by which the foetus can be expelled once fully developed. The former is achieved by amelioration of the tone in the walls of the uterus and hence their compliance i.e., the ease with which the uterine cavity may be dilated. Hence, cavity volume is increased, in human subjects from around 50 ml (Yagel et al., 1992) to over 4,000 ml (Geirsson et al., 1985), so as to accommodate the growing foetus without undue elevation of intra-luminal pressure (Fisk et al., 1992). However, little is known of the changes in contractile dynamics that underlie this 'accommodative' modulation of tone and there is conflicting evidence regarding the spatiotemporal disposition of uterine contractions.

A body of indirect evidence regarding the disposition and timing of individual contractions comes from the qualitative analyses of changes in associated electrical potential in multi-electrodes (Hutchings et al., 2009). The bulk of this work suggests that the propagation of electrical phenomena associated with uterine contractions i.e., localised bursts of activity, is chaotic rather than ordered, with locally varying patterns with re-entry evident in some species (Hutchings et al., 2009; W. J. Lammers, 1996a). A further a body of work suggests that uterine contractions do not progress circumferentially along the long axis of the uterine cavity. Hence, for example, uterine contractions (Norwitz & Robinson, 2001) and associated electrical activity (W. J. Lammers et al., 2008) are relatively reduced around the site of placentation (Daniel, 1960). Again, whilst work indicates that nature and timing of uterine contractions can be modified by hormonal and other stimuli (Van Gestel, IJland, Hoogland, & Evers, 2003), we can find no direct evidence that these stimuli facilitate the spatiotemporal organisation of contractions across the full thickness of the uterine muscle to engender peristaltic progression. Qualitative direct studies of human uterine contraction using two dimensional electro-hysterographic mapping similarly show that the propagating front of electrical burst activity is irregular (Chiara Rabotti et al., 2010) and that uterine contractions vary in frequency and strength between proximal and distal regions and between adjacent sites (R. E. Garfield & Maner, 2007; Norwitz & Robinson, 2001).

Together such findings support a hypothesis that the movement of uterine contents in the appropriate direction could be produced solely by a change in intrauterine pressure i.e., an overall increase in the tone of the wall so as to reduce lumen volume, in both rabbits and in human subjects (Arpad I Csapo, Jaffin, Kerenyi, Lipman, & Wood, 1963; R. Smith, Imtiaz, Banney, Paul, & Young, 2015). Further, evidence suggests that such action could result solely or partly from local mechano-transduction (Roger C Young, 2016). Thus, strips of uterine muscle are sensitive to stretch (Shelkovnikov, Savitskiĭ, & Abramchenko, 1986a) and a mechano-transductive response occurs when a bolus of Tyrode's solution is injected into the uterine cavity. The latter comprises an initial 'early stretch' response when luminal pressure rises above baseline pressure and a subsequent period when rhythmic contractions decrease in amplitude and intra-uterine pressure declines over a period of 20 minutes (Setekleiv, 1964a). Similarly, a number of experiments have shown that hydrostatic (Takeda, 1965) and tensional (Roger C Young & Goloman, 2011) forces can evoke similar contractions in the pregnant uterus. Hence, impairment in the magnitude of mechanoreceptor evoked micro-contractions may act to reduce intrauterine pressure and secure accommodation in a similar manner to that in capacious structures such as the resting urinary bladder (C M Hulls et al., 2017; Lentle et al., 2015b) and gastric fundus (Roger Graham Lentle et al., 2016). Again, hormonal (Mironneau, 1976) and other stimuli (Willets et al., 2009) may act to alter the threshold of such resetting so as to increase intrauterine pressure and engender foetal expulsion. Hence, for example, oxytocin is reported to increase the frequency and intensity of contractions in the oestrogenised uterus via a variety of pathways (Anatoly Shmygol, Gullam, Blanks, & Thornton, 2006).

A number of other studies have suggested that uterine contractions are spatiotemporally organised. An early paper showed orderly progression of electrical activity in the uterine cornua of pregnant ewes (H. Parkington, Harding, & Sigger, 1988). Again, whilst recent multi-electrode studies showed little evidence of tightly ordered proximal to distal propagation of individual uterine contractions, the broad overall direction of the development of propagating electrophysiological bursts was reported to be from proximal to distal along the long axis of the uterus (Wim JEP Lammers, 2013; Mikkelsen, Johansen, Fuglsang-Frederiksen, & Uldbjerg, 2013; Planes, Morucci, Grandjean, & Favretto, 1984; Chiara Rabotti, de Lau, Haazen, Oei, & Mischi, 2013a). Recent

ultrasonographic studies based on cross sectional data have also suggested that the inner, predominantly circular, layer of uterine muscle next to the endometrium i.e., the *stratum subvasculare* may become spatiotemporally organised to form 'peristaltic-like' contractions (Leyendecker et al., 2004). More recently, concerted histological and electrophysiological work in the isolated uterus of the rat, has indicated the presence of myometrial/placental pace-making zones that are closely associated with the site of placentation, prompting a hypothesis that 'spatial organization of these areas likely promotes coordinated delivery of foetuses in a polytocus uterus' (Lutton, Lammers, James, van den Berg, & Blanks, 2018b).

Sensu strictu peristalsis comprises the integrated action of steadily propagating bands of longitudinal and circular muscle contraction to produce a propagating luminal constriction that bears directly against, and imparts impulsion to, the contents of the lumen (W. B. Cannon, 1902; W.B Cannon, 1911). In the small intestine, such integrative action is aided by the anatomical and physiological separation of the longitudinal and circularly orientated smooth muscle (T. K. Smith & Robertson, 1998). There is a similar anatomical demarcation of the longitudinal and circular muscle in the uterine wall of certain species including that of species with a bicornuate uterus such as the rabbit (Lambert, Pelletier, Dufour, & Fortier, 1990). However, the orientations of the long axes of the component myocytes in the wall of the human uterus appear to be less sharply demarcated, although recent work indicates there are higher concentrations of circularly orientated fibres near the cavity and around the tubal openings, and higher concentrations of longitudinally orientated fibres near the serosa (Weiss et al., 2006a). Other work indicates that the wall of the human uterus consists of localised masses of smooth muscle (Huszar & Naftolin, 1984) whose long axes are extensively intertwined (Weiss et al., 2006a), an anatomy which led one worker to hypothesize that this structure and the manner of its interconnection by interstitial tissue provide for local mechanical function (Aleksey G Savitsky et al., 2013).

Were uterine contractions organised to form peristalsis in order to directly propel the uterine content then we would expect that their direction of propagation would vary with function. Hence, the human uterus is reported to exhibit intermittent contraction (J. V. Kelly, 1962) during menstruation to void cellular debris (Bulletti et al., 2000), during the proliferative phase of the menstrual cycle to secure retrograde transport of

spermatozoa (Eytan, Jaffa, Har-Toov, Dalach, & Elad, 1999) and during early pregnancy to secure the proper placement of the conceptus in the uterine cavity (SUSAN Wray, 1993). Currently we can find no definitive evidence that these events are organised to propagate in the appropriate direction.

Conversely, if the uterus were to act primarily on a basis of mechanotransduction and the movement of the contents to be consequent on changes in volume or intrauterine pressure, then the direction of their movement could be determined by concomitant reciprocal variation in the level of occlusion of the proximal i.e., tubal, or the distal i.e., cervical openings of the cavity rather than by change in the spatial organisation and sequence of contraction. This would obviate any need for changes in direction of contraction via neural or myogenic means.

In the current work we use various video spatiotemporal mapping (VSTM) techniques to directly quantify and statistically evaluate the temporal and spatial form, area, and coordination of spontaneous contractions in the wall of the pregnant uterus of the rabbit maintained *in situ* prior to and at term and after dosage with increasing quantities of oxytocin and after subsequent dosage with salbutamol. This, with a view to comparing the spatial and temporal characteristics of contractions during the accommodative and expulsive phases of uterine action during pregnancy with those obtained from multi-electrode electro-physiological and other studies. Further, to determine whether in the latter phase the spatial pattern of contractions are consistent with direct propulsion of contents by peristalsis, or by expulsion from the resetting of uterine tone.

7.3 Materials and Methods

All the experimental procedures were approved by the Massey University Animal Ethics Committee (MUAEC approval number 17/100) and complied with the New Zealand Code of Practice for the Care and Use of Animals for Scientific Purposes.

7.3.1 Anaesthesia

Each rabbit was maintained on 100% oxygen in a clear acrylic induction chamber for five minutes prior to administration of the anaesthetic. Halothane (4%) was then given in 100% oxygen until the animal lost its righting reflex and surgical anaesthesia induced with alfaxalone IV (2-3 mg/kg) via a 20 G catheter in the cephalic vein. The animal was then intubated with a 3.5 mm cuffed endotracheal tube and anaesthesia subsequently maintained by a combination of halothane (EtHal 0.8-1.2%) in oxygen and intravenous alfaxalone maintained at 0.1-0.2 mg/kg/min.

Arterial blood gases were monitored by a 22 G catheter and mechanical ventilation used to maintain normocapnia. Peak systolic blood pressure was maintained above 60 mmHg with intravenous noradrenaline (0.5-1.5 µg/kg/min) when necessary, and body temperature was maintained at 38-39°C via forced-air warming.

7.3.2 Procedure

Eight pregnant New Zealand white rabbits were obtained from a commercial breeder and maintained on commercial feed, which was available *ad libitum* with water until immediately prior to the procedure. Following administration of anaesthetic (see above) the animal was placed in a supine position and the abdomen was opened with a vertical ventral paramedian incision sited lateral to the line of the breast tissue. The anterior surface of the left cornua of the uterus was exposed and lightly dusted with carbon black. The animal was then rotated to the left into a semi-prone position so that the left cornua of the uterus, and contained foetuses, could prolapse laterally through the incision into an organ bath perfused with oxygenated (95% O_2, 5% CO_2) Earle's-HEPES buffered saline (HS) of pH 7.35, comprising 124.0 mM NaCl, 5.4 mM KCl, 0.8 mM $MgSO_4$, 1.0 mM NaH_2PO_4, 14.3 mM $NaHCO_3$, 10.0 mM HEPES, 1.8 mM $CaCl_2$ and 5.0 mM glucose maintained at 37°C and continuously recirculated at a flow rate of 160 ml/min (Supplementary Data 1).

The carbon-dusted anterior surface of the left cornua was adjusted to face the video camera (Supplementary Data 1). Myoelectrical activity in uterine wall was recorded with two multi-stranded stainless-steel wire

electrodes (see below). Note that it was not possible to insert electrodes into the area of the uterus undergoing VSTM as the presence of the wire interfered with the video image and hence the subsequent analysis.

Image sequences were recorded on a video camera mounted above the organ bath to capture the three most distal foetuses in the left cornua of the uterus and saved as uncompressed AVI video files for off-line processing. Hence the motility pattern over the surface of each cornua was subsequently evaluated by cross-correlation techniques in one or two dimensions using the techniques described below.

An intravenous line was inserted through which requisite doses of the pharmaceutical agent oxytocin was given (Phoenix. Vetpharm (NZ) Ltd). Oxytocin is a known specific activator of uterine contractility at term (A.-R. Fuchs, Fuchs, Husslein, & Soloff, 1984). Salbutamol (GlaxoSmithKline (NZ) Ltd) is known to inhibit contractions in the gravid uterus (McDevitt, Wallace, Roberts, & Whitfield, 1975). Salbutamol was added directly to the organ bath super perfusate to give a bath concentration of 174 nmol/L. The latter route was chosen to minimize the generation of any systemic e.g., cardiovascular effects that could have a confounding effect on uterine motility.

At the conclusion of the recordings the anesthetised animal was euthanised with an IV bolus of pentobarbitone (125 mg/Kg) (National Veterinary Supplies Ltd. Auckland, New Zealand). The crown rump lengths of the foetuses from the eight pregnant rabbits were subsequently determined post mortem and used to determine their gestational age (Evans & Sack, 1973) and hence the duration of the pregnancy. This enabled the preparations to be categorised on a basis of their gestation.

The temporal correlations of the various parameters derived by spatiotemporal mapping were subsequently correlated with those of the electrophysiological recordings. The variations in the various quantified temporal and spatial parameters of uterine contractions were subsequently compared according to gestational age so as to identify any significant cross correlation.

Video spatiotemporal mapping (VSTM) allows the local movement of the distinctive visual features, (in this case formed by the carbon particles) between successive frames to be quantified by the displacements of

reference points on a grid of equally spaced points within a rectangular region of interest (ROI). Linear strain rates can be recorded either along the longitudinal or the radial dimensions of the uterine cornua. Conventionally, strain rates have a negative value when the distance between a given pair of markers is decreasing i.e., the tissue is contracting, and a positive value when the distance between markers is lengthening i.e., the tissue is expanding. Thus L-type spatiotemporal (ST) maps i.e., unidimensional plots of the variation in linear strain rate at all points along an appropriately curved longitudinal line of interest (LOI) and along a straight radial LOI (x-axis) over time (y-axis), were generated from the video recordings (Fig. 7-1). The longitudinal LOIs were positioned along the central axis of the anterior surface of the cornua and the radial LOIs orthogonal to this i.e., vertically across the anterior surface overlying the mid-point of the foetus.

The speed and direction (radial or longitudinal) of propagation of a burst of contractions, or of its component individual contractions, across the surface of the uterus can be directly determined from these unidimensional maps. Hence, the (acute) angle formed between the front of a propagating contraction and the horizontal axis is inversely proportional to its speed of propagation, a shallow angle indicating a faster speed. The direction of movement of the propagating front is indicated by the direction of the acute angle i.e., left to right or right to left. The frequencies of the burst type contractions can be determined from the points of intersection of successive bursts on a vertical line on the ST map in the time dimension. Further, the profile of frequencies between 1 and 10 cycles per minute (cpm) of all contractile events including burst contractions could be assessed from Fast Fourier transforms taken along the same vertical transects of the L-type ST maps over a period of 300 seconds, derived in Microsoft Excel. The Fast Fourier transforms could then be compared between the two gestational age groups and between the three doses of oxytocin within each group. The amplitudes and durations of the individual and burst contractions can be determined from vertical transects and similarly compared.

Area strain rates (ASR) at each reference point on the ellipses can determined from the local displacement rates of markers using the same technique that was described in a previous paper (Lentle et al., 2015b). Briefly, ASR are expressed as the percentage change in muscle area per unit time, i.e., % s^{-1}. Like linear strain rates,

ASRs have a negative value when area is decreasing and a positive value when area is increasing. Unidimensional plots of the variation in ASR over time (A-type plots) can be plotted in the same manner as L-type maps. Alternatively, two-dimensional plots of variation in ASR can be overlaid onto real time video frames to produce two-dimensional A-type plots. The sensitivity of the ASR mapping method is well established. Hence, for example, ASR maps derived from myocardial MRI have been shown to provide discrimination between normal and ischemic zones than other indices of strain (Azhari et al., 1995).

A sequence of uni-dimensional (A-type or L-type) and two-dimensional (A-type) ST maps, were prepared. The latter were superimposed on corresponding video images of the uterine cornua to enable the patterns of motility on its surface to be directly visualised. The area of superimposition was limited by a user-specified standardised ellipsoidal masks with their longitudinal axes located on and aligned with the longitudinal axis of the cornua and their radial axis position across the midline of the foetal outline. Each data set was taken from ellipse that occupied 45% of the anterior uterine surface. This proportion was chosen in order to exclude all sites that were close to the edge of the organ profile in which artefacts from rotational movement of the organ and parallax could occur (Supplementary Data 1). Hence the 45% area of the 18-21 day gestation group (110 mm^2) was significantly smaller than that of the 28-day gestation group (695 mm^2). Thus, comparisons of data between the two gestational ages could be confounded by differences in total area. Hence a further data set was taken in which the area of the ellipse on the 28 day group identical to that on the 18 day group i.e., 110 mm^2 with the longitudinal axis of the ellipse similarly located on the longitudinal axis of the cornua so as to standardise for area. The resulting ASRs were colour-coded such that rapidly contracting areas appeared yellow (-ve ASR), more slowly contracting areas appeared red and expanding areas appeared blue (+ve ASR).

The two-dimensional parameters of groups of propagating patches of contraction (PPCs) within the ellipse of A-type ST maps of controls and following the various treatments were each determined from 300 video frames taken at one second intervals over a five-minute period. Each original video image was imported into ArcGIS (v10.4 1999-2015 Esri Inc). In this analysis component pixels in which the strain rate was below

-4% s^{-1}, were classified as contracting and coloured yellow. Correspondingly, component pixels where strain was zero, or greater than -4% s^{-1} i.e., stretched, were classified as not contracting and coloured blue.

7.3.3 Electrophysiology

Myoelectrical activity in the uterine wall was recorded synchronously with VSTM by a pair of stranded stainless-steel wire electrodes (Part no. AS632, Cooner Wire Company, Chatsworth, California, USA). The bared tips (1–2 mm long) of the electrodes were implanted into the muscle layer by puncturing the outer serosa with a sterile 23 G needle which also served to insert the wire electrode. The exposed tips of the electrodes were hooked to ensure they remained secure in the muscle. The bipolar electrodes were placed strategically in a location on the gravid uterus that was close to the site of VSTM. Each pair of electrodes were positioned approximately 4–5 mm apart. A grounding needle electrode was inserted subcutaneously on a bony face of the tibia of each subject. The electrodes were connected via shielded cables to a bio amplifier (Animal Bio amp ML136, AD Instruments, Dunedin, New Zealand) and Powerlab data acquisition system (Power-lab 8/35, AD Instruments). Raw myoelectric data was recorded using LabChart 8 Pro v8.1.13 at a rate of 1 Kbyte per second and stored on a PC for future analysis. This was filtered with a band-pass digital filter set between 0.2 and 40 Hz so as to distinguish contractile activity from gross movement artefacts and line noise.

7.3.4 Further Data Processing and Statistics

Mean durations of uterine contractions were derived from pixel counts of consecutive events on 300 second vertical transects of area type i.e., A-type maps. Mean frequencies were calculated from fast Fourier transforms of the same vertical transects.

We adapted parameters that were originally developed in the FRAGSTATS software suite (McGarigal, Cushman, & Ene, 2012) to describe the spatial structure of patches of vegetation in landscapes to quantify the changes in shape and size of uterine contractions during their development and involution. Hence successive classified raster plots were exported from ArcGIS as GeoTIFF's, for processing by FRAGSTAT, i.e., In order to determine (McGarigal et al., 2012):-

1) Patch density (%PLAND). The total areas of all patch contractions occurring in a given A-type ST elliptical map as a percentage of the total area of the ellipse,

2) Largest Patch Index (LPI). The mean area of the largest patch contraction as a percentage of the total area of the ellipse,

3) Number of Patches (NP). The mean number of patches within the ellipses,

4) MPS. Mean patch size in mm^2

The values for the various parameters were subsequently compared by one way ANOVA or by repeated measures ANOVA, where relevant, in IBM® SPSS® Statistics (Version 25) to determine the significance of differences between gestational age and the effects of administration of oxytocin and salbutamol. Unless otherwise stated, all results are presented as the mean ± SE of the mean observation for each animal.

7.4 Results

Spontaneous local uterine contractile activity was successfully recorded in four rabbits at mid gestation (18-21 days) and four at late gestation (28 days) and after increasing IV doses of oxytocin and subsequent dosage with salbutamol at various sites across the left uterine cornua.

7.4.1 Mid gestation (18-21 days)

7.4.1.1 Unidimensional plots

Unidimensional plots of variation in linear (see later) and area strain rate (Fig 7-1) each showed short-lived contractions that occurred over a range of frequencies from 0.5 and 10 cpm and propagated rapidly over short distances in the radial and in the longitudinal plane. Consequently, they were angled slightly to the left or right of the ST map. There was no tendency for the direction of propagation of an individual contraction to change (Fig 7-1).

There were no significant differences, on repeated measures ANOVA, in the durations or the frequencies of contractions or their direction of propagation (Fig. 7-2) (Table 2), following the IV administration of increasing doses oxytocin.

7.4.1.2 Two dimensional plots

Two dimensional plots of variation in area strain rate showed spontaneous short- lived contractile activity occurred in pleomorphic patches at all sites on the uterine cornua in all rabbits of 18-21 days gestation (Supplementary Data 2). These patches increased in size by peripheral growth and by aggregation with smaller contractions and decreased in size by the reverse process. The sites of such intermittent contraction were randomly distributed across the entire radial surface of the cornua overlying and around each foetus.

Following treatment with increasing IV doses of oxytocin there were no significant increases, on repeated measures ANOVA, either in the densities of contractions within the 45% ellipse i.e., contraction density, or in mean number of patches, the largest patch index or the mean patch area (Fig. 7-3) (Table 3A).

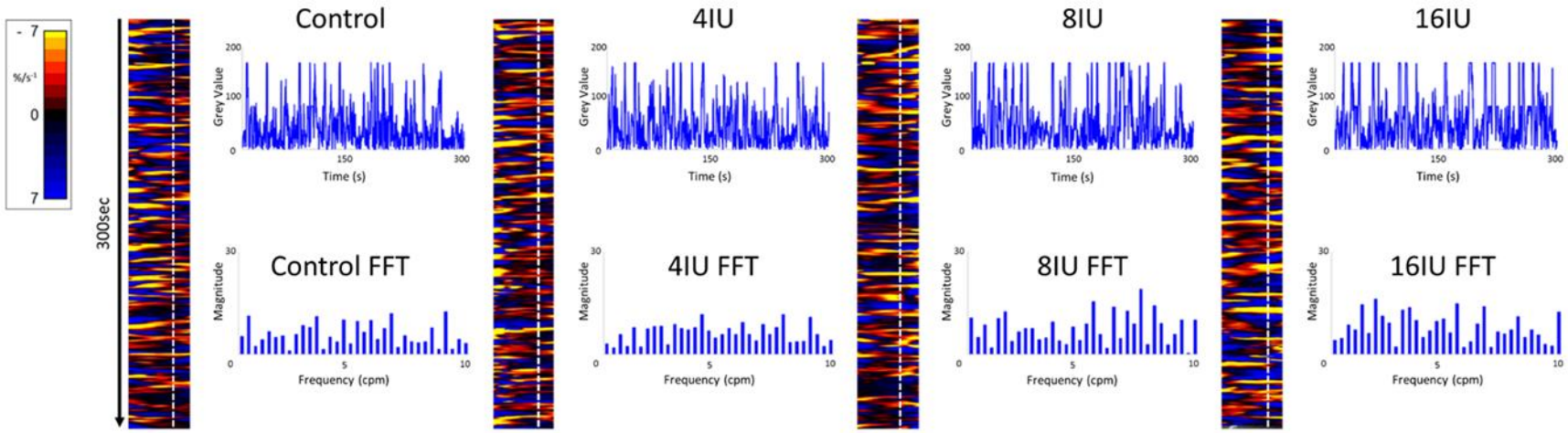

Figure 7-1 Unidimensional plots of temporal and positional variation in area strain rate, vertical transects, and their fast Fourier transforms before and following IV administration of increasing doses of oxytocin from a rabbit uterus at day 18 of gestation.

7.4.2 Late gestation (28 days)

7.4.2.1 Unidimensional plots

Unidimensional plots of variation in linear (Fig 7-4) and area (Fig 7-5) strain rate showed no evidence of spontaneous emergence in late gestation of consecutive, radially disposed, bands of circular and longitudinal contractions, such as are seen in peristalsis, either in the radial or the longitudinal transects of plots of variation in area strain rate. Similarly, there was no evidence of temporal or spatial coordination after increasing doses of oxytocin (Fig 7-5). Thus, localised longitudinal and circular components of contractions continued to occur irregularly, and on occasion concurrently, with no evidence of temporal or regional (Fig 7-5) organisation.

At 28 days gestation the mean frequency of contractions was significantly increased, and the durations significantly reduced, on one-way ANOVA compared with those at 18-21 days gestation (Fig. 7-3A and B) (Table 2).

Conversely, increasing IV doses of oxytocin (from 8 to 16 IU) caused local contractions to become grouped into broader, more regular, composite bands of significantly longer duration and lower frequency on one-way ANOVA (Figs 7-3, 4, 5) (Table 2). The changes in mean frequency were also reflected in the fast Fourier transforms of the vertical transects of the unidimensional maps of variation in area strain rate, by an increase in the lower frequencies around 10 cpm (Fig 7-5). There was also an increasing tendency for the composite burst contractions to propagate proximally rather than distally and to propagate across the entire length of the unidimensional plot (Fig 41).

Unidimensional area strain rate plots taken with LOIs traversing two successive foetuses and spanning the region between the two (Fig 7-6), showed that on occasion, composite contractions propagated from the wall that overlay one foetus onto the wall overlying the neighbouring foetus. However, the bulk of the data showed no consistent correlation of the activities in the two sites (Fig 7-6).

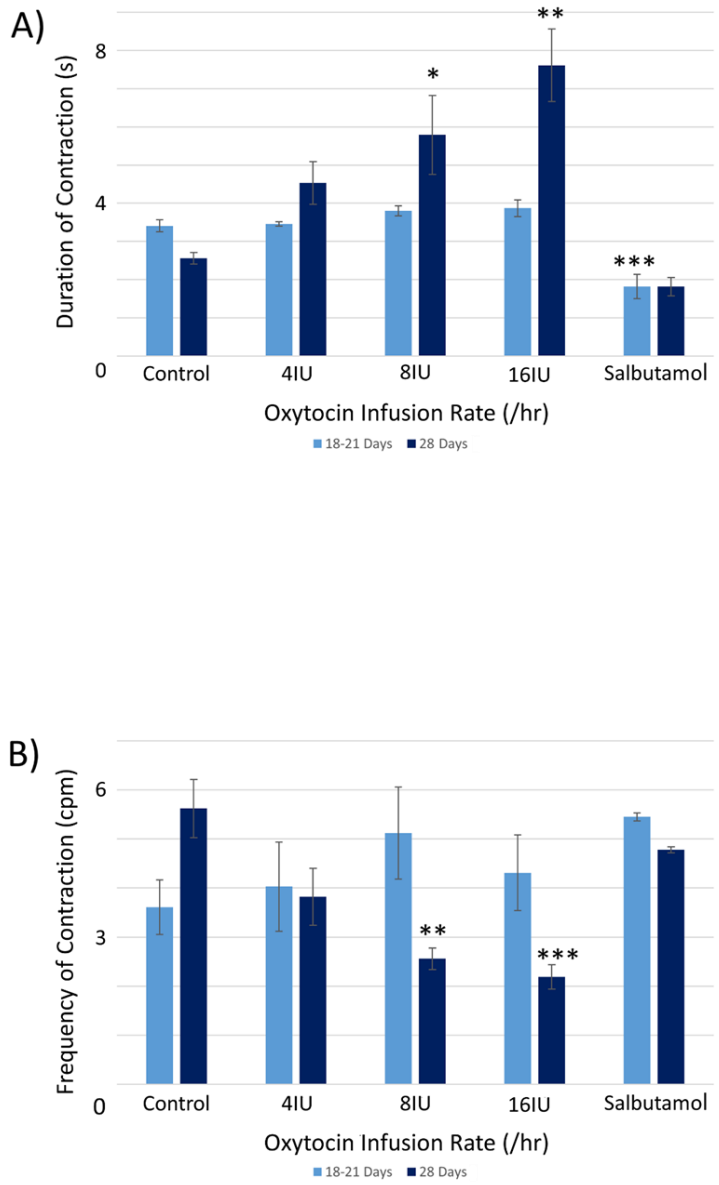

Figure 7-2 Effects of gestational growth, oxytocin, and salbutamol on durations (A) and frequencies (B) of uterine contractions in the gravid rabbit at 18-21 days and at 28 days on parameters derived from unidimensional VSTM.

Differences from control on repeated measures ANOVA following dosage with IV oxytocin; *$p < 0.05$, **$p < 0.01$, ***$p < 0.001$.

A)

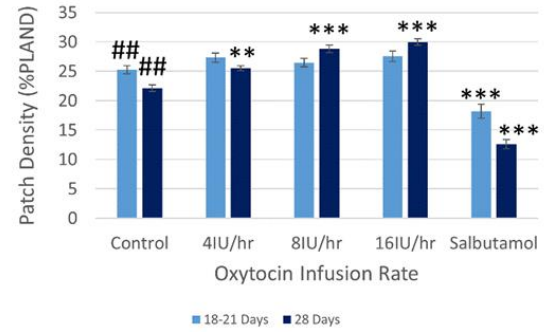
Patch Density (%PLAND)
35
30
25
20
15
10
5
0
##
##
**
***
***
***
***
Control
4IU/hr
8IU/hr
16IU/hr
Salbutamol
Oxytocin Infusion Rate
18-21 Days
28 Days

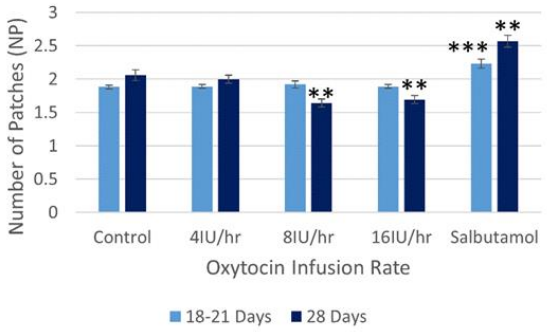
Number of Patches (NP)
3
2.5
2
1.5
1
0.5
0
**
**
***
**
Control
4IU/hr
8IU/hr
16IU/hr
Salbutamol
Oxytocin Infusion Rate
18-21 Days
28 Days

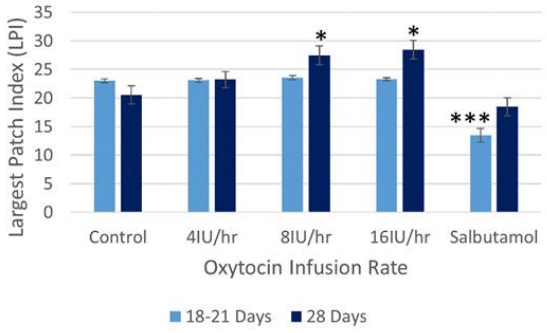
Largest Patch Index (LPI)
35
30
25
20
15
10
5
0
*
*
***
Control
4IU/hr
8IU/hr
16IU/hr
Salbutamol
Oxytocin Infusion Rate
18-21 Days
28 Days

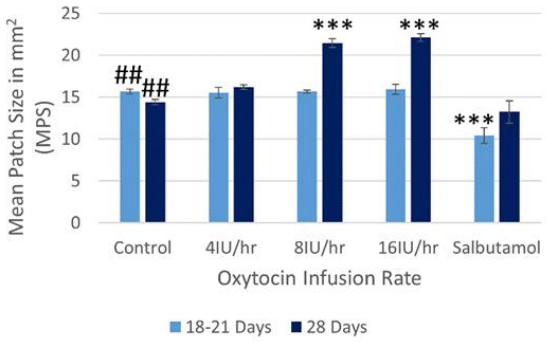
Mean Patch Size in mm²
(MPS)
25
20
15
10
5
0
##
##
***
***
***
Control
4IU/hr
8IU/hr
16IU/hr
Salbutamol
Oxytocin Infusion Rate
18-21 Days
28 Days

B)

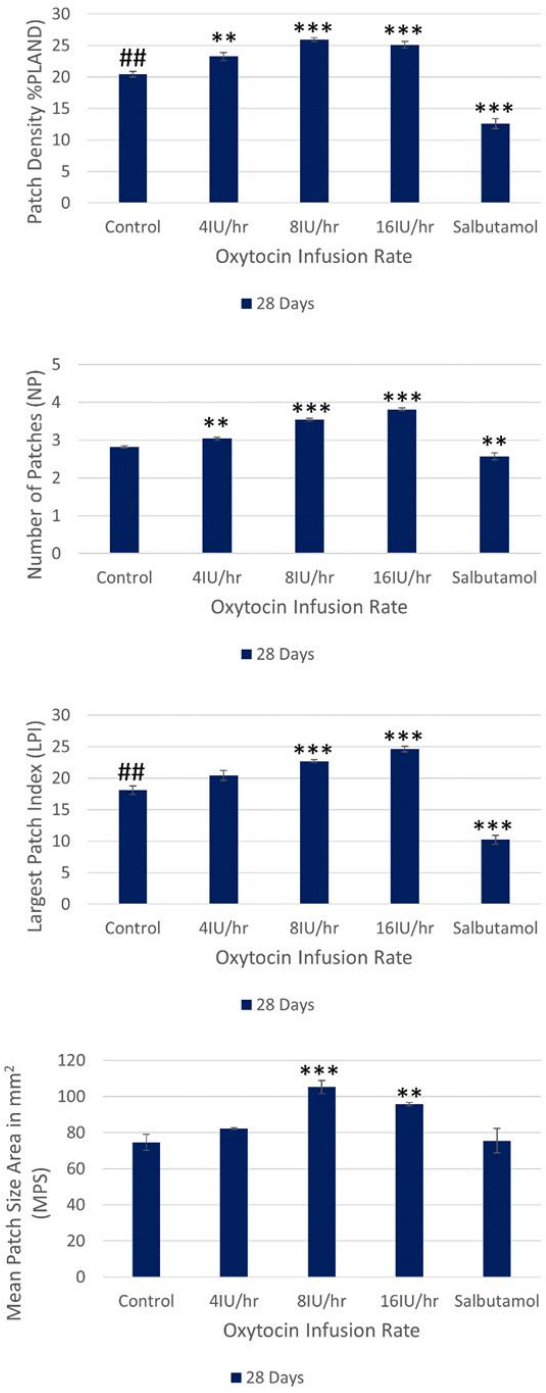

Figure 7-3 Effects of gestational growth, oxytocin and salbutamol on parameters derived from two dimensional VSTMs of the gravid rabbit uterus using A) an ellipse of 110mm2 at 18-21 days and at 28 days and B) an ellipse of vs 695mm2 at 28 days only.

Differences from control on repeated measures ANOVA following dosage with IV oxytocin; *p< 0.05, **p <0.01, ***p < 0.001. Differences between controls on one-way ANOVA; ## p < 0.02.

7.4.2.2 Two dimensional plots

The same spontaneous short-lived contractile activity occurred in pleomorphic patches at all sites on the uterine cornua in all rabbits of 28 days gestation (Fig 7-7A) (Video 1 and 2) as did at 18-21 days gestation (Supplementary Data 2). When the patterns of spontaneous contractile activity in the controls at 28 days gestation were compared with those at 18-21 days gestation, using an ellipsoid mask of identical size (110 mm^2) there were no significant differences either in the number of patches or areas of largest patches (LPI) (Fig. 39A) (Table 3A). Again, with the smaller mask, both the densities of contraction (%PLAND) and mean patch size (MPS) were significantly lower on ANOVA at 28 days gestation than at 18-21 days gestation (Fig.7-3A) (Table 3A). However, the values for MPS were significantly greater when contraction data obtained with the (larger) 695 mm^2 ellipse taken at 28 days gestation was compared with the data from the (smaller) 110mm^2 ellipse taken at 18-21 days (Fig. 7-3B) (Table 3B), indicating that patch size increased with the uterine enlargement, but there was not a significant decrease in contraction density (%PLAND).

Whilst none of these parameters changed significantly after treatment with increasing doses of oxytocin at 18-21 days gestation, they increased significantly following dosage at 28 days gestation (Fig 7-3B) (Video 2) (Table 3B). Hence, there was a significant increase in the contraction density (%PLAND) on repeated measures ANOVA within the 695 mm^2 ellipses in rabbits of 28 days gestation ($p<0.05$, df 3,9, $f = 18.46$) (Fig 7-4) (Table 3B). Similarly, there were significant increases on repeated measures ANOVA in the largest patch index and in MPS (Fig 7-3B) (Table 3B). Similar results were obtained with data from the smaller mask size (110 mm^2) (Fig 7-3A) (Table 3A).

7.4.3 Effects of salbutamol after oxytocin

Addition of salbutamol directly to the organ bath superperfusate, to a concentration of 174 nmol/L, following treatment with increasing doses of oxytocin at 20 days caused the contractions to fragment into their short-

lived, component, individual micro-contractions (Figs. 7-2, 7-3 and Supplementary Data 3) (Tables 2 and 3) with corresponding reduction in their duration and distance of propagation despite the lack of effect of oxytocin.

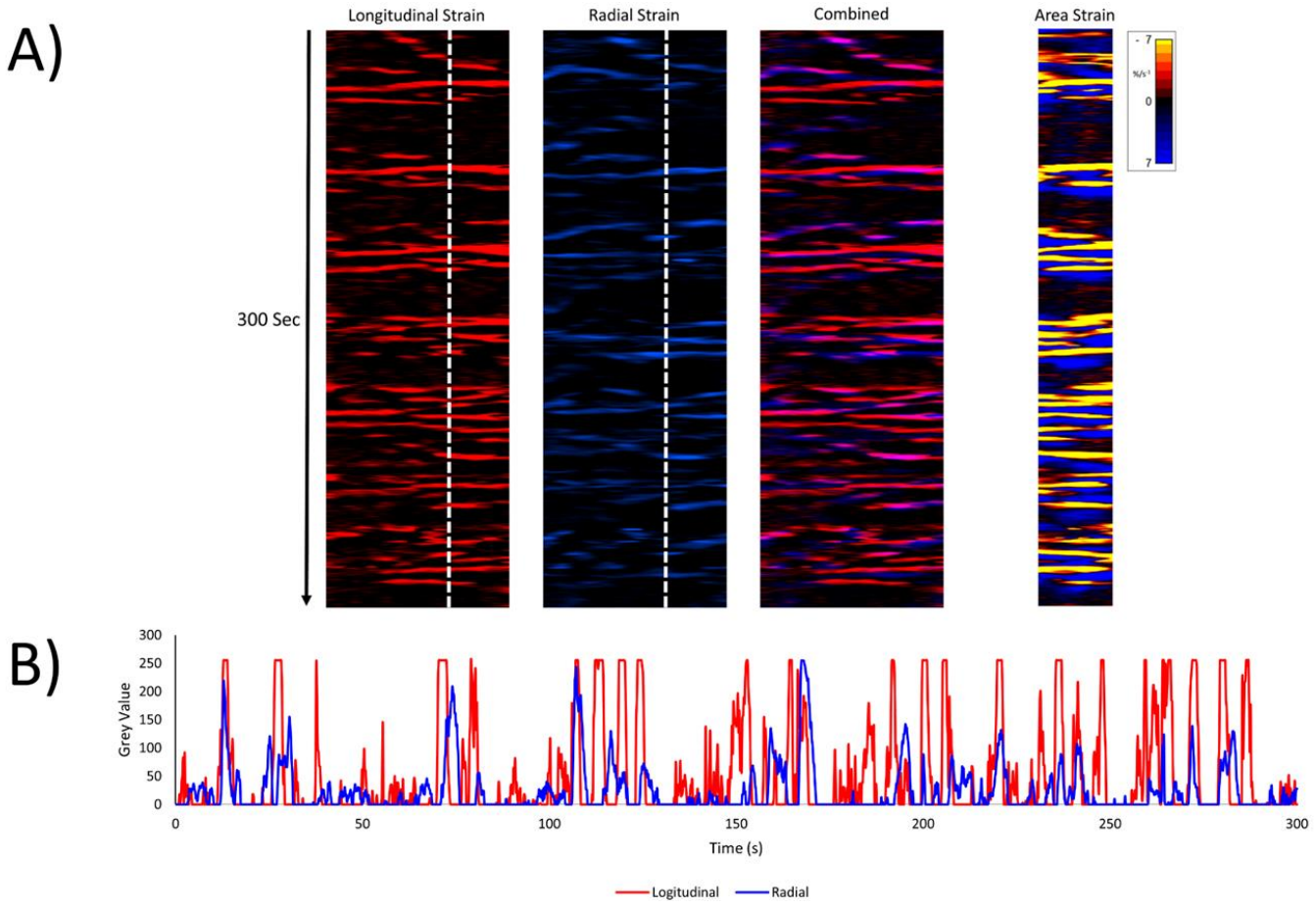

Figure 7-4 Component unidimensional plots of radial and longitudinal strain rate and area strain rate in the cornua of a rabbit uterus at 28 days of gestation.

Consecutive columns in (A) are concurrent. The plots of linear strain rate in the longitudinal (red) (1st column) and radial (blue) (2nd column) direction, the overlay of the two (with longitudinal shown as pink) (3rd column) and the concurrent map of area strain rate plot (4th column) show no tendency to form consistent sequences contraction. Superimposition of plots from vertical transects of first and second columns (B) demonstrates the lack of synergy between contractions in radially and longitudinally orientated smooth muscle.

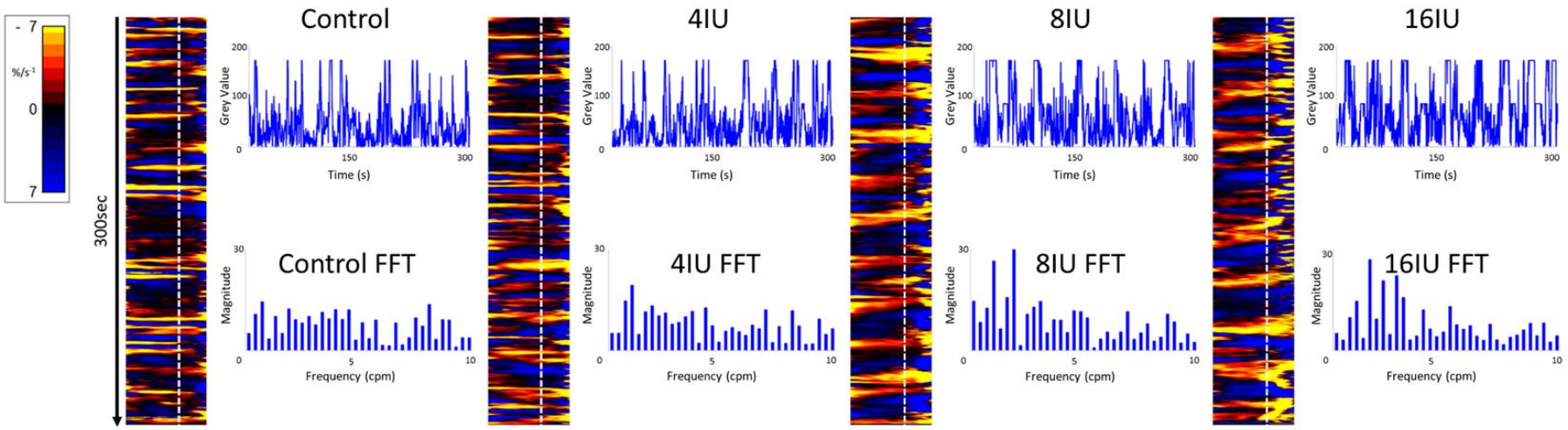

Figure 7-5 Unidimensional plots of variation in area strain rate, their vertical transects, and fast Fourier transforms of contractile activity in a uterine cornua of a gravid rabbit of 28 days gestation, before and following increasing intravenous doses (4, 8 and 16 IU) of oxytocin.

Note the increase in duration and decrease in predominant frequencies at the higher doses of oxytocin.

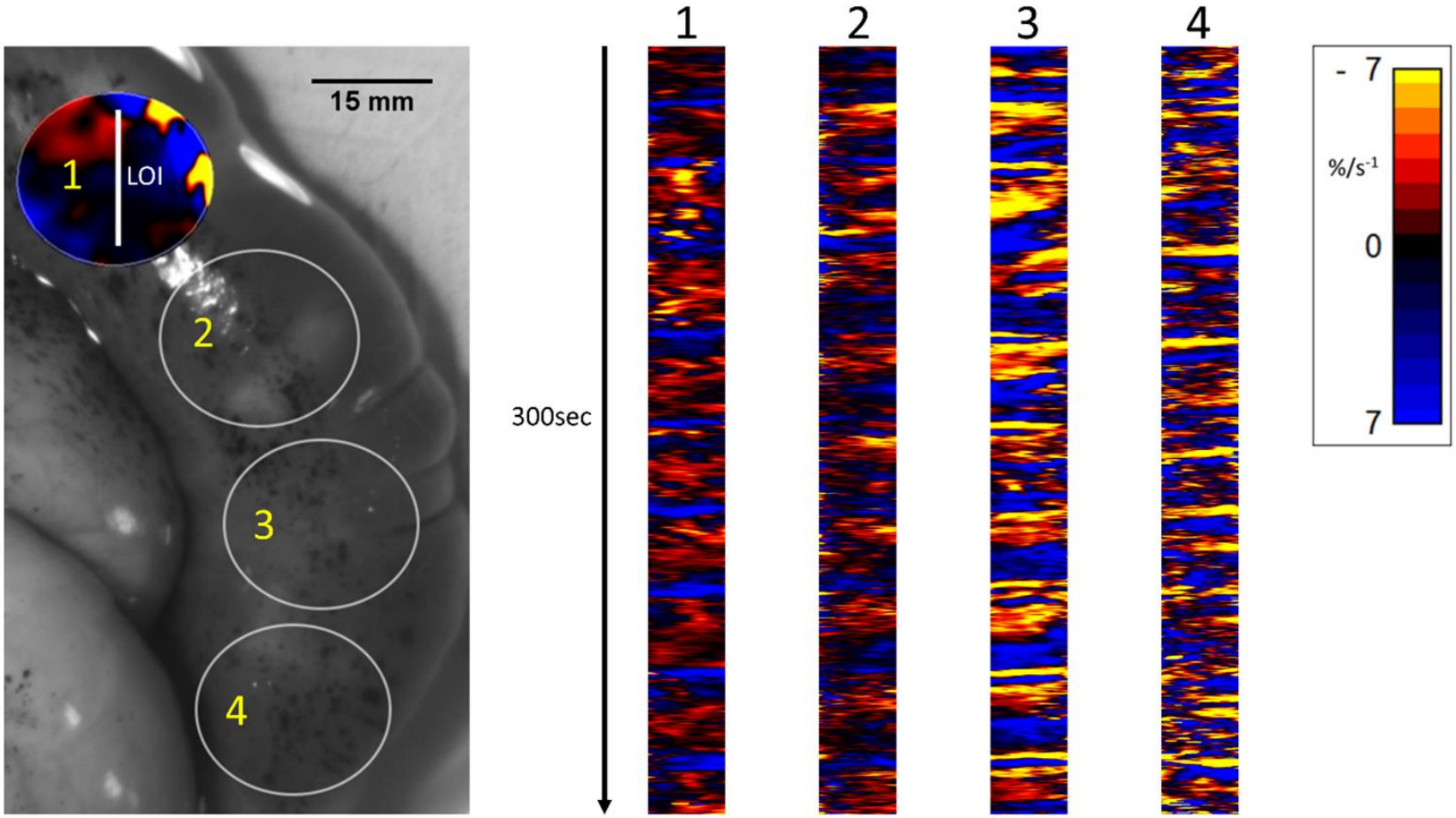

Figure 7-6 Temporal sequence of unidimensional maps showing variation in area strain rate from contractile activity in adjacent foetuses in a rabbit uterine cornua of day 28 gestation, following intravenous administration of 16 IU oxytocin.

The circles (right) represent the sites of VSTM sampling for L Maps (Left) site 1 overlies the distal pole of the first foetus in the cornua, site 2 the interval between the foetuses (distended with displaced amniotic fluid), site 3 the proximal pole of the next foetus and site 4 the distal pole of that foetus.

Hence there were significant reductions on ANOVA in duration (F (4, 15) = 17.77, p = 0.004) %PLAND (F (4, 15) = 19.72, p = 0.0003), largest patch index (LPI) (F (4, 15) = 49.14, p = 0.0005) and the number of patches (F(4, 15) = 11.22, p = 0.0005) and compared to those after dosage with oxytocin.

Addition of salbutamol directly to the organ bath superperfusate, to a concentration of 174 nmol/L, following treatment with increasing doses of oxytocin at 28 days caused the relatively prolonged contractions of lower frequency and longer duration that formed after dosage with oxytocin to fragment into their short-lived, component, individual micro-contractions (Figs 7-2, 7-3 and Supplementary Data 3) (Tables 2 and 3) with corresponding reductions in their duration and distance of propagation. Hence there were significant reductions on ANOVA in duration (F (4, 15) = 22.28, p = 0.002) and %PLAND (F (4, 15) = 130.02, p = 0.0005) and number of patches (F (4, 15) = 27.37, p = 0.0005) and compared to those after dosage with oxytocin. Hence, salbutamol had similar effects after dosage with oxytocin regardless of gestational age and the lack of any significant effects of oxytocin at 20 days gestation.

7.4.4 Electrophysiology

The electrophysiological recordings taken at sites adjacent to those of VSTM (a total of four rabbits) had overall frequencies of burst type events that were of a similar order of magnitude to those of micro-contractions with a similar relative increase following dosage with IV oxytocin (Supplementary Data 4). Hence the mean frequencies during control periods (N=4) were 1.72 ± 0.86 Hz, that following 4 IU of oxytocin was 2.39 ± 1.20 Hz, that following 8 IU was 2.75 ± 1.37 Hz and that following 16 IU was 3.48 ± 1.74 Hz. Likewise, the frequencies in these recordings decreased to 0.51 ± 0.29 Hz following addition of salbutamol.

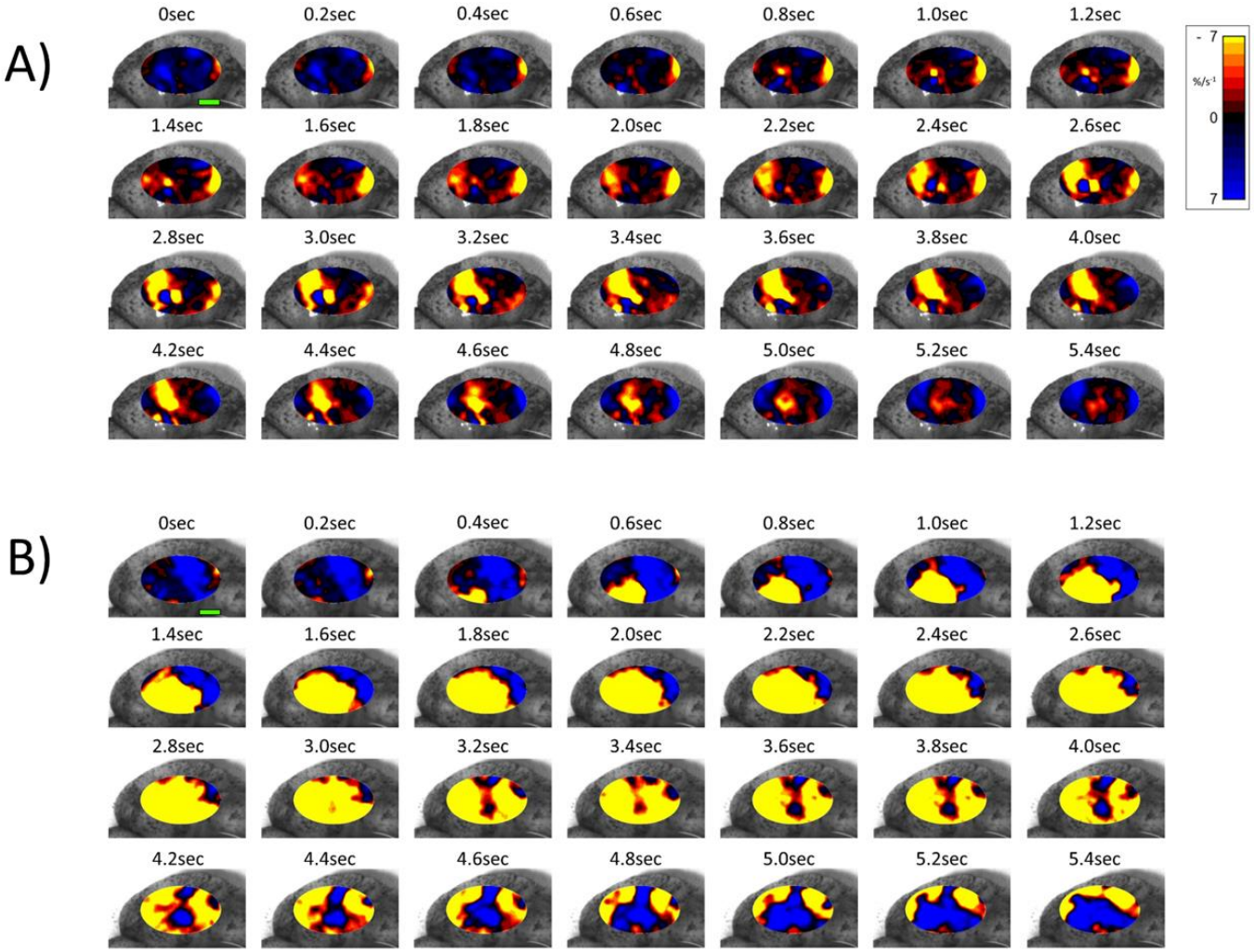

Figure 7-7 Temporal sequence of two-dimensional maps showing changes in area strain rate from spontaneous contractions in a representative rabbit uterus at 28 days gestation before (A) and after dosage with oxytocin (B) overlaid onto the anterior surface of the uterus.

Decrease in size from active contraction shown as red (high) and yellow (medium) levels of negative strain rate with stasis or relaxation shown in blue. Green Scale bar at time 0 sec of each contractile sequence represents 10 mm.

7.5 Discussion

This is the first study to use one and two-dimensional VSTM to directly quantify the location and timing of uterine contractile activity at different stages of gestation and in response to oxytocin and salbutamol. The results provide new insights into gestational changes in the mechanics of myometrial contraction as well as providing reciprocal illumination regarding the results of existing electrophysiological studies (Wim JEP Lammers, 2013).

Hence, our work shows that ongoing, spontaneous, pleomorphic, localised patches of contraction occurred on an ongoing basis at sites that were distributed across the entire surface of the uterus throughout the middle and later stages of pregnancy. Further, that their overall frequency increased, and duration decreased with increase in length of gestation whilst their frequency decreased, and their duration increased following the administration of oxytocin. Whilst this finding fits in with prior electrophysiological work (W Lammers et al., 2013; W. J. Lammers, 1996a; Wim JEP Lammers, 2013) and in this sense are not novel, it is important to confirm these prior findings as the validity of electrophysiological evidence has recently been called into question. Hence, it was hypothesised that the results of multi-electrode studies in the gastric body and antrum were an epiphenomenon that resulted from the relative movements of electrodes relative to the tissue during its contraction (O. Bayguinov et al., 2011; Rhee et al., 2011). In the case of the gastric antrum, the criticism was in part refuted by concurrent spatiotemporal mapping and electrophysiological recording in the anterior surface of the antrum when myogenic contraction was pharmacologically inhibited (Angeli et al., 2013), but similar work has not until now been carried out with regard to uterine contractile activity. The ongoing nature of contractions found in this study also fits in with prior studies showing that ongoing oscillations in amniotic pressure that were associated with uterine contractions continued throughout pregnancy (H. Alvarez & Caldeyro, 1950a). Similarly, they fit in with work measuring localised changes in intra-myogenic pressure at various sites in the uterine wall (Caldeyro-Barcia & Poseiro, 1959) and with the results of a number of electrophysiological studies using multiple electrodes (Wim JEP Lammers, 2013).

The pattern of aggregation of adjacent patches of contraction and their subsequent decay by the reverse process (Fig. 7-7 & Supplementary Data 2) (Videos 1 and 2) suggests that their disposition is governed primarily by local myogenic rather than concerted neurogenic activity. This statistically supported conclusion, based on the direct quantitative spatiotemporal data, fits in with reported electro-physiological events i.e., irregular, sometimes re-entrant, patterns of propagation of excitation (Wim JEP Lammers, 2013).

The significant overall decrease in the density of patch contractions and their duration, and the increase in the frequencies of contractions with the length of gestation, together suggest that the concomitant increase in uterine size and cavity volume from smooth muscle hypertrophy (Owens & Schwartz, 1982) results in a decrease in connectivity between adjacent myocytes (Fig 7-8). This in turn causes the compliance of the uterine wall and its mechano-sensitivity to progressively decrease, allowing the uterine cavity to accommodate the growing foetus (Fig 7-8). Whilst it is possible that such accommodation could result from extrinsic neurogenic signalling, our results suggest that it is myogenic in origin (see below). This fits in with the findings that the capacity of the uterus to accommodate the growing foetus is preserved in uterine transplants in which extrinsic neural connections have necessarily been severed (Brännström et al., 2015), and the fact that no functional intrinsic neutral network has yet been identified in the uterine wall.

Given the reported increase in densities of oxytocin receptors in late pregnancy (A.-R. Fuchs et al., 1984), the tendency at late gestation for component patches of contraction to be larger, of longer duration and to propagate over greater distances after dosage with oxytocin, fit in with the electrophysiological findings that electrical connectivity between myocytes increases in later pregnancy (R. Garfield, Yallampalli, Chard, & Grudzinskas, 1994) and the progressive recruitment of action potentials to form more sustained, faster moving, composite bursts of contractions (Caldeyro-Barcia & Alvarez, 1952; WJ Lammers, Arafat, el-Kays, & el-Sharkawy, 1994; W. J. Lammers, 1996a; J. M. Marshall, 1962a) (Video 2).

The finding that contractions that originate at sites on the uterine wall which overlie one foetus may on occasion propagate to neighbouring foetuses, indicates the extent of such increased connectivity and mitigates

against a hypothesis of a single localised peri-placental origin of excitation (W Lammers et al., 2013) i.e., pacemaker in this species.

Together the findings regarding the spatiotemporal distribution of uterine contractions after the administration of increasing doses of oxytocin render it unlikely that the reorganisation of contractile activity during late gestation could induce concerted direct distal-ward propulsion of a contained foetus and thus could be classified as peristaltic. Hence, uterine contractile activity in late gestation continued to consist of pleomorphic patches that were randomly distributed across the surface of the uterus around and overlying each foetus, did not form distally progressing bands, and did not comprise synchronous separate longitudinal and circumferential patches of contraction such as have been reported in peristalsis (N. J. Spencer, M. Walsh, & T. K. Smith, 1999) (Fig. 7-6). Further, the overall trend of direction of propagation of patches was from distal to proximal, rather than from proximal to distal. It is therefore more likely that late gestational reorganisation progressively reduces the mean compliance of the uterine walls and thus promotes expulsion by volumetric reduction. The lack of any consistent site of origin of contractions, notably in regions adjacent to the placenta (Lutton et al., 2018b) suggests that under our experimental conditions, where the uterus was maintained *in situ*, there was no pacemaker induced coordination of contractile activity. The trend of distal to proximal progression of patches of contraction possibly results from uterine smooth muscle being drawn from the proximal pole of each foetus toward the distal pole.

The reorganisation of smaller individual patches of uterine contraction into larger, more numerous, pleomorphic propagating patches of lower frequency and longer duration following dosage with oxytocin at 28 weeks gestation is similar to the changes that occur in the isolated urinary bladder following administration of cholinergic agents and promotes expulsion of urine (Corrin Murray Hulls, Lentle, King, Chambers, & Reynolds, 2019; Lentle et al., 2015b). Hence, in both cases it appears that the changes in the patterns of contraction accompany a change in function from accommodation to expulsion and may involve a local resetting of myogenic connectivity, although that of the bladder occurs more promptly than that of the uterus.

The effect of salbutamol in reducing the duration and overall distance of propagation of composite contractions and inducing their fragmentation into component individual contractions regardless of the length of gestation, fits in with its reported pharmacological action in reducing the excitability of myocytes via the generation of cAMP (Hajagos-Tóth, Falkay, & Gáspár, 2009; Zingg & Laporte, 2003) and the connectivity of myocytic tight junctions (Ou, Orsino, & Lye, 1997). Whilst it is possible that it could act to reduce the excitability of intermediary cells such as interstitial cajal-like cells, their reported electro-physiological characteristics do not fit in with such a role (Duquette et al., 2005). The overall effects of salbutamol in reducing the overall incidence of contractions and hence overall uterine tone are in line with the reported effects on general contraction (Abel & Hollingsworth, 1986) and cavity pressure (Abel & Hollingsworth, 1985) in the intact uterus of the rat.

Apart from providing a greater understanding of uterine function, the reciprocal changes in the frequency duration, area and density of uterine contractions that were found to occur with increasing gestation, and following dosage with oxytocin at 28 days, may provide a useful means for identifying the switching of uterine function from accommodation to expulsion, although further work is needed to confirm that similar changes occur in human subjects. Again, the demonstration that the VSTM methodology is able to directly quantify changes in the development and disposition of uterine contractions in the rabbit preparation following administration of pharmaceuticals lays the ground for statistically based assays of other agents that influence myometrial contractility at various stages of uterine function.

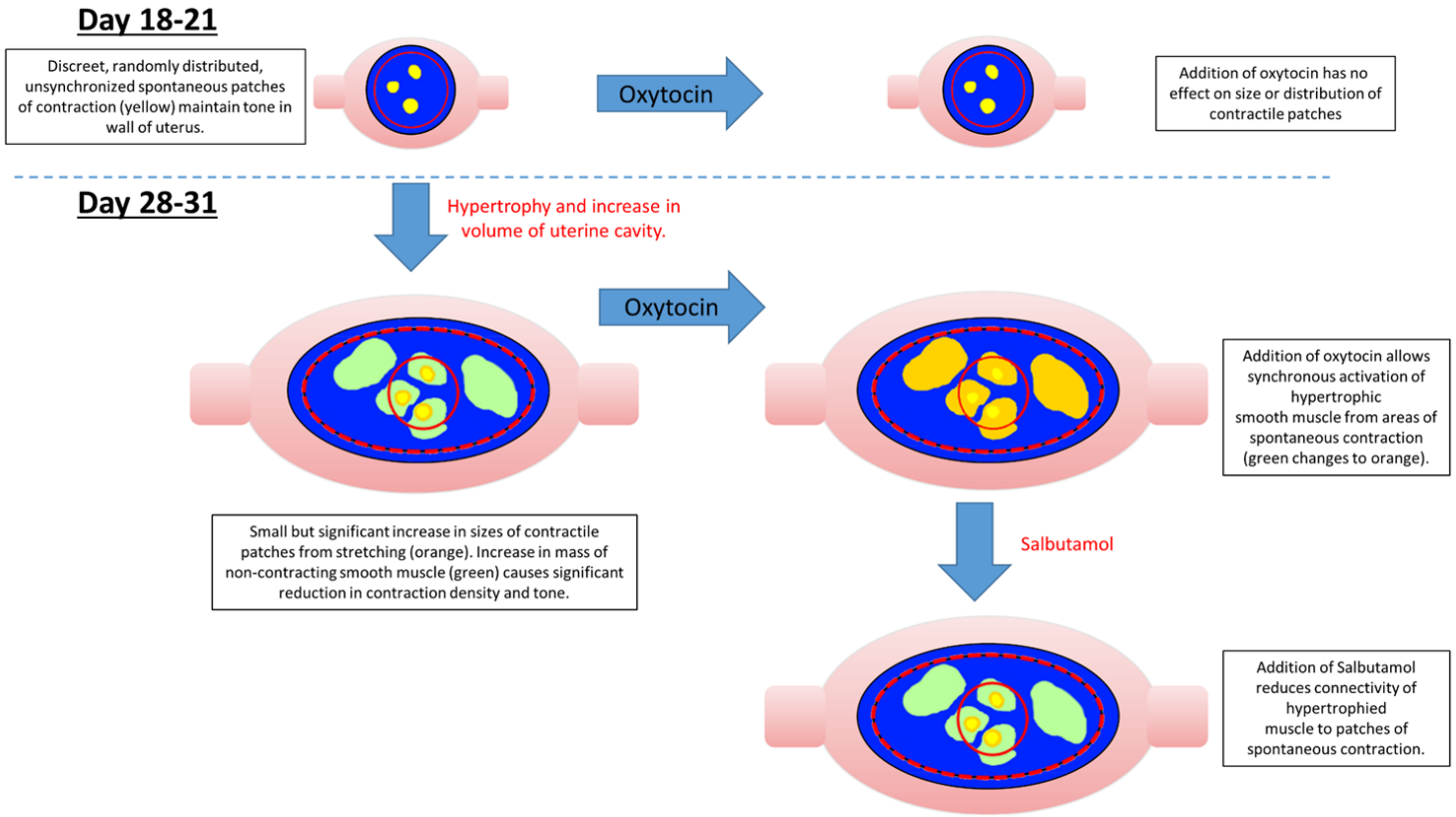

Figure 7-8 Possible mechanism for variation in the distribution, size and number of spontaneous uterine contractions in the gravid uterus rabbit with gestation, oxytocin, and salbutamol.

References

Abel, M. H., & Hollingsworth, M. (1985). The potencies and selectivities of four calcium antagonists as inhibitors of uterine contractions in the rat in vivo. *British Journal of Pharmacology, 85*(1), 263-269.

Abel, M. H., & Hollingsworth, M. (1986). The effects of long-term infusion of salbutamol, diltiazem and nifedipine on uterine contractions in the ovariectomized, post-partum rat. *British Journal of Pharmacology, 88*(3), 577-584.

Alvarez, H., & Caldeyro, R. (1950). Contractility of the human uterus recorded by new methods. *Surgery Gynecology and Obstetrics, 91*(1), 1-13.

Angeli, T. R., Du, P., Paskaranandavadivel, N., Janssen, P. W., Beyder, A., Lentle, R. G., . . . O'Grady, G. (2013). The bioelectrical basis and validity of gastrointestinal extracellular slow wave recordings. *The Journal of Physiology, 591*(18), 4567-4579.

Azhari, H., Weiss, J. L., Rogers, W. J., Siu, C. O., & Shapiro, E. P. (1995). A noninvasive comparative study of myocardial strains in ischemic canine hearts using tagged MRI in 3-D. *American Journal of Physiology, 268*(5), H1918-1926.

Bayguinov, O., Hennig, G., & Sanders, K. (2011). Movement based artifacts may contaminate extracellular electrical recordings from GI muscles. *Neurogastroenterology and Motility, 23*(11), 1029-e1498.

Brännström, M., Johannesson, L., Bokström, H., Kvarnström, N., Mölne, J., Dahm-Kähler, P., . . . Diaz-Garcia, C. (2015). Livebirth after uterus transplantation. *The Lancet, 385*(9968), 607-616.

Bulletti, C., de Ziegler, D., Polli, V., Diotallevi, L., Ferro, E. D., & Flamigni, C. (2000). Uterine contractility during the menstrual cycle. *Human Reproduction, 15*(suppl_1), 81-89.

Caldeyro-Barcia, R., & Alvarez, H. (1952). Abnormal uterine action in labour. *J Obstet Gynaecol Br Emp, 59*, 646.

Caldeyro-Barcia, R., & Poseiro, J. J. (1959). Oxytocin and contractility of the pregnant human uterus. *Annals of the New York Academy of Sciences, 75*(2), 813-830.

Cannon, W. B. (1902). The movements of the intestines studied by means of the Röntgen rays. *American Journal of Physiology, 6*(5), 251-277.

Cannon, W. B. (1911). *The mechanical factors of digestion*. London: Edward Arnold.

Csapo, A. I., Jaffin, H., Kerenyi, T., Lipman, J. I., & Wood, C. (1963). Volume and activity of the pregnant human uterus. *American Journal of Obstetrics and Gynecology, 85*(6), 819-835.

Daniel, E. E. (1960). Effect of the placenta on the electrical activity of the cat uterus in vivo and in vitro. *American Journal of Obstetrics and Gynecology, 80*(2), 229-244.

Duquette, R., Shmygol, A., Vaillant, C., Mobasheri, A., Pope, M., Burdyga, T., & Wray, S. (2005). Vimentin-positive, c-kit-negative interstitial cells in human and rat uterus: a role in pacemaking? *Biology of reproduction, 72*(2), 276-283.

Evans, H., & Sack, W. O. (1973). Prenatal development of domestic and laboratory mammals: growth curves, external features and selected references. *Anatomia, Histologia, Embryologia, 2*(1), 11-45.

Eytan, O., Jaffa, A. J., Har-Toov, J., Dalach, E., & Elad, D. (1999). Dynamics of the intrauterine fluid–wall interface. *Annals of Biomedical Engineering, 27*(3), 372-379.

Fisk, N., Ronderos-Dumit, D., Tannirandorn, Y., Nicolini, U., Talbert, D., & Rodeck, C. (1992). Normal amniotic pressure throughout gestation. *BJOG: An International Journal of Obstetrics & Gynaecology, 99*(1), 18-22.

Fuchs, A.-R., Fuchs, F., Husslein, P., & Soloff, M. S. (1984). Oxytocin receptors in the human uterus during pregnancy and parturition. *American Journal of Obstetrics and Gynecology, 150*(6), 734-741.

Garfield, R., & Yallampalli, C. (1994). Structure and function of uterine muscle. *The uterus*, 54-93.

Garfield, R. E., & Maner, W. L. (2007). *Physiology and electrical activity of uterine contractions.* Paper presented at the Seminars in Cell and Developmental Biology.

Geirsson, R., Ogston, S., Patel, N., & Christie, A. (1985). Growth of total intrauterine, intra-amniotic and placental volume in normal singleton pregnancy measured by ultrasound. *BJOG: An International Journal of Obstetrics & Gynaecology, 92*(1), 46-53.

Hajagos-Tóth, J., Falkay, G., & Gáspár, R. (2009). Modification of the effect of nifedipine in the pregnant rat myometrium: the influence of progesterone and terbutaline. *Life Sciences, 85*(15-16), 568-572.

Hulls, C. M., Lentle, R. G., King, Q. M., Chambers, J. P., & Reynolds, G. W. (2019). Pharmacological modulation of the spatiotemporal disposition of micromotions in the intact resting urinary bladder of the rabbit; their pattern is under both myogenic and autonomic control. *BJU International*

Hulls, C. M., Lentle, R. G., King, Q. M., Reynolds, G. W., & Chambers, J. (2017). Spatiotemporal analysis of spontaneous myogenic contractions in the urinary bladder of the rabbit: timing and patterns reflect reported electrophysiology. *American Journal of Physiology-Renal Physiology, 313*(3), F687-F698.

Huszar, G., & Naftolin, F. (1984). The myometrium and uterine cervix in normal and preterm labor. *New England Journal of Medicine, 311*(9), 571-581.

Hutchings, G., Williams, O., Cretoiu, D., & Ciontea, S. M. (2009). Myometrial interstitial cells and the coordination of myometrial contractility. *Journal of Cellular and Molecular Medicine, 13*(10), 4268-4282.

Kelly, J. V. (1962). Myometrial Participation in Human Sperm Transport: A Dilemma. *Fertility and Sterility, 13*(1), 84-92. 10.1016/S0015-0282(16)34387-4

Lambert, F., Pelletier, G., Dufour, M., & Fortier, M. (1990). Specific properties of smooth muscle cells from different layers of rabbit myometrium. *American Journal of Physiology-Cell Physiology, 258*(5), C794-C802.

Lammers, W., Arafat, K., el-Kays, A., & el-Sharkawy, T. Y. (1994). Spatial and temporal variations in local spike propagation in the myometrium of the 17-day pregnant rat. *American Journal of Physiology-Cell Physiology, 267*(5), C1210-C1223.

Lammers, W., Morrison, J., Lubbad, L., Stephen, B., & Hammad, F. (2013). *Electrical propagation in the guinea pig urinary bladder.* Paper presented at the Proceedings of The Physiological Society.

Lammers, W. J. (1996). Circulating excitations and re-entry in the pregnant uterus. *Pflügers Archiv European Journal of Physiology, 433*(3), 287-293.

Lammers, W. J. (2013). The electrical activities of the uterus during pregnancy. *Reproductive Sciences, 20*(2), 182-189.

Lammers, W. J., Mirghani, H., Stephen, B., Dhanasekaran, S., Wahab, A., Al Sultan, M. A., & Abazer, F. (2008). Patterns of electrical propagation in the intact pregnant guinea pig uterus. *American Journal of Physiology-Regulatory, Integrative and Comparative Physiology, 294*(3), R919-R928.

Lentle, R. G., Reynolds, G. W., Hulls, C. M., & Chambers, J. (2016). Advanced spatiotemporal mapping methods give new insights into the coordination of contractile activity in the stomach of the rat. *American Journal of Physiology-Gastrointestinal and Liver Physiology*, ajpgi. 00308.02016.

Lentle, R. G., Reynolds, G. W., Janssen, P. W. M., Hulls, C. M., King, Q. M., & Chambers, J. (2015). Characterisation of the contractile dynamics of the resting ex vivo urinary bladder of the pig. *BJU International, 116*(6), 973-983.

Leyendecker, G., Kunz, G., Herbertz, M., Beil, D., Huppert, P., Mall, G., . . . Wildt, L. (2004). Uterine peristaltic activity and the development of endometriosis. *Annals of the New York Academy of Sciences, 1034*(1), 338-355.

Lutton, E. J., Lammers, W. J., James, S., van den Berg, H. A., & Blanks, A. M. (2018). Identification of uterine pacemaker regions at the myometrial–placental interface in the rat. *The Journal of Physiology*

Marshall, J. M. (1962). Regulation of activity in uterine smooth muscle. *Physiological Reviews, 42*, 213-227.

McDevitt, D., Wallace, R., Roberts, A., & Whitfield, C. (1975). The uterine and cardiovascular effects of salbutamol and practolol during labour. *BJOG: An International Journal of Obstetrics & Gynaecology, 82*(6), 442-448.

McGarigal, K., Cushman, S., & Ene, E. (2012). FRAGSTATS v4: spatial pattern analysis program for categorical and continuous maps. University of Massachusetts, Amherst, Massachusetts, USA. *goo. gl/aAEbMk*

Mikkelsen, E., Johansen, P., Fuglsang-Frederiksen, A., & Uldbjerg, N. (2013). Electrohysterography of labor contractions: propagation velocity and direction. *Acta Obstetricia et Gynecologica Scandinavica, 92*(9), 1070-1078.

Mironneau, J. (1976). Effects of oxytocin on ionic currents underlying rhythmic activity and contraction in uterine smooth muscle. *Pflügers Archiv, 363*(2), 113-118.

Norwitz, E. R., & Robinson, J. N. (2001). *A systematic approach to the management of preterm labor.* Paper presented at the Seminars in Perinatology.

Ou, C.-W., Orsino, A., & Lye, S. J. (1997). Expression of connexin-43 and connexin-26 in the rat myometrium during pregnancy and labor is differentially regulated by mechanical and hormonal signals. *Endocrinology, 138*(12), 5398-5407.

Owens, G. K., & Schwartz, S. M. (1982). Alterations in vascular smooth muscle mass in the spontaneously hypertensive rat. Role of cellular hypertrophy, hyperploidy, and hyperplasia. *Circulation Research, 51*(3), 280-289.

Parkington, H., Harding, R., & Sigger, J. (1988). Co-ordination of electrical activity in the myometrium of pregnant ewes. *Reproduction, 82*(2), 697-705.

Planes, J., Morucci, J., Grandjean, H., & Favretto, R. (1984). External recording and processing of fast electrical activity of the uterus in human parturition. *Medical and Biological Engineering and Computing, 22*(6), 585-591.

Rabotti, C., de Lau, H., Haazen, N., Oei, G., & Mischi, M. (2013). *Ultrasound analysis of the uterine wall movement for improved electrohysterographic measurement and modeling.* Paper presented at the Engineering in Medicine and Biology Society (EMBC), 2013 35th Annual International Conference of the IEEE.

Rabotti, C., Mischi, M., Oei, S. G., & Bergmans, J. W. (2010). Noninvasive estimation of the electrohysterographic action-potential conduction velocity. *IEEE Transactions on Biomedical Engineering, 57*(9), 2178.

Rhee, P. L., Lee, J. Y., Son, H. J., Kim, J. J., Rhee, J. C., Kim, S., . . . Ward, S. M. (2011). Analysis of Pacemaker Activity in the Human Stomach. *Journal of Physiology, 589*(24), 6105–6118.

Savitsky, A. G., Savitsky, G. A., Ivanov, D. O., Mikhailov, A. V., Kurganskiy, A. V., & Mill, K. V. (2013). The myogenic mechanism of synchronization and coordination for uterine myocytes contractions during labor. *The Journal of Maternal-Fetal & Neonatal Medicine, 26*(6), 566-570.

Setekleiv, J. (1964). Uterine motility of the estrogenized rabbit. *Acta Physiologica, 62*(1-2), 79-93.

Shelkovnikov, S., Savitskiĭ, G., & Abramchenko, V. (1986). Spontaneous contractile activity of isolated strips of uterine myometrium depending on the degree of stretching. *Fiziologiia Cheloveka, 12*(6), 1016.

Shmygol, A., Gullam, J., Blanks, A., & Thornton, S. (2006). Multiple mechanisms involved in oxytocin-induced modulation of myometrial contractility. *Acta Pharmacologica Sinica, 27*(7), 827-832.

Smith, R., Imtiaz, M., Banney, D., Paul, J. W., & Young, R. C. (2015). Why the heart is like an orchestra and the uterus is like a soccer crowd. *American Journal of Obstetrics and Gynecology, 213*(2), 181-185.

Smith, T. K., & Robertson, W. J. (1998). Synchronous movements of the longitudinal and circular muscle during peristalsis in the isolated guinea-pig distal colon. *Journal of Physiology, 506*(2), 563-577.

Spencer, N. J., Walsh, M., & Smith, T. K. (1999). Does the guinea-pig ileum obey the 'law of the intestine'? *Journal of Physiology, 517*(3), 889-898.

Takeda, H. (1965). Generation and propagation of uterine activity in situ. *Fertility and Sterility, 16*(1), 113-119.

Van Gestel, I., IJland, M., Hoogland, H., & Evers, J. (2003). Endometrial wave-like activity in the non-pregnant uterus. *Human Reproduction Update, 9*(2), 131-138.

Weiss, S., Jaermann, T., Schmid, P., Staempfli, P., Boesiger, P., Niederer, P., . . . Bajka, M. (2006). Three-dimensional fiber architecture of the nonpregnant human uterus determined ex vivo using magnetic resonance diffusion tensor imaging. *The Anatomical Record, 288*(1), 84-90.

Willets, J. M., Brighton, P. J., Mistry, R., Morris, G. E., Konje, J. C., & Challiss, R. J. (2009). Regulation of oxytocin receptor responsiveness by G protein-coupled receptor kinase 6 in human myometrial smooth muscle. *Molecular Endocrinology, 23*(8), 1272-1280.

Wray, S. (1993). Uterine contraction and physiological mechanisms of modulation. *American Journal of Physiology-Cell Physiology, 264*(1), C1-C18.

Yagel, S., Ben-Chetrit, A., Anteby, E., Zacut, D., Hochner-Celnikier, D., & Ron, M. (1992). The effect of ethinyl estradiol on endometrial thickness and uterine volume during ovulation induction by clomiphene citrate. *Fertility and Sterility, 57*(1), 33-36.

Young, R. C. (2016). Mechanotransduction mechanisms for coordinating uterine contractions in human labor. *152*(2), R51. 10.1530/rep-16-0156

Young, R. C., & Goloman, G. (2011). Mechanotransduction in rat myometrium: coordination of contractions of electrically and chemically isolated tissues. *Reproductive Sciences, 18*(1), 64-69.

Zingg, H. H., & Laporte, S. A. (2003). The oxytocin receptor. *Trends in Endocrinology & Metabolism, 14*(5), 222-227.

7.6 Supplementary Data

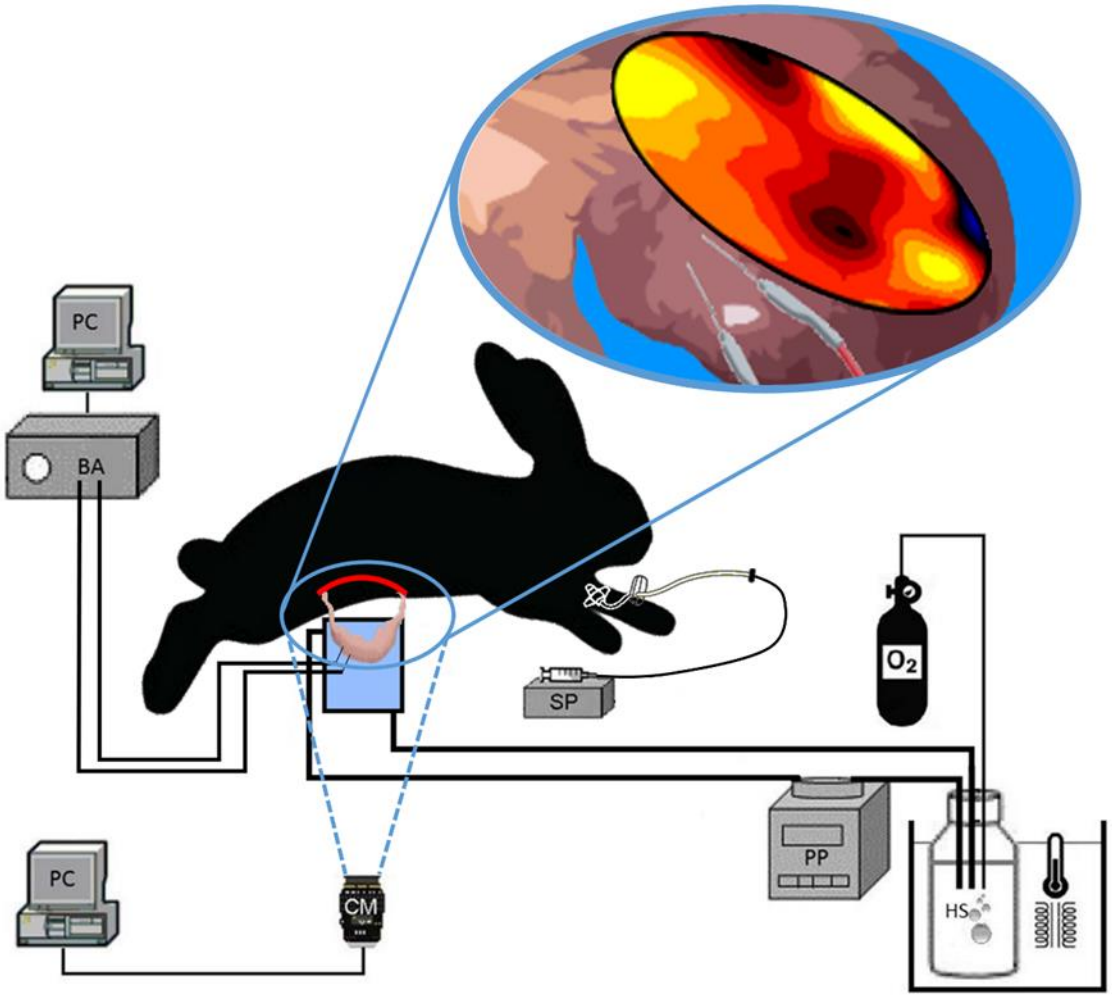

Supplementary Data 1 Experimental setup for recording VSTM in the gravid uterus of the anaesthetised rabbit.

The anterior surface of the prolapsing uterus is positioned in the organ bath with its anterior surface to the right and filmed by an appropriately positioned video camera. The elliptical mask of the VSTM covered 45% of its anterior surface. The electrophysiological electrodes were positioned just outside of the filmed area. PC, personal computer; BA, bio amplifier; CM, video camera; SP, syringe pump; PP, peristaltic pump; HS, reservoir of Earle's–HEPES solution.

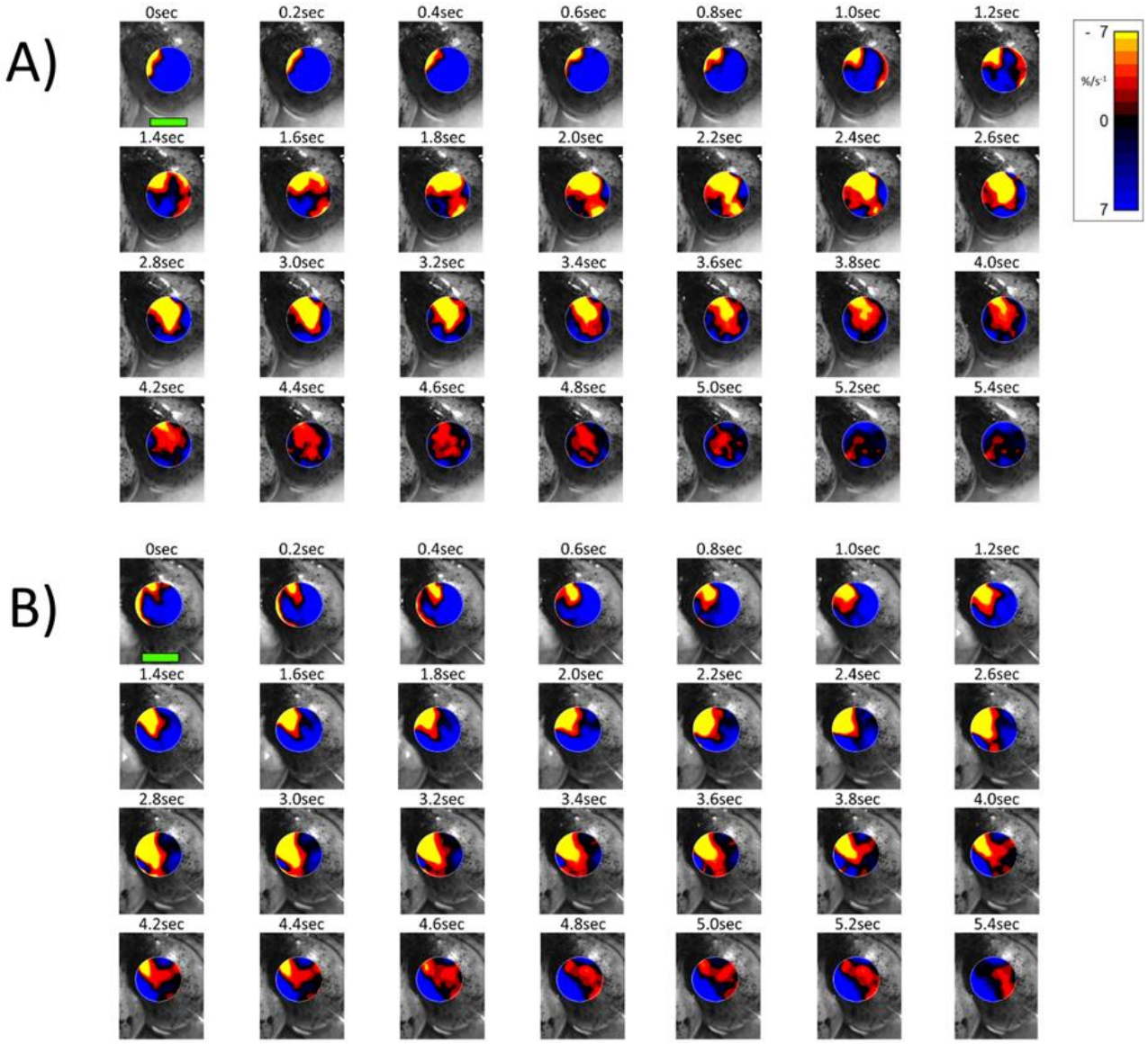

Supplementary Data 2 Temporal sequence of two-dimensional maps showing variation in area strain from spontaneous contractions in a representative rabbit uterus at 20 days gestation before (A) and after (B) dosage with 16 IU of oxytocin.

Decrease in size from active contraction shown as red (high) and yellow (medium) levels of negative strain rate with stasis or relaxation shown in blue. Green scale bar at time 0sec in each contractile sequence represents 10 mm.

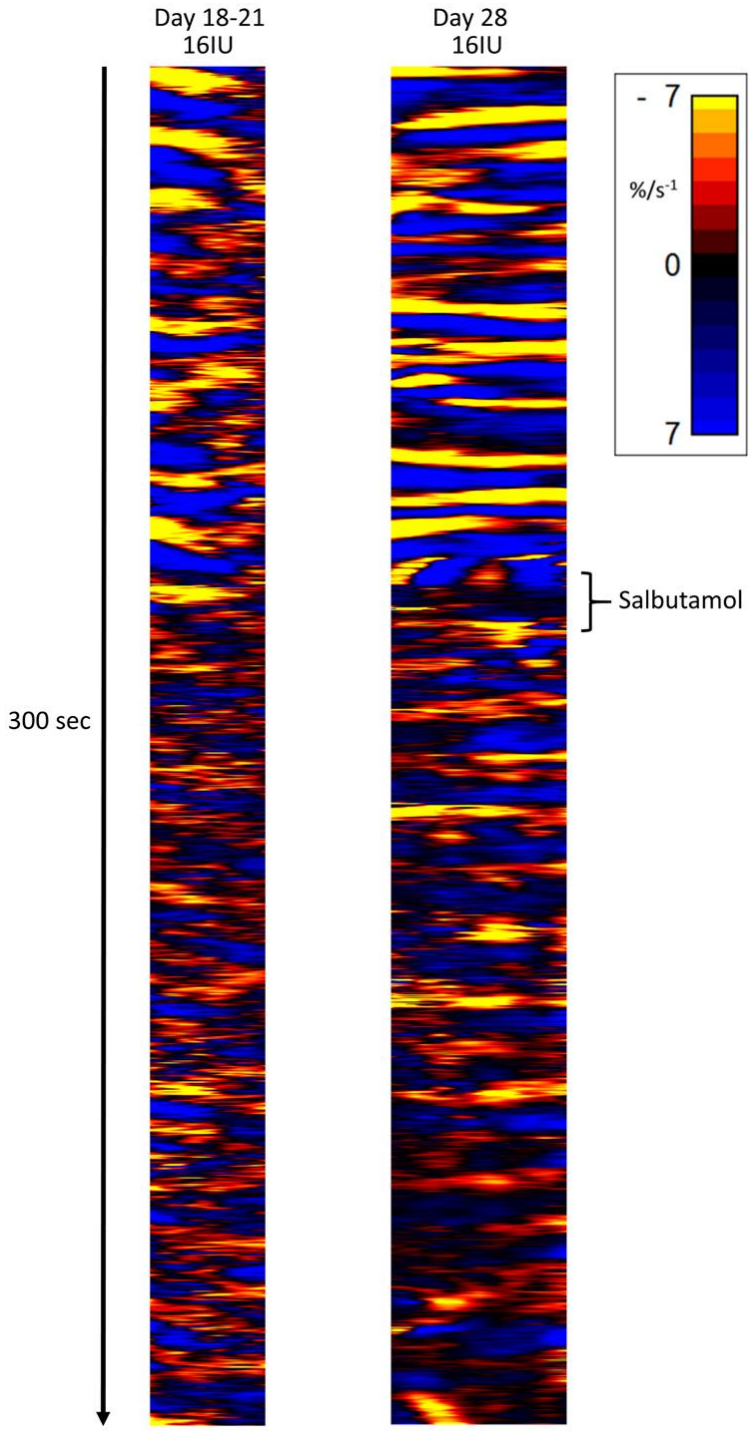

Supplementary Data 3 Temporal sequence of unidimensional maps showing variation in area strain rate from component contractions after commencement of continuing maximal dosage with oxytocin a rabbit uterus at 18-21 and 28 days gestation and subsequent dosage with salbutamol (174 nmol/L).

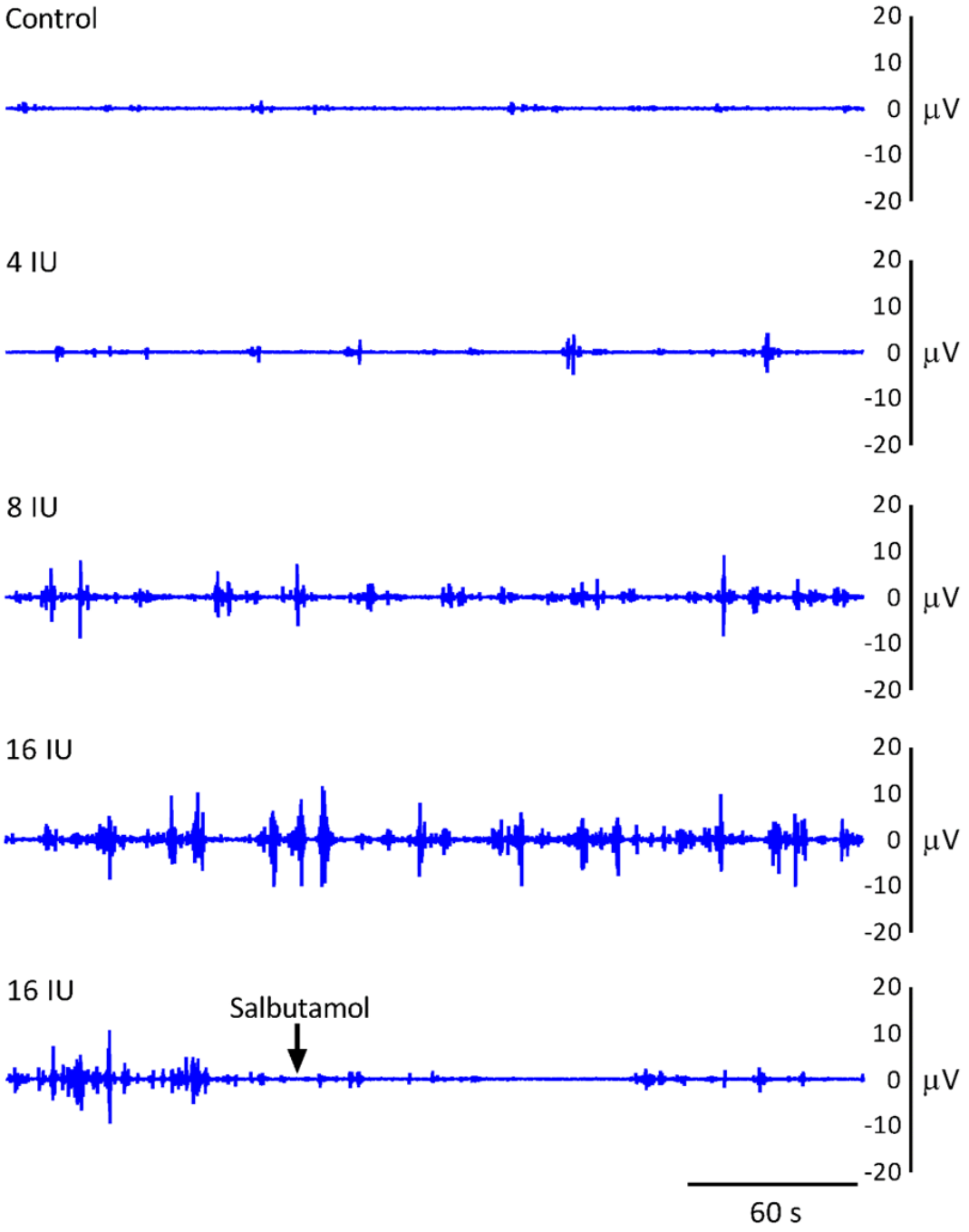

Supplementary Data 4 Temporal sequences of myoelectric activity in the wall of the gravid uterus of the rabbit taken concurrently with VSTM.

Representative tracings (300 s duration) of myoelectrical activity in the wall of the gravid rabbit uterus (28 days) of resting activity (Control), and that stimulated by IV oxytocin at various doses (4, 8, 16 IU) and reduction of activity with Salbutamol. All traces were filtered (band pass 0.2-40 Hz) for potential gross movement artefacts and line noise.

		OXYTOCIN INFUSION RATE			
Duration of Contraction (s)	Control	4 IU/hr.	8 IU/hr.	16 IU/hr.	Salbutamol
Day 18-21 of Gestation	3.4±0.16	3.46±0.06	3.80±0.13	3.87±0.22	1.82±0.32***
Day 28 of Gestation	2.56±0.15##	4.53±0.56	5.79±1.03*	7.61±0.95**	1.82±0.24

		OXYTOCIN INFUSION RATE			
Frequency of Contractions (CPM)	Control	4 IU/hr.	8 IU/hr.	16 IU/hr.	Salbutamol
Day 18-21 of Gestation	3.61±0.56	4.03±0.91	5.12±0.94	4.31±0.77	5.45±0.08
Day 28 of Gestation	5.62±0.59#	3.82±0.58	2.56±.22**	2.19±0.25***	4.78±0.06

N=4, *P < 0.05, **P < 0.01, ***P < 0.001

Table 2 Quantitative data derived from vertical transects of ST maps of variation in strain rate from contraction in the gravid uterus of the rabbit.

Mean durations of contractions were derived from pixel counts of consecutive contractions on 300 second vertical transects of unidimensional A-maps. Mean frequencies were calculated from fast Fourier transforms of the same vertical transects.

Differences between controls at different gestations on one-way ANOVA # < 0.05, ##P < 0.01, N=4.

Differences between corresponding treatment and control on one-way ANOVA; *P < 0.05, **P < 0.01, ***P < 0.001. N=4.

A) Comparison on a basis of standard ellipse size (110 mm^2).

	OXYTOCIN INFUSION RATE				
Day 18-21 of Gestation FragStat Metrics	Control	4 IU/hr.	8 IU/hr.	16 IU/hr.	Salbutamol
Patch density (% Landscape of Mask)	25.27±0.67##	27.33±0.80	26.47±0.70	27.54±0.88	18.21±1.21***
Number of Patches (NP)	1.88±0.03	1.89±0.03	1.92±0.05	1.89±0.03	2.23±0.07***
Largest Patch Index (LPI)	23.02±0.33	23.09±0.36	23.59±0.39	23.29±0.26	13.48±1.22***
Mean Patch Size Area in mm^2 (Area MN)	15.67±0.28##	15.51±0.62	15.65±0.18	15.93±0.60	10.41±0.94***

	OXYTOCIN INFUSION RATE				
Day 28 of Gestation FragStat Metrics	Control	4 IU/hr.	8 IU/hr.	16 IU/hr.	Salbutamol
Patch density (% Landscape of Mask)	22.10±0.55##	25.51±0.43**	28.83±0.66***	29.96±0.57***	12.59±0.79***
Number of Patches (NP)	2.06±0.08	2.00±0.06	1.64±0.06**	1.69±0.06**	2.57±0.09**
Largest Patch Index (LPI)	20.57±1.56	23.24±1.42	27.50±1.66*	28.46±1.59*	18.46±1.59
Mean Patch Size Area in mm^2 (Area MN)	14.39±0.32##	16.18±0.27*	21.43±0.53***	22.12±0.47***	13.23±1.33

B) Comparison on a basis of percentage surface area of cornua (45% of width i.e., 110 mm^2 at 18-21 day vs 695 mm^2 at 28 days).

	OXYTOCIN INFUSION RATE				
FragStat Metrics	Control	4 IU/hr.	8 IU/hr.	16 IU/hr.	Salbutamol
% Landscape of Mask (PLAND) Δ	20.45±0.44##	23.23±0.64**	25.90±0.35***	25.09±0.54***	12.59±0.79***
Number of Patches (NP) Δ	2.82±0.03	3.04±0.04**	3.54±0.04***	3.81±0.04**	2.57±0.09**
Largest Patch Index (LPI) ΔΔ	18.07±0.69	20.42±0.78	22.67±0.23***	24.59 0.43***	10.23±0.70***
Mean Patch Size Area in mm^2 ΔΔ (Area MN)	74.50±4.41##	82.22±0.59	105.18±3.58***	95.77±0.87**	75.50±6.81

Table 3 Variation of Indices of contractile activity within ellipses of A-type maps with gestation, oxytocin and ellipse size.

Data was obtained from A-type ST maps of strain rate. Each parameter value was determined from 300 video frames (one every second over a period of 5 minutes) n=4 animals in all cases.

Differences from control on repeated measures ANOVA following dosage with IV oxytocin; *P < 0.05, **P < 0.01, ***P < 0.001.

Differences between controls on one-way ANOVA; ## p < 0.02.

Differences on doubly repeated measures ANOVA comparing responses to IV oxytocin at day 18-21 with those at day 28 as the significance of interaction term between gestation and oxytocin responses; Δ p<0.001 ΔΔ p <0.005.

DRC 16

MASSEY UNIVERSITY
TE KUNENGA KI PŪREHUROA
UNIVERSITY OF NEW ZEALAND

GRADUATE RESEARCH SCHOOL

STATEMENT OF CONTRIBUTION
DOCTORATE WITH PUBLICATIONS/MANUSCRIPTS

We, the candidate and the candidate's Primary Supervisor, certify that all co-authors have consented to their work being included in the thesis and they have accepted the candidate's contribution as indicated below in the *Statement of Originality*.

Name of candidate:	Corrin Hulls
Name/title of Primary Supervisor:	Prof RG Lentle
In which chapter is the manuscript /published work:	Chapter 7

Please select one of the following three options:

(●) The manuscript/published work is published or in press

- Please provide the full reference of the Research Output:

Front. Endocrinol., 21 November 2019
Sec. Reproduction
https://doi.org/10.3389/fendo.2019.00802

( ) The manuscript is currently under review for publication – please indicate:

- The name of the journal:

Frontiers in Endocrionology

- The percentage of the manuscript/published work that was contributed by the candidate: 70%
- Describe the contribution that the candidate has made to the manuscript/published work:

Conducted the experiment (practical work)
Process of evaluate of results
statistical procedures

( ) It is intended that the manuscript will be published, but it has not yet been submitted to a journal

Candidate's Signature:	
Date:	3-10-22
Primary Supervisor's Signature:	PROFESSOR ROGER LENTLE
Date:	2/10/22

This form should appear at the end of each thesis chapter/section/appendix submitted as a manuscript/ publication or collected as an appendix at the end of the thesis.

8 General Discussion and Conclusion

This thesis describes a body of work that investigates smooth muscle motility in two capacious organs, the bladder and gravid uterus of the rabbit, e using a variety of spatiotemporal mapping techniques. The results of which suggest their patchy, localised smooth muscle contractile activity could represent ongoing resetting of smooth muscle tone in order to adjust wall compliance. Further, that upregulation of control of tone could cause evacuation of the lumen contents in the gravid uterus. Again, that control of tone may be largely autonomous.

Hence, I was able to describe the motility (i.e., stationary and migrating), velocity, duration, frequency, and strength and size of contractile activity. Further, I was able to evaluate changes in area of contraction and effects of various pharmaceuticals (bladder) and hormones (gravid uterus). Again, I was able to assess concurrent variances in intravesical pressure and electromyography measurements in the *ex vivo* bladder and *in vivo* gravid uterus, respectively. The use of these advanced spatiotemporal techniques described in this thesis allowed a more comprehensive understanding of smooth muscle motility and function in the bladder and gravid uterus than has previously been reported. The significance and implications of these findings will be discussed below.

8.1 Discussion of Results

8.1.1 Motility of the *ex vivo* Rabbit Bladder

Whereas the general characteristics and disposition of 'micro-motions' on the surface of the bladder has been described in previous publications (Lentle et al., 2015a), quantitative evaluation of their genesis and involution and accompanying changes in area and distribution have not. This thesis describes propagating myogenic patches of the wall of the *ex vivo* rabbit bladder, which were coined propagating patch

contractions (PPC's), and were comprised of nearly synchronous cyclic propagating individual contractions or PIC's.

The frequency and speed of propagation of tonic contractions in the intact urinary bladder of the rabbit maintained *ex vivo* were broadly similar to those reported in intact bladders of pigs *in vivo* and *ex vivo* (Lentle et al., 2015a). Furthermore, the results of spatiotemporal mapping are broadly similar to those based on published electrophysiological recordings (Hammad et al., 2014) but provide additional insight into the organization of contractile behaviour of the whole organ. Hence, like PPC's and PIC's, the occurrence, and amplitudes of patches of spontaneous variation in electrical potential, i.e., electrical waves, increased with the stretch of the bladder wall.

PPC's differed from those of electrical waves in the fact that they as they propagated vertically, they simultaneously enlarged in the transverse dimension, whereas electrical waves have been reported to propagate rarely in the transverse dimension. Further, in our work, the spatiotemporal configuration with PPC's, with their component PIC's each propagating at a faster rate of propagation of the PPC, suggests that PPC's and their component PIC's result from the establishment of linkage between successive myocyte syncytia within electrical patches of excitation generated by ICC's. This hypothesis is supported by the fact that electrophysiological patches of excitation were observed to cover as much as 80% of the elliptical area of analysis on the anterior surface of the rabbit bladder. Hence, PPC's would likely contain many such electrophysiological patches.

The occasional breakdown of organization of regular PPC's and their replacement by desynchronized bouts of irregularly timed PIC's that propagated over more limited distances than those of PPC's fit with reported electrophysiological findings (Hikaru Hashitani, Yanai, et al., 2004b; Kubota et al., 2006b) that action potentials and synchronous contractions could occur in either in bursts or singly and irregularly in sheets of smooth muscle in the guinea pig. It also fits suggests there may be some change in the participation of ICC-like cells influencing the propagation of electrical waves (Hammad et al., 2014). The finding that the administration of drugs such as imitinab, which may disrupt the function of ICC's, similarly caused contractile bursts of action potentials to revert to faster irregular successions of individual action potentials

(Kubota et al., 2006b), with a frequency was that within the range exhibited by PIC's reported in this thesis, further supports a hypothesis that ICC's are responsible for the synchronization of PIC's within PPC's.

Observations on the morphology of developing an involuting PPC's and our quantitative studies on the variation in area and shape off PPC's during cycles of intravesical pressure indicate that the sizes of PPC's increase and decrease by a combination aggregation, hence, that increase in excitation may lead to growth of PPC's by incremental extension of chains of coupled oscillators (Imtiaz, von der Weid, & van Helden, 2010) and to the interlinking of such chains when smaller propagated contractions approximate and fuse, whereas the reverse process occur at times when the excitation and size of the PPC's are declining.

The occurrence of Temporal Patch Domains (TPD's) (stacked area spatiotemporal maps used to determine the size, shape, and position of sites on the anterior surface), and of PPC's and PICs within them, has not been previously reported. The sudden shifts in the locations of TPD's and changes in the direction of propagation of PIC's within PPC's lead us to hypothesize that such a behaviour is more likely to result from changes in the organization and linkage of spontaneous oscillation chains of loosely coupled ICC's (Huizinga et al., 2015; Specht & Bortoff, 1972) than from linkage with permanent sites where populations of ICC's or myocytes have an inherently more rapid rhythm, i.e., pacemakers (Lammers & Stephen, 2008).

In sum, this work enabled the identification of three principle parameters; PPC's, PIC's, and TPD's, which mirror the fundamental properties previously described electro physiologically (Hammad et al., 2014) i.e., contractile activity occurs spontaneously, propagates for a finite distance until spontaneous termination, occurs in the vertical dimension. Hence, TPD's influence the initiation of autonomous contractile activity, and PPC's influence the frequency and extent of propagation of PIC's and may influence the magnitude of the preceding stretch, i.e., background tone. Both low and high threshold stretch sensitive neural receptors (Fig 8-1A) have been identified in the wall of the bladder in both *in vivo* and *in vitro* studies (Sengupta & Gebhart, 1995; Xu & Gebhart, 2008; Zagorodnyuk, Costa, & Brookes, 2006; Vladimir P Zagorodnyuk, Ian L Gibbins, Marcello Costa, Simon JH Brookes, & Sarah J Gregory, 2007). High threshold mechano-transduction likely takes place in the outer muscular layers as it is not affected by removal of the urothelium and lamina propria (Vladimir P Zagorodnyuk et al., 2007). The firing rates of neural mechanoreceptor

circuits increase with increase in intracystic pressure (Iggo, 1955; Satchell & Vaughan, 1994). However, no morphologically complex specialised nerve endings such as intraganglionic laminar endings have been identified (Vladimir P Zagorodnyuk, Simon JH Brookes, & Nick J Spencer, 2010; Vladimir P Zagorodnyuk et al., 2007). Hence the less complex 'antenna like' nerve endings in smooth muscle are the likely sites of mechanosensitivity.

The find that carbachol increased the size, frequency, speed, and distance of propagation of bladder (Fig 8-1B) PPCs in a patchy configuration after dosage supports a hypothesis that compliance is locally adjusted via mechanoreceptor sensitivity and not via global initiation of smooth muscle contraction. Furthermore, it appears that uniform global cholinergic contraction is unlikely (or only when voiding) in the resting bladder given that resting can also be modulated by non-adrenergic, non-cholinergic agonists, and that levels of cholinergic stimulation are low (J. Gillespie, 2004b).

The addition of isoprenaline temporarily halted the incorporation of PICs into PPCs, and reduced patch size and total area undergoing contraction. Reducing or eliminating PPC's (but not randomly sited PIC's) is in line with reports that β-adrenergic agonists reduce the amplitude and frequency of oscillation of intravesical pressure (J. I. Gillespie et al., 2012a). The selective suppression of PPC's, with persistence of PICs after dosage of isoprenaline, suggests the adrenergic agonists either decrease the excitability of ICC-like cells (Fig 8-1C), i.e., their ability to coordinate myocyte contraction to form large PPC's, or directly reduce the excitability of myocytes, rendering IC's unable to fire them. It could be hypothesized that the bladder has the capacity to switch between these two states whereby PPC's allow the elasticity of the wall to be continually dynamically assessed and 'anticipatory' adjustment of bladder capacity made; whereas in the state where PPC's are reduced, a combination of diffuse uncoordinated contraction and passive mechanical properties of the tissue occurs (Gregersen, 2003).

The RhoA kinase (ROCK) inhibitor Y-27632 reduced both largest patch index, mean patch size and the duration of PPC's. These observations are keeping with its effect in reducing the excitability of myocytes and hence the ability of PICs to form and increase in size. Again its effect on the duration of PPC's fits in

with its reported effect in reducing amplitude and the regularity of burst type contractions in strips of guinea pig detrusor (Hikaru Hashitani, Brading, et al., 2004).

Carbenoxolone, a gap junction blocker, decreased the duration of PPC's after treatment which would suggest that its effect on gap junctions (Fig 8-1C) decreases the rate at which PIC's are incorporated into PPC's in order to maintain them.

Both carbenoxolone and ROCK inhibition decreased the duration of PPCs. Carbenoxolone also prolonged duration and accelerated PPC propagation velocity. The authors postulate that these differences arise from differing effects of these agents on myocytes and interstitial cells within the stress environment of the bladder, influencing the development, coordination, and propagation of PPCs.

The results from dosage with parasympathetic and sympathetic agonists indicate that the relative proportions of the two contractile regimes (PPC's and PIC's) over the surface of the bladder may be influenced by autonomic input. Hence the rate of formation of PPC's (i.e., their frequency and the distance of their propagation, and the consequent general increase in the areas undergoing contraction at any given time), is promoted by cholinergic receptors, presumably M_2 type in the rabbit (Schneider et al., 2004). Further, the fact that the c-kit receptor inhibitor imatinib disrupts such synchronisation in the bladder suggests that ICC (Fig 8-1C) may be involved in such synchronisation (Kubota et al., 2006a).

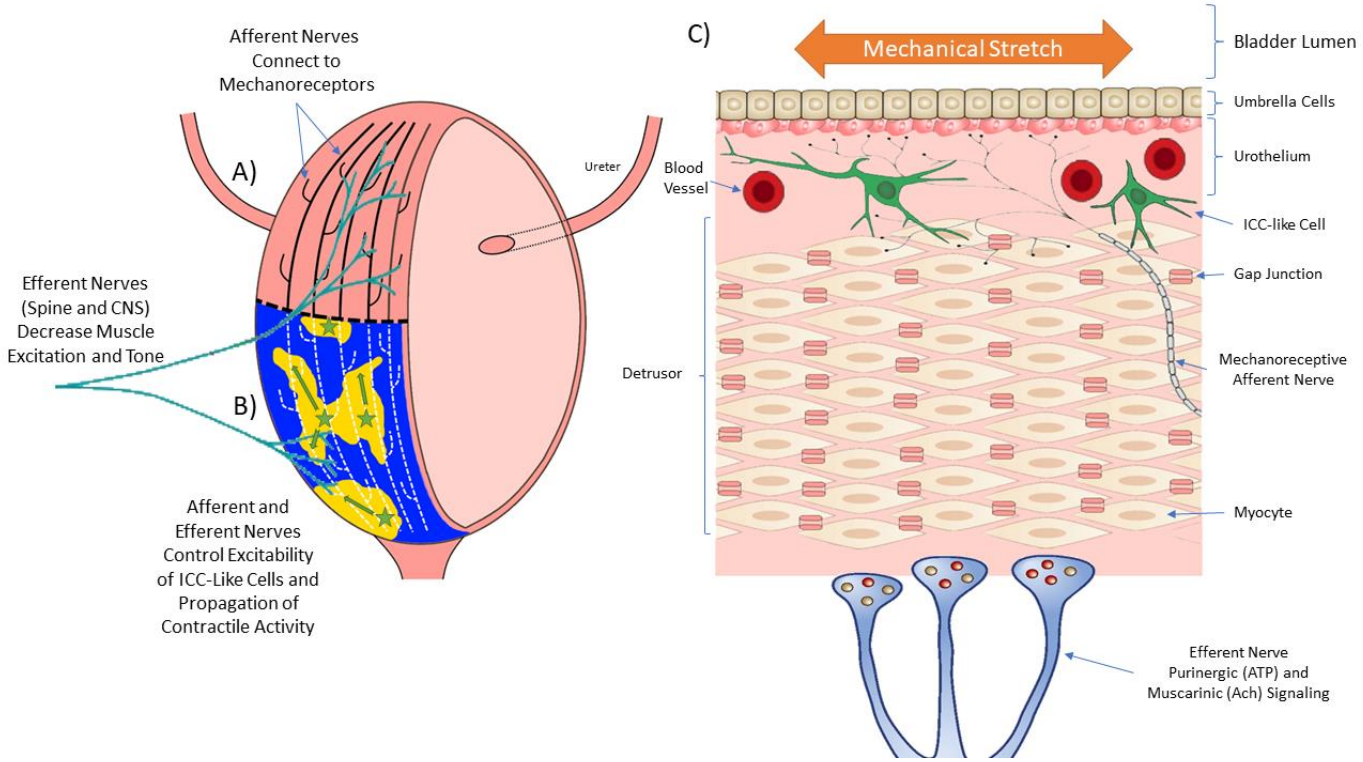

Figure 8-1 Bladder micromotions in urinary storage.

A) Upper 2-D representation of bladder in an intact animal. Afferent nerves are found throughout the bladder wall and are distension sensitive. Central projections of afferents are characterised as distention sensitive mechanoreceptors and behave as in series tension receptors. Efferent nerves contract and relax the bladder.

B) Lower 2-D representation of the bladder in an intact animal with overlayed spatiotemporal map of area strain. This illustration conveys the propagating pattern of micro-motility, yellow indicating motile, and stars indicating initiation points of the micro-contractions. Myogenic propagation of patch contractions are enhanced by stimulation (either by increasing the intravesical volume or by extrinsic application of agonists).

C) Overview of storage control and cell layers of the wall of the urinary bladder. Storage reflexes are activated during bladder filling and are organized primarily in the CNS whereas voiding is mediated by reflex mechanisms that are organized in the brain (Sympathetic efferent nerves). During storage, mechanical stretch of the bladder wall causes mechanoreceptive afferent nerve signalling. Detrusor contractile activity (or micromotions) are modulated by the urothelium, ICC-like cells, and the functional syncytium of gap junctions in the smooth muscle. ICC-like cell inhibition may thus be a means to reduce initiation of microcontractility.

8.1.2 Motility of the *in vivo* Gravid Rabbit Uterus

This thesis is the first body of work to use one and two-dimensional video spatiotemporal mapping (VSTM) to directly quantify the location and timing of uterine contractile activity at different stages of gestation and in response to oxytocin and salbutamol. The results provide new insights into gestational changes in mechanics of myometrial contraction as well as providing reciprocal illumination regarding the results of existing electrophysiological studies (W. J. Lammers, 2013).

The tone of the uterine wall is modulated to accommodate any increase in the volume of the contents and mitigate any consequent increase in intraluminal pressure. Hence, the uterus is reported to 'contract' intermittently (J. V. Kelly, 1962) during the menses to void cellular debris (Bulletti et al., 2000) and during the proliferative phase to secure retrograde transport of spermatozoa (Eytan et al., 1999), similarly during early pregnancy to secure the proper placement of the conceptus in the uterine cavity, as well to void the foetus at term (SUSAN Wray, 1993). Ongoing uterine contractions occur at frequency between one and four cycles per minute and of varying amplitude and duration in the non-pregnant uterus throughout the menstrual cycle (Bulletti et al., 2000) and may be accentuated during days 1-10 of the menstrual period (A. Csapo & Pinto-Dantas, 1966). However, as far as we are aware, their disposition and transit across the surface of the uterus has not been directly mapped. Ultrasonographic studies have suggested that the inner, predominantly circular, muscle layer next to the endometrium i.e., the stratum subvasculare undergoes 'peristaltic like' contraction (Leyendecker et al., 2004). However, such studies are necessarily based on cross sectional data and thus cannot provide evidence of the area of contraction (see below) and its propagation across the surface of the uterus.

This thesis describes ongoing, spontaneous, pleomorphic, localized patches of contraction occurring on an ongoing basis at sites distributed across the entire surface of the uterus throughout the middle and latter stages of pregnancy. Further, their overall frequency increased, and duration decreased with increase in length of gestation whilst their frequency decreased, and duration increased following administration of oxytocin. Whilst these findings fit in with prior physiological work (Hammad et al., 2014; W. J. Lammers, 1996b; W. J. Lammers, 2013) and in this sense are not novel, it is important to confirm these prior findings.

Moreover, the ongoing contractions found in this study also fits with prior studies showing that ongoing oscillations in amniotic pressure that were associated with uterine contractions continued throughout pregnancy (H. Alvarez & Caldeyro, 1950b). Similarly, they fit in with the work measuring localized changes in intra-myogenic pressure at the various sites in the uterine wall (Caldeyro-Barcia & Poseiro, 1959) and with results of a number of electrophysiological studies using multiple electrodes (W. J. Lammers, 2013).

What is new and novel is the identification and observation using VSTM of adjacent contractile patches similar to micro contractions seen in the urinary bladder. Moreover, the pattern of peripheral aggregation of contractile patches and enlargement the subsequent decay by the reverse process was also similar. The reorganization of smaller individual patches of uterine contraction into larger, more numerous, pleomorphic propagating patches of lower frequency and longer duration following dosage of oxytocin at 28 weeks gestation is similar to changes that occur in the isolated urinary bladder following the administration of cholinergic agents and promotes expulsion of urine (C M Hulls et al., 2017; Lentle et al., 2015a).

In the gravid uterus, the density and duration of contractions decreased, and their frequency increased with the length of gestation in the non-labouring uterus suggesting that the concomitant increase in uterine size and cavity volume from smooth muscle hypertrophy (Owens & Schwartz, 1982) results in a decrease in connectivity between adjacent myocytes. The result of this growth is an increase in compliance of the uterine wall to accommodate the growing foetus but also a progressive decrease to wall mechanosensitivity. Evidence summarized below suggests that accommodation is a of myogenic origin rather than from extrinsic neurogenic signalling.

It is well known that densities of oxytocin receptors increase in late pregnancy (A.-R. Fuchs et al., 1984). The observation that component patches of contraction to be larger, of longer duration and to propagate over greater distances after dosage with oxytocin, is supported by the electrophysiological findings that the electrical connectivity between myocytes increases in later pregnancy (R. Garfield et al., 1994) and the progressive recruitment of action potentials to form more sustained, faster moving, composite bursts of contractions (Caldeyro-Barcia & Alvarez, 1952; WJ Lammers et al., 1994; W. J. Lammers, 1996b; J. M.

Marshall, 1962b) (also see Supplementary Video 2). Moreover, it was observed that contractions that originate at sites on the uterine wall which overlie one foetus may on occasion propagate to neighbouring foetuses further suggesting increased connectivity between myocytes and also mitigates against a hypothesis of a single localized peri-placental origin of excitation (Hammad et al., 2014) i.e., pacemaker in this species.

The spatiotemporal distribution of uterine contractions after the administration of increasing doses of oxytocin render it unlikely that the reorganization of contractile activity during late gestation could induce direct distal-ward propulsion of a contained foetus and thus could not be classified as peristaltic. Contractile activity in late gestation continued to consist of pleomorphic patches that were randomly distributed across the surface of the uterus and overlying each foetus, did not form distally progressing bands, and did not comprise synchronous separate longitudinal and circumferential patches of contraction such has been reported in peristalsis (N. Spencer, M. Walsh, & T. K. Smith, 1999). Further, the overall trend of direction of propagation of patches was distal to proximal, rather than from proximal to distal. It is therefore more likely that late gestational reorganization progressively reduces the mean compliance of the uterine wall and thus promotes expulsion by volumetric reduction. Moreover, the trend of distal to proximal progression of patches of contraction possibly results from uterine smooth muscle being drawn from the proximal pole of each foetus toward the distal pole.

The effect of salbutamol in reducing the duration and overall distance of propagation of composite contractions and inducing their fragmentation into component individual contractions regardless of length of gestation , fits in with the reported pharmacological action in reducing the excitability of myocytes via the generation of cAMP (Hajagos-Tóth et al., 2009; Zingg & Laporte, 2003). The overall effects of salbutamol in reducing the overall incidence of contractions and hence overall uterine tone are in line with the reported effects on general contraction (Abel & Hollingsworth, 1986) and the cavity pressure (Abel & Hollingsworth, 1985) in the intact uterus of the rat.

8.2 Conclusion

The characteristics of smooth muscle contraction that are associated with the maintenance of tone during accommodation appear to be to be similar in the capacious organs discussed. Hence, it appears there is patchy rather than uniform local revision of the state of tonal contraction over the surfaces of the various capacious organs during accommodation that can undergo neural modulation.

The similarity of the frequencies and speeds of propagation of tonal revision to those of coordinated myogenic phasic contractile events renders it difficult to distinguish the former from the latter. Hence events of tonal revision can only be distinguished by their patchiness, their lack of constancy in two dimensional area and the lack of consistency in their direction of their propagation. This raises questions as to the nature of a number of myogenic contractile phenomena that are currently evidenced only by 'unidimensional' spatiotemporal, electrophysiological or manometric evidence.

It is noteworthy that, whilst the component myocytes of some capacious organs are grouped into 'circularly' and 'longitudinally' axially aligned layers, the extent of their modulation by coupled oscillation (Publicover & Sanders, 1989) or cross frequency coupling (Jan D Huizinga et al., 2015) appears to be limited as they consistently lack the concerted unidirectional propagation such as occurs with antral propagating contractions (O'Grady et al., 2010) in the stomach. Indeed, the demonstration that a number of these organs exhibit two tonal contractile regimes, the first in which there is randomly distributed isolated unsynchronised contraction of small groups of myocytes that is seen in the bladder a and of similar timing to a reported pattern of the electrical activity (Hikaru Hashitani, Brading, et al., 2004), the second in which there is synchronised contraction of larger patches of myocytes that is similar in timing to a second reported pattern of 'bursts' of electrical activity of (Hikaru Hashitani, Brading, et al., 2004), suggests that the synchronisation of component myocytes is episodic. The fact that the c-kit receptor inhibitor imitinab disrupts such synchronisation in some of these organs suggests that ICC may be involved in such synchronisation (Kubota et al., 2006a; Popescu et al., 2006).

There appears to be less similarity in regard to the mechanisms that secure the voiding contractions in these capacious structures. Whilst the actuation of the necessary shorter term increase in tone may be ultimately dependent upon a mechanosensitive myogenic reflex, the relative contributions of autonomic, hormonal, mechanical and voluntary reflexes that reset the threshold of this reflex and aid in the relatively rapid expulsion of the contents, appear to vary between organs.

8.3 Implications of the Research Study

8.3.1 The Bladder

The study identified three principal parameters, PICs, PPCs, and TPDs, which mirror the fundamental properties that influence intravesical pressure in the bladder (M. Drake et al., 2003). Hence, TPDs influence the initiation of autonomous contractile activity, and PPCs influence the frequency and extent of propagation of contained PICs and may influence the magnitude of preceding stretch, i.e., background tone. Furthermore, analyses of the origin and transit of macroscopic patches of negative strain rate (PPCs) across the anterior surface of the bladder support a hypothesis that PPCs result from the facilitation of the inherent rhythmicity and frequency of contraction of myocytes by patches of ICCs that become synchronized in the manner of coupled oscillators (Jan D Huizinga et al., 2015). This loose coupling is prone to break down, allowing myocytes to contract at their own inherent frequency. Further, the differences in the effects of the sympathomimetic and parasympathomimetic agonists, with the former affecting the size and speed of propagation of PPCs and the latter the genesis of component PICs and the formation of PPCs, suggest that disorders in the formation of micro contractions (Vahabi & Drake, 2015) may be better treated by combinations of sympathomimetic and parasympatholytic agents so as to influence the size and frequency of PPCs as well as their formation. Moreover, these results indicate that disorders of bladder wall contraction and the genesis of PPCs from PICs may result from disorders in either neurogenic or myogenic signalling. Further, the ability of spatiotemporal mapping to detect the subtle differences in contraction patterns and associated changes in intravesical pressure that result from treatment with myogenically active agents suggests that it may be useful in detecting those changes that lead to the development of overactive bladder syndrome and hence its aetiology. Changes in the characteristics of low

amplitude rhythmic contractions in subjects with detrusor overactivity that have been identified in cystometric recordings by Fast Fourier Transform (FFT) algorithm (Cullingsworth et al., 2018) may therefore be further resolved by the use of ST mapping techniques. Whilst population-based registries, such as those of bladder cancer, may provide insight into the incidence of frankly pathological bladder conditions (Vatandoust et al., 2018) direct spatiotemporal studies on human subjects are needed to provide direct evidence of normal and abnormal bladder function.

8.3.2 The Uterus

In regard to the gravid uterus, apart from providing a greater understanding of uterine function, the reciprocal changes in the frequency duration, area and density of uterine contractions that were found to occur with increasing gestation, and following dosage with oxytocin at 28 days, may provide a useful means for identifying the switching of uterine function from accommodation to expulsion, although further work is needed to confirm that similar changes occur in human subjects. Again, the demonstration that the VSTM methodology is able to directly quantify changes in the development and disposition of uterine contractions in the rabbit preparation following administration of pharmaceuticals lays the ground for statistically based assays of other agents that influence myometrial contractility at various stages of uterine function.

8.4 Limitations of the Research Study

8.4.1 Limited Planes of View

Video spatiotemporal mapping comprises the comparison through time of the spatial position of an object or of distinctive features of the object. Both studies (the urinary bladder and gravid uterus) used only one high definition camera to capture the motion of distinctive features in the areas under investigation. Because only one camera was used, it limited observations to only one specific surface i.e., the anterior surfaces of the bladder and one gravid horn of the bicornuate uterus of the rabbit. Therefore, the motility

captured and analysed was only from one plane, and motility that may have occurred in the posterior, and/or lateral aspects of the organs went unrecorded. Comparisons of motility between different areas of the bladder or uterus where therefore unable to be compared. Further, the limitation of one camera prevented the simultaneous filming of the other cornu of the bicornuate uterus.

8.4.2 Image Quality

As well as being only able to capture the contractile activity of one surface of an organ, the convex nature of the organs themselves prevent the organ surface to be mapped in its entirety. When footage of the organ is captured, the principal axis of the camera is 90° to the surface. This means the focal length is at its most defined at the centre of the curvature. However, from the centre of the image, depending on the curvature, the focal length increases. In areas at the periphery of a large spherical structure where angulation of the surface is high, video footage will be unfocused and ill defined. Because the robustness of VSTM relies on the quality of the footage, distortion at the edges of an image will result in strain rates that may be significantly underestimated. Further, artefacts can be generated by minor organ rotation at the edges and foreshortening from angulation of the surface can occur. Therefore, only areas of high definition and fidelity could be analysed and thus maps of area strain were restricted to a user defined ellipsoid mask of 45% of the anterior surface of the bladder and gravid uterus.

8.4.3 Pharmacological Constraints

Both the bladder and uterus lent themselves to pharmacological modulation. In both cases, the organs were maintained and super perfused in oxygenated (95% O_2, 5% CO_2) HEPES buffer solution maintained at 37°C. The *ex vivo* bladder and *in vivo* uterus organ baths contained a volume of 300 and 500ml respectively plus an additional reservoir for recirculation of 150mls. When preparing for the measurement of physiological tissue responses to drug concentrations particular attention needs to be made to how much antagonist/agonist needs to be added to the bath to illicit a response. In most cases, information on drug fluid concentrations could be found in previous publications that tested isolated muscle strips in small,

isolated tissue baths of approximately 5-50ml. However, because motility was being assessed in whole organ preparations with a total recirculating fluid volume of up to 750ml, it was impractical emptying the same drug concentration into this large volume. Again, as some drugs required dilution in solvents (DMSO, ethanol, acetate) whereby the addition of large volumes of said drug and vehicle could be toxic to the tissue. Further, the addition of such large volumes of pharmaceutical agents could cause the drug to precipitate out of solution e.g., the gap junction blocker 18-α glycyrrhetinic acid (18-α-GA). Therefore, drugs were restricted to those that were non-toxic to the tissue and practical to use. The example of this was seen in the use of carbenoxolone in the bladder rather than (18-α-GA) as it is a modestly potent, reasonably effective, water-soluble blocker of gap junctions (Rozental, Srinivas, & Spray, 2001). However, it is a "dirty" drug in respect to its specificity. Thus, evidence suggests it also suppresses action potentials and blocks calcium channels (Connors, 2012). Even though no drug is absolutely specific, the work should be repeated with a more targeted gap junction antagonist such as 18β-GA isomers or oxybutynin if the conclusions are to be upheld.

8.5 Future research

As illustrated in this thesis, the technique of spatiotemporal mapping offers unique insight into the contractile activity of smooth muscle in *ex vivo* capacious structures. However, there is additional work required to completely understand the hierarchical modality of bladder accommodative control.

Future work is required is to see if similar contractile activity can be observed *in vivo.* This would require the adaptation of the method to film the bladder via endoscopy or cystoscope. This would enable characterisation of contractile activity *in vivo* with the opportunity to describe normal contractile behaviour as well as dysmotility. Further, there would be the ability to quantify the effects of therapeutic agents.

The use of spatiotemporal mapping techniques can also be used to address other problems. Overactive bladder (OAB) also known as "Overactive Bladder Syndrome" is defined by the International Continence Society as "urinary urgency, usually accompanied by increased daytime frequency and/or nocturia (having

to wake at night one or more times to urinate) with urinary incontinence (OAB-wet) or without (OAB-dry), in the absence of urinary tract infection or other detectable disease". When OAB is associated with overactivity of the bladder detrusor muscle (diagnosed by cystometry) the condition is termed Detrusor Overactivity (DO). DO demonstrably manifests itself through involuntary detrusor muscle contraction.

The injection of Onabotulinum Neurotoxin A (BoNT-A), or botox, into the urinary bladder wall is one commonly used treatment for overactive bladder (OAB). However, the precise mechanism of the clinical effect is incompletely understood. The evidence regarding its use is limited and largely gleaned from observation in human research subjects. There is thus a real need for animal studies in order to provide more detail to its mode of action. The methods for quantifying bladder motility in this thesis could be readily used in an *in vivo* model such as the anesthetized rabbit.

Additionally, techniques described in this thesis, if adapted for use with an hysteroscope, could provide a useful means for identifying the switching of uterine function from accommodation to expulsion and the identification of dysfunctional labour, notably dystocia.

9 References

Abdu, F., Hicks, G. A., Hennig, G., Allen, J. P., & Grundy, D. (2002). Somatostatin sst2 receptors inhibit peristalsis in the rat and mouse jejunum. *American Journal of Physiology-Gastrointestinal and Liver Physiology, 282*(4), G624-G633.

Abel, M. H., & Hollingsworth, M. (1985). The potencies and selectivities of four calcium antagonists as inhibitors of uterine contractions in the rat in vivo. *British journal of pharmacology, 85*(1), 263.

Abel, M. H., & Hollingsworth, M. (1986). The effects of long-term infusion of salbutamol, diltiazem and nifedipine on uterine contractions in the ovariectomized, post-partum rat. *British journal of pharmacology, 88*(3), 577-584.

Adrian, A., Dun, E., Tica, V., & Cojocaru, O. The autonomic innervation of the uterus.

Aguilar, H. N., & Mitchell, B. F. (2010). Physiological pathways and molecular mechanisms regulating uterine contractility. *Hum Reprod Update, 16*(6), 725-744. 10.1093/humupd/dmq016

Ajalloueian, F., Lemon, G., Hilborn, J., Chronakis, I. S., & Fossum, M. (2018). Bladder biomechanics and the use of scaffolds for regenerative medicine in the urinary bladder. *Nature Reviews Urology, 15*(3), 155-174. 10.1038/nrurol.2018.5

Akerlund, M. (1998). Uterine contractions in non-pregnant women. How are they handled? what is their significance? *Lakartidningen, 95*(4), 284-287.

Alexander, R. S. (1973). Viscoplasticity of smooth muscle of urinary bladder. *American Journal of Physiology-Legacy Content, 224*(3), 618-622.

Almasri, A. M., Ratz, P. H., & Speich, J. E. (2010). Length adaptation of the passive-to-active tension ratio in rabbit detrusor. *Ann Biomed Eng, 38*(8), 2594-2605. 10.1007/s10439-010-0021-7

Alvarez, H., & Caldeyro, R. (1950a). Contractility of the human uterus recorded by new methods. *Surgery Gynecology and Obstetrics, 91*(1), 1-13.

Alvarez, H., & Caldeyro, R. (1950b). Contractility of the human uterus recorded by new methods. *Surgery, gynecology & obstetrics, 91*(1), 1-13.

Alvarez, W. C., & Zimmermann, A. (1927). The absence of inhibition ahead of peristaltic rushes. *American Journal of Physiology, 83*(1), 52-59.

Anderson, K.-E. (1993). Pharmacology of lower urinary tract smooth muscles and penile erectile tissues. *Pharmacological Reviews, 45*(3), 253-308.

Anderson, K. E. (1993). Pharmacology of lower urinary tract smooth muscles and penile erectile tissues. *Pharmacol Rev, 45*(3), 253-308.

Anderson, U., Carson, C., Johnston, L., Joshi, S., Gurney, A., & McCloskey, K. (2013). Functional expression of KCNQ (Kv7) channels in guinea pig bladder smooth muscle and their contribution to spontaneous activity. *British journal of pharmacology, 169*(6), 1290-1304.

Andersson, K.-E. (2002). Potential benefits of muscarinic M3 receptor selectivity. *European Urology Supplements, 1*(4), 23-28.

Andersson, K.-E., & Arner, A. (2004). Urinary Bladder Contraction and Relaxation: Physiology and Pathophysiology. *Physiological Reviews, 84*(3), 935-986. 10.1152/physrev.00038.2003

Andersson, K.-E., & Gratzke, C. (2007). Pharmacology of α 1-adrenoceptor antagonists in the lower urinary tract and central nervous system. *Nature Clinical Practice Urology, 4*(7), 368-378.

Andersson, K.-E., Holmquist, F., Fovaeus, M., Hedlund, H., & Sundler, R. (1991). Muscarinic receptor stimulation of phosphoinositide hydrolysis in the human isolated urinary bladder. *The Journal of urology, 146*(4), 1156-1159.

Andersson, K.-E., Ingemarsson, I., & Persson, C. (1975). Effects of terbutaline on human uterine motility at term. *Acta Obstetricia et Gynecologica Scandinavica, 54*(2), 165-172.

Andersson, K. E. (2017). On the Site and Mechanism of Action of beta3-Adrenoceptor Agonists in the Bladder. *Int Neurourol J, 21*(1), 6-11. 10.5213/inj.1734850.425

Andersson, K. E., Boedtkjer, D. B., & Forman, A. (2017). The link between vascular dysfunction, bladder ischemia, and aging bladder dysfunction. *Ther Adv Urol, 9*(1), 11-27. 10.1177/1756287216675778

Angeli, T. R., Du, P., Paskaranandavadivel, N., Janssen, P. W., Beyder, A., Lentle, R. G., . . . O'Grady, G. (2013). The bioelectrical basis and validity of gastrointestinal extracellular slow wave recordings. *The Journal of Physiology, 591*(18), 4567-4579.

Anssari-Benam, A., Bucchi, A., & Saccomandi, G. (2021). Modelling the Inflation and Elastic Instabilities of Rubber-Like Spherical and Cylindrical Shells Using a New Generalised Neo-Hookean Strain Energy Function. *Journal of Elasticity* 10.1007/s10659-021-09823-x

Apodaca, G. (2004). The uroepithelium: not just a passive barrier. *Traffic, 5*(3), 117-128.

Apostolakis, E., Rice, K. E., Longo, L. D., Seron-Ferre, M., & Yellon, S. M. (1993). Time of day of birth and absence of endocrine and uterine contractile activity rhythms in sheep. *American Journal of Physiology-Endocrinology and Metabolism, 264*(4), E534-E540.

Appukuttan, S., Padmakumar, M., Young, J. S., Brain, K. L., & Manchanda, R. (2018). Investigation of the Syncytial Nature of Detrusor Smooth Muscle as a Determinant of Action Potential Shape. *Frontiers in Physiology, 9*(1300) 10.3389/fphys.2018.01300

Arrowsmith, S., Keov, P., Muttenthaler, M., & Gruber, C. W. (2018). Contractility measurements of human uterine smooth muscle to aid drug development. *JoVE (Journal of Visualized Experiments)*(131), e56639.

Ashokkumar, M., & Ajayan, P. M. (2021). Materials science perspective of multifunctional materials derived from collagen. *International Materials Reviews, 66*(3), 160-187.

Aslanidi, O., Atia, J., Benson, A., van Den Berg, H., Blanks, A., Choi, C., . . . Holden, A. (2011). Towards a computational reconstruction of the electrodynamics of premature and full term human labour. *Progress in biophysics and molecular biology, 107*(1), 183-192.

Azhari, H., Weiss, J. L., Rogers, W. J., Siu, C. O., & Shapiro, E. P. (1995). A noninvasive comparative study of myocardial strains in ischemic canine hearts using tagged MRI in 3-D. *American Journal of Physiology, 268*(5), H1918-1926.

Baah-Dwomoh, A., McGuire, J., Tan, T., & De Vita, R. (2016). Mechanical properties of female reproductive organs and supporting connective tissues: a review of the current state of knowledge. *Applied Mechanics Reviews, 68*(6)

Baguma-Nibasheka, M., Wentworth, R. A., Green, L. R., Jenkins, S. L., & Nathanielsz, P. W. (1998). Differences in the in vitro sensitivity of ovine myometrium and mesometrium to oxytocin and prostaglandins E2 and F2α. *Biology of reproduction, 58*(1), 73-78.

Baillargeon, B., Rebelo, N., Fox, D. D., Taylor, R. L., & Kuhl, E. (2014). The living heart project: a robust and integrative simulator for human heart function. *European Journal of Mechanics-A/Solids, 48*, 38-47.

Balasteghin, K. T., Nardo, A., Amaro, J., & Padovani, C. (2003). Experimental model of bladder instability in rabbits. *International braz j urol, 29*, 62-71.

Balducci, J., Risek, B., Gilula, N. B., Hand, A., Egan, J. F., & Vintzileos, A. M. (1993). Gap junction formation in human myometrium: a key to preterm labor? *American Journal of Obstetrics and Gynecology, 168*(5), 1609-1615.

Ballaro, A. (2008). The elusive electromyogram in the overactive bladder: a spark of understanding. *The Annals of The Royal College of Surgeons of England, 90*(5), 362-367.

Ballaro, A., Mundy, A., Fry, C., & Craggs, M. (2003). Bladder electrical activity: the elusive electromyogram. *BJU International, 92*(1), 78-84.

Bannowsky, A., & Juenemann, K.-P. (2003). Innervation and function of the female urinary bladder and urethra. *EAU Update Series, 1*(3), 120-127.

Barrington, F. (1915). The effect of division of the hypogastric nerves on frequency of micturition. *Experimental Physiology, 9*(3), 261-264.

Basicmedicalkey. (2022). The reproductive systems. Retrieved 24082022 2022 from https://basicmedicalkey.com/the-reproductive-systems/

Bayguinov, O., Hennig, G., & Sanders, K. (2011). Movement based artifacts may contaminate extracellular electrical recordings from GI muscles. *Neurogastroenterology and Motility, 23*(11), 1029-e1498.

Bayguinov, P. O., Hennig, G. W., & Smith, T. K. (2010a). Ca2+ imaging of activity in ICC-MY during local mucosal reflexes and the colonic migrating motor complex in the murine large intestine. *The Journal of Physiology, 588*(22), 4453-4474.

Bayguinov, P. O., Hennig, G. W., & Smith, T. K. (2010b). Calcium activity in different classes of myenteric neurons underlying the migrating motor complex in the murine colon. *The Journal of Physiology, 588*(3), 399-421.

Bayliss, W. M. (1902). On the local reactions of the arterial wall to changes of internal pressure. *The Journal of physiology, 28*(3), 220-231. 10.1113/jphysiol.1902.sp000911

Bazer, F. W. (1975). Uterine protein secretions: relationship to development of the conceptus. *Journal of Animal Science, 41*(5), 1376-1382.

Beeson, J., & Martens, M. (2004). Variable intrauterine pressure catheter (IUPC) tracings with two catheters. *American Journal of Obstetrics & Gynecology, 191*(6), S151.

Benard, T., Bouchoucha, M., Dupres, M., & Cugnenc, P. H. (1997). In vitro analysis of rat intestinal wall movements at rest and during propagated contraction: a new method. *American Journal of Physiology, 273*(4), G776-784.

Bengtsson, B., Chow, E., & Marshall, J. (1984). Activity of circular muscle of rat uterus at different times in pregnancy. *American Journal of Physiology-Cell Physiology, 246*(3), C216-C223.

Benham, C., & Tsien, R. (1987). A novel receptor-operated Ca 2+-permeable channel activated by ATP in smooth muscle. *Nature, 328*(6127), 275-278.

Bergman, R. A. (1968). Uterine smooth muscle fibers in castrate and estrogen-treated rats. *The Journal of cell biology, 36*(3), 639.

Berridge, M. J. (2008). Smooth muscle cell calcium activation mechanisms. *Journal of Physiology, 586*(21), 5047-5061.

Berthoud, H. R., Hennig, G., Campbell, M., Volaufova, J., & Costa, M. (2002). Video-based spatio-temporal maps for analysis of gastric motility in vitro: effects of vagal stimulation in guinea-pigs. *Neurogastroenterology and Motility, 14*(6), 677-688.

Bhattacharjee, A. K., Pomponio, J. W., Evans, S. A., Pervitsky, D., & Gordon, R. K. (2013). Discovery of subtype selective muscarinic receptor antagonists as alternatives to atropine using in silico pharmacophore modeling and virtual screening methods. *Bioorganic & medicinal chemistry, 21*(9), 2651-2662.

Bijos, D., & Drake, M. (2015). *SPREADING OF MICROMOTIONS IN JUVENILE RAT BLADDER: ORIGIN POINTS, DIRECTIONALITY AND FUNCTION OF GAP JUNCTIONS.* Paper presented at the Neurourology and Urodynamics.

Birnholz, J. C. (1984). Ultrasonic visualization of endometrial movements. *Fertility and Sterility, 41*(1), 157-158.

Blok, B., Pannek, J., Castro-Diaz, D., Del Popolo, G., Groen, J., & Hamid, R. (2019). EAU Guidelines on Neuro-urology. 2015. *In*, European Association of Urology Guidelines Office 2018.

Bø, K., Lilleås, F., Talseth, T., & Hedland, H. (2001). Dynamic MRI of the pelvic floor muscles in an upright sitting position. *Neurourology and Urodynamics: Official Journal of the International Continence Society, 20*(2), 167-174.

Bo, W. J., Odor, D. L., & Rothrock, M. (1968). The fine structure of uterine smooth muscle of the rat uterus at various time intervals following a single injection of estrogen. *American Journal of Anatomy, 123*(2), 369-383.

Boberg, L., Szekeres, F. L., & Arner, A. (2018). Signaling and metabolic properties of fast and slow smooth muscle types from mice. *Pflügers Archiv-European Journal of Physiology, 470*(4), 681-691.

Bogeski, G., Shafton, A. D., Kitchener, P. D., Ferens, D. M., & Furness, J. B. (2005). A quantitative approach to recording peristaltic activity from segments of rat small intestine in vivo. *Neurogastroenterology and Motility, 17*(2), 262-272.

Bond, M., Kitazawa, T., Somlyo, A., & Somlyo, A. (1984). Release and recycling of calcium by the sarcoplasmic reticulum in guinea-pig portal vein smooth muscle. *The Journal of physiology, 355*(1), 677-695.

Bonnans, C., Chou, J., & Werb, Z. (2014). Remodelling the extracellular matrix in development and disease. *Nature reviews Molecular cell biology, 15*(12), 786-801.

Borsdorf, M., Tomalka, A., Stutzig, N., Morales-Orcajo, E., Bol, M., & Siebert, T. (2019). Locational and Directional Dependencies of Smooth Muscle Properties in Pig Urinary Bladder. *Front Physiol, 10*, 63. 10.3389/fphys.2019.00063

Bottari, S., Vokaer, A., Kaivez, E., Lescrainier, J., & Vauquelin, G. (1985). Regulation of alpha-and beta-adrenergic receptor subclasses by gonadal steroids in human myometrium. *Acta Physiologica Hungarica, 65*(3), 335-346.

Bowditch, H. (1897). Movements of the alimentary canal. *Science, 5*, 901-902.

Bozler, E. (1941). Influence of estrone on the electric characteristics and the motility of uterine muscle. *Endocrinology, 29*(2), 225-227.

Brading, A. (1987). Physiology of Bladder Smooth Muscle. In M. Torrens & J. F. B. Morrison (Eds.), *The Physiology of the Lower Urinary Tract* (pp. 161-191). London: Springer London. 10.1007/978-1-4471-1449-9_6

Brading, A. (2006). Spontaneous activity of lower urinary tract smooth muscles: correlation between ion channels and tissue function. *The Journal of Physiology, 570*(1), 13-22.

Brading, A. F. (1997). A myogenic basis for the overactive bladder. *Urology, 50*(6, Supplement 1), 57-67. https://doi.org/10.1016/S0090-4295(97)00591-8

Brading, A. F. (2006). Spontaneous activity of lower urinary tract smooth muscles: correlation between ion channels and tissue function. *J Physiol, 570*(Pt 1), 13-22. 10.1113/jphysiol.2005.097311

Bramich, N. J., & Brading, A. F. (1996). Electrical properties of smooth muscle in the guinea-pig urinary bladder. *The Journal of physiology, 492*(1), 185-198.

Brännström, M., Johannesson, L., Bokström, H., Kvarnström, N., Mölne, J., Dahm-Kähler, P., . . . Diaz-Garcia, C. (2015). Livebirth after uterus transplantation. *The Lancet, 385*(9968), 607-616.

Brauer, M. M., & Smith, P. G. (2015). Estrogen and female reproductive tract innervation: cellular and molecular mechanisms of autonomic neuroplasticity. *Autonomic Neuroscience, 187*, 1-17.

Braverman, A. S., Doumanian, L. R., & Ruggieri, M. R. (2006). M2 and M3 muscarinic receptor activation of urinary bladder contractile signal transduction. II. Denervated rat bladder. *Journal of Pharmacology and Experimental Therapeutics, 316*(2), 875-880.

Braverman, A. S., Tibb, A. S., & Ruggieri, M. R. (2006). M2 and M3 muscarinic receptor activation of urinary bladder contractile signal transduction. I. Normal rat bladder. *Journal of Pharmacology and Experimental Therapeutics, 316*(2), 869-874.

Brierley, S. M. (2010). Molecular basis of mechanosensitivity. *Autonomic Neuroscience, 153*(1-2), 58-68.

Brindley, G. (1977). A substitute for hermeticity in implantable pressure sensors [proceedings]. *The Journal of physiology, 272*(1), 7P-8P.

Brosens, J. J., Barker, F. G., & deSouza, N. M. (1998). Myometrial zonal differentiation and uterine junctional zone hyperplasia in the non-pregnant uterus. *Human reproduction update, 4*(5), 496-502.

Buchmiller-Crair, T. L., Gregg, J. P., Rivera, F. A., Choi, R. S., Diamond, J. M., & Fonkalsrud, E. W. (2001). Delayed disaccharidase development in a rabbit model of intrauterine growth retardation. *Pediatric research, 50*(4), 520-524.

Buhimschi, C. S., Buhimschi, I. A., Malinow, A. M., & Weiner, C. P. (2003). Myometrial thickness during human labor and immediately post partum. *American Journal of Obstetrics and Gynecology, 188*(2), 553-559.

Buhimschi, C. S., Buhimschi, I. A., Norwitz, E. R., Sfakianaki, A. K., Hamar, B., Copel, J. A., . . . Weiner, C. P. (2005). Sonographic myometrial thickness predicts the latency interval of women with preterm premature rupture of the membranes and oligohydramnios. *American Journal of Obstetrics and Gynecology, 193*(3), 762-770.

Bulbring, E. (1987). Catecholamine action on smooth muscle. *Pharmacol Rev, 39*, 49-96.

Bülbring, E. (1955). Correlation between membrane potential, spike discharge and tension in smooth muscle. *Journal of Physiology, 128*(1), 200-221.

Bulletti, C., de Ziegler, D., Polli, V., Diotallevi, L., Ferro, E. D., & Flamigni, C. (2000). Uterine contractility during the menstrual cycle. *Human Reproduction, 15*(suppl_1), 81-89.

Burns, A. J., Lomax, A., Torihashi, S., Sanders, K. M., & Ward, S. M. (1996). Interstitial cells of Cajal mediate inhibitory neurotransmission in the stomach. *Proceedings of the National Academy of Sciences, 93*(21), 12008-12013.

Burnstock, G. (1980). Purinergic nerves and receptors. *Progress in biochemical pharmacology, 16*, 141-154.

Burnstock, G. (2014). Purinergic signalling in the urinary tract in health and disease. *Purinergic signalling, 10*(1), 103-155.

Burnstock, G., & Prosser, C. (1960). Responses of smooth muscles to quick stretch; relation of stretch to conduction. *American Journal of Physiology--Legacy Content, 198*(5), 921-925.

Caldeyro-Barcia, R., & Alvarez, H. (1952). Abnormal uterine action in labour. *J Obstet Gynaecol Br Emp, 59*, 646.

Caldeyro-Barcia, R., & Poseiro, J. J. (1959). Oxytocin and contractility of the pregnant human uterus. *Annals of the New York Academy of Sciences, 75*(2), 813-830.

Camilleri, M., Bharucha, A. E., Di Lorenzo, C., Hasler, W., Prather, C., Rao, S., & Wald, A. (2008). American Neurogastroenterology and Motility Society consensus statement on intraluminal measurement of gastrointestinal and colonic motility in clinical practice. *Neurogastroenterology and Motility, 20*(12), 1269-1282.

Cannon, W. B. (1898). The movements of the stomach studied by means of the Röntgen rays. *American Journal of Physiology, 1*(3), 359-382.

Cannon, W. B. (1902). The movements of the intestines studied by means of the Röntgen rays. *American Journal of Physiology, 6*(5), 251-277.

Cannon, W. B. (1911). *The mechanical factors of digestion*. London: Edward Arnold.

Carsten, M. E. (1968). Tropomyosin from smooth muscle of the uterus. *Biochemistry, 7*(3), 960-967.

Carter, A. M., Naaktgeboren, C., & Van Zon-Van Wagtendonk, A. (1971). Parturition in the rabbit: spontaneous uterine activity during late pregnancy, parturition and the post partum period and its relation to normal behaviour. *European Journal of Obstetrics & Gynecology, 1*(2), 37-68.

Caspo, A. (1975). The" seesaw" theory of the regulatory mechanism of pregnancy. *American Journal of Obstetrics and Gynecology, 121*(4), 578-581.

Chakrabarty, B., Bijos, D. A., Vahabi, B., Clavica, F., Kanai, A. J., Pickering, A. E., . . . Drake, M. J. (2019). Modulation of bladder wall micromotions alters intravesical pressure activity in the isolated bladder. *Frontiers in Physiology, 9*, 1937.

Chalubinski, K., Deutinger, J., & Bernaschek, G. (1993). Vaginosonography for recording of cycle-related myometrial contractions. *Fertility and Sterility, 59*(1), 225-228.

Chang, S. L., Chung, J. S., Yeung, M. K., Howard, P. S., & Macarak, E. J. (1999). Roles of the lamina propria and the detrusor in tension transfer during bladder filling. *Scandinavian journal of urology and nephrology. Supplementum, 201*, 38-45. 10.1080/003655999750042132

Chang, S. L., Howard, P. S., Koo, H. P., & Macarak, E. J. (1998). Role of type III collagen in bladder filling. *Neurourology and Urodynamics: Official Journal of the International Continence Society, 17*(2), 135-145.

Chard, T., Grudzinskas, J. G., & Grudzinskas, J. (1994). *The uterus*: Cambridge University Press.

Chen, J.-H., Yang, Z., Yu, Y., & Huizinga, J. D. (2016). Haustral boundary contractions in the proximal 3-taeniated rabbit colon. *American Journal of Physiology, 310*(3), G181-192.

Chen, J.-H., Zhang, Q., Yu, Y., Li, K., Liao, H., Jiang, L., . . . Chen, S. (2013). Neurogenic and myogenic properties of pan-colonic motor patterns and their spatiotemporal organization in rats. *PloS one, 8*(4), e60474.

Chen, J., & McCallum, R. W. (1992). Gastric slow wave abnormalities in patients with gastroparesis. *American Journal of Gastroenterology, 87*(4)

Cheng, F., Birder, L. A., Kullmann, F. A., Hornsby, J., Watton, P. N., Watkins, S., . . . Robertson, A. M. (2018). Layer-dependent role of collagen recruitment during loading of the rat bladder wall. *Biomechanics and modeling in mechanobiology, 17*(2), 403-417.

Cheng, Y., Mansfield, K., Sandow, S., Sadananda, P., Burcher, E., & Moore, K. (2011). Porcine bladder urothelial, myofibroblast, and detrusor muscle cells: characterization and ATP release. *Frontiers in pharmacology, 2*, 27.

Chess-Williams, R. (2002). Muscarinic receptors of the urinary bladder: detrusor, urothelial and prejunctional. *Autonomic and Autacoid Pharmacology, 22*(3), 133-145.

Christ, G. J., & Hodges, S. (2006). Molecular mechanisms of detrusor and corporal myocyte contraction: identifying targets for pharmacotherapy of bladder and erectile dysfunction. *British journal of pharmacology, 147 Suppl 2*(Suppl 2), S41-S55. 10.1038/sj.bjp.0706627

Christensen, A. P., & Corey, D. P. (2007). TRP channels in mechanosensation: direct or indirect activation? *Nature Reviews Neuroscience, 8*(7), 510-521.

ClinicalGate. (2015, 18 March). Smooth muscle and the cardiovascular and lymphatic systems. Retrieved 27 March 2020 from https://clinicalgate.com/smooth-muscle-and-the-cardiovascular-and-lymphatic-systems/

Coakley, F. V., Glenn, O. A., Qayyum, A., Barkovich, A. J., Goldstein, R., & Filly, R. A. (2004). Fetal MRI: a developing technique for the developing patient. *American Journal of Roentgenology, 182*(1), 243-252.

Cohen, L. H. (1972). Ultrasonic measurements of early fetal growth.

Cohen, W. R. (2017). Clinical assessment of uterine contractions. *Int J Gynaecol Obstet, 139*(2), 137-142. 10.1002/ijgo.12270

Cole, M., Shaffer, E., & Scott, R. (1987). Gallbladder pressure, compliance, and hysteresis during cyclic volume change. *Canadian journal of physiology and pharmacology, 65*(10), 2124-2130.

Collins, C., Klausner, A. P., Herrick, B., Koo, H. P., Miner, A. S., Henderson, S. C., & Ratz, P. H. (2009). Potential for control of detrusor smooth muscle spontaneous rhythmic contraction by cyclooxygenase products released by interstitial cells of Cajal. *Journal of cellular and molecular medicine, 13*(9b), 3236-3250.

Collins, C. W., & Winters, J. C. (2014). AUA/SUFU adult urodynamics guideline: a clinical review. *Urologic Clinics, 41*(3), 353-362.

Collins, J., Borojevic, R., Verdu, E., Huizinga, J., & Ratcliffe, E. (2014). Intestinal microbiota influence the early postnatal development of the enteric nervous system. *Neurogastroenterology and Motility, 26*(1), 98-107.

Connors, B. W. (2012). Tales of a Dirty Drug: Carbenoxolone, Gap Junctions, and Seizures: Carbenoxolone and Seizures. *Epilepsy currents, 12*(2), 66-68.

Conrad, J. T., Johnson, W. L., Kuhn, W. K., & Hunter, C. A. (1966). Passive stretch relationships in human uterine muscle. *American Journal of Obstetrics & Gynecology, 96*(8), 1055-1059.

Coolsaet, B. (1984). Cystometry. *Clinical gynecologic urology*, 59.

Coolsaet, B. (1985). Bladder compliance and detrusor activity during the collection phase. *Neurourology and Urodynamics, 4*(4), 263-273.

Coolsaet, B., Van Mastrigt, R., Van Duyl, W., & Huygen, R. (1976). Viscoelastic properties of bladder wall strips at constant elongation. *Investigative urology, 13*(6), 435.

Coolsaet, B. L., Van Duyl, W. A., Os-Bossagh, V., & De Bakker, H. V. (1993). New concepts in relation to urge and detrusor activity. *Neurourology and Urodynamics, 12*(5), 463-471.

Corner, G. W., & Csapo, A. (1953). Action of the ovarian hormones on uterine muscle. *British medical journal, 1*(4812), 687-693. 10.1136/bmj.1.4812.687

Cortivo, R., Pagano, F., Passerini, G., Abatangelo, G., & Castellani, I. (1981). Elastin and collagen in the normal and obstructed urinary bladder. *British Journal of Urology, 53*(2), 134-137.

Cosgrove, M., LaJoie, W., & Jones, W. (1977). Further observations of the detrusor electromyogram. *Urologia internationalis, 32*(2-3), 123-126.

Costa, M., Dodds, K. N., Wiklendt, L., Spencer, N. J., Brookes, S. J., & Dinning, P. G. (2013). Neurogenic and myogenic motor activity in the colon of the guinea pig, mouse, rabbit, and rat. *American Journal of Physiology-Gastrointestinal and Liver Physiology, 305*(10), G749-G759.

Costa, M., Wiklendt, L., Arkwright, J. W., Spencer, N. J., Omari, T., Brookes, S. J., & Dinning, P. G. (2013). An experimental method to identify neurogenic and myogenic active mechanical states of intestinal motility.

Craggs, M., & Stephenson, J. (1976). The real bladder electromyogram. *British Journal of Urology, 48*(6), 443-451.

Crankshaw, D. (1984). Muscarinic cholonoceptors in the rabbits myometrium: A study of the relationship between binding and response. *European journal of pharmacology, 101*(1-2), 1-10.

Cretoiu, D., Ciontea, S. M., Popescu, L., Ceafalan, L., & Ardeleanu, C. (2006). Interstitial Cajal-like cells (ICLC) as steroid hormone sensors in human myometrium: immunocytochemical approach. *Journal of cellular and molecular medicine, 10*(3), 789-795.

Csapo, A. (1956). Progesterone "block". *American Journal of Anatomy, 98*(2), 273-291.

Csapo, A. (1962). Smooth muscle as a contractile unit. *Physiological reviews. Supplement, 5*, 7-33.

Csapo, A. (1970). The diagnostic significance of the intrauterine pressure. *Obstetrical & gynecological survey, 25*(6), 515-543.

Csapo, A. I., Jaffin, H., Kerenyi, T., Lipman, J. I., & Wood, C. (1963). Volume and activity of the pregnant human uterus. *American Journal of Obstetrics and Gynecology, 85*(6), 819-835.

Csapo, A. I., & Lloyd-Jacob, M. A. (1962). Placenta, uterine volume, and the control of the pregnant uterus in rabbits. *American Journal of Obstetrics and Gynecology, 83*(8), 1073-1082. https://doi.org/10.1016/S0002-9378(16)35943-9

Csapo, A. I., Pulkkinen, M. O., & Wiest, W. (1973). Effects of luteectomy and progesterone replacement therapy in early pregnant patients. *American Journal of Obstetrics and Gynecology, 115*(6), 759-765.

Csapo, A. I., & Takeda, H. (1965). Effect of progesterone on the electric activity and intrauterine pressure of pregnant and parturient rabbits. *American Journal of Obstetrics and Gynecology, 91*(2), 221-231.

Cullingsworth, Z. E., Kelly, B. B., Deebel, N. A., Colhoun, A. F., Nagle, A. S., Klausner, A. P., & Speich, J. E. (2018). Automated quantification of low amplitude rhythmic contractions (LARC) during real-world urodynamics identifies a potential detrusor overactivity subgroup. *PLoS One, 13*(8), e0201594.

Cushny, A. R. (1906). On the movements of the uterus. *The Journal of physiology, 35*(1-2), 1.

Daly, D., Rong, W., Chess-Williams, R., Chapple, C., & Grundy, D. (2007). Bladder afferent sensitivity in wild-type and TRPV1 knockout mice. *The Journal of physiology, 583*(2), 663-674.

Danforth, D. (1947). The fibrous nature of the human cervix, and its relation to the isthmic segment in gravid and nongravid uteri. *American Journal of Obstetrics and Gynecology, 53*(4), 541-560.

Daniel, E. E. (1960). Effect of the placenta on the electrical activity of the cat uterus in vivo and in vitro. *American Journal of Obstetrics and Gynecology, 80*(2), 229-244.

Davidson, J. S., & Baumgarten, I. M. (1988). Glycyrrhetinic acid derivatives: a novel class of inhibitors of gap-junctional intercellular communication. Structure-activity relationships. *Journal of Pharmacology and Experimental Therapeutics, 246*(3), 1104-1107.

Davidson, R. A., & McCLOSKEY, K. D. (2005). Morphology and localization of interstitial cells in the guinea pig bladder: structural relationships with smooth muscle and neurons. *The Journal of urology, 173*(4), 1385-1390.

Davis, M. J., & Hill, M. A. (1999). Signaling mechanisms underlying the vascular myogenic response. *Physiological Reviews, 79*(2), 387-423.

Dawood, M. Y., Wang, C., Gupta, R., & Fuchs, F. (1978). Fetal contribution to oxytocin in human labor. *Obstetrics and gynecology, 52*(2), 205-209.

de Groat, W. C., Griffiths, D., & Yoshimura, N. (2015). Neural control of the lower urinary tract. *Comprehensive Physiology, 5*(1), 327.

De Jongh, R., Van Koeveringe, G. A., Van Kerrebroeck, P. E. V., Markerink-van Ittersum, M., De Vente, J., & Gillespie, J. I. (2007). The effects of exogenous prostaglandins and the identification of constitutive

cyclooxygenase I and II immunoreactivity in the normal guinea pig bladder. *BJU international, 100*(2), 419-429. 10.1111/j.1464-410X.2007.07011.x

de Loubens, C., Lentle, R. G., Hulls, C., Janssen, P. W., Love, R. J., & Chambers, J. P. e. (2014). Characterisation of Mixing in the Proximal Duodenum of the Rat during Longitudinal Contractions and Comparison with a Fluid Mechanical Model Based on Spatiotemporal Motility Data. *PloS one, 9*(4), e95000.

de Loubens, C., Lentle, R. G., Love, R. J., Hulls, C., & Janssen, P. W. M. (2013). Fluid mechanical consequences of pendular activity, segmentation, and pyloric outflow in the proximal duodenum of the rat and the guinea pig. *Journal of the Royal Society Interface, 10*(83), 20130027.

de Vries, K., Lyons, E. A., Ballard, G., Levi, C. S., & Lindsay, D. J. (1990). Contractions of the inner third of the myometrium. *American Journal of Obstetrics and Gynecology, 162*(3), 679-682.

Degani, S., Leibovitz, Z., Shapiro, I., Gonen, R., & Ohel, G. (1998). Myometrial thickness in pregnancy: longitudinal sonographic study. *Journal of ultrasound in medicine, 17*(10), 661-665.

Devedeux, D., Marque, C., Mansour, S., Germain, G., & Duchêne, J. (1993). Uterine electromyography: a critical review. *American Journal of Obstetrics and Gynecology, 169*(6), 1636-1653.

Di Lorenzo, C., Hillemeier, C., Hyman, P., Loening-Baucke, V., Nurko, S., Rosenberg, A., & Taminiau, J. (2002). Manometry studies in children: minimum standards for procedures. *Neurogastroenterology and Motility, 14*(4), 411-420.

Dinning, P., Wiklendt, L., Maslen, L., Gibbins, I., Patton, V., Arkwright, J., . . . Brookes, S. (2014a). Quantification of in vivo colonic motor patterns in healthy humans before and after a meal revealed by high-resolution fiber-optic manometry. *Neurogastroenterology and Motility, 26*(10), 1443-1457.

Dinning, P., Wiklendt, L., Maslen, L., Gibbins, I., Patton, V., Arkwright, J., . . . Brookes, S. (2014b). Quantification of in vivo colonic motor patterns in healthy humans before and after a meal revealed by high-resolution fiber-optic manometry. *Neurogastroenterology and Motility, 26*(10), 1443-1457.

Dinning, P. G., Costa, M., Brookes, S., & Spencer, N. J. (2012). Neurogenic and myogenic motor patterns of rabbit proximal, mid, and distal colon. *American Journal of Physiology-Gastrointestinal and Liver Physiology, 303*(1), G83-G92.

Dinning, P. G., Szczesniak, M. M., & Cook, I. J. (2008). Twenty four hour spatiotemporal mapping of colonic propagating sequences provides pathophysiological insight into constipation. *Neurogastroenterology and Motility, 20*(9), 1017-1021.

Dodds, K. N., Travis, L., Beckett, E. A., & Spencer, N. J. (2021). Identification of a novel distension-evoked motility pattern in the mouse uterus. *American Journal of Physiology-Regulatory, Integrative and Comparative Physiology, 321*(3), R317-R327.

Dörje, F., Wess, J., Lambrecht, G., Tacke, R., Mutschler, E., & Brann, M. (2012). Antagonist binding profiles of five cloned human muscarinic receptor subtypes.

Drake, M., Harvey, I., & Gillespie, J. (2003). Autonomous activity in the isolated guinea pig bladder. *Experimental physiology, 88*(1), 19-30.

Drake, M., Mills, I., & Gillespie, J. (2001). Model of peripheral autonomous modules and a myovesical plexus in normal and overactive bladder function. *The Lancet, 358*(9279), 401-403.

Drake, M. J., Fry, C. H., & Eyden, B. (2006). Structural characterization of myofibroblasts in the bladder. *BJU international, 97*(1), 29-32.

Drake, M. J., Gardner, B. P., & Brading, A. F. (2003). Innervation of the detrusor muscle bundle in neurogenic detrusor overactivity. *BJU International, 91*(7), 702-710.

Drake, M. J., Harvey, I. J., Gillespie, J. I., & Van Duyl, W. A. (2005). Localized contractions in the normal human bladder and in urinary urgency. *BJU international, 95*(7), 1002-1005.

Drake, M. J., Hedlund, P., Harvey, I. J., Pandita, R. K., Andersson, K.-E., & Gillespie, J. I. (2003). Partial outlet obstruction enhances modular autonomous activity in the isolated rat bladder. *The Journal of urology, 170*(1), 276-279.

Drake, M. J., Kanai, A., Bijos, D. A., Ikeda, Y., Zabbarova, I., Vahabi, B., & Fry, C. H. (2017). The potential role of unregulated autonomous bladder micromotions in urinary storage and voiding dysfunction; overactive bladder and detrusor underactivity. *BJU Int, 119*(1), 22-29. 10.1111/bju.13598

Dubin, N., Ghodgaonkar, R., & King, T. (1979). Role of prostaglandin production in spontaneous and oxytocin-induced uterine contractile activity in in vitro pregnant rat uteri. *Endocrinology, 105*(1), 47-51.

Dunford, J. R., Lutton, E. J., Atia, J., Blanks, A. M., & van den Berg, H. A. (2019). Computational physiology of uterine smooth muscle. *Science progress, 102*(2), 103-126.

Duquette, R., Shmygol, A., Vaillant, C., Mobasheri, A., Pope, M., Burdyga, T., & Wray, S. (2005). Vimentin-positive, c-kit-negative interstitial cells in human and rat uterus: a role in pacemaking? *Biology of reproduction, 72*(2), 276-283.

Durnwald, C. P., & Mercer, B. M. (2008). Myometrial thickness according to uterine site, gestational age and prior cesarean delivery. *J Matern Fetal Neonatal Med, 21*(4), 247-250. 10.1080/14767050801926709

Eastham, J. E., & Gillespie, J. I. (2013). The concept of peripheral modulation of bladder sensation. *Organogenesis, 9*(3), 224-233.

Eglen, R., Bonhaus, D., Calixto, J., Choppin, A., Leung, E., Loeb, M., . . . Hegde, S. (1997). *Characterization of the interaction of tolterodine at muscarinic receptor subtypes in vitro and in vivo.* Paper presented at the British journal of pharmacology.

Eglen, R., & Nahorski, S. (2000). The muscarinic M5 receptor: a silent or emerging subtype? *British journal of pharmacology, 130*(1), 13.

Ek, A., Alm, P., Andersson, K. E., & Persson, C. (1977). Adrenergic and cholinergic nerves of the human urethra and urinary bladder. A histochemical study. *Acta physiologica scandinavica, 99*(3), 345-352.

Ekman-Ordeberg, G., Stjernholm, Y., Wang, H., Stygar, D., & Sahlin, L. (2003). Endocrine regulation of cervical ripening in humans—potential roles for gonadal steroids and insulin-like growth factor-I. *Steroids, 68*(10-13), 837-847.

Ekman, G., Malmström, A., Uldbjerg, N., & Ulmsten, U. (1986). Cervical collagen: an important regulator of cervical function in term labor. *Obstetrics and gynecology, 67*(5), 633-636.

Elbadawi, A. (1995). Pathology and pathophysiology of detrusor in incontinence. *The Urologic clinics of North America, 22*(3), 499-512.

Elmer, M., Alm, P., & Thorbert, G. (1980). Electrical field stimulation of myometrial strips from non-pregnant and pregnant guinea-pigs. *Acta physiologica scandinavica, 108*(3), 209-213.

Eroschenko, V. P. (2008). *DiFiore's atlas of histology with functional correlations*: Lippincott Williams & Wilkins.

Escalante-Gaytán, J., Esquivel-Arizmendi, C. G., Ledesma-Ramírez, C. I., Pliego-Carrillo, A. C., García-González, M. T., & Reyes-Lagos, J. J. (2019). Usefulness of the electrohysterography in the clinical field as a technique for uterine monitoring: A literature review. *Ginecología y Obstetricia de México, 87*(01), 46-59.

Escalante, N., & Pino, J. (2017). Arrangement of Muscle Fibers in the Myometrium of the Human Uterus: A Mesoscopic Study. *MOJ Anatomy & Physiology, 4*(2), 131-135.

Evans, H., & Sack, W. O. (1973). Prenatal development of domestic and laboratory mammals: growth curves, external features and selected references. *Anatomia, Histologia, Embryologia, 2*(1), 11-45.

Ewalt, D. H., Howard, P. S., Blyth, B., Snyder III, H. M., Duckett, J. W., Levin, R. M., & Macarak, E. J. (1992). Is lamina propria matrix responsible for normal bladder compliance? *The Journal of urology, 148*(2), 544-549.

Eytan, O., Jaffa, A. J., Har-Toov, J., Dalach, E., & Elad, D. (1999). Dynamics of the intrauterine fluid–wall interface. *Annals of Biomedical Engineering, 27*(3), 372-379.

Fang, S., McLean, J., Shi, L., Vink, J.-S. Y., Hendon, C. P., & Myers, K. M. (2021). Anisotropic mechanical properties of the human uterus measured by spherical indentation. *Annals of biomedical engineering, 49*(8), 1923-1942.

Farrer-Brown, G., Beilby, J., & Tarbit, M. (1970). The blood supply of the uterus: 1. Arterial vasculature. *BJOG: An International Journal of Obstetrics & Gynaecology, 77*(8), 673-681.

Ferguson, D., Kennedy, I., & Burton, T. (1997). ATP is released from rabbit urinary bladder epithelial cells by hydrostatic pressure changes–possible sensory mechanism? *The Journal of physiology, 505*(2), 503-511.

Ferrell, C. L., Garrett, W. N., & Hinman, N. (1976). Growth, Development and Composition of the Udder and Gravid Uterus of Beef Heifers during Pregnancy. *Journal of Animal Science, 42*(6), 1477-1489. 10.2527/jas1976.4261477x

Finkbeiner, A. E. (1999). In vitro responses of detrusor smooth muscle to stretch and relaxation. *Scand J Urol Nephrol Suppl, 201*, 5-11. 10.1080/003655999750042088

Finkbeiner, A. E., & O'Donnell, P. D. (1990). Responses of detrusor smooth muscle to stretch and relaxation: in vitro study. *Urology, 36*(2), 193-198.

Fisk, N., Ronderos-Dumit, D., Tannirandorn, Y., Nicolini, U., Talbert, D., & Rodeck, C. (1992). Normal amniotic pressure throughout gestation. *BJOG: An International Journal of Obstetrics & Gynaecology, 99*(1), 18-22.

Fowler, C. J., Griffiths, D., & De Groat, W. C. (2008). The neural control of micturition. *Nature Reviews Neuroscience, 9*(6), 453-466.

Frazier, E. P., Peters, S. L., Braverman, A. S., Ruggieri, M. R., & Michel, M. C. (2008). Signal transduction underlying the control of urinary bladder smooth muscle tone by muscarinic receptors and β-adrenoceptors. *Naunyn-Schmiedeberg's Archives of Pharmacology, 377*(4-6), 449-462.

Freed, A. D., & Doehring, T. C. (2005). Elastic model for crimped collagen fibrils.

Frei, W., & Chen, C.-C. (1977). Fast Boundary Detection: A Generalizationand New Algorithm. *IEEE Transactions on Computers, 26*(10)

Fry, C., Cooklin, M., Birns, J., & Mundy, A. (1999). Measurement of intercellular electrical coupling in guinea-pig detrusor smooth muscle. *The Journal of urology, 161*(2), 660-664.

Fry, C., Gallegos, C., & Montgomery, B. (1994). The actions of extracellular H+ on the electrophysiological properties of isolated human detrusor smooth muscle cells. *The Journal of physiology, 480*(1), 71-80.

Fry, C. H., & McCloskey, K. D. (2019). Spontaneous Activity and the Urinary Bladder. In H. Hashitani & R. J. Lang (Eds.), *Smooth Muscle Spontaneous Activity: Physiological and Pathological Modulation* (pp. 121-147). Singapore: Springer Singapore. 10.1007/978-981-13-5895-1_5

Fry, C. H., Meng, E., & Young, J. S. (2010). The physiological function of lower urinary tract smooth muscle. *Auton Neurosci, 154*(1-2), 3-13. 10.1016/j.autneu.2009.10.006

Fry, C. H., Sui, G.-P., Severs, N. J., & Wu, C. (2004). Spontaneous activity and electrical coupling in human detrusor smooth muscle: implications for detrusor overactivity? *Urology, 63*(3), 3-10.

Fry, C. H., Young, J., Jabr, R. I., McCarthy, C., Ikeda, Y., & Kanai, A. J. (2012). Modulation of spontaneous activity in the overactive bladder: the role of P2Y agonists. *American Journal of Physiology-Renal Physiology, 302*(11), F1447-F1454.

Fuchs, A.-R. (1978). Hormonal control of myometrial function during pregnancy and parturition. *European Journal of Endocrinology, 89*(4_Suppla), S9-NP.

Fuchs, A.-R., Fuchs, F., Husslein, P., & Soloff, M. S. (1984). Oxytocin receptors in the human uterus during pregnancy and parturition. *American Journal of Obstetrics and Gynecology, 150*(6), 734-741.

Fuchs, A.-R., Fuchs, F., Husslein, P., Soloff, M. S., & Fernstrom, M. J. (1982). Oxytocin receptors and human parturition: a dual role for oxytocin in the initiation of labor. *Science, 215*(4538), 1396-1398.

Fuchs, A. R., & Fuschs, F. (1984). Endocrinology of human parturition: a review. *BJOG: An International Journal of Obstetrics & Gynaecology, 91*(10), 948-967.

Gabella, G., Bulbring, E., Brading, A., Jones, A., & Tomita, T. (1981). Smooth muscle: An assessment of current knowledge. In *Edward Arnold* (pp. 1-46).

Garfield, R. (1986). Structural studies of innervation on nonpregnant rat uterus. *American Journal of Physiology-Cell Physiology, 251*(1), C41-C54.

Garfield, R., Blennerhassett, M., & Miller, S. (1988). Control of myometrial contractility: role and regulation of gap junctions. *Oxford reviews of reproductive biology, 10*, 436-490.

Garfield, R., & Somlyo, A. (1985). Structure of smooth muscle. In *Calcium and contractility* (pp. 1-36): Springer.

Garfield, R., Yallampalli, C., Chard, T., & Grudzinskas, J. (1994). Structure and function of uterine muscle. *The uterus*, 54-93.

Garfield, R. E., & Maner, W. L. (2007). *Physiology and electrical activity of uterine contractions.* Paper presented at the Seminars in Cell and Developmental Biology.

Garrioch, D. (1978). The effect of indomethacin on spontaneous activity in the isolated human myometrium and on the response to oxytocin and prostaglandin. *BJOG: An International Journal of Obstetrics & Gynaecology, 85*(1), 47-52.

Geiger, B., & Ginsberg, D. (1991). The cytoplasmic domain of adherens-type junctions. *Cell Motility, 20*(1), 1-6. 10.1002/cm.970200102

Geiger, B., Yehuda-Levenberg, S., & Bershadsky, A. (1995). Molecular interactions in the submembrane plaque of cell-cell and cell-matrix adhesions. *Cells Tissues Organs, 154*(1), 46-62.

Geirsson, R., Ogston, S., Patel, N., & Christie, A. (1985). Growth of total intrauterine, intra-amniotic and placental volume in normal singleton pregnancy measured by ultrasound. *BJOG: An International Journal of Obstetrics & Gynaecology, 92*(1), 46-53.

Geisler, K., Künzel, J., Grundtner, P., Müller, A., Beckmann, M. W., & Dittrich, R. (2012). The perfused swine uterus model: long-term perfusion. *Reproductive Biology and Endocrinology, 10*(1), 1-10.

Gevaert, T., Ost, D., & De Ridder, D. (2006). Comparison study of autonomous activity in bladders from normal and paraplegic rats. *Neurourology and Urodynamics, 25*(4), 368-378.

Ghulé, V. V., Gray, C., Galimberti, A., & Anumba, D. O. (2012). Prostaglandin-induced cervical remodelling in humans in the first trimester is associated with increased expression of specific tight junction, but not gap junction proteins. *Journal of translational medicine, 10*(1), 40.

Gilbert, T. W., Wognum, S., Joyce, E. M., Freytes, D. O., Sacks, M. S., & Badylak, S. F. (2008). Collagen fiber alignment and biaxial mechanical behavior of porcine urinary bladder derived extracellular matrix. *Biomaterials, 29*(36), 4775-4782.

Gillespie, E. C. (1950). Principles of uterine growth in pregnancy. *American Journal of Obstetrics and Gynecology, 59*(5), 949-959.

Gillespie, J. (2004a). The autonomous bladder: a view of the origin of bladder overactivity and sensory urge. *BJU international, 93*(4), 478-483.

Gillespie, J. (2004b). Modulation of autonomous contractile activity in the isolated whole bladder of the guinea pig. *BJU international, 93*(3), 393-400.

Gillespie, J., Harvey, I., & Drake, M. (2003). Agonist-and nerve-induced phasic activity in the isolated whole bladder of the guinea pig: evidence for two types of bladder activity. *Experimental physiology, 88*(3), 343-357.

Gillespie, J. I., Palea, S., Guilloteau, V., Guerard, M., Lluel, P., & Korstanje, C. (2012a). Modulation of non-voiding activity by the muscarinergic antagonist tolterodine and the β3-adrenoceptor agonist mirabegron in conscious rats with partial outflow obstruction. *BJU international, 110*(2b), E132-E142.

Gillespie, J. I., Palea, S., Guilloteau, V., Guerard, M., Lluel, P., & Korstanje, C. (2012b). Modulation of non-voiding activity by the muscarinergic antagonist tolterodine and the β3-adrenoceptor agonist mirabegron in conscious rats with partial outflow obstruction. *BJU International, 110*(2b)

Gillespie, P. G., & Walker, R. G. (2001). Molecular basis of mechanosensory transduction. *Nature, 413*(6852), 194-202.

Gloeckner, D. C., Sacks, M. S., Fraser, M. O., Somogyi, G. T., De Groat, W. C., & Chancellor, M. B. (2002). Passive biaxial mechanical properties of the rat bladder wall after spinal cord injury. *The Journal of urology, 167*(5), 2247-2252.

Goerttler, K. (1968). Structure of the human uterus wall. *Archiv fur Gynakologie, 205*(4), 334-342.

Goto, M., & Woodbury, J. (1958). *Effects of stretch and NaCl on transmembrane potentials and tension of pregnant rat uterus.* Paper presented at the Federation Proceedings.

Gray, S. M., McGeown, J. G., McMurray, G., & McCloskey, K. D. (2013). Functional innervation of Guinea-pig bladder interstitial cells of cajal subtypes: neurogenic stimulation evokes in situ calcium transients. *PLoS One, 8*(1), e53423.

Gregersen, H. (2003). *Biomechanics of the gastrointestinal tract: new perspectives in motility research and diagnostics*: Springer Science & Business Media.

Gregersen, H., & Christensen, J. (2000). Gastrointestinal tone. *Neurogastroenterology & Motility, 12*(6), 501-508.

Griffin, C. S., Thornbury, K. D., Hollywood, M. A., & Sergeant, G. P. (2018). Muscarinic receptor-induced contractions of the detrusor are impaired in TRPC4 deficient mice. *Scientific reports, 8*(1), 1-11.

Grover, A., Kwan, C., & Daniel, E. (1981). Na--Ca exchange in rat myometrium membrane vesicles highly enriched in plasma membranes. *American Journal of Physiology-Cell Physiology, 240*(5), C175-C182.

Guharay, F., & Sachs, F. (1984). Stretch-activated single ion channel currents in tissue-cultured embryonic chick skeletal muscle. *The Journal of physiology, 352*(1), 685-701.

Guneyli, S., Ward, E., Peng, Y., Nehal Yousuf, A., Trilisky, I., Westin, C., . . . Oto, A. (2017). MRI evaluation of benign prostatic hyperplasia: Correlation with international prostate symptom score. *Journal of Magnetic Resonance Imaging, 45*(3), 917-925.

Gunja-Smith, Z., & Woessner Jr, J. F. (1985). Content of the collagen and elastin cross-links pyridinoline and the desmosines in the human uterus in various reproductive states. *American Journal of Obstetrics and Gynecology, 153*(1), 92-95.

Gurtovenko, A. A., & Anwar, J. (2007). Modulating the structure and properties of cell membranes: the molecular mechanism of action of dimethyl sulfoxide. *The journal of physical chemistry B, 111*(35), 10453-10460.

Gwynne, R. M., Thomas, E. A., Goh, S. M., Sjovall, H., & Bornstein, J. C. (2004). Segmentation induced by intraluminal fatty acid in isolated guinea-pig duodenum and jejunum. *Journal of Physiology, 556*(2), 557-569.

Haase, E. B., Buchman, J., Tietz, A. E., & Schramm, L. P. (1997). Pregnancy-induced uterine neuronal degeneration in the rat. *Cell and tissue research, 288*(2), 293-306.

Habteyes, F. (2014). Modeling Acute Changes in Bladder Wall Tension, Shape and Compliance During Filling.

Hai, C.-M., & Murphy, R. A. (1988). Regulation of shortening velocity by cross-bridge phosphorylation in smooth muscle. *American Journal of Physiology-Cell Physiology, 255*(1), C86-C94.

Hajagos-Tóth, J., Falkay, G., & Gáspár, R. (2009). Modification of the effect of nifedipine in the pregnant rat myometrium: the influence of progesterone and terbutaline. *Life sciences, 85*(15-16), 568-572.

Haluska, G. J., & Novy, M. J. (1993). *Hormonal modulation of uterine activity during primate parturition.* Paper presented at the Seminars in reproductive endocrinology.

Hamill, O. P., & Martinac, B. (2001). Molecular basis of mechanotransduction in living cells. *Physiological Reviews, 81*(2), 685-740.

Hammad, F. T., Stephen, B., Lubbad, L., Morrison, J. F., & Lammers, W. (2014). Macroscopic electrical propagation in the guinea pig urinary bladder. *American Journal of Physiology-Renal Physiology, 307*(2), F172-F182.

Hanna-Mitchell, A. T., Beckel, J. M., Barbadora, S., Kanai, A. J., de Groat, W. C., & Birder, L. A. (2007). Non-neuronal acetylcholine and urinary bladder urothelium. *Life sciences, 80*(24-25), 2298-2302.

Hariss, D., Marsh, K., Birmingham, A., & Hill, S. (1995). Expression of muscarinic M 3 receptor coupled to inositol phospholipid hydrolysis in human detrusor cultured smooth cells. *J. Urol, 154*, 1241-1245.

Hashitani, H. (2006). Interaction between interstitial cells and smooth muscles in the lower urinary tract and penis. *J Physiol, 576*(Pt 3), 707-714. 10.1113/jphysiol.2006.116632

Hashitani, H., & Brading, A. F. (2003a). Electrical properties of detrusor smooth muscles from the pig and human urinary bladder. *British Journal of Pharmacology, 140*(1), 146-158.

Hashitani, H., & Brading, A. F. (2003). Electrical properties of detrusor smooth muscles from the pig and human urinary bladder. *Br J Pharmacol, 140*(1), 146-158. 10.1038/sj.bjp.0705319

Hashitani, H., & Brading, A. F. (2003b). Ionic basis for the regulation of spontaneous excitation in detrusor smooth muscle cells of the guinea-pig urinary bladder. *British journal of pharmacology, 140*(1), 159-169.

Hashitani, H., Brading, A. F., & Suzuki, H. (2004). Correlation between spontaneous electrical, calcium and mechanical activity in detrusor smooth muscle of the guinea-pig bladder. *British journal of pharmacology, 141*(1), 183-193.

Hashitani, H., Fukuta, H., Takano, H., Klemm, M. F., & Suzuki, H. (2001). Origin and propagation of spontaneous excitation in smooth muscle of the guinea-pig urinary bladder. *Journal of Physiology, 530*(2), 273-286.

Hashitani, H., & Lang, R. J. (2010). Functions of ICC-like cells in the urinary tract and male genital organs. *Journal of cellular and molecular medicine, 14*(6a), 1199-1211.

Hashitani, H., Yanai, Y., & Suzuki, H. (2004a). Role of interstitial cells and gap junctions in the transmission of spontaneous Ca^{2+} signals in detrusor smooth muscles of the guinea-pig urinary bladder. *Journal of Physiology, 559*(2), 567-581.

Hashitani, H., Yanai, Y., & Suzuki, H. (2004b). Role of interstitial cells and gap junctions in the transmission of spontaneous Ca2+ signals in detrusor smooth muscles of the guinea-pig urinary bladder. *The Journal of physiology, 559*(2), 567-581.

Heinricius, G. (1889). En metod att grafiskt atergiva kontraktioner hos en icke gravid livmoder. *Finsk Lakaresallsk Handl, 31*, 349.

Hennessy, R. J., Kinsella, A., & Waddington, J. L. (2002). 3D laser surface scanning and geometric morphometric analysis of craniofacial shape as an index of cerebro-craniofacial morphogenesis: initial application to sexual dimorphism. *Biological Psychiatry, 51*(6), 507-514.

Hennig, G. W., Costa, M., Chen, B. N., & Brookes, S. J. H. (1999). Quantitative analysis of peristalsis in the guinea-pig small intestine using spatio-temporal maps. *Journal of Physiology, 517*, 575-590.

Hennig, G. W., Gregory, S., Brookes, S. J. H., & Costa, M. (2010). Non-peristaltic patterns of motor activity in the guinea-pig proximal colon. *Neurogastroenterology and Motility, 22*, e207–217.

Hennig, G. W., Spencer, N. J., Jokela-Willis, S., Bayguinov, P. O., Lee, H., Ritchie, L. A., . . . Sanders, K. M. (2010). ICC-MY coordinate smooth muscle electrical and mechanical activity in the murine small intestine. *Neurogastroenterology and Motility, 22*(5), e138-151.

Heppner, T., Bonev, A., & Nelson, M. (1997). Ca (2+)-activated K+ channels regulate action potential repolarization in urinary bladder smooth muscle. *American Journal of Physiology-Cell Physiology, 273*(1), C110-C117.

Heppner, T. J., Tykocki, N. R., Hill-Eubanks, D., & Nelson, M. T. (2016). Transient contractions of urinary bladder smooth muscle are drivers of afferent nerve activity during filling. *J Gen Physiol, 147*(4), 323-335. 10.1085/jgp.201511550

Hill, W. G. (2015). Control of urinary drainage and voiding. *Clin J Am Soc Nephrol, 10*(3), 480-492. 10.2215/CJN.04520413

Hinman, F., & Cox, C. E. (1967). Residual Urine Volume in Normal-Male Subjects. *The Journal of urology, 97*(4), 641-645.

Hirst, G., & Ward, S. (2003). Interstitial cells: involvement in rhythmicity and neural control of gut smooth muscle. *The Journal of physiology, 550*(2), 337-346.

Hocaoglu, Y., Roosen, A., Herrmann, K., Tritschler, S., Stief, C., & Bauer, R. M. (2012). Real-time magnetic resonance imaging (MRI): anatomical changes during physiological voiding in men. *BJU international, 109*(2), 234-239.

Homma, Y., Battista, J., Sb, B., Griffiths, D., Hilton, P., Kramer, G., . . . Rosier, P. (2002). In (pp. 317-372).

Honnebier, M. B. O., Jenkins, S. L., Wentworth, R. A., Figueroa, J. P., & Nathanielsz, P. W. (1991). Temporal structuring of delivery in the absence of a photoperiod: preparturient myometrial activity of the rhesus monkey is related to maternal body temperature and depends on the maternal circadian system. *Biology of reproduction, 45*(4), 617-625.

Hossler, F. E., & Monson, F. C. (1995). Microvasculature of the rabbit urinary bladder. *The Anatomical Record, 243*(4), 438-448.

House, M., Bhadelia, R. A., Myers, K., & Socrate, S. (2009). Magnetic resonance imaging of three-dimensional cervical anatomy in the second and third trimester. *European Journal of Obstetrics & Gynecology and Reproductive Biology, 144*, S65-S69.

Hsu, K.-F., Pan, H.-A., Hsu, Y.-Y., Wu, C.-M., Chung, W.-J., & Huang, S.-C. (2014). Enhanced myometrial autophagy in postpartum uterine involution. *Taiwanese Journal of Obstetrics and Gynecology, 53*(3), 293-302.

Huang, Y., Sammali, F., Blank, C., Kuijsters, N., Rabotti, C., Schoot, B., & Mischi, M. (2018). *Quantitative ultrasound imaging and characterization of uterine peristaltic waves.* Paper presented at the 2018 IEEE International Ultrasonics Symposium (IUS).

Huber, A., Hudelist, G., Czerwenka, K., Husslein, P., Kubista, E., & Singer, C. F. (2005). Gene expression profiling of cervical tissue during physiological cervical effacement. *Obstetrics & Gynecology, 105*(1), 91-98.

Huizinga, J. D., Lammers, W. J. E. P., Mikkelsen, H. B., Zhu, Y., & Wang, X. Y. (2010). Toward a Concept of Stretch Coupling in Smooth Muscle: A Thesis by Lars Thuneberg on Contractile Activity in Neonatal Interstitial Cells of Cajal. *Anatomical Record, 293*(9), 1543-1552.

Huizinga, J. D., Parsons, S. P., Chen, J.-H., Pawelka, A., Pistilli, M., Li, C., . . . Tong, M. (2015). Motor patterns of the small intestine explained by phase-amplitude coupling of two pacemaker activities: the critical importance of propagation velocity. *American Journal of Physiology-Cell Physiology, 309*(6), C403-C414.

Hulls, C., Lentle, R. G., de Loubens, C., Janssen, P. W., Chambers, P., & Stafford, K. J. (2012). Spatiotemporal mapping of ex vivo motility in the caecum of the rabbit. *Journal of Comparative Physiology B, 182*(2), 287-297.

Hulls, C., Lentle, R. G., de Loubens, C., Janssen, P. W. M., Chambers, P., & Stafford, K. J. (2012). Spatiotemporal mapping of ex vivo motility in the caecum of the rabbit. *Journal of Comparative Physiology. B, Biochemical, Systemic, and Environmental Physiology, B182*, 287-297. 10.1007/s00360-011-0610-2

Hulls, C. M., Lentle, R. G., King, Q., Reynolds, G. W., & Chambers, J. P. (2017). Spatiotemporal analysis of spontaneous myogenic contractions in the urinary bladder of the rabbit: timing and patterns reflect reported electrophysiology. *American Journal of Physiology-Renal Physiology, 313*(3), F687-F698.

Hulls, C. M., Lentle, R. G., King, Q. M., Chambers, J. P., & Reynolds, G. W. (2019). Pharmacological modulation of the spatiotemporal disposition of micromotions in the intact resting urinary bladder of the rabbit; their pattern is under both myogenic and autonomic control. *BJU International*

Hurd, W. W., & Falcone, T. (2007). Clinical reproductive medicine and surgery. St Louis, Mo: Mosby. In: Elsevier.

Huszar, G., & Naftolin, F. (1984). The myometrium and uterine cervix in normal and preterm labor. *New England Journal of Medicine, 311*(9), 571-581.

Hutchings, G., Williams, O., Cretoiu, D., & Ciontea, S. M. (2009). Myometrial interstitial cells and the coordination of myometrial contractility. *Journal of Cellular and Molecular Medicine, 13*(10), 4268-4282.

Igawa, Y., & Michel, M. C. (2013). Pharmacological profile of β3-adrenoceptor agonists in clinical development for the treatment of overactive bladder syndrome. In (Vol. 386, pp. 177-183): Springer.

Igawa, Y., YAMAZAKI, Y., TAKEDA, H., KAIDOH, K., AKAHANE, M., AJISAWA, Y., . . . ANDERSSON, K.-E. (2001). Relaxant effects of isoproterenol and selective β3-adrenoceptor agonists on normal, low compliant and hyperreflexic human bladders. *The Journal of urology, 165*(1), 240-244.

Iggo, A. (1955). Tension receptors in the stomach and the urinary bladder. *The Journal of physiology, 128*(3), 593-607.

Ikeda, Y., Fry, C., Hayashi, F., Stolz, D., Griffiths, D., & Kanai, A. (2007). Role of gap junctions in spontaneous activity of the rat bladder. *American Journal of Physiology-Renal Physiology, 293*(4), F1018-F1025.

Imtiaz, M. S., von der Weid, P. Y., & van Helden, D. F. (2010). Synchronization of Ca2+ oscillations: a coupled oscillator-based mechanism in smooth muscle. *The FEBS journal, 277*(2), 278-285.

Ishikawa, M., & Fuchs, A.-R. (1978). Electrical and mechanical activity of rat uterus in vivo during the estrous cycle. *American Journal of Obstetrics and Gynecology, 132*(6), 611-619.

Izumi, H. (1985). Changes in the mechanical properties of the longitudinal and circular muscle tissues of the rat myometrium during gestation. *British journal of pharmacology, 86*(1), 247.

Jähne, B. (2004). *Practical Handbook on Image Processing for Scientific and Technical Applications* (2nd ed.). Boca Raton: CRC Press.

Janssen, P. W. M., & Lentle, R. G. (2013). Spatiotemporal Mapping Techniques for Quantifying Gut Motility. In L. K. Cheng & G. Farrugia (Eds.), *New Advances in Gastrointestinal Motility Research* (pp. 219-241). New York: Springer.

Janssen, P. W. M., Lentle, R. G., Chambers, P., Reynolds, G. W., De Loubens, C., & Hulls, C. M. (2014). Spatiotemporal organization of standing postprandial contractions in the distal ileum of the anesthetized pig. *Neurogastroenterology and Motility, 26*(11), 1651-1662.

Janssen, P. W. M., Lentle, R. G., Hulls, C., Ravindran, V., & Amerah, A. M. (2009). Spatiotemporal mapping of the motility of the isolated chicken caecum. *Journal of Comparative Physiology. B, Biochemical, Systemic, and Environmental Physiology, B179*(5), 593-604.

Jelen, K., Lopot, F., Budka, Š., Novacek, V., & Sedlacek, R. (2008). Rheological properties of myometrium: experimental quantification and mathematical modeling. *Neuroendocrinology Letters, 29*(4), 454.

Jenkin, G., & Young, I. R. (2004). Mechanisms responsible for parturition; the use of experimental models. *Animal Reproduction Science, 82*, 567-581.

Jespersen, B., Tykocki, N. R., Watts, S. W., & Cobbett, P. J. (2015). Measurement of smooth muscle function in the isolated tissue bath-applications to pharmacology research. *JoVE (Journal of Visualized Experiments)*(95), e52324.

Jezior, J. R., Brady, J. D., Rosenstein, D. I., McCammon, K. A., Miner, A. S., & Ratz, P. H. (2001). Dependency of detrusor contractions on calcium sensitization and calcium entry through LOE-908-sensitive channels. *British journal of pharmacology, 134*(1), 78-87.

Ji, G., Barsotti, R. J., Feldman, M. E., & Kotlikoff, M. I. (2002). Stretch-induced calcium release in smooth muscle. *The Journal of General Physiology, 119*(6), 533-543.

Ji, H., Long, V., Briody, V., & Chien, E. K. (2011). Progesterone modulates integrin α2 (ITGA2) and α11 (ITGA11) in the pregnant cervix. *Reproductive sciences, 18*(2), 156-163.

John, H., Walch, M., Lehmann, T., & Maake, C. (2009). Connexin45 expression in the human obstructed detrusor muscle. *World journal of urology, 27*(3), 411-418.

John, H., Wang, X., Wehrli, E., Hauri, D., & Maake, C. (2003). Evidence of gap junctions in the stable nonobstructed human bladder. *The Journal of urology, 169*(2), 745-749.

Johnston, L., Carson, C., Lyons, A. D., Davidson, R. A., & McCloskey, K. D. (2008). Cholinergic-induced Ca2+ signaling in interstitial cells of Cajal from the guinea pig bladder. *American Journal of Physiology-Renal Physiology, 294*(3), F645-F655.

Johnston, L., Woolsey, S., Cunningham, R. M., O'Kane, H., Duggan, B., Keane, P., & McCloskey, K. D. (2010). Morphological expression of KIT positive interstitial cells of Cajal in human bladder. *The Journal of urology, 184*(1), 370-377.

Jünemann, K., Scheepe, J., Persson-Jünemann, C., Schmidt, P., Abel, K., Zwick, A., . . . Alken, P. (1994). Basic experimental studies on corpus cavernosum electromyography and smooth-muscle electromyography of the urinary bladder. *World journal of urology, 12*(5), 266-273.

Kagami, K., Ono, M., Iizuka, T., Matsumoto, T., Hosono, T., Sekizuka-Kagami, N., . . . Fujiwara, H. (2020). A novel third mesh-like myometrial layer connects the longitudinal and circular muscle fibers-A potential stratum to coordinate uterine contractions. *Scientific reports, 10*(1), 1-7.

Kajioka, S., Nakayama, S., McMurray, G., Abe, K., & Brading, A. F. (2002). Ca2+ channel properties in smooth muscle cells of the urinary bladder from pig and human. *European journal of pharmacology, 443*(1-3), 19-29.

Kanai, A., & Andersson, K. E. (2010). Bladder afferent signaling: recent findings. *J Urol, 183*(4), 1288-1295. 10.1016/j.juro.2009.12.060

Kane, M., Morgan, P., & Coonan, C. (1997). Peptide growth factors and preimplantation development. *Human reproduction update, 3*(2), 137-157.

Karim, S., & Hillier, K. (1979). Prostaglandins in the control of animal and human reproduction. *British medical bulletin, 35*(2), 173.

Kasza, K. E., Rowat, A. C., Liu, J., Angelini, T. E., Brangwynne, C. P., Koenderink, G. H., & Weitz, D. A. (2007). The cell as a material. *Current Opinion in Cell Biology, 19*(1), 101-107.

Kawarabayashi, T., & Marshall, J. M. (1981). Factors Influencing Circular Muscle Activity in the Pregnant Rat Uterus1. *Biology of reproduction, 24*(2), 373-379. 10.1095/biolreprod24.2.373

Kaya, C., & Şahin, B. (2016). The role of extracellular matrix proteins in the urinary tract: a literature review. *Composition and Function of the Extracellular Matrix in the Human Body*

Keelan, J. A., Coleman, M., & Mitchell, M. D. (1997). The molecular mechanisms of term and preterm labor: recent progress and clinical implications. *Clinical obstetrics and gynecology, 40*(3), 460-478.

Kelly, J. V. (1962). Myometrial Participation in Human Sperm Transport: A Dilemma. *Fertility and Sterility, 13*(1), 84-92. 10.1016/S0015-0282(16)34387-4

Kelly, P. (2020). Solid Mechanics Lecture Notes Part 1. 185-193.

KIER, W. M., & SMITH, K. K. (1985). Tongues, tentacles and trunks: the biomechanics of movement in muscular-hydrostats. *Zoological Journal of the Linnean Society, 83*(4), 307-324. https://doi.org/10.1111/j.1096-3642.1985.tb01178.x

Kinder, M., Gommer, E., Janknegt, R., & Van Waalwijk van Doorn, E. (1997). A method for the electromyographic mapping of the detrusor smooth muscle. *Archives of physiology and biochemistry, 105*(7), 673-690.

Kinder, R., & Mundy, A. (1987). Pathophysiology of Idiopathic Detrusor Instability and Detrusor Hyper-reflexia: An in vitro Study of Human Detrusor Muscle. *British Journal of Urology, 60*(6), 509-515.

Kirber, M. T., Walsh, J. V., & Singer, J. J. (1988). Stretch-activated ion channels in smooth muscle: a mechanism for the initiation of stretch-induced contraction. *Pflügers Archiv European Journal of Physiology, 412*(4), 339-345.

Kirsch, R. A. (1971). Computer determination of the constituent structure of biological images. *Computers and Biomedical Research, 4*(3), 315-328.

Klevmark, B. (1974). Motility of the Urinary Bladder in Cats during Filling at Physiological Rates: I. Intravesical Pressure Patterns Studied by a New Methods of Cystometry. *Acta Physiologica, 90*(3), 565-577.

Klöckner, U., & Isenberg, G. (1985). Action potentials and net membrane currents of isolated smooth muscle cells (urinary bladder of the guinea-pig). *Pflügers Archiv, 405*(4), 329-339.

Koh, B. H., Roy, R., Hollywood, M. A., Thornbury, K. D., McHale, N. G., Sergeant, G. P., . . . Koh, S. D. (2012). Platelet-derived growth factor receptor-α cells in mouse urinary bladder: a new class of interstitial cells. *Journal of Cellular and Molecular Medicine, 16*(4), 691-700.

Kondo, A., & Susset, J. G. (1973). Physical properties of the urinary detrusor muscle: a mechanical model based upon the analysis of stress relaxation curve. *Journal of biomechanics, 6*(2), 141-151.

Kories, C., Czyborra, C., Fetscher, C., Schneider, T., Krege, S., & Michel, M. C. (2003). Gender comparison of muscarinic receptor expression and function in rat and human urinary bladder: differential regulation of M2 and M3 receptors? *Naunyn-Schmiedeberg's Archives of Pharmacology, 367*(5), 524-531.

Korossis, S., Bolland, F., Southgate, J., Ingham, E., & Fisher, J. (2009). Regional biomechanical and histological characterisation of the passive porcine urinary bladder: Implications for augmentation and tissue engineering strategies. *Biomaterials, 30*(2), 266-275.

Kraichely, R., & Farrugia, G. (2007a). Mechanosensitive ion channels in interstitial cells of Cajal and smooth muscle of the gastrointestinal tract. *Neurogastroenterology & Motility, 19*(4), 245-252.

Kraichely, R., & Farrugia, G. (2007b). Mechanosensitive ion channels in interstitial cells of Cajal and smooth muscle of the gastrointestinal tract. *Neurogastroenterology and Motility, 19*(4), 245-252.

Kubota, Y., Biers, S. M., Kohri, K., & Brading, A. F. (2006a). Effects of imatinib mesylate (Glivec®) as ac-kit tyrosine kinase inhibitor in the guinea-pig urinary bladder. *Neurourology and Urodynamics, 25*(3), 205-210.

Kubota, Y., Biers, S. M., Kohri, K., & Brading, A. F. (2006b). Effects of imatinib mesylate (Glivec®) as ac-kit tyrosine kinase inhibitor in the guinea-pig urinary bladder. *Neurourology and Urodynamics: Official Journal of the International Continence Society, 25*(3), 205-210.

Kubota, Y., Kojima, Y., Shibata, Y., Imura, M., Sasaki, S., & Kohri, K. (2011). Role of KIT-positive interstitial cells of Cajal in the urinary bladder and possible therapeutic target for overactive bladder. *Advances in urology, 2011*

Kuijsters, N. P. M., Methorst, W. G., Kortenhorst, M. S. Q., Rabotti, C., Mischi, M., & Schoot, B. C. (2017). Uterine peristalsis and fertility: current knowledge and future perspectives: a review and meta-analysis. *Reproductive BioMedicine Online, 35*(1), 50-71.

Kunz, G., Beil, D., Deiniger, H., Einspanier, A., Mall, G., & Leyendecker, G. (1997). The uterine peristaltic pump. In *The Fate of the Male Germ Cell* (pp. 267-277): Springer.

Kunz, G., Beil, D., Deininger, H., Wildt, L., & Leyendecker, G. (1996). The dynamics of rapid sperm transport through the female genital tract: evidence from vaginal sonography of uterine peristalsis and hysterosalpingoscintigraphy. *Human Reproduction, 11*(3), 627-632.

Kunz, G., Herbertz, M., Noe, M., & Leyendecker, G. (1998). Sonographic evidence for the involvement of the utero-ovarian counter-current system in the ovarian control of directed uterine sperm transport. *Human reproduction update, 4*(5), 667-672.

Kunz, G., & Leyendecker, G. (2002). Uterine peristaltic activity during the menstrual cycle: characterization, regulation, function and dysfunction. *Reproductive BioMedicine Online, 4*, 5-9. 10.1016/s1472-6483(12)60108-4

Kurjak, A., Latin, V., Mandruzzato, G., D'Addario, V., & Rajhvajn, B. (1984). Ultrasound diagnosis and perinatal management of fetal genito-urinary abnormalities. *J Perinat Med, 12*(6), 291-312.

Laforet, J., Rabotti, C., Mischi, M., & Marque, C. (2013). Improved multi-scale modeling of uterine electrical activity. *Irbm, 34*(1), 38-42.

Lagou, M., Drake, M. J., & Gillespie, J. I. (2004). Volume-induced effects on the isolated bladder: a possible local reflex. *BJU international, 94*(9), 1356-1365.

Lambert, F., Pelletier, G., Dufour, M., & Fortier, M. (1990). Specific properties of smooth muscle cells from different layers of rabbit myometrium. *American Journal of Physiology-Cell Physiology, 258*(5), C794-C802.

Lammers, W., Arafat, K., el-Kays, A., & el-Sharkawy, T. Y. (1994). Spatial and temporal variations in local spike propagation in the myometrium of the 17-day pregnant rat. *American Journal of Physiology-Cell Physiology, 267*(5), C1210-C1223.

Lammers, W., Morrison, J., Lubbad, L., Stephen, B., & Hammad, F. (2013). *Electrical propagation in the guinea pig urinary bladder.* Paper presented at the Proceedings of The Physiological Society.

Lammers, W. J. (1996a). Circulating excitations and re-entry in the pregnant uterus. *Pflügers Archiv European Journal of Physiology, 433*(3), 287-293.

Lammers, W. J. (1996b). Circulating excitations and re-entry in the pregnant uterus. *Pflügers Archiv, 433*(3), 287-293.

Lammers, W. J. (2013). The electrical activities of the uterus during pregnancy. *Reprod Sci, 20*(2), 182-189. 10.1177/1933719112446082

Lammers, W. J. (2013). The electrical activities of the uterus during pregnancy. *Reproductive sciences, 20*(2), 182-189.

Lammers, W. J., Mirghani, H., Stephen, B., Dhanasekaran, S., Wahab, A., Al Sultan, M. A., & Abazer, F. (2008). Patterns of electrical propagation in the intact pregnant guinea pig uterus. *American Journal of Physiology-Regulatory, Integrative and Comparative Physiology, 294*(3), R919-R928.

Lammers, W. J., Stephen, B., Al-Sultan, M. A., Subramanya, S. B., & Blanks, A. M. (2015). The location of pacemakers in the uteri of pregnant guinea pigs and rats. *American Journal of Physiology-Regulatory, Integrative and Comparative Physiology, 309*(11), R1439-R1446.

Lammers, W. J. E. P., Dhanasekaran, S., Slack, J. R., & Stephen, B. (2001). Two-dimensional high-resolution motility mapping in the isolated feline duodenum: methodology and initial results. *Neurogastroenterology and Motility, 13*(4), 309-323.

Lammers, W. J. E. P., & Slack, J. R. (2001). Of slow waves and spike patches. *News in physiological sciences, 16*, 138-144.

Lammers, W. J. E. P., & Stephen, B. (2008). Origin and propagation of individual slow waves along the intact feline small intestine. *Experimental Physiology, 93*(3), 334-346.

Lammers, W. J. E. P., Ver Donck, L., Schuurkes, J. A. J., & Stephen, B. (2003). Longitudinal and circumferential spike patches in the canine small intestine in vivo. *American Journal of Physiology, 285*(5), G1014-1027.

Lang, R. J., Tonta, M. A., Zoltkowski, B. Z., Meeker, W. F., Wendt, I., & Parkington, H. C. (2006). Pyeloureteric peristalsis: role of atypical smooth muscle cells and interstitial cells of Cajal-like cells as pacemakers. *The Journal of physiology, 576*(3), 695-705.

Latini, C., Frontini, A., Morroni, M., Marzioni, D., Castellucci, M., & Smith, P. (2008). Remodeling of uterine innervation. *Cell and tissue research, 334*(1), 1-6.

Lavoie, B., Balemba, O. B., Nelson, M. T., Ward, S. M., & Mawe, G. M. (2007). Morphological and physiological evidence for interstitial cell of Cajal-like cells in the guinea pig gallbladder. *The Journal of Physiology, 579*(2), 487-501.

Lecci, A., Giuliani, S., Meini, S., & Maggi, C. (1995). Pharmacological analysis of the local and reflex responses to bradykinin on rat urinary bladder motility in vivo. *British journal of pharmacology, 114*(3), 708-714.

Lee, K., Mitsui, R., Kajioka, S., Naito, S., & Hashitani, H. (2016). Role of PTHrP and sensory nerve peptides in regulating contractility of muscularis mucosae and detrusor smooth muscle in the guinea pig bladder. *The Journal of urology, 196*(4), 1287-1294.

Lee, Y. H., Hwang, M. K., Morgan, K., & Taggart, M. J. (2001). Receptor-coupled contractility of uterine smooth muscle: from membrane to myofilaments. *Experimental physiology, 86*(2), 283-288.

Lentle, R. G., De Loubens, C., Hulls, C., Janssen, P. W. M., Golding, M. D., & Chambers, J. P. (2012). A comparison of the organization of longitudinal and circular contractions during pendular and segmental activity in the duodenum of the rat and guinea pig. *Neurogastroenterology and Motility, 24*(7), 686-e298.

Lentle, R. G., Janssen, P. W. M., Asvarujanon, P., Chambers, P., Stafford, K. J., & Hemar, Y. (2007). High definition mapping of circular and longitudinal motility in the terminal ileum of the brushtail possum *Trichosurus*

vulpecula with watery and viscous perfusates. *Journal of Comparative Physiology. B, Biochemical, Systemic, and Environmental Physiology, B177*(5), 543-556.

Lentle, R. G., Janssen, P. W. M., Asvarujanon, P., Chambers, P., Stafford, K. J., & Hemar, Y. (2008). High definition spatiotemporal mapping of contractile activity in the isolated proximal colon of the rabbit. *Journal of Comparative Physiology. B, Biochemical, Systemic, and Environmental Physiology, B178*, 257-268.

Lentle, R. G., Janssen, P. W. M., DeLoubens, C., Lim, Y. F., Hulls, C., & Chambers, P. (2013). Mucosal microfolds augment mixing at the wall of the distal ileum of the brushtail possum. *Neurogastroenterology and Motility, 25*(11), 881-e700.

Lentle, R. G., Janssen, P. W. M., Goh, K., Chambers, P., & Hulls, C. (2010). Quantification of the Effects of the Volume and Viscosity of Gastric Contents on Antral and Fundic Activity in the Rat Stomach Maintained *Ex Vivo*. *Digestive Diseases and Sciences, 55*(12), 3349-3360.

Lentle, R. G., Reynolds, G. W., Hulls, C. M., & Chambers, J. (2016). Advanced spatiotemporal mapping methods give new insights into the coordination of contractile activity in the stomach of the rat. *American Journal of Physiology-Gastrointestinal and Liver Physiology*, ajpgi. 00308.02016.

Lentle, R. G., Reynolds, G. W., Hulls, C. M., & Chambers, J. P. (2016). Advanced spatiotemporal mapping methods give new insights into the coordination of contractile activity in the stomach of the rat. *American Journal of Physiology-Gastrointestinal and Liver Physiology, 311*(6), G1064-G1075. 10.1152/ajpgi.00308.2016

Lentle, R. G., Reynolds, G. W., & Janssen, P. W. (2013). Gastrointestinal tone; its genesis and contribution to the physical processes of digestion. *Neurogastroenterol Motil, 25*(12), 931-942. 10.1111/nmo.12223

Lentle, R. G., Reynolds, G. W., Janssen, P. W., Hulls, C. M., King, Q. M., & Chambers, J. P. (2015a). Characterisation of the contractile dynamics of the resting ex vivo urinary bladder of the pig. *BJU Int, 116*(6), 973-983. 10.1111/bju.13132

Lentle, R. G., Reynolds, G. W., Janssen, P. W. M., Hulls, C. M., King, Q. M., & Chambers, J. (2015b). Characterisation of the contractile dynamics of the resting ex vivo urinary bladder of the pig. *BJU International, 116*(6), 973-983.

Leppert, P. C., & Yu, S. Y. (1991). Three-Dimensional Structures of Uterine Elastic Fibers: Scanning Electron Microscopic Studies. *Connective Tissue Research, 27*(1), 15-31. 10.3109/03008209109006992

Levin, R. M., Goldman, M., & Wein, A. J. (1984). Effect of lsoproterenol and EGTA on the volume-pressure relationship of the in vitro whole bladder preparation. *Neurourology and Urodynamics, 3*(2), 133-139. 10.1002/nau.1930030207

Levin, R. M., Ruggieri, M. R., Velagapudi, S., Gordon, D., Altman, B., & Wein, A. J. (1986). Relevance of spontaneous activity to urinary bladder function: an in vitro and in vivo study. *Journal of Urology, 136*(2), 517-521.

Levin, R. M., Ruggieri, M. R., & Wein, A. J. (1988). Identification of receptor subtypes in the rabbit and human urinary bladder by selective radio-ligand binding. *The Journal of urology, 139*(4), 844-848.

Levin, R. M., Shofer, F. S., & Wein, A. J. (1980). Cholinergic, adrenergic and purinergic response of sequential strips of rabbit urinary bladder. *Journal of Pharmacology and Experimental Therapeutics, 212*(3), 536-540.

Lewis, S. A. (2000). Everything you wanted to know about the bladder epithelium but were afraid to ask. *American Journal of Physiology-Renal Physiology, 278*(6), F867-F874.

Lewitus, E., & Soligo, C. (2011). Life-History Correlates of Placental Structure in Eutherian Evolution. *Evolutionary Biology, 38*(3), 287-305. 10.1007/s11692-011-9115-x

Leyendecker, G., Kunz, G., Herbertz, M., Beil, D., Huppert, P., Mall, G., . . . Wildt, L. (2004). Uterine peristaltic activity and the development of endometriosis. *Annals of the New York Academy of Sciences, 1034*(1), 338-355.

Li, Y., Reznichenko, M., Tribe, R. M., Hess, P. E., Taggart, M., Kim, H., . . . Morgan, K. G. (2009). Stretch activates human myometrium via ERK, caldesmon and focal adhesion signaling. *PLoS One, 4*(10), e7489.

Liang, K. L., Bursova, J. O., Lam, F., Chen, X., & Obukhov, A. G. (2019). Ex Vivo Method for Assessing the Mouse Reproductive Tract Spontaneous Motility and a MATLAB-based Uterus Motion Tracking Algorithm for Data Analysis. *JoVE (Journal of Visualized Experiments)*(151), e59848.

Liu, L., Ishida, Y., Okunade, G., Shull, G. E., & Paul, R. J. (2006). Role of plasma membrane Ca2+-ATPase in contraction-relaxation processes of the bladder: evidence from PMCA gene-ablated mice. *American Journal of Physiology-Cell Physiology, 290*(4), C1239-C1247.

Loch-Caruso, R. K., Criswell, K. A., Grindatti, C. M., & Brant, K. A. (2003). Sustained inhibition of rat myometrial gap junctions and contractions by lindane. *Reproductive Biology and Endocrinology, 1*(1), 1-13.

Longhurst, P. A., Kang, J., Wein, A. J., & Levin, R. M. (1990). Comparative length-tension relationship of urinary bladder strips from hamsters, rats, guinea-pigs, rabbits and cats. *Comparative biochemistry and physiology. A, Comparative physiology, 96*(1), 221-225.

Longhurst, P. A., & Levendusky, M. (1999). Pharmacological characterization of β-adrenoceptors mediating relaxation of the rat urinary bladder in vitro. *British journal of pharmacology, 127*(7), 1744-1750.

Lucovnik, M., Maner, W. L., Chambliss, L. R., Blumrick, R., Balducci, J., Novak-Antolic, Z., & Garfield, R. E. (2011). Noninvasive uterine electromyography for prediction of preterm delivery. *American Journal of Obstetrics and Gynecology, 204*(3), 228. e221-228. e210.

Lukacz, E. S., Sampselle, C., Gray, M., Macdiarmid, S., Rosenberg, M., Ellsworth, P., & Palmer, M. H. (2011). A healthy bladder: a consensus statement. *International journal of clinical practice, 65*(10), 1026-1036. 10.1111/j.1742-1241.2011.02763.x

Lutton, E. J., Lammers, W. J., James, S., van den Berg, H. A., & Blanks, A. M. (2018a). Identification of uterine pacemaker regions at the myometrial–placental interface in the rat. *The Journal of physiology, 596*(14), 2841-2852.

Lutton, E. J., Lammers, W. J., James, S., van den Berg, H. A., & Blanks, A. M. (2018b). Identification of uterine pacemaker regions at the myometrial–placental interface in the rat. *The Journal of Physiology*

Lye, S., Mitchell, J., Nashman, N., Oldenhof, A., Ou, R., Shynlova, O., & Langille, L. (2001). Role of mechanical signals in the onset of term and preterm labor. *Frontiers of Hormone Research, 27*, 165-178.

Lynn, P., Zagorodnyuk, V., Hennig, G., Costa, M., & Brookes, S. (2005). Mechanical activation of rectal intraganglionic laminar endings in the guinea pig distal gut. *The Journal of Physiology, 564*(2), 589-601.

Lyons, E. A., Taylor, P. J., Zheng, X. H., Ballard, G., Levi, C. S., & Kredentser, J. V. (1991). Characterization of subendometrial myometrial contractions throughout the menstrual cycle in normal fertile women. *Fertility and Sterility, 55*(4), 771-774.

Mackler, A. M., Ducsay, C. A., Veldhuis, J. D., & Yellon, S. M. (1999). Maturation of spontaneous and agonist-induced uterine contractions in the peripartum mouse uterus. *Biology of reproduction, 61*(4), 873-878.

Maggi, C. A., Santicioli, P., & Meli, A. (1984). The effects of topical capsaicin on rat urinary bladder motility in vivo. *European journal of pharmacology, 103*(1-2), 41-50.

Makhlouf, G. M., & Murthy, K. S. (2006). Cellular physiology of gastrointestinal smooth muscle. In L. R. Johnson (Ed.), *Physiology of the Gastrointestinal Tract* (4th ed.). New York: Raven Press.

Maland, C. O. (1928). Spontaneous contractions of the pregnant human uterus. A preliminary report: Ko Chi Sun: Bulletin of Johns Hopkins Hospital, 1925, xxxvi, 280. *American Journal of Obstetrics & Gynecology, 16*(3), 450. 10.1016/S0002-9378(28)91001-7

Malik, M., Roh, M., & England, S. K. (2021). Uterine contractions in rodent models and humans. *Acta Physiologica, 231*(4), e13607.

Malkowicz, S. B., Wein, A. J., Elbadawi, A., Arsdalen, K. V., Ruggieri, M. R., & Levin, R. M. (1986). Acute Biochemical and Functional Alterations in The Partially Obstructed Rabbit Urinary Bladder. *Journal of Urology, 136*(6), 1324-1329. doi:10.1016/S0022-5347(17)45331-6

Malmgren, A., Andersson, K.-E., Andersson, P., Fovaeus, M., & Sjögren, C. (1990). Effects of cromakalim (BRL 34915) and pinacidil on normal and hypertrophied rat detrusor in vitro. *The Journal of urology, 143*(4), 828-834.

Malmqvist, U., Arner, A., & Uvelius, B. (1991). Contractile and cytoskeletal proteins in smooth muscle during hypertrophy and its reversal. *American Journal of Physiology-Cell Physiology, 260*(5), C1085-C1093. 10.1152/ajpcell.1991.260.5.C1085

Malmqvist, U., Arner, A., & Uvelius, B. (1991). Lactate dehydrogenase activity and isoform distribution in normal and hypertrophic smooth muscle tissue from the rat. *Pflügers Archiv, 419*(3), 230-234. 10.1007/BF00371100

Mandile, O. (2017). Intrauterine Pressure Catheter. *Embryo Project Encyclopedia*

Manoogian, S. J., Bisplinghoff, J. A., Kemper, A. R., & Duma, S. M. (2012). Dynamic material properties of the pregnant human uterus. *Journal of biomechanics, 45*(9), 1724-1727.

Marsal, K. (1983). Ultrasonic assessment of fetal activity. *Clinics in Obstetrics and Gynaecology, 10*(3), 541-563.

Marsden, A. L., & Feinstein, J. A. (2015). Computational modeling and engineering in pediatric and congenital heart disease. *Current opinion in pediatrics, 27*(5), 587.

Marshall, J. (1981). Effects of ovarian steroids and pregnancy on adrenergic nerves of uterus and oviduct. *American Journal of Physiology-Cell Physiology, 240*(5), C165-C174.

Marshall, J. M. (1962a). Regulation of activity in uterine smooth muscle. *Physiological Reviews, 42*, 213-227.

Marshall, J. M. (1962b). Regulation of activity of uterine smooth muscle. *Physiol. Rev., 42*, 213-235.

Marshall, J. M., & Kroeger, E. (1973). Adrenergic influences on uterine smooth muscle. *Philosophical Transactions of the Royal Society of London. B, Biological Sciences, 265*(867), 135-148.

Martin, T., Janzen, C., Li, X., Del Rosario, I., Chanlaw, T., Choi, S., . . . Devaskar, S. U. (2020). Characterization of uterine motion in early gestation using MRI-based motion tracking. *Diagnostics, 10*(10), 840.

Martínez-Burnes, J., Muns, R., Barrios-García, H., Villanueva-García, D., Domínguez-Oliva, A., & Mota-Rojas, D. (2021). Parturition in mammals: Animal models, pain and distress. *Animals, 11*(10), 2960.

Mattiasson, A., Andersson, K.-E., Elbadawi, A., Morgan, E., & Sjögren, C. (1987). Interaction between adrenergic and cholinergic nerve terminals in the urinary bladder of rabbit, cat and man. *The Journal of urology, 137*(5), 1017-1019.

McCarthy, M., & McCarthy, L. (2019). The evolution of the urinary bladder as a storage organ: scent trails and selective pressure of the first land animals in a computational simulation. *SN Applied Sciences, 1*(12), 1-13.

McCLOSKEY, K. D. (2005). Characterization of outward currents in interstitial cells from the guinea pig bladder. *The Journal of urology, 173*(1), 296-301.

McCLOSKEY, K. D. (2006). Calcium currents in interstitial cells from the guinea-pig bladder. *BJU international, 97*(6), 1338-1343.

McCloskey, K. D. (2010a). Interstitial cells in the urinary bladder—localization and function. *Neurourology and Urodynamics: Official Journal of the International Continence Society, 29*(1), 82-87.

McCloskey, K. D. (2010b). Interstitial cells in the urinary bladder—localization and function. *Neurourology and Urodynamics, 29*(1), 82-87.

McCloskey, K. D., & Gurney, A. M. (2002a). Kit positive cells in the guinea pig bladder. *The Journal of urology, 168*(2), 832-836.

McCloskey, K. D., & Gurney, A. M. (2002b). Kit positive cells in the guinea pig bladder. *Journal of Urology, 168*(2), 832-836.

McDevitt, D., Wallace, R., Roberts, A., & Whitfield, C. (1975). The uterine and cardiovascular effects of salbutamol and practolol during labour. *BJOG: An International Journal of Obstetrics & Gynaecology, 82*(6), 442-448.

McEvoy, A., & Sabir, S. (2021). Physiology, Pregnancy Contractions. In *StatPearls [Internet]*: StatPearls Publishing.

McGarigal, K. (2014). Fragstats v4: Spatial Pattern Analysis Program for Categorical and Continuous Maps-Help manual. *Amherst: University of Massachusetts. Recuperado de http://www. umass. edu/landeco/research/fragstats/fragstats. html*

McGarigal, K., Cushman, S., & Ene, E. (2012). FRAGSTATS v4: spatial pattern analysis program for categorical and continuous maps. University of Massachusetts, Amherst, Massachusetts, USA. *goo. gl/aAEbMk*

McGarigal, K., Cushman, S. A., Neel, M. C., & Ene, E. (2002). FRAGSTATS: spatial pattern analysis program for categorical maps.

McGarigal, K., & Marks, B. J. (1995). Spatial pattern analysis program for quantifying landscape structure. *Gen. Tech. Rep. PNW-GTR-351. US Department of Agriculture, Forest Service, Pacific Northwest Research Station*

McHugh, R., McDicken, W., Bow, C., Anderson, T., & Boddy, K. (1978). An ultrasonic pulsed Doppler instrument for monitoring human fetal breathing in utero. *Ultrasound in Medicine and Biology, 3*(4), 381-384.

McKinley, M. P., O'loughlin, V. D., Pennefather-O'Brien, E., & Harris, R. T. (2006). *Human anatomy*: McGraw-Hill Higher Education Boston, MA.

Melville, J., Macagno, E., & Christensen, J. (1975). Longitudinal contractions in the duodenum: their fluid-mechanical function. *American Journal of Physiology, 228*(6), 1887-1892.

Merkur, H. (1979). Normal and abnormal antenatal ultrasonic cardiographic patterns. *BJOG: An International Journal of Obstetrics & Gynaecology, 86*(7), 533-539.

Metaxa-Mariatou, V., McGavigan, C., Robertson, K., Stewart, C., Cameron, I., & Campbell, S. (2002). Elastin distribution in the myometrial and vascular smooth muscle of the human uterus. *MHR: Basic science of reproductive medicine, 8*(6), 559-565.

Mierke, C. T. (2022). Viscoelasticity, like forces, plays a role in mechanotransduction. *Frontiers in Cell and Developmental Biology, 10*

Miftahof, R. N., & Nam, H. G. (2013). *Biomechanics of the human urinary bladder*: Springer Science & Business Media.

Mikkelsen, E., Johansen, P., Fuglsang-Frederiksen, A., & Uldbjerg, N. (2013). Electrohysterography of labor contractions: propagation velocity and direction. *Acta Obstetricia et Gynecologica Scandinavica, 92*(9), 1070-1078.

Miodonski, A., Litwin, J., Nowogrodzka-Zagorska, M., & Gorczyca, J. (2001). Vascular architecture of normal human urinary bladder and its remodeling in cancer, as revealed by corrosion casting. *Italian journal of anatomy and embryology= Archivio italiano di anatomia ed embriologia, 106*(2 Suppl 1), 221-228.

Mironneau, J. (1976). Effects of oxytocin on ionic currents underlying rhythmic activity and contraction in uterine smooth muscle. *Pflügers Archiv, 363*(2), 113-118.

Mischi, M., Rabotti, C., Kuijsters, N., & Schoot, B. C. (2015). *Quantitative ultrasound imaging of the uterus for improved embryo implantation: Preliminary study.* Paper presented at the 2015 IEEE International Conference on Digital Signal Processing (DSP).

Mitchell, B. F., & Taggart, M. J. (2009). Are animal models relevant to key aspects of human parturition? *Am J Physiol Regul Integr Comp Physiol, 297*(3), R525-545. 10.1152/ajpregu.00153.2009

Mizrahi, J., Karni, Z., & Polishuk, W. (1980). Isotropy and anisotropy of uterine muscle during labor contraction. *Journal of biomechanics, 13*(3), 211-218.

Monaghan, K. P., Johnston, L., & McCloskey, K. D. (2012). Identification of PDGFRα positive populations of interstitial cells in human and guinea pig bladders. *The Journal of urology, 188*(2), 639-647.

Mondragon, E., Yoshida, K., & Meyers, K. (2013). Characterizing the biomechanical and biochemical properties of mouse uterine tissue. *Columbia Undergraduate Science Journal, 7*

Monson, F. C., Goldschmidt, M., Zderic, S., Ruggieri, M., Levin, R., & Wein, A. (1988). Use of a previously undescribed elastic lamina of the serosa to characterize connective tissue hypertrophy of the rabbit bladder wall following partial outlet obstruction. *Neurourology and Urodynamics, 7*(4), 385-396.

Montgomery, B. S., & Fry, C. H. (1992). The action potential and net membrane currents in isolated human detrusor smooth muscle cells. *The Journal of urology, 147*(1), 176-184.

Morales-Orcajo, E., Siebert, T., & Böl, M. (2018). Location-dependent correlation between tissue structure and the mechanical behaviour of the urinary bladder. *Acta biomaterialia, 75*, 263-278.

Morrione, T. G., & Seifter, S. (1962). Alteration in the collagen content of the human uterus during pregnancy and post partum involution. *Journal of Experimental Medicine, 115*(2), 357-365.

Morrison, J. (1999). The activation of bladder wall afferent nerves. *Experimental physiology, 84*(1), 131-136.

Mosso, A., & Pellacani, P. (1882). Arch. ital. de biol. *T. I*, 97.

Mosso, A., & Pellacani, P. (1882). Sur la fonction de la vessie. *Archives Italiennes de Biologie, 1*, 291–324.

Murakumo, M., Ushiki, T., Abe, K., Matsumura, K., Shinno, Y., & Koyanagi, T. (1995). Three-dimensional arrangement of collagen and elastin fibers in the human urinary bladder: a scanning electron microscopic study. *The Journal of urology, 154*(1), 251-256.

Muybridge, E. (1887). Complete human and animal locomotion. *New York*

Nagatomi, J., Toosi, K. K., Grashow, J. S., Chancellor, M. B., & Sacks, M. S. (2005). Quantification of bladder smooth muscle orientation in normal and spinal cord injured rats. *Annals of biomedical engineering, 33*(8), 1078-1089.

Nagle, A. S., Klausner, A. P., Varghese, J., Bernardo, R. J., Colhoun, A. F., Barbee, R. W., . . . Speich, J. E. (2017). Quantification of bladder wall biomechanics during urodynamics: a methodologic investigation using ultrasound. *Journal of biomechanics, 61*, 232-241.

Nagle, A. S., Speich, J. E., De Wachter, S. G., Ghamarian, P. P., Le, D. M., Colhoun, A. F., . . . Klausner, A. P. (2017). Non-invasive characterization of real-time bladder sensation using accelerated hydration and a novel sensation meter: an initial experience. *Neurourology and Urodynamics, 36*(5), 1417-1426.

Natali, A., Audenino, A., Artibani, W., Fontanella, C., Carniel, E., & Zanetti, E. (2015). Bladder tissue biomechanical behavior: Experimental tests and constitutive formulation. *Journal of biomechanics, 48*(12), 3088-3096.

Nathanielsz, P. W., Barbera OM Honnebier, M., Mecenas, C., Jenkins, S., Holland, M., & Demarest, K. (1997). Effect of the oxytocin antagonist atosiban (1-deamino-2-D-tyr (OET)-4-thr-8-orn-vasotocin/oxytocin) on nocturnal myometrial contractions, maternal cardiovascular function, transplacental passage, and fetal oxygenation in the pregnant baboon during the last third of gestation. *Biology of reproduction, 57*(2), 320-324.

Neal, K. B., Parry, L. J., & Bornstein, J. C. (2009). Strain specific genetics, anatomy and function of enteric neural serotonergic pathways in inbred mice. *Journal of Physiology, 587*(3), 567-586.

Nishinaka, K., & Fukuda, Y. (1991). Changes in extracellular matrix materials in the uterine myometrium of rats during pregnancy and postparturition. *Pathology International, 41*(2), 122-132.

Nobe, K., Sutliff, R. L., Kranias, E. G., & Paul, R. J. (2001). Phospholamban regulation of bladder contractility: evidence from gene-altered mouse models. *The Journal of physiology, 535*(3), 867-878.

Norman, M., Ekman, G., & Malmström, A. (1993). Changed proteoglycan metabolism in human cervix immediately after spontaneous vaginal delivery. *Obstetrics and gynecology, 81*(2), 217-223.

Norwitz, E. R., Lockwood, C. J., & Barss, V. A. Physiology of parturition UpToDate.

Norwitz, E. R., & Robinson, J. N. (2001). *A systematic approach to the management of preterm labor.* Paper presented at the Seminars in Perinatology.

Notman, R., Noro, M., O'Malley, B., & Anwar, J. (2006). Molecular basis for dimethylsulfoxide (DMSO) action on lipid membranes. *Journal of the American Chemical Society, 128*(43), 13982-13983.

O'Grady, G., Angeli, T. R., Du, P., Lahr, C., Lammers, W. J., Windsor, J. A., . . . Cheng, L. K. (2012). Abnormal initiation and conduction of slow-wave activity in gastroparesis, defined by high-resolution electrical mapping. *Gastroenterology, 143*(3), 589-598. e583.

O'Grady, G., Du, P., Cheng, L. K., Egbuji, J. U., Lammers, W. J., Windsor, J. A., & Pullan, A. J. (2010). Origin and propagation of human gastric slow-wave activity defined by high-resolution mapping. *American Journal of Physiology-Gastrointestinal and Liver Physiology, 299*(3), G585-G592.

Ohe, M. R., Hanson, R. B., & Camilleri, M. (1994). Comparison of simultaneous recordings of human colonic contractions by manometry and a barostat. *Neurogastroenterology and Motility, 6*(3), 213-222.

Olson, D. M., Mijovic, J. E., & Sadowsky, D. W. (1995). Control of human parturition. *Seminars in Perinatology, 19*(1), 52-63. https://doi.org/10.1016/S0146-0005(95)80047-6

Omari, E. A., Varghese, T., Kliewer, M. A., Harter, J., & Hartenbach, E. M. (2015). Dynamic and quasi-static mechanical testing for characterization of the viscoelastic properties of human uterine tissue. *Journal of biomechanics, 48*(10), 1730-1736.

Osa, T., Ogasawara, T., & Kato, S. (1983). Effects of magnesium, oxytocin, and prostaglandin F2α on the generation and propagation of excitation in the longitudinal muscle of rat myometrium during late pregnancy. *The Japanese Journal of Physiology, 33*(1), 51-57.

Ou, C.-W., Orsino, A., & Lye, S. J. (1997). Expression of connexin-43 and connexin-26 in the rat myometrium during pregnancy and labor is differentially regulated by mechanical and hormonal signals. *Endocrinology, 138*(12), 5398-5407.

Owens, G. K., & Schwartz, S. M. (1982). Alterations in vascular smooth muscle mass in the spontaneously hypertensive rat. Role of cellular hypertrophy, hyperploidy, and hyperplasia. *Circulation research, 51*(3), 280-289.

Owman, C., Rosengren, E., & Sjöberg, N.-O. (1967). Adrenergic innervation of the human female reproductive organs: a histochemical and chemical investigation. *Obstetrics & Gynecology, 30*(6), 763-773.

Park, K. J., Hennig, G. W., Lee, H. T., Spencer, N. J., Ward, S. M., Smith, T. K., & Sanders, K. M. (2006). Spatial and temporal mapping of pacemaker activity in interstitial cells of Cajal in mouse ileum in situ. *American Journal of Physiology, 290*(5), C1411-1427.

Parkington, H., Harding, R., & Sigger, J. (1988). Co-ordination of electrical activity in the myometrium of pregnant ewes. *Reproduction, 82*(2), 697-705.

Parkington, H. C. (1985). Some properties of the circular myometrium of the sheep throughout pregnancy and during labour. *The Journal of physiology, 359*(1), 1-15.

Parkington, H. C., Tonta, M. A., Brennecke, S. P., & Coleman, H. A. (1999). Contractile activity, membrane potential, and cytoplasmic calcium in human uterine smooth muscle in the third trimester of pregnancy and during labor. *American Journal of Obstetrics and Gynecology, 181*(6), 1445-1451.

Parsons, B. A., Drake, M. J., Gammie, A., Fry, C. H., & Vahabi, B. (2012). The validation of a functional, isolated pig bladder model for physiological experimentation. *Frontiers in pharmacology, 3*

Parsons, B. A., Drake, M. J., Gammie, A., Fry, C. H., & Vahabi, B. (2012). The validation of a functional, isolated pig bladder model for physiological experimentation. *Front Pharmacol, 3*, 52. 10.3389/fphar.2012.00052

Parsons, S. P., & Huizinga, J. D. (2015). Effects of gap junction inhibition on contraction waves in the murine small intestine in relation to coupled oscillator theory. *American Journal of Physiology-Gastrointestinal and Liver Physiology, 308*(4), G287-G297.

Parsons, S. P., & Huizinga, J. D. (2016). Spatial Noise in Coupling Strength and Natural Frequency within a Pacemaker Network; Consequences for Development of Intestinal Motor Patterns According to a Weakly Coupled Phase Oscillator Model. *Frontiers in neuroscience, 10*

Pearsall, G. W., & Roberts, V. L. (1978). Passive mechanical properties of uterine muscle (myometrium) tested in vitro. *Journal of biomechanics, 11*(4), 167-176. https://doi.org/10.1016/0021-9290(78)90009-X

Petkov, G. V. (2011). Role of potassium ion channels in detrusor smooth muscle function and dysfunction. *Nat Rev Urol, 9*(1), 30-40. 10.1038/nrurol.2011.194

Pewowaruk, R., Rutkowski, D., Hernando, D., Kumapayi, B. B., Bushman, W., & Roldán-Alzate, A. (2020). A pilot study of bladder voiding with real-time MRI and computational fluid dynamics. *PLoS One, 15*(11), e0238404.

Peyron, R., Aubeny, E., Targosz, V., Silvestre, L., Renault, M., Elkik, F., . . . Baulieu, E.-E. (1993). Early termination of pregnancy with mifepristone (RU 486) and the orally active prostaglandin misoprostol. *New England Journal of Medicine, 328*(21), 1509-1513.

Planes, J., Morucci, J., Grandjean, H., & Favretto, R. (1984). External recording and processing of fast electrical activity of the uterus in human parturition. *Medical and Biological Engineering and Computing, 22*(6), 585-591.

Plum, F., & Colfelt, R. H. (1960). The genesis of vesical rhythmicity. *Archives of Neurology, 2*(5), 487-496.

Poley, R. N., Dosier, C. R., Speich, J. E., Miner, A. S., & Ratz, P. H. (2008). Stimulated calcium entry and constitutive RhoA kinase activity cause stretch-induced detrusor contraction. *European journal of pharmacology, 599*(1-3), 137-145.

Popescu, L. M., Vidulescu, C., Curici, A., Caravia, L., Simionescu, A. A., Ciontea, S. M., & Simion, S. (2006). Imatinib inhibits spontaneous rhythmic contractions of human uterus and intestine. *European journal of pharmacology, 546*(1-3), 177-181.

Prayer, D., Brugger, P. C., & Prayer, L. (2004). Fetal MRI: techniques and protocols. *Pediatric radiology, 34*(9), 685-693.

Publicover, N. G., & Sanders, K. M. (1989). Are relaxation oscillators an appropriate model of gastrointestinal electrical activity? *American Journal of Physiology-Gastrointestinal and Liver Physiology, 256*(2), G265-G274.

Rabotti, C., de Lau, H., Haazen, N., Oei, G., & Mischi, M. (2013a). *Ultrasound analysis of the uterine wall movement for improved electrohysterographic measurement and modeling.* Paper presented at the Engineering in Medicine and Biology Society (EMBC), 2013 35th Annual International Conference of the IEEE.

Rabotti, C., de Lau, H., Haazen, N., Oei, G., & Mischi, M. (2013b). *Ultrasound analysis of the uterine wall movement for improved electrohysterographic measurement and modeling.* Paper presented at the 2013 35th Annual International Conference of the IEEE Engineering in Medicine and Biology Society (EMBC).

Rabotti, C., & Mischi, M. (2015). Propagation of electrical activity in uterine muscle during pregnancy: a review. *Acta Physiol (Oxf), 213*(2), 406-416. 10.1111/apha.12424

Rabotti, C., Mischi, M., Oei, S. G., & Bergmans, J. W. (2010). Noninvasive estimation of the electrohysterographic action-potential conduction velocity. *IEEE Transactions on Biomedical Engineering, 57*(9), 2178-2187.

Raines, D. A., & Cooper, D. B. (2017). Braxton Hicks Contractions.

Ramsey, E. (1994). Anatomy of the human uterus. *The uterus*, 18-40.

Rao, S. S., Sadeghi, P., Beaty, J., Kavlock, R., & Ackerson, K. (2001). Ambulatory 24-h colonic manometry in healthy humans. *American Journal of Physiology-Gastrointestinal and Liver Physiology, 280*(4), G629-G639.

Rasmussen, H., Rumessen, J. J., Hansen, A., Smedts, F., & Horn, T. (2009). Ultrastructure of Cajal-like interstitial cells in the human detrusor. *Cell and Tissue Research, 335*(3), 517.

Ratz, P. H., & Speich, J. E. (2010). Evidence that actomyosin cross bridges contribute to "passive" tension in detrusor smooth muscle. *Am J Physiol Renal Physiol, 298*(6), F1424-1435. 10.1152/ajprenal.00635.2009

Read, C. P., Word, R. A., Ruscheinsky, M. A., Timmons, B. C., & Mahendroo, M. S. (2007). Cervical remodeling during pregnancy and parturition: molecular characterization of the softening phase in mice. *Reproduction, 134*(2), 327-340.

Refuerzo, J. S., Leonard, F., Bulayeva, N., Gorenstein, D., Chiossi, G., Ontiveros, A., . . . Godin, B. (2016). Uterus-targeted liposomes for preterm labor management: studies in pregnant mice. *Scientific reports, 6*(1), 1-12.

Rhee, P. L., Lee, J. Y., Son, H. J., Kim, J. J., Rhee, J. C., Kim, S., . . . Ward, S. M. (2011). Analysis of Pacemaker Activity in the Human Stomach. *Journal of Physiology, 589*(24), 6105–6118.

Richter, O., Bartz, C., Dowaji, J., Kupka, M., Reinsberg, J., Ulrich, U., & Rath, W. (2006). Contractile reactivity of human myometrium in isolated non-pregnant uteri. *Human Reproduction, 21*(1), 36-45.

Riemer, R. K., & Heymann, M. A. (1998). Regulation of uterine smooth muscle function during gestation. *Pediatric research, 44*(5), 615-627.

Roberts, R. R., Bornstein, J. C., Bergner, A. J., & Young, H. M. (2008). Disturbances of colonic motility in mouse models of Hirschsprung's disease. *American Journal of Physiology, 294*(4), G996-G1008.

Roberts, R. R., Ellis, M., Gwynne, R. M., Bergner, A. J., Lewis, M. D., Beckett, E. A., . . . Young, H. M. (2010). The first intestinal motility patterns in fetal mice are not mediated by neurons or interstitial cells of Cajal. *Journal of Physiology, 588*(7), 1153-1169.

Robertson, A. (1999). Behaviour of the human bladder during natural filling: the Newcastle experience of ambulatory monitoring and conventional artificial filling cystometry. *Scandinavian Journal of Urology and Nephrology, 33*(201), 19-24.

Roccabianca, S., & Bush, T. R. (2016). Understanding the mechanics of the bladder through experiments and theoretical models: where we started and where we are heading. *Technology, 4*(01), 30-41.

Rong, W., Spyer, K. M., & Burnstock, G. (2002). Activation and sensitisation of low and high threshold afferent fibres mediated by P2X receptors in the mouse urinary bladder. *The Journal of physiology, 541*(2), 591-600.

Rood, K. M. (2012). Complications associated with insertion of intrauterine pressure catheters: an unusual case of uterine hypertonicity and uterine perforation resulting in fetal distress after insertion of an intrauterine pressure catheter. *Case reports in obstetrics and gynecology, 2012*

Roosen, A., Wu, C., Sui, G., Chowdhury, R. A., Patel, P. M., & Fry, C. H. (2009). Characteristics of spontaneous activity in the bladder trigone. *European Urology, 56*(2), 346-354.

Rosier, P. F., Schaefer, W., Lose, G., Goldman, H. B., Guralnick, M., Eustice, S., . . . Hashim, H. (2017). International Continence Society Good Urodynamic Practices and Terms 2016: urodynamics, uroflowmetry, cystometry, and pressure-flow study. *Neurourology and Urodynamics, 36*(5), 1243-1260.

Ross, R., & Klebanoff, S. J. (1967). Fine structural changes in uterine smooth muscle and fibroblasts in response to estrogen. *The Journal of cell biology, 32*(1), 155-167.

Rozental, R., Srinivas, M., & Spray, D. C. (2001). How to close a gap junction channel. In *Connexin Methods and Protocols* (pp. 447-476): Springer.

Rüegg, J. (1971). Smooth muscle tone. *Physiological Reviews, 51*(1), 201-248.

Russ, J. C. (2006). *The Image Processing Handbook* (5th ed.). Boca Raton: CRC Press.

Sam, P., Jiang, J., & LaGrange, C. A. (2021). Anatomy, abdomen and pelvis, sphincter urethrae. In *StatPearls [Internet]*: StatPearls Publishing.

Sammali, F., Blank, C., Huang, Y., Kuijsters, N., Rabotti, C., Schoot, B., & Mischi, M. (2018). *Quantitative analysis of uterine motion outside pregnancy by dedicated ultrasound speckle tracking.* Paper presented at the 2018 IEEE International Ultrasonics Symposium (IUS).

Sammali, F., Kuijsters, N. P., Huang, Y., Blank, C., Rabotti, C., Schoot, B. C., & Mischi, M. (2018). Dedicated ultrasound speckle tracking for quantitative analysis of uterine motion outside pregnancy. *IEEE transactions on ultrasonics, ferroelectrics, and frequency control, 66*(3), 581-590.

Sanders, K. M. (1996). A case for interstitial cells of Cajal as pacemakers and mediators of neurotransmission in the gastrointestinal tract. *Gastroenterology, 111*(2), 492-515.

Sanders, K. M., Ward, S. M., & Koh, S. D. (2014). Interstitial cells: regulators of smooth muscle function. *Physiological Reviews*

Sartori, A. M., Kessler, T. M., & Schwab, M. E. (2021). Methods for assessing lower urinary tract function in animal models. *European Urology Focus, 7*(1), 186-189.

Satchell, P., & Vaughan, C. (1994). Bladder wall tension and mechanoreceptor discharge. *Pflügers Archiv, 426*(3-4), 304-309.

Savitsky, A. G., Savitsky, G. A., Ivanov, D. O., Mikhailov, A. V., Kurganskiy, A. V., & Mill, K. V. (2013). The myogenic mechanism of synchronization and coordination for uterine myocytes contractions during labor. *J Matern Fetal Neonatal Med, 26*(6), 566-570. 10.3109/14767058.2012.738261

Savitsky, A. G., Savitsky, G. A., Ivanov, D. O., Mikhailov, A. V., Kurganskiy, A. V., & Mill, K. V. (2013). The myogenic mechanism of synchronization and coordination for uterine myocytes contractions during labor. *The Journal of Maternal-Fetal & Neonatal Medicine, 26*(6), 566-570.

Schatz, F. (1872). Beiträge zur physiologischen Geburtskunde. *Archiv fur Gynakologie, 4*(1), 34-111.

Schneider, T., Fetscher, C., Krege, S., & Michel, M. C. (2004). Signal transduction underlying carbachol-induced contraction of human urinary bladder. *Journal of Pharmacology and Experimental Therapeutics, 309*(3), 1148-1153.

Schofield, B. M., & Wood, C. (1964). Length—tension relation in rabbit and human myometrium. *The Journal of physiology, 175*(1), 125.

Schreiber, D., Klotz, M., Laures, K., Clasohm, J., Bischof, M., & Schäfer, K.-H. (2014). The mesenterially perfused rat small intestine: A versatile approach for pharmacological testings. *Annals of Anatomy-Anatomischer Anzeiger, 196*(2), 158-166.

Schwartz, S. M., & Mecham, R. (1995). *The Vascular Smooth Muscle Cell*: Elsevier.

Seerden, T. C., Lammers, W., De Winter, B. Y., De Man, J. G., & Pelckmans, P. A. (2005). Spatiotemporal electrical and motility mapping of distension-induced propagating oscillations in the murine small intestine. *American Journal of Physiology, 289*(6), G1043-1951.

Seki, N., Karim, O., & Mostwin, J. L. (1992). Changes in electrical properties of guinea pig smooth muscle membrane by experimental bladder outflow obstruction. *American Journal of Physiology-Renal Physiology, 262*(5), F885-F891.

Sengupta, J., & Gebhart, G. (1995). Mechanosensitive afferent fibers in the gastrointestinal and lower urinary tracts. *Visceral pain, progress in pain research and management, 5*, 75-98.

Setekleiv, J. (1964a). Uterine motility of the estrogenized rabbit. *Acta Physiologica, 62*(1-2), 79-93.

Setekleiv, J. (1964b). Uterine Motility of the Estrogenized Rabbit: I. Isotonic and Isometric Recording in vivo. Influence of Anesthesia and Temperature. *Acta physiologica scandinavica, 62*(1-2), 68-78.

Setoguchi, M., Ohya, Y., Abe, I., & Fujishima, M. (1997). Stretch activated whole cell currents in smooth muscle cells from mesenteric resistance artery of guinea pig. *Journal of Physiology, 501*(2), 343-353.

Seydewitz, R., Menzel, R., Siebert, T., & Böl, M. (2017). Three-dimensional mechano-electrochemical model for smooth muscle contraction of the urinary bladder. *Journal of the mechanical behavior of biomedical materials, 75*, 128-146.

Shafik, A., El-Sibai, O., Shafik, A. A., & Shafik, I. (2004). Identification of interstitial cells of Cajal in human urinary bladder: concept of vesical pacemaker. *Urology, 64*(4), 809-813.

Shafik, A., El-Sibai, O., & Shafik, I. (2004). Identification of c-kit-positive cells in the uterus. *International Journal of Gynecology & Obstetrics, 87*(3), 254-255.

Sheldon, R. E., Shmygol, A., van den Berg, H. A., & Blanks, A. M. (2015). Functional and morphological development of the womb throughout life. *Sci Prog, 98*(Pt 2), 103-127. 10.3184/003685015X14308363103415

Shelkovnikov, S., Savitskiĭ, G., & Abramchenko, V. (1986a). Spontaneous contractile activity of isolated strips of uterine myometrium depending on the degree of stretching. *Fiziologiia Cheloveka, 12*(6), 1016.

Shelkovnikov, S., Savitskiĭ, G., & Abramchenko, V. (1986b). Spontaneous contractile activity of isolated strips of uterine myometrium depending on the degree of stretching. *Fiziologiia Cheloveka, 12*(6), 1016-1020.

Sherrington, C. S. (1892). Notes on the Arrangement of some Motor Fibres in the Lumbo-Sacral Plexus. *The Journal of physiology, 13*(6), 621-772. 10.1113/jphysiol.1892.sp000428

Sherrington, C. S. (1892a). Notes on the arrangement of some motor fibres in the lumbo-sacral plexus. *Journal of Physiology, 13*(6), 621–772.

Sherrington, C. S. (1892b). Notes on the Arrangement of some Motor Fibres in the Lumbo-Sacral Plexus. *The Journal of Physiology, 13*(6), 621-772.

Sheth, S. S., Hajari, A. R., Lulla, C. P., & Kshirsagar, D. (2017). Sonographic evaluation of uterine volume and its clinical importance. *Journal of Obstetrics and Gynaecology Research, 43*(1), 185-189. 10.1111/jog.13189

Shmygol, A., Blanks, A., Bru-Mercier, G., Astle, S., & Thornton, S. (2006). *Tissue-level Ca2+ signalling in human myometrium: a possible role for ICCs.* Paper presented at the Proc Physiol Soc.

Shmygol, A., Gullam, J., Blanks, A., & Thornton, S. (2006). Multiple mechanisms involved in oxytocin-induced modulation of myometrial contractility. *Acta Pharmacologica Sinica, 27*(7), 827-832.

Sigger, J., Harding, R., & Jenkin, G. (1984). Relationship between electrical activity of the uterus and surgically isolated myometrium in the pregnant and non-pregnant ewe. *Reproduction, 70*(1), 103-114.

Sigurdson, W., Ruknudin, A., & Sachs, F. (1992). Calcium imaging of mechanically induced fluxes in tissue-cultured chick heart: role of stretch-activated ion channels. *American Journal of Physiology-Heart and Circulatory Physiology, 262*(4), H1110-H1115.

Simon, C., & Einspanier, A. (2009). The hormonal induction of cervical remodeling in the common marmoset monkey (Callithrix jacchus). *Reproduction (Cambridge, England), 137*(3), 517-525.

Smet, P. J., Jonavicius, J., Marshall, V., & De Vente, J. (1996). Distribution of nitric oxide synthase-immunoreactive nerves and identification of the cellular targets of nitric oxide in guinea-pig and human urinary bladder by cGMP immunohistochemistry. *Neuroscience, 71*(2), 337-348.

Smith, R., Imtiaz, M., Banney, D., Paul, J. W., & Young, R. C. (2015). Why the heart is like an orchestra and the uterus is like a soccer crowd. *American Journal of Obstetrics and Gynecology, 213*(2), 181-185.

Smith, T. K., & Robertson, W. J. (1998). Synchronous movements of the longitudinal and circular muscle during peristalsis in the isolated guinea-pig distal colon. *Journal of Physiology, 506*(2), 563-577.

Sobel, I. (1970). *Camera models and machine perception*. DTIC Document.

Sokolowski, P., Saison, F., Giles, W., McGrath, S., Smith, D., Smith, J., & Smith, R. (2010). Human uterine wall tension trajectories and the onset of parturition. *PLoS One, 5*(6)

Solomon, E., Yasmin, H., Duffy, M., Rashid, T., Akinluyi, E., & Greenwell, T. J. (2018). Developing and validating a new nomogram for diagnosing bladder outlet obstruction in women. *Neurourology and Urodynamics, 37*(1), 368-378.

Somlyo, A., & Somlyo, A. (1998). From pharmacomechanical coupling to G-proteins and myosin phosphatase. *Acta physiologica scandinavica, 164*(4), 437-448.

Somlyo, A. P. (1984). Cell physiology: cellular site of calcium regulation. *Nature, 309*(5968), 516-517.

Specht, P. C., & Bortoff, A. (1972). Propagation and electrical entrainment of intestinal slow waves. *The American journal of digestive diseases, 17*(4), 311-316.

Speich, J. E., Almasri, A. M., Bhatia, H., Klausner, A. P., & Ratz, P. H. (2009). Adaptation of the length-active tension relationship in rabbit detrusor. *American Journal of Physiology-Renal Physiology, 297*(4), F1119-F1128.

Speich, J. E., Borgsmiller, L., Call, C., Mohr, R., & Ratz, P. H. (2005). ROK-induced cross-link formation stiffens passive muscle: reversible strain-induced stress softening in rabbit detrusor. *American Journal of Physiology-Cell Physiology, 289*(1), C12-C21.

Speich, J. E., Dosier, C., Borgsmiller, L., Quintero, K., Koo, H. P., & Ratz, P. H. (2007). Adjustable passive length-tension curve in rabbit detrusor smooth muscle. *J Appl Physiol (1985), 102*(5), 1746-1755. 10.1152/japplphysiol.00548.2006

Speich, J. E., Quintero, K., Dosier, C., Borgsmiller, L., Koo, H. P., & Ratz, P. H. (2006). A mechanical model for adjustable passive stiffness in rabbit detrusor. *J Appl Physiol (1985), 101*(4), 1189-1198. 10.1152/japplphysiol.00396.2006

Speich, J. E., Southern, J. B., Henderson, S., Wilson, C. W., Klausner, A. P., & Ratz, P. H. (2012). Adjustable passive stiffness in mouse bladder: regulated by Rho kinase and elevated following partial bladder outlet obstruction. *American Journal of Physiology-Renal Physiology, 302*(8), F967-F976.

Spencer, N., Walsh, M., & Smith, T. K. (1999). Does the guinea-pig ileum obey the 'law of the intestine'? *The Journal of physiology, 517*(3), 889-898.

Spencer, N. J., Bayguinov, P., Hennig, G. W., Park, K. J., Lee, H.-T., Sanders, K. M., & Smith, T. K. (2007). Activation of neural circuitry and Ca2+ waves in longitudinal and circular muscle during CMMCs and the consequences of rectal aganglionosis in mice. *American Journal of Physiology-Gastrointestinal and Liver Physiology, 292*(2), G546-G555.

Spencer, N. J., Nicholas, S. J., Sia, T., Staikopoulos, V., Kyloh, M., & Beckett, E. A. (2013). By what mechanism does ondansetron inhibit colonic migrating motor complexes: does it require endogenous serotonin in the gut wall? *Neurogastroenterology and Motility, 25*(8), 677-685.

Spencer, N. J., Walsh, M., & Smith, T. K. (1999). Does the guinea-pig ileum obey the 'law of the intestine'? *Journal of Physiology, 517*(3), 889-898.

Spitz, I. M., & Bardin, C. (1993). Mifepristone (RU 486)--a modulator of progestin and glucocorticoid action. *New England Journal of Medicine, 329*(6), 404-412.

Strauss, J. D., & Murphy, R. A. (1996). Regulation of cross-bridge cycling in smooth muscle. In *Biochemistry of smooth muscle contraction* (pp. 341-353): Elsevier.

Strege, P. R., Ou, Y., Sha, L., Rich, A., Gibbons, S. J., Szurszewski, J. H., . . . Farrugia, G. (2003). Sodium current in human intestinal interstitial cells of Cajal. *American Journal of Physiology, 285*(6), G1111-1121.

Streng, T., Hedlund, P., Talo, A., ANDERSSON, K. E., & Gillespie, J. I. (2006). Phasic non-micturition contractions in the bladder of the anaesthetized and awake rat. *BJU International, 97*(5), 1094-1101.

Strobl, K. H., Sepp, W., Wahl, E., Bodenmuller, T., Suppa, M., Seara, J. F., & Hirzinger, G. (2004). *The DLR multisensory hand-guided device: The laser stripe profiler.* Paper presented at the Robotics and Automation, 2004. Proceedings. ICRA'04. 2004 IEEE International Conference on.

Sugaya, K., & de Groat, W. C. (2000). Influence of temperature on activity of the isolated whole bladder preparation of neonatal and adult rats. *American Journal of Physiology, 278*(1), R238-246.

Sugaya, K., Roppolo, J. R., Yoshimura, N., Card, J. P., & de Groat, W. C. (1997). The central neural pathways involved in micturition in the neonatal rat as revealed by the injection of pseudorabies virus into the urinary bladder. *Neuroscience Letters, 223*(3), 197-200.

Sui, G., Rothery, S., Dupont, E., Fry, C., & Severs, N. (2002). Gap junctions and connexin expression in human suburothelial interstitial cells. *BJU international, 90*(1), 118-129.

Sui, G. P., Wu, C., & Fry, C. H. (2003). A description of Ca2+ channels in human detrusor smooth muscle. *BJU Int, 92*(4), 476-482. 10.1046/j.1464-410x.2003.04356.x

Suzuki, H., & Tsutsumi, Y. (1981). Intraluminal pressure changes in the oviduct, uterus, and cervix of the mated rabbit. *Biology of reproduction, 24*(4), 723-733.

Swee, M. H., Parks, W. C., & Pierce, R. A. (1995). Developmental Regulation of Elastin Production.: EXPRESSION OF TROPOELASTIN PRE-mRNA PERSISTS AFTER DOWN-REGULATION OF STEADY-STATE mRNA LEVELS (∗). *Journal of Biological Chemistry, 270*(25), 14899-14906.

Széll, E. A., Somogyi, G. T., de Groat, W. C., & Szigeti, G. P. (2003). Developmental changes in spontaneous smooth muscle activity in the neonatal rat urinary bladder. *American Journal of Physiology-Regulatory, Integrative and Comparative Physiology, 285*(4), R809-R816.

Tack, J., & Sifrim, D. (2000). A little rest and relaxation. *Gut, 47*(1), 11-12.

Takeda, H. (1965). Generation and propagation of uterine activity in situ. *Fertility and Sterility, 16*(1), 113-119.

Tan, L. K., Tan, H. K., & Ng, L. K. (2008). P39.02: Uterine volume during pregnancy - A cross sectional study. *Ultrasound in Obstetrics & Gynecology, 32*(3), 445-445. https://doi.org/10.1002/uog.6082

Tang, Y., Ballarini, R., Buehler, M. J., & Eppell, S. J. (2010). Deformation micromechanisms of collagen fibrils under uniaxial tension. *Journal of The Royal Society Interface, 7*(46), 839-850.

Tare, M., Coleman, H., & Parkington, H. C. (2002). Glycyrrhetinic derivatives inhibit hyperpolarization in endothelial cells of guinea pig and rat arteries. *American Journal of Physiology-Heart and Circulatory Physiology, 282*(1), H335-H341.

Tasaka, K., & Farrar, J. T. (1969). Mechanics of small intestinal muscle function in the dog. *American Journal of Physiology, 217*(4), 1224-1229.

Tasian, G., Cunha, G., & Baskin, L. (2010). Smooth muscle differentiation and patterning in the urinary bladder. *Differentiation, 80*(2-3), 106-117.

Taylor, C. A., & Figueroa, C. (2009). Patient-specific modeling of cardiovascular mechanics. *Annual review of biomedical engineering, 11*, 109.

Taylor, C. A., & Steinman, D. A. (2010). Image-based modeling of blood flow and vessel wall dynamics: applications, methods and future directions. *Annals of biomedical engineering, 38*(3), 1188-1203.

Terzidou, V., Sooranna, S. R., Kim, L. U., Thornton, S., Bennett, P. R., & Johnson, M. R. (2005). Mechanical stretch up-regulates the human oxytocin receptor in primary human uterine myocytes. *J Clin Endocrinol Metab, 90*(1), 237-246. 10.1210/jc.2004-0277

Testut, L. L. A. (1984). *Tratado de anatoma humana. Vol.1, Vol.1*. Barcelona [etc.]: Salvat.

Thompson, T. R., & Little, R. W. (1970). End effects in a truncated semi-infinite cone. *The Quarterly Journal of Mechanics and Applied Mathematics, 23*(2), 185-196.

Thorbert, G. (1978). Regional changes in structure and function of adrenergic nerves in guinea-pig uterus during pregnancy. *Acta Obstetricia et Gynecologica Scandinavica, 57*(sup79), 2-32.

Thorburn, G., Challis, J., & Robinson, J. (1977). The endocrinology of parturition. *Cellular Biology of the Uterus, Wynn, RM (Ed), Plenum Press, New York*, 653.

Thuneberg, L., & Peters, S. (2001). Toward a concept of stretch-coupling in smooth muscle. I. Anatomy of intestinal segmentation and sleeve contractions. *Anatomical Record, 262*(1), 110-124.

Tica, A. A., Dun, E., Tica, V., Cojocaru, V., Tica, O. S., & Berceanu, S. (2011). The autonomic innervation of the uterus A short review on pharmacological aspects. *GINECO RO, 7*(2), 86-91.

Tobin, G., & Sjögren, C. (1998). Prejunctional facilitatory and inhibitory modulation of parasympathetic nerve transmission in the rabbit urinary bladder. *Journal of the autonomic nervous system, 68*(3), 153-156.

Tomita, T. (1990). Spread of excitation in smooth muscle. *Progress in Clinical and Biological Research, 327*, 361.

Toner, J., & Adler, N. (1985). The role of uterine luminal fluid in uterine contractions, sperm transport and fertility of rats. *Reproduction, 74*(1), 295-302.

Tops, L. F., Bax, J. J., Zeppenfeld, K., Jongbloed, M. R., Lamb, H. J., van der Wall, E. E., & Schalij, M. J. (2005). Fusion of multislice computed tomography imaging with three-dimensional electroanatomic mapping to guide radiofrequency catheter ablation procedures. *Heart Rhythm, 2*(10), 1076-1081.

Tribe, R. M. (2001). Regulation of human myometrial contractility during pregnancy and labour: are calcium homeostatic pathways important? *Experimental physiology, 86*(2), 247-254.

Turner, W., & Brading, A. (1997). Smooth muscle of the bladder in the normal and the diseased state: pathophysiology, diagnosis and treatment. *Pharmacology and Therapeutics, 75*(2), 77-110.

Uchiyama, T., & Chess-Williams, R. (2004). Muscarinic receptor subtypes of the bladder and gastrointestinal tract. *Journal of smooth muscle research, 40*(6), 237-247.

Umans, B. D., & Liberles, S. D. (2018). Neural sensing of organ volume. *Trends in neurosciences, 41*(12), 911-924.

Urology, E. A. o. (2022). Oncology endorses EAU Guideline on Muscle-Invasive and Metastatic Bladder Cancer. Retrieved 19/08/2022 2022 from https://uroweb.org/news/american-society-of-clinical-oncology-endorses-eau-guideline-on-muscle-invasive-and-metastatic-bladder-cancer

Ursillo, R. (1961). Electrical activity of the isolated nerve-urinary bladder strip preparation of the rabbit. *American Journal of Physiology-Legacy Content, 201*(3), 408-412.

USHIKI, T., & MURAKUMO, M. (1991). Scanning electron microscopic studies of tissue elastin components exposed by a KOH-collagenase or simple KOH digestion method. *Archives of histology and cytology, 54*(4), 427-436.

Vahabi, B., & Drake, M. J. (2015). Physiological and pathophysiological implications of micromotion activity in urinary bladder function. *Acta Physiologica, 213*(2), 360-370.

Van Doorn, E. V. W., Remmers, A., & Janknegt, R. (1992). Conventional and extramural ambulatory urodynamic testing of the lower urinary tract in female volunteers. *The Journal of urology, 147*(5), 1319-1325.

Van Duyl, W. (1980). *Determination and interpretation of micromotion in urinary bladder smooth muscle: viscomotion model.* Paper presented at the Proceedings, 20th International Congress of Biological Engineers, London.

van Duyl, W. A. (2021). Biomechanics of urinary bladder: slow-filling and slow-emptying cystometry and accommodation. *Bladder, 8*(1)

Van Gestel, I., IJland, M., Hoogland, H., & Evers, J. (2003). Endometrial wave-like activity in the non-pregnant uterus. *Human Reproduction Update, 9*(2), 131-138.

Van Os-Bossagh, P., Kosterman, L., Hop, W., Westerhof, B., De Bakker, J., Drogendijk, A., & Van Duyl, W. (2001). Micromotions of bladder wall in chronic pelvic pain (CPP): a pilot study. *International Urogynecology Journal, 12*(2), 89-96.

Vatandoust, S., Kichenadasse, G., O'Callaghan, M., Vincent, A. D., Kopsaftis, T., Walsh, S., . . . Moretti, K. (2018). Localised prostate cancer in elderly men aged 80–89 years, findings from a population-based registry. *BJU international, 121*, 48-54.

Visser, A., & Van Mastrigt, R. (1999). Intracellular recording of spontaneous electrical activity in human urinary bladder smooth muscle strips. *Archives of physiology and biochemistry, 107*(3), 257-270.

Visser, A., & van Mastrigt, R. (2000). The role of intracellular and extracellular calcium in mechanical and intracellular electrical activity of human urinary bladder smooth muscle. *Urological research, 28*(4), 260-268.

Visser, A. J., & van Mastrigt, R. (2001). Intracellular electrical activity in human urinary bladder smooth muscle: the effect of high sucrose medium. *Urologia internationalis, 66*(4), 205-211.

Vlaskovska, M., Kasakov, L., Rong, W., Bodin, P., Bardini, M., Cockayne, D. A., . . . Burnstock, G. (2001). P2X3 knock-out mice reveal a major sensory role for urothelially released ATP. *Journal of Neuroscience, 21*(15), 5670-5677.

Waelchli, R. (2007). Current Therapy in Equine Reproduction. *The Canadian Veterinary Journal, 48*(5), 486.

Wang, M., Xing, N., Wu, L., Huang, W. C., Xu, Z., & Liu, G. (2018). Regulation of Spontaneous Contractions in Intact Rat Bladder Strips and the Effects of Hydrogen Peroxide. *Biomed Res Int, 2018*, 2925985. 10.1155/2018/2925985

Wang, P., Luthin, G., & Ruggieri, M. (1995). Muscarinic acetylcholine receptor subtypes mediating urinary bladder contractility and coupling to GTP binding proteins. *The Journal of pharmacology and experimental therapeutics, 273*(2), 959.

Wang, Y., Fang, Q., Lu, Y., Song, B., Li, W., & Li, L. (2010). Effects of mechanical stretch on interstitial cells of Cajal in guinea pig bladder. *Journal of Surgical Research, 164*(1), e213-e219.

Wang, Z. S., He, Z., & Chen, J. D. (2004). Chaotic behavior of gastric migrating myoelectrical complex. *IEEE Transactions on Biomedical Engineering, 51*(8), 1401-1406.

Ward, S. M., Morris, G., Reese, L., Wang, X.-Y., & Sanders, K. M. (1998). Interstitial cells of Cajal mediate enteric inhibitory neurotransmission in the lower esophageal and pyloric sphincters. *Gastroenterology, 115*(2), 314-329.

Wasserman, N. F., Spilseth, B., Golzarian, J., & Metzger, G. J. (2015). Use of MRI for lobar classification of benign prostatic hyperplasia: potential phenotypic biomarkers for research on treatment strategies. *AJR. American journal of roentgenology, 205*(3), 564.

Wathes, D. C., & Porter, D. (1982). Effect of uterine distension and oestrogen treatment on gap junction formation in the myometrium of the rat. *Reproduction, 65*(2), 497-505.

Watton, P., Hill, N., & Heil, M. (2004). A mathematical model for the growth of the abdominal aortic aneurysm. *Biomechanics and modeling in mechanobiology, 3*(2), 98-113.

Weiss, S., Jaermann, T., Schmid, P., Staempfli, P., Boesiger, P., Niederer, P., . . . Bajka, M. (2006a). Three-dimensional fiber architecture of the nonpregnant human uterus determined ex vivo using magnetic resonance diffusion tensor imaging. *The Anatomical Record, 288*(1), 84-90.

Weiss, S., Jaermann, T., Schmid, P., Staempfli, P., Boesiger, P., Niederer, P., . . . Bajka, M. (2006b). Three-dimensional fiber architecture of the nonpregnant human uterus determined ex vivo using magnetic resonance diffusion tensor imaging. *The Anatomical Record Part A: Discoveries in Molecular, Cellular, and Evolutionary Biology: An Official Publication of the American Association of Anatomists, 288*(1), 84-90.

Wellner, M.-C., & Isenberg, G. (1993). Stretch Activated Nonselective Cation Channels in Urinary Bladder Myocytes: Importance for Pacemaker Potentials and Myogenic Response. *EXS, 66*, 93-99.

Wellner, M.-C., & Isenberg, G. (1994). Stretch effects on whole-cell currents of guinea-pig urinary bladder myocytes. *The Journal of physiology, 480*(3), 439-448.

Wellner, M. C., & Isenberg, G. (1993). Properties of stretch-activated channels in myocytes from the guinea-pig urinary bladder. *The Journal of physiology, 466*(1), 213-227. 10.1113/jphysiol.1993.sp019717

Wibberley, A., Chen, Z., Hu, E., Hieble, J. P., & Westfall, T. D. (2003). Expression and functional role of Rho-kinase in rat urinary bladder smooth muscle. *British journal of pharmacology, 138*(5), 757-766.

Wildt, L., Kissler, S., Licht, P., & Becker, W. (1998). Sperm transport in the human female genital tract and its modulation by oxytocin as assessed by hysterosalpingoscintigraphy, hysterotonography, electrohysterography and Doppler sonography. *Human reproduction update, 4*(5), 655-666.

Willecke, K., Eiberger, J., Degen, J., Eckardt, D., Romualdi, A., Güldenagel, M., . . . Söhl, G. (2002). Structural and functional diversity of connexin genes in the mouse and human genome.

Willets, J. M., Brighton, P. J., Mistry, R., Morris, G. E., Konje, J. C., & Challiss, R. J. (2009). Regulation of oxytocin receptor responsiveness by G protein-coupled receptor kinase 6 in human myometrial smooth muscle. *Molecular Endocrinology, 23*(8), 1272-1280.

Willocks, J., & Dunsmore, I. R. (1971). Assessment of gestational age and prediction of dysmaturity by ultrasonic fetal cephalometry. *BJOG: An International Journal of Obstetrics & Gynaecology, 78*(9), 804-808.

Wilson, L., & Kurzrok, R. (1938). Studies on the motility of the human uterus in vivo. *Endocrinology, 23*(1), 79-86.

Wilson, R., Allen, M., Nandi, M., Giles, H., & Thornton, S. (2001). Spontaneous contractions of myometrium from humans, non-human primate and rodents are sensitive to selective oxytocin receptor antagonism in vitro. *British Journal of Obstetrics and Gynaecology, 108*(9), 960-966.

Wilson, R. L., & Worthen, N. J. (1979). Ultrasonic demonstration of myometrial contractions in intrauterine pregnancy. *American Journal of Roentgenology, 132*(2), 243-247.

Winkelstein, B. A. (2012). *Orthopaedic biomechanics*: CRC Press.

Wiseman, O., Fowler, C., & Landon, D. (2003). The role of the human bladder lamina propria myofibroblast. *BJU international, 91*(1), 89-93.

Won, K.-J., Sanders, K. M., & Ward, S. M. (2005). Interstitial cells of Cajal mediate mechanosensitive responses in the stomach. *Proceedings of the National Academy of Sciences, 102*(41), 14913-14918.

Won, K. J., Sanders, K. M., & Ward, S. M. (2005). Interstitial cells of Cajal mediate mechanosensitive responses in the stomach. *Proceedings of the National Academy of Sciences of the United States of America, 102*(41), 14913-14918.

Wood, C. (1999). Control of parturition in ruminants. *Journal of reproduction and fertility. Supplement, 54*, 115-126.

Wray, S. (1993). Uterine contraction and physiological mechanisms of modulation. *American Journal of Physiology-Cell Physiology, 264*(1), C1-C18.

Wray, S., Burdyga, T., Noble, D., Noble, K., Borysova, L., & Arrowsmith, S. (2015). Progress in understanding electro-mechanical signalling in the myometrium. *Acta Physiologica, 213*(2), 417-431.

Wray, S., Jones, K., Kupittayanant, S., Li, Y., Matthew, A., Monir-Bishty, E., . . . Shmygol, A. V. (2003). Calcium signaling and uterine contractility. *J Soc Gynecol Investig, 10*(5), 252-264. 10.1016/s1071-5576(03)00089-3

Wu, C., & Fry, C. (2001). Na+/Ca2+ exchange and its role in intracellular Ca2+ regulation in guinea pig detrusor smooth muscle. *American Journal of Physiology-Cell Physiology, 280*(5), C1090-C1096.

Wu, C., Kentish, J. C., & Fry, C. H. (1995). Effect of pH on Myofilament Ca sup 2 Plus-Sensitivity in Alphatoxin Permeabilized Guinea Pig Detrusor Muscle. *The Journal of urology, 154*(5), 1921-1924.

Wu, C., Sui, G., & Fry, C. (2004). Purinergic regulation of guinea pig suburothelial myofibroblasts. *The Journal of physiology, 559*(1), 231-243.

Wu, X., & Davis, M. J. (2001). Characterization of stretch-activated cation current in coronary smooth muscle cells. *American Journal of Physiology, 280*(4), H1751-1761.

Wuttke, W. (1989). Endocrinology. In R. F. Schmidt & G. Thews (Eds.), *Human Physiology* (pp. 371-399). Berlin, Heidelberg: Springer Berlin Heidelberg. 10.1007/978-3-642-73831-9_17

Xu, L., & Gebhart, G. F. (2008). Characterization of mouse lumbar splanchnic and pelvic nerve urinary bladder mechanosensory afferents. *Journal of neurophysiology, 99*(1), 244-253.

Yagel, S., Ben-Chetrit, A., Anteby, E., Zacut, D., Hochner-Celnikier, D., & Ron, M. (1992). The effect of ethinyl estradiol on endometrial thickness and uterine volume during ovulation induction by clomiphene citrate. *Fertility and Sterility, 57*(1), 33-36.

Yamada, K. M., & Geiger, B. (1997). Molecular interactions in cell adhesion complexes. *Current Opinion in Cell Biology, 9*(1), 76-85. https://doi.org/10.1016/S0955-0674(97)80155-X

Yamanishi, T., Chapple, C., & Chess-Williams, R. (2001). Which muscarinic receptor is important in the bladder? *World journal of urology, 19*(5), 299-306.

Yamazaki, Y., Takeda, H., Akahane, M., Igawa, Y., Nishizawa, O., & Ajisawa, Y. (1998). Species differences in the distribution of β-adrenoceptor subtypes in bladder smooth muscle. *British Journal of Pharmacology, 124*(3), 593-599.

Yeomans, E. R., Hoffman, B. L., Gilstrap, L. C., & Cunningham, F. G. (2017). *Cunningham and Gilstrap's Operative Obstetrics*: McGraw Hill Professional.

Yoshida, M., Inadome, A., Maeda, Y., Satoji, Y., Masunaga, K., Sugiyama, Y., & Murakami, S. (2006). Non-neuronal cholinergic system in human bladder urothelium. *Urology, 67*(2), 425-430.

Yoshida, M., Miyamae, K., Iwashita, H., Otani, M., & Inadome, A. (2004). Management of detrusor dysfunction in the elderly: changes in acetylcholine and adenosine triphosphate release during aging. *Urology, 63*(3), 17-23.

Yoshimura, N., & Chancellor, M. B. (2002). Current and future pharmacological treatment for overactive bladder. *The Journal of urology, 168*(5), 1897-1913.

Yoshino, M., Wang, S., & Kao, C. (1997). Sodium and calcium inward currents in freshly dissociated smooth myocytes of rat uterus. *The Journal of general physiology, 110*(5), 565-577.

Young, J. S., Matharu, R., Carew, M. A., & Fry, C. H. (2012). Inhibition of stretching-evoked ATP release from bladder mucosa by anticholinergic agents. *BJU international, 110*(8b), E397-E401.

Young, R., & Hession, R. (1999). Three-dimensional structure of the smooth muscle in the term-pregnant human uterus. *Obstetrics & Gynecology, 93*(1), 94-99.

Young, R. C. (2016). Mechanotransduction mechanisms for coordinating uterine contractions in human labor. *152*(2), R51. 10.1530/rep-16-0156

Young, R. C. (2016). Mechanotransduction mechanisms for coordinating uterine contractions in human labor. *Reproduction, 152*(2), R51-61. 10.1530/REP-16-0156

Young, R. C., & Barendse, P. (2014). Linking myometrial physiology to intrauterine pressure; how tissue-level contractions create uterine contractions of labor. *PLoS Comput Biol, 10*(10), e1003850. 10.1371/journal.pcbi.1003850

Young, R. C., & Goloman, G. (2011). Mechanotransduction in rat myometrium: coordination of contractions of electrically and chemically isolated tissues. *Reproductive Sciences, 18*(1), 64-69.

Young, R. C., Smith, L. H., & McLaren, M. D. (1993). T-type and L-type calcium currents in freshly dispersed human uterine smooth muscle cells. *American Journal of Obstetrics and Gynecology, 169*(4), 785-792.

Yu, Y.-L., He, Q., Li, G.-H., & Cheng, S. (2017). The dome wall of bladder acts as a pacemaker site in detrusor instability in rats. *Medical science monitor: international medical journal of experimental and clinical research, 23*, 2400.

Zagorodnyuk, V. P., Brookes, S. J., & Spencer, N. J. (2010). Structure-function relationship of sensory endings in the gut and bladder. *Auton Neurosci, 153*(1-2), 3-11. 10.1016/j.autneu.2009.07.018

Zagorodnyuk, V. P., Brookes, S. J., & Spencer, N. J. (2010). Structure–function relationship of sensory endings in the gut and bladder. *Autonomic Neuroscience: Basic and Clinical, 153*(1), 3-11.

Zagorodnyuk, V. P., Costa, M., & Brookes, S. J. (2006). Major classes of sensory neurons to the urinary bladder. *Autonomic Neuroscience: Basic and Clinical, 126*, 390-397.

Zagorodnyuk, V. P., Gibbins, I. L., Costa, M., Brookes, S. J., & Gregory, S. J. (2007). Properties of the major classes of mechanoreceptors in the guinea pig bladder. *The Journal of physiology, 585*(1), 147-163.

Zagorodnyuk, V. P., Gibbins, I. L., Costa, M., Brookes, S. J., & Gregory, S. J. (2007). Properties of the major classes of mechanoreceptors in the guinea pig bladder. *J Physiol, 585*(Pt 1), 147-163. 10.1113/jphysiol.2007.140244

Zakar, T., & Hertelendy, F. (2007). Progesterone withdrawal: key to parturition. *American Journal of Obstetrics and Gynecology, 196*(4), 289-296.

Zamir, E., & Geiger, B. (2001). Molecular complexity and dynamics of cell-matrix adhesions. *Journal of cell science, 114*(20), 3583-3590.

Zanetti, E. M., Perrini, M., Bignardi, C., & Audenino, A. L. (2012). Bladder tissue passive response to monotonic and cyclic loading. *Biorheology, 49*(1), 49-63.

Zara, F., & Dupuis, O. (2017). Uterus – Biomechanical modeling of uterus. Application to a childbirth simulation. In P. Yohan & O. Jacques (Eds.), *Biomechanics of Living Organs: Hyperelastic Constitutive Laws for Finite Element Modeling* (pp. 325-346): Elsevier.

Zeeman, G. G., Khan-Dawood, F. S., & Dawood, M. Y. (1997). Oxytocin and its receptor in pregnancy and parturition: current concepts and clinical implications. *Obstetrics & Gynecology, 89*(5), 873-883.

Zhang, X., & DiSanto, M. E. (2011). Rho-kinase, a common final path of various contractile bladder and ureter stimuli. In *Urinary Tract* (pp. 543-568): Springer.

Zhang, Y., Qian, J., Zaltzhendler, O., Bshara, M., Jaffa, A. J., Grisaru, D., . . . Elad, D. (2019). Analysis of in vivo uterine peristalsis in the non-pregnant female mouse. *Interface focus, 9*(4), 20180082.

Zingg, H. H., & Laporte, S. A. (2003). The oxytocin receptor. *Trends in Endocrinology & Metabolism, 14*(5), 222-227.